CIVIL ENGINEERING STUDIES
STRUCTURAL RESEARCH SERIES NO. 350

EXACT SOLUTIONS OF SOME DYNAMIC PROBLEMS OF INDENTATION AND TRANSIENT LOADINGS OF AN ELASTIC HALF SPACE

By
J. C. THOMPSON
and
A. R. ROBINSON

A Technical Report
of a Research Program
Sponsored by
THE OFFICE OF NAVAL RESEARCH
DEPARTMENT OF THE NAVY
Contract N00014-67-A-0305-0010

UNIVERSITY OF ILLINOIS
URBANA, ILLINOIS
SEPTEMBER, 1969

EXACT SOLUTIONS OF SOME DYNAMIC PROBLEMS OF INDENTATION AND TRANSIENT LOADINGS OF AN ELASTIC HALF SPACE

by

J. CARL THOMPSON

and

A. R. ROBINSON

A technical Report
of a Research Program
Sponsored by
THE OFFICE OF NAVAL RESEARCH
DEPARTMENT OF THE NAVY
Contract N00014-67-A-0305-0010

UNIVERSITY OF ILLINOIS
URBANA, ILLINOIS

SEPTEMBER, 1969

ACKNOWLEDGMENT

This report was prepared as a doctoral dissertation by Mr. J. C. Thompson and was submitted to the Graduate College of the University of Illinois, Urbana, in partial fulfillment of the requirements for the degree of Doctor of Philosophy. The work was done under the supervision of Dr. A. R. Robinson, Professor of Civil Engineering.

The investigation was conducted as part of a research program supported by the Office of Naval Research, Contract N00014-67-A-0305-0010, Numerical and Approximate Methods of Stress Analysis.

The numerical results were obtained with the use of the IBM 360 50-75 computer system of the Department of Computer Science of the University of Illinois.

TABLE OF CONTENTS

Page

LIST OF FIGURES

1. INTRODUCTION

1.1. General Remarks

When two solids collide, the general character of the behavior of the media in the region of contact depends strongly on the speed of impact of the two bodies. If this speed is very low, a very accurate estimate of the magnitude and distribution of the contact stress can be obtained by a quasi-static analysis. This is the type of solution obtained if one uses the Hertz Theory of Impact [1].†

If the speed of impact is very high (hypervelocity impact), one or both of the solids may liquefy in the zone of contact. For impact problems of this type results obtained by a hydrodynamic analysis compare reasonably well with results obtained experimentally [2].

The method of characteristics can be used, as in Ref. [3], to obtain exact solutions for certain problems involving the longitudinal impact of elastic-plastic bars of finite length.

The purely elastic dynamic contact problem should be a reasonable model for some intermediate speeds of contact. Inelastic behavior in regions near mathematical singularities will not be taken into account. The contact problems considered in this study involve the indentation of a linearly elastic half space by arbitrarily-shaped rigid dies. The solutions obtained take full account of the transient character of the disturbance and are exact within the limits of the classical theory of elasticity. The method which is used to solve these impact problems is also used to obtain the general solution

---

† Numbers in square brackets refer to entries in the List of References.

for any problem involving transient loads acting on the surface of a linearly elastic half space. This class of boundary value problems has been studied in considerable detail by Smirnov and Sobolev [4,5,6], by Cagniard [7], and by Ewing, Jardetzky and Press (8], and many others. However, it is only the first pair of authors who have obtained solutions using a method which does not lead to formidable mathematical difficulties. With the aid of the method which was developed Smirnov and Sobolev and later modified by Kostrov [9], solutions can be obtained almost by inspection for any boundary load problem as well as for many impact problems. It is this method which is used to solve the dynamic contact problems that are considered in this study.

Kostrov was partially successful in solving the problem in which a rigid wedge- or cone-shaped die indents an elastic half space.† In the only case considered by Kostrov the rate of indentation was assumed to be both constant and slow enough that the speed of the boundary of the contact region would never exceed the speed of the Rayleigh (surface) wave. This condition was imposed because it was incorrectly reasoned that greater indentation speeds would require an infinite flow of power across the surface of the die.

There is a second fundamental error in Kostrov's work. In determining the final deformed shape of the surface of the half space in the region beneath the die, Kostrov failed to consider the displacement which each point would have at the instant that it came in contact with the die. Even in static contact problems, the final shapes of the deformed contacting bodies are matched,

---

† For brevity in what follows a rigid wedge-shaped die is referred to as a wedge, a rigid cone-shaped die as a cone.

and the approach cannot be calculated without considering the deformations of the entire body (see Ref. [1]). Kostrov assumed that the deformed position of a surface point beneath the die could be determined simply by multiplying the downward speed of the die by the length of time that the point in question has been in contact with the die. Fortunately, the actual deformation of the surface beneath the contact stresses determined by Kostrov is a wedge or conical shape. Thus, the solution obtained by Kostrov is not wrong but is correct for a wedge or cone with some different apex angle.

1.2. Objectives of the Study

The first purpose of this report is to determine the contact stress for the wedge and cone problems including cases in which the speed of the boundary of the contact region is greater than the speed of the surface wave. It will be seen later that once these stresses are known, it is not difficult to determine the transient disturbance at any point in the half space.

The rigid wedge- and cone-shaped dies are assumed to be shallow enough that the usual assumptions of the small displacement theory of elasticity are satisfied and that displacements normal to these dies are essentially normal to the original position of the surface of the half space.

It will be shown that the small displacement theory of elasticity predicts that the stress field is singular beneath the apex of a wedge or cone for all indentation velocities and that another singularity is present at the edge of the contact zone for a certain range of indentation velocities. As indicated above, the inevitable non-linear behavior of the half space near these points is not considered.

As one might expect, the stress near the edge of the region of contact is strongly dependent on the speed of the boundary of this region

relative to the speeds of the dilatation, shear, and surface waves. For reasons that will be apparent later, the following four ranges of speeds must be solved separately:

1) the speed of the boundary† is less than the speed of the surface wave,
2) the speed of the boundary is in the small range between the speeds of the surface and shear waves,
3) the speed of the boundary is between the speeds of the shear and dilatation waves, and
4) the speed of the boundary exceeds the speed of the dilatation wave.

In what follows, these ranges of speed will be referred to as the "slow," "first intermediate," "second intermediate" and "superseismic" ranges, respectively.

To solve these problems, all possible distributions of contact stress which cause surface points within the region of contact to move downward with the same constant velocity will be determined. It is then a simple matter to select from these that single stress distribution which causes a wedge- or cone-shaped deformation of the surface of the half space within the region of contact.

The second purpose of this study is the derivation of the closed form solution for "superseismic" contact problems which involve an arbitrarily shaped rigid die and a linearly elastic half space. The term "superseismic" is used to describe any contact problem in which the boundary of the region of contact moves along the surface of the half space more rapidly than the

---

† That is, the speed of the edge of the boundary of the contact region.

dilatation wave. It is apparent that the contact must always be superseismic for a finite interval of time if two bodies impact at a point where the surface of each is smooth.

1.3. The Method of Solution

The contact problems considered in the report will be solved by means of a modified form of a self-similar† potential method developed in the early 1930's by V. I. Smirnov and S. L. Sobolev. Using this method, which is explained in detail in Chapter 2, the above authors obtained a closed form solution for both the two- and three-dimensional problem of an impulse acting on the surface of a linearly elastic half space.†† From these results the solution of any problem involving transient loads on the boundary can be obtained by the method of superposition.

Since the work of Smirnov and Sobolev is not well known outside the U.S.S.R., the method of self-similar solutions is developed in detail and used to solve various two- and three-dimensional traction problems, that is, problems with loads acting on the surface of the half space.

The self-similar method, sometimes referred to as the method of functional invariant solutions, is closely related to the d'Alembert approach used for one-dimensional problems. The first step in the solution of the two-dimensional problem is the determination of a suitable function of the space and time variables which identically satisfies the two-dimensional wave equation. Using this function as the argument of any second function, one can easily construct an infinite family of functions, each of which satisfies

---

† See Sec. 2.2 for a definition of the term "self-similar."

†† Because these problems were initially solved by Lamb [10], they are frequently referred to as "Lamb's Problem."

the wave equation identically. In Sec. 2.4, we prove that the function, or superposition of functions of this type, which satisfies the boundary conditions for a given problem, is the complete solution of that problem.

The corresponding three-dimensional problems are only slightly more difficult to solve. Solutions are obtained by a superposition of two-dimensional solutions, as is described in Chapter 2.

It will be shown later that the contact problems mentioned in Sec. 1.2 as well as any problem involving transient loads can easily be solved by self-similar methods.

1.4. Previous Related Studies

It is also possible to solve wave propagation problems by Laplace transform and harmonic wave methods. However, there are certain difficulties inherent in each of these approaches. With the first method, transformations are encountered which are difficult to carry out analytically except for problems such as Lamb's Problem which have boundary conditions that are homogeneous functions of the space and time variables.

Using Laplace transforms, Cagniard [7] solved Lamb's Problem without actually having to carry out any of the transformations. Several other problems have also been solved in the same way [11,12].† Somewhat surprisingly, it does not appear that any of the authors using this approach have recognized that solutions for any problem with homogeneous boundary conditions can be solved as simply as Lamb's Problem. As is shown later in this study, one can solve these same problems almost by inspection using the method of self-similar solutions.

---

† In the literature, this particular method of solving wave propagation problems is frequently referred to as the method of Cagniard.

The relation of the simple Smirnov-Sobolev computation to the more circuitous approach of Cagniard is but one more instance of a very useful principle enunciated by Lame:†

> Lorsqu'on parvient à un résultat simple par des calculs compliqués, il doit exister une manière beaucoup plus directe d'arriver au même résultat; toute simplification qui s'opère, tout facteur qui disparaît dans le cours du calcul primitif, est l'indice certain d'une méthode à chercher, où cette simplification serait toute faite, où ce facteur n'apparaitraît pas.

When wave propagation problems are solved by the harmonic wave method the potentials satisfying the governing wave equations are expressed as functions of the space variables multiplied by a harmonic function of time [8]. However, unless the source of the disturbance varies in a harmonic fashion, one has the formidable task of evaluating a Fourier integral in order to satisfy the boundary and initial conditions for the problem being considered. Even when a "solution" is found which satisfies the boundary conditions, one must introduce a radiation condition†† in order to eliminate any component of the "solution" which is associated with a disturbance originating at infinity.

Craggs [15,16,17,18] has solved several wave propagation problems using a method that was derived independently, but is essentially equivalent to the method of Smirnov and Sobolev. However, the form of the general solution given by Craggs is neither as compact nor as convenient for the study of contact problems as the form of solution that can be derived with the approach of Smirnov and Sobolev.

It has already been indicated that all traction problems and the two types of contact problems mentioned in Sec. 1.2 can be solved in a

---

† See Ref. [13], page 111.

†† See Ref. [14], page 189.

straightforward manner by the self-similar method. This approach has also been used to solve such diverse problems as the growth of tension and shear cracks [19,20], the reflection and refraction of waves within a multi-layered medium [21,22], and the diffraction of plane waves at the edge of a narrow slit [23]. Additional problems that have been solved by this method can be found in Refs. [24,25,26].

In Chapters 2 and 3, where solutions are derived for many traction problems, reference is made to papers in which the problems are solved by other methods. No attempt is made to discuss these papers except to remark that the self-similar method gives solutions in a few lines where the other methods often involve pages of detailed calculations.

1.5. Organization of the Study

Chapter 2 contains the motivation and development of a method of solving two-dimensional wave propagation problems by means of self-similar potentials. To illustrate the use of this method, solutions are obtained for several problems which have been solved previously by more complicated methods. These include the problem in which a line of impulses acts in an infinite body, and problems in which line impulses and fixed and moving line loads act on the surface of a half space. This chapter also contains a complete description of the variation of the stresses and displacements in the vicinity of the surface wave and wave fronts for the problem in which an impulse acts vertically downward at a point on the surface of a half space.

A method of solving axially symmetric three-dimensional wave propagation problems is developed in Chapter 3. Solutions are found for the three-dimensional impulse problems whose two-dimensional counterparts were solved in Chapter 2.

In Chapter 4, problems which involve rigid dies pressed into an elastic half space are considered. Initially, the plane strain problem is solved for a wedge-shaped die moving at a constant rate into the half space. The solution is then obtained for the three-dimensional problem in which an axially symmetric conical die penetrates the elastic medium at a constant rate. Next, it is shown how the solution can be obtained for any problem in which a die of arbitrary shape indents the half space rapidly enough to cause the boundary of the region of contact to move along the surface of the half space more rapidly than the speed of the dilatation wave.

The stress and velocity fields for the wedge and cone problems are evaluated numerically by techniques described in Chapter 5. These techniques are presented in great detail, since some care is required in performing integrations in the vicinity of the singularities associated with the wave fronts.

Chapter 6 contains a description of the results obtained by the methods of Chapter 5 and a comparison of the solutions for point loads and slowly indenting wedges and cones.

In Chapter 7, the results obtained for the contact problems solved in this study are summarized. In addition, some further problems of technical interest which might be solved by the method of self-similar potentials are described.

1.6. Notation

The symbols used in this study are defined where they first appear. For convenience, frequently used symbols are listed below.

a Speed of the P wave ($\sqrt{\frac{\lambda+2\mu}{\rho}}$).

b	Speed of the S wave ($\sqrt{\frac{\mu}{\rho}}$).
c	Speed of the Rayleigh (surface) wave (except in Secs. 2.2, 2.3 and 2.4).
c_1	Speed of the P wave (same as a).
c_2	Speed of the S wave (same as b).
$F_{\alpha b}(\theta)$	See Eq. (4.25).
G_1, G_2	See Eq. (3.41).
H	Heaviside step function.
i	$\sqrt{-1}$.
I_h, I_v	Line impulses on the surface of a half space in the horizontal and vertical directions, respectively.
r, ω, y	Cylindrical space coordinates.
$R(\theta^2)$	Rayleigh function (see Eq. (2.56)).
t	Time coordinate.
t_1	Arrival time of the P wave.
t_2	Arrival time of the S wave.
t_H, t_S, t_P	Arrival times of the head, S and P waves, respectively.
t_{PM}, t_{SM}	Arrival times of the Mach fronts associated with the P and S waves, respectively.
Δt	Increment of time.
u_x, u_y	Components of the displacement field for plane strain problems.
u_r, u_y	Components of the displacement field for axially symmetric problems.
u_x^*, u_y^*, u_z^*	Complex displacements associated with u_x, u_y and u_r.
u_r^P, u_y^P	P-wave displacement components.
u_r^S, u_y^S	S-wave displacement components.
v_x, v_y	Components of the velocity fields for plane strain problems.

v_r, v_y	Components of the velocity field for axially symmetric problems.
v_x^*, v_y^*, v_r^*	Complex velocities associated with v_x, v_y and v_r.
v_r^P, v_y^P	P-wave velocity components.
v_r^S, v_y^S	S-wave velocity components.
v_r^R, v_y^R	Velocities associated with surface wave disturbances.
V	Downward velocity of the rigid die
x, y, z	Cartesian space coordinates.
(x_0, y_0) or (r_0, y_0)	Coordinates of a specific point.
α	Speed of the boundary of the region of contact (for Chapters 4, 5 and 6).
$\beta(\theta^2)$	Argument, i.e. phase of the Rayleigh function.
γ	Apex angle of a rigid wedge or cone.
$\delta(x)$	Dirac delta function.
δ_1	See Eq. (2.18).
δ_2	See Eq. (2.18).
δ_1'	$\partial\delta_1/\partial\theta_1$.
δ_2'	$\partial\delta_2/\partial\theta_2$.
θ_1, θ_2	See Eqs. (2.30).
θ_P, θ_S	Value of θ at a point on the front of the P and S waves, respectively.
λ, μ	Lamé constants of elasticity.
ξ_1, ξ_2	See Eqs. (6.6) and (6.10).
ρ	Density of the elastic solid.
$\sigma_x, \sigma_y, \sigma_z$	Normal stresses for plane strain problems.
$\sigma_r, \sigma_\omega, \sigma_y$	Normal stresses for axially symmetric problems.

$\sigma_x^*, \sigma_y^*, \sigma_z^*$	Complex normal stresses associated with σ_x, σ_y and σ_z.
$\sigma_y^{*'}$	$\partial\sigma_y^*/\partial\theta$ for plane strain problems; $\partial\sigma_y^*/\partial\theta^2$ for axially symmetric problems.
$\sigma_r^P, \sigma_\omega^P, \sigma_y^P$	Normal stress components for the P wave.
$\sigma_r^S, \sigma_\omega^S, \sigma_y^S$	Normal stress components for the S wave.
$\sigma_r^R, \sigma_\omega^R, \sigma_y^R$	Normal stress components associated with the Rayleigh wave.
Σ_y, T_{xy}	Fictitious tractions (see Eqs. (2.87)).
Σ_y^*, T_{xy}^*	Fictitious complex tractions (see Eqs. (2.87)).
$\tau_{xy}, \tau_{xz}, \tau_{yz}$	Shear stresses for plane strain problems.
$\tau_{ry}, \tau_{r\omega}, \tau_{y\omega}$	Shear stresses for axially symmetric problems.
τ_{xy}^*	Complex shear stress associated with τ_{xy}.
$\tau_{ry}^P, \tau_{ry}^S, \tau_{ry}^R$	Components of τ_{ry} associated with the P, S and Rayleigh waves, respectively.
φ, ψ	Scalar irrotational and equivoluminal potentials for plane strain problems.
Φ, Ψ	Complex irrotational and equivoluminal potentials associated with φ and ψ.

2. STRESS WAVE PROPAGATION IN AN ELASTIC MEDIUM

2.1. General Equations

When stress waves propagate in a homogeneous, isotropic solid which has elastic properties defined by the Lamé constants λ and μ, the equations of motion can be expressed in terms of the displacements as follows,

$$\begin{aligned}
(\lambda + \mu)\frac{\partial \Delta}{\partial x} + \mu\nabla^2 u_x &= \rho\frac{\partial^2 u_x}{\partial t^2} \\
(\lambda + \mu)\frac{\partial \Delta}{\partial y} + \mu\nabla^2 u_y &= \rho\frac{\partial^2 u_y}{\partial t^2} \\
(\lambda + \mu)\frac{\partial \Delta}{\partial z} + \mu\nabla^2 u_z &= \rho\frac{\partial^2 u_z}{\partial t^2}
\end{aligned} \tag{2.1}$$

where $$\nabla^2 = \frac{\partial^2}{\partial x^2} + \frac{\partial^2}{\partial y^2} + \frac{\partial^2}{\partial z^2} \quad ,$$

ρ is the density of the solid, u_x, u_y, and u_z are the components of a displacement vector $\overline{U}$, and Δ is the dilatation,

$$\nabla = \frac{\partial u_x}{\partial x} + \frac{\partial u_y}{\partial y} + \frac{\partial u_z}{\partial z} \quad .$$

For linear wave propagation problems it is customary to express the displacement vector as the sum of the gradient of a scalar potential φ and the curl of a vector potential $\overline{\psi}$, i.e.

$$\overline{U} = \text{grad } \varphi + \text{curl } \overline{\psi} \tag{2.2}$$

where $\overline{\psi}$ satisfies the condition $\operatorname{div} \overline{\psi} = 0$. The first term is an irrotational displacement; the second is equivoluminal.

For the equations of motion to be satisfied, it is both a necessary and sufficient condition that the potentials satisfy the wave equations,

$$\begin{aligned} \left(\nabla^2 - \frac{1}{c_1^2} \frac{\partial^2}{\partial t^2}\right) \varphi &= 0 \\ \left(\nabla^2 - \frac{1}{c_2^2} \frac{\partial^2}{\partial t^2}\right) \overline{\psi} &= 0 \end{aligned} \tag{2.3}$$

where $$c_1 = \sqrt{\frac{\lambda + 2\mu}{\rho}} \quad \text{and} \quad c_2 = \sqrt{\frac{\mu}{\rho}} \ .$$

The constants c_1 and c_2 are the speeds of the irrotational and equivoluminal waves, respectively. In what follows the customary geophysical designation of P and S waves will be used in place of the awkward terms "irrotational" and "equivoluminal."

The sufficiency of Eqs. (2.3) can be established by straightforward substitution of (2.2) into the equations of motion (2.1). The necessity of Eq. (2.3) is more difficult to prove. The initial proof is due to Duhem [27]. Later, the sufficiency was proved in a more straightforward manner by Sobolev [4] and by Sternberg [28].

For the plane strain problem in which the displacements are zero in the z direction, the components of $\overline{\psi}$ in the x and y directions are zero. The complete solution of the two-dimensional wave propagation problem is then given by the scalar potentials φ and ψ_z which satisfy the equations,

$$\left(\nabla^2 - \frac{1}{c_1^2}\frac{\partial^2}{\partial t^2}\right)\varphi = 0$$

$$\left(\nabla^2 - \frac{1}{c_2^2}\frac{\partial^2}{\partial t^2}\right)\psi_z = 0 \qquad (2.4)$$

where ψ_z is the z-component of $\bar{\psi}$, and ∇^2 has been redefined as

$$\nabla^2 = \left(\frac{\partial^2}{\partial x^2} + \frac{\partial^2}{\partial y^2}\right)$$

The differential operator of either of Eqs. (2.4) is sometimes referred to as the d'Alembertian.

In terms of the scalar potentials the components of the displacement vector are given as

$$u_x = \frac{\partial\varphi}{\partial x} + \frac{\partial\psi}{\partial y}\,, \quad u_y = \frac{\partial\varphi}{\partial y} - \frac{\partial\psi}{\partial x}\,, \quad u_z = 0\,, \qquad (2.5)$$

where $\psi = \psi_z$.

Along a boundary, Eqs. (2.4) are coupled in an involved manner by the equations which express the boundary conditions as functions of the potentials of the P and S waves. The least complicated problems involving a boundary concern the propagation of stress waves in a semi-infinite medium whose only boundary is the y = 0 plane. However, these problems are still difficult to solve by means of the harmonic wave method of Ewing, Jardetzky and Press [8], or by the particular Laplace transform approach that is generally referred to as Cagniard's method [7]. By contrast, if the self-similar† potential method of Smirnov and Sobolev [5,6] is used, the required

† See Sec. 2.2 for the definition of the term "self-similar."

P- and S-wave potentials can be determined almost directly from the equations for the boundary tractions or displacements on the y = 0 surface. This method is hardly described at all in the non-Russian literature, and its description in the Russian references, which are difficult to obtain, is somewhat less than satisfactory. Therefore, a motivation and derivation of the Smirnov-Sobolev method is given in the next section.

2.2. Self-Similar Solutions of the Two-Dimensional Wave Equations

Consider the class of wave propagation problems for the half plane $y \geq 0$ that are solved by "self-similar" potentials. A potential is said to be self-similar if for $t < 0$ its value is zero and for $t > 0$ its value is constant on any straight line passing through the origin of the x, y, t space. Thus, if φ and ψ are self-similar potentials, they must satisfy the equations

$$\begin{aligned} \varphi &= \psi = 0 \quad \text{for } t < 0 \\ \varphi &= \varphi(x/t, y/t) \quad \text{for } t > 0 \\ \psi &= \psi(x/t, y/t) \quad \text{for } t > 0 \end{aligned} \tag{2.6}$$

The condition of self-similarity means physically that the loading is applied initially at the origin. In the work that follows, solutions are obtained for a wide variety of problems of this type.

2.2.1. Determination of Self-Similar Potentials Associated with the Characteristic Surfaces of the Wave Equations

Each of Eqs. (2.3) can be written in the form

$$\left(\nabla^2 - \frac{1}{c^2}\frac{\partial^2}{\partial t^2}\right) \cdot g = 0 \tag{2.7}$$

with c and g replacing c_1 and φ, and c_2 and ψ, in the first and second of Eqs. (2.3), respectively. Obviously, any solution of Eq. (2.7) can be modified to give a solution of each of Eqs. (2.3).

The characteristic surfaces for Eq. (2.7) can be determined in the following manner [29]. Let any surface in the x, y, t space be denoted symbolically as $S = S(x,y,t) = 0$. A system of mutually orthogonal coordinates λ_1, λ_2, λ_3 is chosen such that λ_2 and λ_3 lie in the surface $S = 0$, and λ_1 is always directed normal to that surface. Along $S = 0$, the derivatives of g with respect to λ_2 and λ_3 are customarily referred to as interior derivatives while the derivatives of g with respect to λ_1 are referred to as exterior derivatives [29].

In terms of this new coordinate system, Eq. (2.7) has the form

$$\sum_{i=1}^{3}\sum_{j=1}^{3} a^{ij}\frac{\partial^2 g}{\partial\lambda_i\partial\lambda_j} + \sum_{i=1}^{3} a^{i}\frac{\partial g}{\partial\lambda_i} = 0 \qquad (2.8)$$

where $\lambda_i = \lambda_i(x,y,t)$ $\qquad i = 1,2,3$

and the a^{ij}'s and a^{i}'s are determined from the equations

$$\begin{aligned} a^{ij} &= \frac{\partial\lambda_i}{\partial x}\frac{\partial\lambda_j}{\partial x} + \frac{\partial\lambda_i}{\partial y}\frac{\partial\lambda_j}{\partial y} - \frac{1}{c^2}\frac{\partial\lambda_i}{\partial t}\frac{\partial\lambda_j}{\partial t} \\ a^{i} &= \frac{\partial^2\lambda_i}{\partial x^2} + \frac{\partial^2\lambda_i}{\partial y^2} - \frac{\partial^2\lambda_i}{\partial t^2} \qquad i,j = 1,2,3. \end{aligned} \qquad (2.9)$$

Let us assume that the values of g and $\partial g/\partial\lambda_1$ are specified at every point on $S = 0$. If the coefficient of the $\partial^2 g/\partial\lambda_1^2$ term in Eq. (2.8) is not zero, i.e., $a^{11} \neq 0$, this equation can be used to determine the value of $\partial^2 g/\partial\lambda_1^2$ at every point on $S = 0$. Then by taking successive derivatives

of Eq. (2.8) with respect to the exterior coordinate λ_1, all the higher order exterior derivatives of g can also be found. In this way, the value of g on S = 0 can be extended to fill the entire x, y, t space.

When $a^{11} = 0$ the surface S = 0 is called a characteristic surface. Along such a surface neither $\partial^2 g/\partial\lambda_1^2$ nor any higher order exterior derivative of g can be found. Consequently, these derivatives may have discontinuous values of any magnitude on a characteristic surface.

To determine the equation for the characteristic surface, set i = j = 1 and $a^{11} = 0$ in Eq. (2.9). Then the complete integral of the first order partial differential equation,

$$\left(\frac{\partial\lambda_1}{\partial x}\right)^2 + \left(\frac{\partial\lambda_1}{\partial y}\right)^2 - \frac{1}{c^2}\left(\frac{\partial\lambda_1}{\partial t}\right)^2 = 0 \tag{2.10}$$

defines the characteristic surfaces of Eq. (2.7). This integral† is

$$\lambda_1 = \alpha_o ct + \alpha_1 x + \alpha_2 y = K \tag{2.11}$$

where K is a constant and the α's are parameters which satisfy the equation

$$\alpha_o^2 = \alpha_1^2 + \alpha_2^2 \tag{2.12}$$

If the initial disturbance is concentrated at the origin of the $y \geq 0$ half space, it is only the characteristic surfaces through that point which are of interest. On these surfaces, K must be zero. Without loss of generality, Eq. (2.11) can then be simplified further by dividing through by $\alpha_o c$. The result is

---

† See Ref. [29], p. 199.

$$t + \frac{\alpha_1}{\alpha_o c} x + \frac{\alpha_2}{\alpha_o c} y = 0 \tag{2.13}$$

It is apparent from Eq. (2.13) that α_1/α_o can be expressed in terms of α_2/α_o, or α_2/α_o in terms of α_1/α_o. The latter of these is chosen since it yields the simpler form of Eq. (2.13) at points on the y = 0 surface where boundary conditions must be satisfied. Consequently, a convenient form of Eq. (2.13) is given by the equation

$$t - \theta x - y\sqrt{c^{-2}-\theta^2} = 0 \tag{2.14}$$

where $\theta = \dfrac{-\alpha_1}{\alpha_o c}$ and

$$\frac{\alpha_2}{\alpha_o c} = -\sqrt{c^{-2} - \theta^2}\ \dagger \tag{2.15}$$

The characteristic surfaces defined by Eq. (2.14) for values of θ in the range $-c^{-1} \leq \theta \leq c^{-1}$ are planes, each of which is tangent to the cone

$$c^2t^2 = x^2 + y^2 \tag{2.16}$$

It follows that each characteristic plane can be parameterized uniquely by the value of θ on its surface. For convenience, these surfaces are denoted symbolically by the equation $S(\theta) = 0$. The intersection of several of these surfaces and the t = 1 plane is shown schematically in Fig. 1.

---

† The negative sign is taken so that the results of the work which follows will agree with the results obtained by Smirnov and Sobolev [5], and by Kostrov [9]. The radical itself is specified as equal to $+c^{-1}$ at the origin and is analytic everywhere in the θ plane except across cuts outward along the real axis from $+c^{-1}$ and $-c^{-1}$.

Since the characteristic surfaces are planes, the λ_1, λ_2, λ_3 coordinate system can be taken as Cartesian. The a^i coefficients defined by the second of Eqs. (2.9) are then identically equal to zero. As a result, the only terms in Eq. (2.8) which have non-zero coefficients are those which are differentiated at least once with respect to λ_2 or λ_3. Because these coordinates lie in the characteristic surface, the wave equation will be satisfied identically by any function which has a constant value on each of these surfaces.

The quantity θ which has been introduced parametrizes each characteristic surface. Therefore, it would appear that θ or any sufficiently smooth function of θ solves the wave equation. This can be verified as follows. Assume that $f(\theta)$ has continuous first and second derivatives except at $t = 0$ where all the derivatives are necessarily discontinuous. Then the left-hand side of Eq. (2.7) can be rewritten as

$$\frac{d^2f(\theta)}{d\theta^2}\left[\left(\frac{\partial\theta}{\partial x}\right)^2 + \left(\frac{\partial\theta}{\partial y}\right)^2 - \frac{1}{c^2}\left(\frac{\partial\theta}{\partial t}\right)^2\right] + \frac{df(\theta)}{d(\theta)}\left[\left(\frac{\partial^2\theta}{\partial y^2}\right) + \left(\frac{\partial^2\theta}{\partial y^2}\right) - \frac{1}{c^2}\left(\frac{\partial^2\theta}{\partial t^2}\right)\right] \tag{2.17}$$

The various derivatives of θ can be found from Eq. (2.14). For convenience, a new variable δ is defined as follows:

$$\delta \equiv t - \theta x - y\sqrt{c^{-2} - \theta^2} = 0 \tag{2.18}$$

Then
$$\frac{\partial\theta}{\partial x} = -\frac{\partial\delta}{\partial x}\Big/\frac{\partial\delta}{\partial\theta} = \frac{\theta}{\delta'} \tag{2.19}$$

where
$$\delta' = \frac{\partial\delta}{\partial\theta} = -x + \frac{y\theta}{\sqrt{c^{-2} - \theta^2}} \tag{2.20}$$

and

$$\begin{aligned}\frac{\partial^2\theta}{\partial x^2} &= \frac{1}{\delta'}\frac{\partial\theta}{\partial x} - \frac{\theta}{(\delta')^2}\left[\frac{\partial\delta'}{\partial x} + \frac{\partial\delta'}{\partial\theta}\frac{\partial\theta}{\partial x}\right] \\ &= \frac{1}{\delta'}\left[\frac{\partial\theta}{\partial x} + \frac{\theta}{\delta'} - \frac{\theta}{\delta'}\frac{\partial\delta'}{\partial\theta}\frac{\partial\theta}{\partial x}\right] \\ &= \frac{1}{\delta'}\left[2\frac{\theta}{\delta'} - \frac{\partial\delta'}{\partial\theta}\cdot\frac{\theta^2}{\delta'^2}\right] \\ &= \frac{1}{\delta'}\cdot\frac{\partial}{\partial\theta}\left[\frac{\theta^2}{\delta'}\right]\end{aligned} \tag{2.21}$$

Thus, $\frac{\partial\theta}{\partial x} = \frac{\theta}{\delta'}$ and $\frac{\partial^2\theta}{\partial x^2} = \frac{1}{\delta'}\frac{\partial}{\partial\theta}\left[\frac{\theta^2}{\delta'}\right]$

In the same way it can be shown that

$$\begin{aligned}&\frac{\partial\theta}{\partial y} = \frac{\sqrt{c^{-2}-\theta^2}}{\delta'}\quad,\quad \frac{\partial^2\theta}{\partial y^2} = \frac{1}{\delta'}\frac{\partial}{\partial\theta}\left[\frac{c^{-2}-\theta^2}{\delta'}\right], \\ &\frac{\partial\theta}{\partial t} = -\frac{1}{\delta'}\quad,\ \text{and}\quad \frac{\partial^2\theta}{\partial t^2} = \frac{1}{\delta'}\frac{\partial}{\partial\theta}\left[\frac{1}{\delta'}\right].\end{aligned} \tag{2.22}$$

If these expressions are used to evaluate the quantities within the brackets of (2.17), the following results are obtained:

$$\left[\left(\frac{\partial\theta}{\partial x}\right)^2 + \left(\frac{\partial\theta}{\partial y}\right)^2 - \frac{1}{c^2}\left(\frac{\partial\theta}{\partial t}\right)^2\right] = \frac{1}{(\delta')^2}\left[\theta^2 + c^{-2} - \theta^2 - c^{-2}\right] = 0 \tag{2.23}$$

and

$$\left[\frac{\partial^2\theta}{\partial x^2} + \frac{\partial^2\theta}{\partial y^2} - \frac{1}{c^2}\frac{\partial^2\theta}{\partial t^2}\right] = \frac{1}{\delta'}\frac{\partial}{\partial\theta}\left[\frac{\theta^2 + c^{-2} - \theta^2 - c^{-2}}{\delta'}\right] = 0 \tag{2.24}$$

Since $\frac{d^2f(\theta)}{d\theta^2}$ and $\frac{df(\theta)}{d\theta}$ are finite everywhere, expression (2.17) is identically zero and we have verified that $f(\theta)$ satisfies the wave equation, i.e.

$$(\nabla^2 - \frac{1}{c^2}\frac{\partial^2}{\partial t^2})\, f(\theta) = 0 \qquad (2.25)$$

Nowhere in this verification was it necessary to consider that the point in question in the x, y, t space lay outside the cone, i.e. that θ satisfied the condition $|\theta| \leq c^{-1}$. It was only necessary that θ be defined by Eq. (2.18). Thus, it is possible to interpret Eq. (2.18) and the corresponding function $f(\theta)$ for points inside the cone.

Solving Eq. (2.18) for θ yields

$$\theta = \frac{xt}{r^2} \pm i\,\frac{y}{r^2}\sqrt{t^2 - r^2/c^2} \qquad (2.26)$$

where $r^2 = x^2 + y^2$ and $i = \sqrt{-1}$.

Except along the $y = 0$ surface θ has two possible complex values at each point inside the cone. Since these are merely conjugate pairs, one of them can be chosen arbitrarily. The following definition of θ is taken to conform with the definition used by Smirnov and Sobolev [5]:

$$\theta = \frac{xt}{r^2} + \frac{iy\sqrt{t^2 - r^2/c^2}}{r^2} \qquad (2.27)$$

The other possible value at each point is given by the equation

$$\bar{\theta} = \frac{xt}{r^2} - \frac{iy\sqrt{t^2 - r^2/c^2}}{r^2} \qquad (2.28)$$

Inside the cone, $f(\theta)$ and $f(\bar{\theta})$ are generally complex. Consequently, both the real and imaginary parts of these functions are real analytic functions of the variables x, y, and t. Furthermore, these analytic functions must be self-similar potentials which independently satisfy the wave equation.

It will be seen later that each constant value of θ outside the range $-c^{-1} < \theta < c^{-1}$ corresponds to a straight line which passes through the origin and lies entirely within the cone

$$c^2t^2 = x^2 + y^2 \tag{2.29}$$

The results of this section can be summarized as follows:

1) If θ is defined by Eq. (2.18), then any sufficiently smooth function of θ, $f(\theta)$, is a solution of the two-dimensional wave equation.
2) At points outside the cone, θ and $f(\theta)$ have constant values on planes which are tangent to the cone and fill the entire region of the x, y, t space outside the cone.
3) At points inside the cone, θ and $f(\theta)$ have constant values on every straight line through the origin.

It follows directly that the potentials $\Phi(\theta_1)$ and $\Psi(\theta_2)$ solve the first and second of Eqs. (2.4), respectively, if θ_i is defined implicitly by the equation

$$t - \theta_i x - y\sqrt{c_i^{-2} - \theta_i^2} = 0 \qquad i = 1,2. \tag{2.30}$$

2.3. The Completeness of the Self-Similar Solutions

The purpose of this section is to show that any self-similar solution of the two-dimensional wave equation can be written as a function of the parameter θ defined implicitly by Eq. (2.30). This may be proved as follows.

Since self-similar potentials are functions of the two independent variables x/t and y/t, there must always be a second system of coordinates

$$\begin{aligned} \eta_1 &= \eta_1\left(\frac{x}{t}\,,\,\frac{y}{t}\right) \\ \eta_2 &= \eta_2\left(\frac{x}{t}\,,\,\frac{y}{t}\right) \end{aligned} \tag{2.31}$$

such that the wave equation can be reduced to one of the following canonical forms:

$$\begin{aligned} \left(\frac{\partial^2}{\partial\eta_1^2} + \frac{\partial^2}{\partial\eta_2^2}\right) \cdot g(\eta_1,\eta_2) &= 0 \\ \left(\frac{\partial^2}{\partial\eta_1^2} - \frac{\partial^2}{\partial\eta_2^2}\right) \cdot g(\eta_1,\eta_2) &= 0 \end{aligned} \tag{2.32}$$

Equations (2.32) have general solutions of the form

$$\begin{aligned} g(\eta_1,\eta_2) &= g_1(\eta_1 + i\eta_2) + g_2(\eta_1 - i\eta_2) \\ \text{and} \qquad g(\eta_1,\eta_2) &= g_3(\eta_1 + \eta_2) + g_4(\eta_1 - \eta_2) \end{aligned} \tag{2.33}$$

respectively, where the gi's are arbitrary functions of their arguments.

The required transformation of coordinates, expressed symbolically by Eq. (2.31), has been derived by several authors, including Smirnov and Sobolev [5], and Ward [30].

At points inside the cone the transformation

$$\begin{aligned} \eta_1 &= \frac{xt}{r^2} \\ \eta_2 &= \frac{y\sqrt{t^2 - r^2/c^2}}{r^2} \end{aligned} \tag{2.34}$$

reduces the wave equation to the canonical form given by the first of Eqs. (2.33). Thus, the governing differential equation is elliptic in this region. At points outside the cone the transformation

$$\eta_1 = \frac{xt}{r^2}$$
$$\eta_2 = \frac{y\sqrt{r^2/c^2-t^2}}{r^2} = \frac{iy}{r^2}\sqrt{t^2-r^2/c^2} \tag{2.35}$$

reduces the wave equation to the second of Eqs. (2.33), and the governing equation is hyperbolic. Thus, the surface of the cone separates the regions in the x,y,t space in which the wave equation is hyperbolic (outside) and elliptic (inside). Outside the surface of the cone the radical $\sqrt{t^2-r^2/c^2}$ has an imaginary value, whereas inside the cone it is real-valued. As a result the arguments of each of Eqs. (2.33) can be written in the form

$$\frac{xt}{r^2} \pm \frac{iy\sqrt{t^2-r^2/c^2}}{r^2} \tag{2.36}$$

From Eq. (2.26) of the previous section it may be seen that the above functions are identical with the two possible values of θ which satisfy the equation

$$t - \theta x - y\sqrt{c^{-2} - \theta^2} = 0 \tag{2.37}$$

As a result, every self-similar solution of the two-dimensional wave equation is a function of one of the two possible values of θ which satisfy Eq. (2.25). Moreover, these functions are analytic at every point within the cone defined by Eq. (2.16).

The self-similar problems considered by Craggs in Refs. 15 and 18 were solved by a method which is equivalent to but s less direct than the method developed by Smirnov and Sobolev. Craggs first reduced the number of independent variables from three to two (in the manner described above) and then sought potentials of the same form as those of Eqs. (2.33) which would lead to the satisfaction of the boundary conditions. It will be seen in the work that follows that the solution of these problems can be obtained virtually by inspection with the aid of the method of Smirnov and Sobolev.

2.4. The Mapping of Points in the x,y,t Space into the Complex θ Plane

The variable $\theta(x/t, y/t)$, which is defined implicitly by the equation

$$t - \theta x - y\sqrt{c^{-2} - \theta^2} = 0 \tag{2.38}$$

maps every point in the x,y,t space into the complex θ plane. Solving Eq. (2.38) for θ gives

$$\theta = \frac{xt \pm y\sqrt{r^2/c^2 - t^2}}{r^2} = \frac{xt \pm iy\sqrt{t^2 - r^2/c^2}}{r^2} \tag{2.39}$$

where $r^2 = x^2 + y^2$.

At every point in the x,y,t space both values of θ given by Eq. (2.39) will satisfy Eq. (2.25). However, for self-similar disturbances induced by loads which act initially at the origin, the initial and boundary conditions can be satisfies if θ is defined as a single-valued function by the equations

$$\theta = \frac{xt + iy\sqrt{t^2 - r^2/c^2}}{r^2} \tag{2.40}$$

for points inside the cone and

$$\theta = \frac{xt - y\sqrt{r^2/c^2 - t^2}}{r^2} \quad , \quad x > 0$$
$$\theta = \frac{xt + y\sqrt{r^2/c^2 - t^2}}{r^2} \quad , \quad x < 0 \qquad (2.41)$$

for points outside the cone. The reason for defining θ in this fashion is discussed later.

Figures 2 and 3 show how points in the half space $y \geq 0$ are mapped into the upper half plane of θ. Within the cone, points on each straight line through the origin map into a single point in the θ plane. Specifically, lines that lie in the $y = 0$ surface are mapped into the real axis while those lines that are not in the $y = 0$ surface are mapped into points off the real axis. Typical examples of this mapping are the lines AO, BO, CO, DO, FO and GO in Figs. 2a and 3a, which map into the points A', B', C', D', F' and G', respectively, in Fig. 2b.

In the region of the x,y,t space outside the cone, θ has a constant value on the portion of each tangent plane which is bounded by the $y = 0$ surface and the line of tangency with the cone. It follows that every point in the bounded portion of each plane maps into a single point on the θ plane. Thus the bounded portions of the planes HOH° and JOJ° shown in Fig. 3b map, respectively, into the points H' and J' in the θ plane.

At points outside the cone, θ has been specified by Eq. (2.41) in anticipation of the solution of problems which involve disturbances propagating along the surface more rapidly than the P-waves or S-waves. These waves have plane fronts which are similar to the tangent planes HOH° and JOJ°, which are shown in Fig. 3b.

At points inside the cone, the way in which θ is specified uniquely merely determines whether points in the half space $y > 0$ map into the upper or lower half of the complex θ plane. Both definitions of θ lead to the same final results. The mapping defined by Eq. (2.40) takes points from the half space $y \geq 0$ into the half plane $\mathrm{Im}\theta \geq 0$.

In the previous section it was proved that a self-similar potential for a wave propagation problem must be an analytic function of θ at every point inside the cone except the origin. Since the region maps into and fills the entire region above the real θ axis, it follows that the potentials must be analytic functions everywhere in the half plane $\mathrm{Im}\theta > 0$, with the exception of the point at infinity which corresponds to the origin of the x,y,t space. Furthermore, the $y = 0$ surface, along which the boundary conditions must be satisfied, and the region outside the cone, which is initially free of disturbance, are both mapped into the real θ axis. Thus, the boundary and initial conditions in the x,y,t space simply become boundary conditions on the real θ axis of the half plane $\mathrm{Im}\theta > 0$. Standard mathematical techniques can then be used to determine the potential which satisfies the boundary conditions on the real axis and is analytic in the upper half plane with the exception of the points at infinity.

2.5. Determination of the Self-Similar Potentials

2.5.1. Preliminary Considerations

The determination of the self-similar potentials which solve† a particular wave propagation problem is simplified by the introduction of

† It is actually φ and ψ, the real parts of Φ and Ψ, respectively, which solve the problem.

complex-valued functions for the displacements and stresses. These functions of the independent variables x, y, and t are defined by the equations

$$u_x^* = \frac{\partial \Phi(\theta_1)}{\partial x} + \frac{\partial \Psi(\theta_2)}{\partial y}$$
$$u_y^* = \frac{\partial \Phi(\theta_1)}{\partial y} - \frac{\partial \Psi(\theta_2)}{\partial x} \qquad (2.42)$$

and

$$\sigma_x^* = \lambda \Delta^* + 2\mu \frac{\partial u_x^*}{\partial x}$$
$$\sigma_y^* = \lambda \Delta^* + 2\mu \frac{\partial u_y^*}{\partial y}$$
$$\tau_{xy}^* = \mu\left(\frac{\partial u_x^*}{\partial y} + \frac{\partial u_y^*}{\partial x}\right) \qquad (2.43)$$
$$\sigma_z^* = \lambda \Delta^*$$

where $$\Delta^* = \frac{\partial u_x^*}{\partial x} + \frac{\partial u_y^*}{\partial y} .$$

Since it is the real part of $\Phi(\theta_1)$ and $\Psi(\theta_2)$ which solve the problem, the actual displacements and stresses are given by the equations

$$u_x = \text{Re } u_x^* \qquad \sigma_x = \text{Re } \sigma_x^*$$
$$u_y = \text{Re } u_y^* \qquad \sigma_y = \text{Re } \sigma_y^* \qquad (2.44)$$
$$\sigma_z = \text{Re } \sigma_z^* \qquad \tau_{xy} = \text{Re } \tau_{xy}^*$$

Equations (2.42) and (2.43) can be simplified by means of Eqs. (2.21) and (2.22) which give expressions for the derivatives of self-similar functions. Equations (2.42) become

$$u_x^* = \Phi'(\theta_1) \cdot \frac{\theta_1}{\delta_1'} + \Psi'(\theta_2) \frac{\sqrt{c_2^{-2} - \theta_2^2}}{\delta'} \tag{2.45}$$

$$u_y^* = \Phi'(\theta_1) \cdot \frac{\sqrt{c_1^{-2} - \theta_1^2}}{\delta_1'} - \Psi'(\theta_2) \cdot \frac{\theta_2}{\delta_2'}$$

where $$\delta_i' = - x + y\theta_i \Big/ \sqrt{c_i^{-2} - \theta_i^2}\ , \qquad i = 1,2, \tag{2.46}$$

and $$\Phi'(\theta_1) = \frac{d\Phi(\theta_1)}{d\theta_1} \quad \text{and} \quad \Psi'(\theta_2) \cdot \frac{d\Psi(\theta_2)}{d\theta_2}\ .$$

In what follows, a and b will frequently be used in place of c_1 and c_2.

It can easily be verified that Eqs. (2.43) simplify to the following:

$$\frac{\sigma_y^*}{\mu} = \frac{\partial^2}{\partial t^2} \left\{ \int_0^{\theta_1} (b^{-2} - 2\theta^2)\Phi'(\theta)d\theta - \int_0^{\theta_2} 2\theta\sqrt{b^{-2} - \theta^2}\,\Psi'(\theta)d\theta \right\}$$

$$\frac{\sigma_x^*}{\mu} = \frac{\partial^2}{\partial t^2} \left\{ \int_0^{\theta_1} (b^{-2} + 2\theta^2 - 2\theta^{-2})\Phi'(\theta)d\theta + \int_0^{\theta_2} 2\theta\sqrt{b^{-2} - \theta^2}\,\Psi'(\theta)d\theta \right\}$$

$$= - \frac{\sigma_y^*}{\mu} + \frac{\partial^2}{\partial t^2} \left\{ \int_0^{\theta_1} 2(b^{-2} - a^{-2})\Phi'(\theta)d\theta \right\} \tag{2.47}$$

$$\frac{\tau_{xy}^*}{\mu} = \frac{\partial^2}{\partial t^2} \left\{ \int_0^{\theta_1} 2\theta\sqrt{a^{-2} - \theta^2}\,\Phi'(\theta)d\theta + \int_0^{\theta_2} (b^{-2} - 2\theta^2)\Psi'(\theta)d\theta \right\}$$

$$\frac{\sigma_z^*}{\mu} = \frac{\partial^2}{\partial t^2} \left\{ \int_0^{\theta_1} (b^{-2} - 2a^{-2})\Phi'(\theta)d\theta \right\}$$

where θ is a dummy variable in each integral.

From Eqs. (2.45) and (2.47), it can be seen that the stresses and displacements are expressed in terms of the first derivatives of the potentials rather than the potentials themselves. As a result, the problem is solved in terms of the first derivatives of the potentials and to avoid constant repetition these quantities will be referred to as potentials. This will never lead to ambiguity because $\Phi(\theta_1)$ and $\Psi(\theta_2)$ do not occur in any of the equations.

Since the potentials are homogeneous functions of degree zero, Eqs. (2.45) and (2.47) can only be satisfied by expressions for the displacements and stresses which are homogeneous functions of degree -1 and -2, respectively. That is,

$$\begin{aligned}
&\Phi'(kx,ky,kt) = \Phi'(x,y,t) \quad , \quad \Psi'(kx,ky,kt) = \Psi'(x,y,t) \\
&u_x(kx,ky,kt) = k^{-1}u_x(x,y,t) \quad , \quad u_y(kx,ky,kt = k^{-1}u_y(x,y,t) \\
&\sigma_x(kx,ky,kt) = k^{-2}\sigma_x(x,y,t) \\
&\sigma_y(kx,ky,kt) = k^{-2}\sigma_y(x,y,t) \\
&\sigma_z(kx,ky,kt) = k^{-2}\sigma_z(x,y,t) \\
&\tau_{xy}(kx,ky,kt) = k^{-2}\tau_{xy}(x,y,t)
\end{aligned} \tag{2.48}$$

The problem now is to determine the unique set of potentials, $\Phi'(\theta_1)$ and $\Psi'(\theta_2)$, which solve a wave propagation problem in the half space $y \geq 0$ when the specified boundary tractions satisfy conditions (2.48).

2.5.2. Expressing the Potentials as Functions of Self-Similar Tractions

On the surface $y = 0$, the parameters θ_1 and θ_2 are both equal to t/x. Consequently, for points on that surface, the first and third of Eqs. (2.47)

can be written as follows:

$$\frac{\sigma_y^*}{\mu} = \frac{\partial^2}{\partial t^2} \int_0^\theta \left\{ (b^{-2}-2\theta^2)\Phi'(\theta) - 2\theta \sqrt{b^{-2}-\theta^2}\, \Psi'(\theta) \right\} d\theta$$

$$\frac{\tau_{xy}^*}{\mu} = \frac{\partial^2}{\partial t^2} \int_0^\theta \left\{ 2\theta \sqrt{a^{-2}-\theta^2}\, \Psi'(\theta) + (b^{-2}-2\theta^2)\Psi'(\theta) \right\} d\theta \qquad (2.49)$$

where $\theta = t/x$, and σ_y^* and τ_{xy}^* are unknown complex-valued tractions related to the known tractions, σ_y and τ_{xy}, by the equations

$$\sigma_y = \text{Re}\ \sigma_y^*$$

$$\tau_{xy} = \text{Re}\ \tau_{xy}^* \qquad (2.50)$$

It is convenient to integrate Eqs. (2.49) twice with respect to time. This integration gives

$$\frac{\Sigma_y(\theta)}{\mu} = \int_0^\theta \left\{ (b^{-2}-2\theta^2)\Phi'(\theta) - 2\theta \sqrt{b^{-2}-\theta^2}\, \Psi'(\theta) \right\}$$

$$\frac{T_{xy}^*(\theta)}{\mu} = \int_0^\theta \left\{ 2\theta \sqrt{a^{-2}-\theta^2}\, \Phi'(\theta) + (b^{-2}-2\theta^2)\Psi'(\theta) \right. \qquad (2.51)$$

on $y = 0$, where Σ_y^* and T_{xy}^* are self-similar, complex-valued functions defined by the equations

$$\Sigma_y^*(\theta) = \int_0^t \int_0^{t_1} \sigma_y^*(x,0,t_o)\, dt_o\, dt_1 \qquad (2.52)$$

$$T^*_{xy}(\theta) = \int_0^t \int_0^{t_1} \tau^*_{xy}(x,0,t_o)dt_o dt_1$$

Integrating Eqs. (2.50) twice with respect to time gives

$$\begin{aligned} \Sigma_y &= \mathrm{Re}\ \overset{*}{y} \\ T_{xy} &= \mathrm{Re}\ T^*_{xy} \end{aligned} \tag{2.53}$$

where Σ_y and T_{xy} are self-similar, real-valued functions defined as follows:

$$\begin{aligned} \Sigma_y(\tfrac{t}{x}) &= \int_0^t \int_0^{t_1} \sigma_y(x,0,t_o)dt_o dt_1 \\ T_{xy}(\tfrac{t}{x}) &= \int_0^t \int_0^{t_1} \tau_{xy}(x,0,t_o)dt_o dt_1 \end{aligned} \tag{2.54}$$

It is convenient to consider that Σ_y and T_{xy} are fictitious tractions, and that Σ^*_y and T^*_{xy} are complex-valued fictitious tractions related to Σ_y and T_{xy} in the same way that σ^*_y and τ^*_{xy} are related to the actual tractions, σ_y and τ_{xy}. It will be shown later that Eqs. (2.53) and (2.54) and certain additional conditions determine uniquely the functions Σ^*_y and T^*_{xy}. Hence, the value of the potentials on the y = 0 surface can than be determined by solving Eqs. (2.51). The following result can easily be verified:

$$\Phi'(\theta) = \frac{1}{\mu} \frac{(b^{-2}-2\theta^2)\,\Sigma^{*\prime}_y + 2\theta\sqrt{b^{-2}-\theta^2}\,T^{*\prime}_{xy}}{R(\theta^2)} \tag{2.55}$$

$$\Psi'(\theta) = \frac{1}{\mu} \frac{-2\theta\sqrt{a^{-2}-\theta^2}\ \Sigma_y^{*'} + (b^{-2}-2\theta^2)T_{xy}^{*'}}{R(\theta^2)}$$

where $\Sigma_y^{*'}(\theta) = \frac{d\Sigma_y^{*}(\theta)}{d\theta}$, $T_{xy}^{*'}(\theta) = \frac{dT_{xy}^{*}(\theta)}{d\theta}$ and $R(\theta^2)$ is the Rayleigh function

$$R(\theta^2) = (b^{-2}-2\theta^2)^2 + 4\theta^2\sqrt{a^{-2}-\theta^2}\sqrt{b^{-2}-\theta^2} \tag{2.56}$$

It is not difficult to show that the Rayleigh function has only one zero in the θ^2 plane and that this zero lies on the real θ^2 axis to the right of b^{-2}. In the work that follows, c^{-2} is used to denote this zero. Consequently, $R(c^{-2}) = 0$ and $c^{-2} > b^{-2}$. The dependence of c^{-2} on the value of Poisson's ratio is shown graphically in Fig. 4.

Along the $y = 0$ surface, the potentials of Eq. (2.55) are determined uniquely by the first derivatives of Σ_y^* and T_{xy}^*. Since the $y = 0$ surface maps into the real axes of the θ_0 and θ_2 planes, $\Phi(\theta)$ and $\Psi'(\theta)$ must be the boundary values for Φ' and Ψ' in the θ_1 and θ_2 half planes, respectively. It will now be shown that the value of the potentials at points off the real θ_i ($i = 1,2$) axes† can be determined by substituting θ_1 and θ_2 for θ in the first and second of Eqs. (2.55), respectively. That is, the potentials are defined by the equations

$$\begin{aligned}
\Phi'(\theta_1) &= \frac{1}{\mu} \frac{(b^{-2}-2\theta_1^2)\ \Sigma_y^{*'}(\theta_1) + 2\theta_1\sqrt{b^{-2}-\theta_1^2}\ T_{xy}^{*'}(\theta_1)}{R(\theta_1^2)} \\
\Psi'(\theta_2) &= \frac{1}{\mu} \frac{-2\theta_2\sqrt{a^{-2}-\theta_2^{+2}}\ \Sigma_y^{*'}(\theta_2) + (b^{-2}-2\theta_2^2)T_{xy}^{*'}(\theta_2)}{R(\theta_2^2)}
\end{aligned} \tag{2.57}$$

† The notation θ_i will be used whenever a condition applies to both the θ_1 and θ_2 planes.

where θ_1 and θ_2 are the single-valued functions defined by Eqs. (2.30) of Sec. 2.2.1.

In Sec. 2.3, it was shown that, with the exception of points at infinity, the potentials which solve a wave propagation problem must be analytic functions everywhere in the half planes Im $\theta_i > 0$. These potentials must also be analytic at $\theta_i = 0$ since this point corresponds to the point at infinity in the x/t, y/t plane. These conditions will be satisfied by $\Phi'(\theta_1)$ and $\Psi'(\theta_2)$ of Eqs. (2.57) if, and only if, the functions $\Sigma_y^{*'}(\theta_i)$ and $T_{xy}^{*'}(\theta_i)$ are analytic at $\theta_i = 0$ and at all θ_i off the real axes, with the exception of the point at infinity. It follows that $\Phi'(\theta_i)$ and $\Psi'(\theta_2)$ will be possible solutions if there exist complex-valued fictitious tractions $\Sigma_y^*(\theta_i)$ and $T_{xy}^*(\theta_i)$ which satisfy Eqs. (2.53) on the boundary of the θ_i half-planes and are analytic at $\theta_i = 0$ and at every point off the axes, except at infinity.

The possibility of a singularity at infinity makes the boundary value problem difficult to solve in the θ_i half planes. However, the upper half of the x/t, y/t plane maps into the lower half of the $\eta_i = 1/\theta_i$ planes in such a way that the point at infinity in the former plane corresponds to the point at infinity in the η_i planes. Consequently, functions $\Sigma_y^o(\eta_i)$ and $T_{xy}^o(\eta_i)$, which are equal to $\Sigma_y^*(\theta_i)$ and $T_{xy}^*(\theta_i)$, respectively, must be analytic at infinity if only a finite region of the surface is loaded. Moreover, $\Sigma_y^o(\eta_i)$ and $T_{xy}^o(\eta_i)$ will be analytic at points off the real η_i axes because $\Sigma_y^*(\theta_i)$ and $T_{xy}^*(\theta_i)$ are analytic at points off the real axes, except at infinity. On the real η_i axes, the value of the real parts of $\Sigma_y^o(\eta_i)$ and $T_{xy}^o(\eta_i)$ can be obtained from Eqs. (2.53). Each of these functions is determined uniquely up to an imaginary constant by the conditions given above.†

† Since it is the derivatives of $\Sigma_y^*(\theta)$ and $T_{xy}^*(\theta)$ which are required in Eqs. (2.57), it is convenient to assume that the value of each of the imaginary constants is a zero.

Moreover, each function can be constructed without difficulty using the Cauchy integral theorem for the half plane.† The result is

$$\Sigma_y^*(\theta_i) = \Sigma_y^o(\eta_i) = -\frac{1}{i\pi}\int_{-\infty}^{\infty} \frac{\Sigma_y(\xi/t)}{\xi/t - \eta_i}\, d(\frac{\xi}{t}) = -\frac{1}{i\pi}\int_{-\infty}^{\infty} \frac{\Sigma_y(\xi,t)}{\xi - x}\, d\xi$$

$$T_{xy}^*(\theta_i) = T_{xy}^o(\eta_i) = -\frac{1}{i\pi}\int_{-\infty}^{\infty} \frac{T_{xy}(\xi/t)}{\xi/t - 1/\theta_i}\, d(\frac{\xi}{t}) \tag{2.58}$$

$$= -\frac{1}{i\pi}\int_{-\infty}^{\infty} \frac{T_{xy}(\xi,t)}{\xi - x}\, d\xi$$

With Σ_y^* and T_{xy}^* constructed in this fashion, Eqs. (2.57) define potentials which are possible solutions of the problem in question. The uniqueness of these solutions can be proven as follows.

Suppose there exist a second set of potentials $\Phi_2'(\theta_1)$ and $\Psi_2'(\theta_2)$ which are analytic everywhere off the real θ_i axes except at infinity. If the above potentials are equal to $\Phi'(\theta)$ and $\Psi'(\theta)$ on the real axes then the functions defined by the differences $\Phi_2'(\theta_1) - \Phi'(\theta_1)$ and $\Psi_2'(\theta_2) - \Psi'(\theta_2)$ are both identically zero on the axes. Consequently, these functions are analytic everywhere except at infinity. Since the only analytic function which is zero along a line is zero itself,†† it follows that

$$\Phi_2'(\theta_1) = \Phi'(\theta_1)$$
$$\Psi_2'(\theta_2) = \Psi'(\theta_2) \tag{2.59}$$

---

† The form of the Cauchy integral theorem used here can be obtained directly from the results presented in Ref. [31] page 251.

†† This is the identity theorem [32].

and Eqs. (2.57) define uniquely the potentials which solve the problem being considered.

The results of this section can be summarized as follows. For any problem in which the tractions are homogeneous functions of degree -2,† a unique pair of functions Σ_y^* and T_{xy}^* can be found from Eqs. (2.54) and (2.58). Substituting the derivatives of these functions into Eqs. (2.57) gives the required potentials for the problem in question.

With the potentials known, the displacements and stresses can be calculated directly from Eqs. (2.45) and (2.47). The problem is then completely solved.

The method that has been used to obtain these potentials can easily be extended to problems involving loads acting at the interior of a multi-layered or homogeneous elastic medium. For the homogeneous medium the same results could be obtained by means of the Kelvin solution [1].

2.6. A Line of Impulses on the Surface of a Half Space††

In the previous section it was shown that each pair of self-similar P- and S-wave displacement potentials solves a problem in which the tractions on the boundary are homogeneous functions of degree -2. It follows then from Eq. (2.48) that the fictitious tractions for these problems are necessarily homogeneous functions of degree zero.

---

† The results of this section are generalized in Sec. 2.8 with the result that any problem with homogeneous boundary conditions can be solved by self-similar potentials.

†† This problem was solved initially by Lamb using the method of Laplace transforms [10]. Later, Smirnov and Sobolev solved this problem using self-similar potentials.

Let us now determine the problem that is solved if the fictitious normal and tangential tractions satisfy the following very simple equations:

$$\begin{aligned} \Sigma_y &= -\frac{I_v}{2\alpha} && \text{for } |x| \leq \alpha t \\ &= 0 && \text{for } |x| > \alpha t \\ T_{xy} &= 0 && \text{for all } x\ , \end{aligned} \tag{2.60}$$

where I_v is a constant with units of lb-sec/in. Since Σ_y acts over the expanding region $-\alpha t \leq x \leq +\alpha t$, the resultant of this fictitious traction is a fictitious load of magnitude $I_v \cdot t$. This load acts vertically downward at the origin and is independent of the value of α. Since the actual boundary tractions and loads are the second time derivatives of their respective fictitious counterparts, it follows that, in the limit as α tends to zero, Eq. (2.60) defines the fictitious traction for a problem in which an impulse of magnitude I_v acts vertically downward at the origin at time $t = 0$.

2.6.1. The Potentials for Vertical and Horizontal Impulses

It is now a simple matter to determine the potentials for this problem. If the values of Σ_y and T_{xy} given by Eq. (2.60) are substituted into Eq. (2.58) and the required integration carried out, the following expressions for the self-similar complex-valued tractions are obtained:

$$\begin{aligned} \Sigma_y^*(\theta_i) &= -\frac{I_v}{2\alpha i\pi} \log \frac{1 + \alpha\theta_i}{1 - \alpha\theta_i} \\ T_{xy}^*(\theta_i) &= 0 \qquad\qquad i = 1,2. \end{aligned} \tag{2.61}$$

It can easily be verified that $\Sigma_y = \text{Re}\ \Sigma_y^*$ for all real values of θ_i.

In the limit as α tends to zero the above equations reduce to the following:

$$\begin{aligned} \Sigma_y^*(\theta_i) &= -\frac{I_v}{i\pi}\theta_i \\ T_{xy}^*(\theta_i) &= 0 \qquad\qquad i = 1,2. \end{aligned} \tag{2.62}$$

Therefore,

$$\Sigma_y^{*'}(\theta_i) = -\frac{I_v}{i\pi} \quad , \quad T_{xy}^{*'}(\theta_i) = 0 \tag{2.63}$$

Direct substitution of these results into Eq. (2.57) yields

$$\begin{aligned} \Phi'(\theta_i) &= -\frac{(b^{-2}-2\theta_1^2)}{R(\theta_1^2)}\,\frac{I_v}{i\pi\mu} \\ \Psi'(\theta_2) &= \frac{2\theta_2\sqrt{a^{-2}-\theta_2^2}}{R(\theta_2^2)}\,\frac{I_v}{i\pi\mu} \end{aligned} \tag{2.64}$$

Equations (2.64) define the self-similar potentials which solve the problem of an impulse of magnitude I_v acting vertically downward at the origin at time $t = 0$. The use of a limiting process to solve this problem ensures that the potentials defined by Eq. (2.64) have no component which corresponds to a self-equilibrating stress singularity at any point in the x,y,t space.

For the problem in which an impulse of magnitude I_h acts horizontally in the positive x direction, an almost identical procedure leads to the potentials

$$\Phi'(\theta_1) = \frac{2\theta_1\sqrt{b^{-2}-\theta_1^2}}{R(\theta_1^2)} \cdot \frac{I_v}{i\pi\mu} \tag{2.65}$$

$$\Psi'(\theta_2) = \frac{(b^{-2}-2\theta_2^2)}{R(\theta_2^2)} \cdot \frac{I_h}{i\pi\mu}$$

2.6.2. The Displacement Field for a Vertical Impulse

The equations which define the displacements at any point are found by taking the real part of the expressions obtained when the potentials of Eqs. (2.64) are substituted in Eqs. (2.45). The result is

$$u_x = \mathrm{Re}\left\{\frac{I_v}{i\mu\pi}\left[-\frac{(b^{-2}-2\theta_1^2)\theta_1}{R(\theta_1^2)\delta_1'} + \frac{2\theta_2\sqrt{a^{-2}-\theta_2^2}\sqrt{b^{-2}-\theta_2^2}}{R(\theta_2^2)\delta_2'}\right]\right\}$$

$$u_y = \mathrm{Re}\left\{\frac{I_v}{i\mu\pi}\left[-\frac{(b^{-2}-2\theta_1^2)\sqrt{a^{-2}-\theta_1^2}}{R(\theta_1^2)\delta_1'} - \frac{2\theta_2^2\sqrt{a^{-2}-\theta_2^2}}{R(\theta_2^2)\delta_2'}\right]\right\} \qquad (2.66)$$

where $$\delta_i' = -x + \frac{y\theta_i}{\sqrt{c_i^{-2}-\theta_i^2}} = \frac{i\sqrt{t^2-r^2c_i^{-2}}}{\sqrt{c_i^{-2}-\theta_i^2}} \quad \text{and} \quad r^2 = x^2+y^2 \qquad (2.67)$$

On the y = 0 surface these equations simplify to the following:

$$u_x = \mathrm{Re}\left\{\frac{I_v}{\mu i\pi}\left[\frac{(b^{-2}-2\theta^2)\theta - 2\theta\sqrt{a^{-2}-\theta^2}\sqrt{b^{-2}-\theta^2}}{xR(\theta^2)}\right]\right\}$$

$$u_y = \mathrm{Re}\left\{\frac{I_v}{\mu i\pi}\left[-\frac{b^{-2}\sqrt{a^{-2}-\theta^2}}{xR(\theta^2)}\right]\right\} \qquad (2.68)$$

where $\theta = t/x$.

These equations are equivalent to those obtained by Lamb [10].

For $t > 0$ the displacements are finite and continuous except

(a) at the fronts of the P and S waves where the term $t^2 - r^2c_i^{-2}$ is zero, and

(b) on the $y = 0$ surface at the two positions of the surface wave. At these locations u_x and u_y are unbounded since $R(c^{-2}) = 0$.

A further investigation of Eqs. (2.66) reveals that the irrotational component of the displacement field is zero, as expected, beyond the front of the P wave. However, the equivoluminal component of this field is zero only in the portion of the x,y,t space which maps into the $-a^{-1} \leq \theta_2 \leq a^{-1}$ segment of the real θ_2 axis. The portion of the x,y,t space which maps into the $a^{-1} \leq |\theta_2| \leq b^{-1}$ segments of the real θ_2 axis is bounded by the $y = 0$ surface, the front of the S wave, and the planes along which $|\theta_2| = a^{-1}$.† The equivoluminal component of the displacement field in these regions is customarily referred to as the head wave component.

The head wave disturbances can be thought of as the equivoluminal disturbances which result from the interaction of the front of the P wave and the free surface of the half space. It will be seen in the work that follows that head wave disturbances occur whenever there is no constraint on the displacements of the surface of the half space near the front of the P wave.

2.6.2.1. Displacements Behind the Wave Fronts

It is apparent from Eqs. (2.66) and (2.67) that the P and S wave components of the displacement vary as $(t - rc_i^{-1})^{1/2}$ just behind their respective wave fronts. At points a greater distance behind these fronts, the displacements are finite and continuous.

---

† The mapping of the x,y,t space into the complex θ plane was described in Sec. 2.4.

If a head wave passes through the point being considered, it will do so before the arrival of the S wave. By expanding Eq. (2.66) asymptotically about $\theta_2 = a^{-1}$, it can easily be verified that the equivoluminal component of the displacement at a point just behind this front varies as the square root of the distance between the front and the point in question. That is, these displacements vary in the same way as the imaginary part of the radical $\sqrt{a^{-1} - \theta_2}$.

2.6.2.2. Surface Wave Displacements

The singular displacements near the surface waves are obtained from the asymptotic expansion of Eq. (2.66) about the points $\theta = \pm c^{-1}$. The way in which these displacements vary along the surface has previously been studied by Lamb [10]. In this study the variation at points beneath the $y = 0$ surface is also considered.

Near $\theta = c^{-1}$, the asymptotic expansions of Eqs. (2.66) have the following form:

$$u_x \simeq \mathrm{Re}\left\{\frac{I_v}{i\mu\pi}\left[\frac{C_0}{t(\theta_1-c^{-1})} + \frac{C_1}{t(\theta_2-c^{-1})} + \frac{C_2}{t} + \frac{C_3}{t}(\theta_1-c^{-1}) + \frac{C_4}{t}(\theta_2-c^{-1}) + \ldots\right]\right\}$$

$$u_y \simeq \mathrm{Re}\left\{\frac{I_v}{\mu\pi}\left[\frac{D_0}{t(\theta_1-c^{-1})} + \frac{D_1}{t(\theta_2-c^{-1})} + \frac{D_2}{t} + \frac{D_3}{t}(\theta_1-c^{-1}) + \frac{D_4}{t}(\theta_2-c^{-1}) + \ldots\right]\right\} \tag{2.69}$$

where

$$C_0 = - \frac{c^{-2}(b^{-2} - 2c^{-2})}{R'(c^{-2})}$$

$$C_1 = - \frac{2\sqrt{c^{-2} - a^{-2}}\; c^{-2} \sqrt{c^{-2} - b^{-2}}}{R'(c^{-2})}$$

$$D_0 = \frac{c(b^{-2} - 2c^{-2}) \sqrt{c^{-2} - a^{-2}}}{R'(c^{-2})}$$

$$D_1 = \frac{2c^{-2} \sqrt{c^{-2} - a^{-2}}}{R'(c^{-2})}$$

$$R'(c^{-2}) = \left. \frac{dR(\theta^2)}{d\theta} \right|_{\theta = c^{-1}}$$

and the remaining C's and D's are real-valued constants.

In each of Eqs. (2.69), the first two terms combine to give a displacement which is singular at $\theta = c^{-1}$. These displacements are referred to as the surface wave displacements. The remaining terms in the expansion give a non-singular displacement, the magnitude of which falls off as t^{-1}. Consequently, at a considerable distance from the origin only the surface wave disturbances are significant for points which are on or near the $y = 0$ surface. The patterns of these displacements are found in the following way.

At any given time $t = x_0/c$, the linear approximation of the term $\theta_i - c^{-1}$ near $x_0 = ct$ has the form

$$\theta_i - c^{-1} \simeq - \frac{\xi}{t} c^{-2} + \frac{iy}{t} c^{-1} \sqrt{c^{-2} - c_i^{-2}} \qquad (2.70)$$

where $\xi = x - x_0$. Substituting this result in Eqs. (2.69) yields the following expressions for the surface wave displacements:

$$u_x \simeq \left\{\frac{I_v}{i\mu\pi}\left[\frac{C_0}{-c^{-2}\xi+iyc^{-1}\sqrt{c^{-2}-a^{-2}}}+\frac{C_1}{-c^{-2}\xi+iyc^{-1}\sqrt{c^{-2}-b^{-2}}}\right]\right\}$$

$$u_y \simeq \left\{\frac{I_v}{\mu\pi}\left[\frac{D_0}{-c^{-2}\xi+iyc^{-1}\sqrt{c^{-2}-a^{-2}}}+\frac{D_1}{-c^{-2}\xi+iyc^{-1}\sqrt{c^{-2}-b^{-2}}}\right]\right\} \qquad (2.71)$$

It is apparent from Eqs. (2.71) that the surface wave displacements propagate in a manner which is independent of time. It is also apparent that the magnitude of these displacements at points on a x/y = constant plane through $x_0 = ct$ ($\theta = c^{-1}$) varies inversely as the distance away from the surface wave. The variation of the surface wave displacements along different y = constant planes is shown in Fig. 5, where the curves have been non-dimensionalized by plotting

$$\frac{u_x\left(\frac{\xi}{\epsilon}, \frac{y}{\epsilon}\right)}{u_x(0.0,0.1)} \quad \text{and} \quad \frac{u_y\left(\frac{\xi}{\epsilon}, \frac{y}{\epsilon}\right)}{u_x(0.0,0.1)} \quad \text{vs} \quad \frac{\xi}{\epsilon} \ .$$

2.6.2.3. Displacements on the Surface of the Half Space

At points on the y = 0 surface between the shear and dilatation waves, both u_x and u_y are finite and continuous. Inside the S wave the horizontal displacement is zero on y = 0 except at $\theta = \pm c^{-1}$, where the singular character is given by the first of Eqs. (2.68).

The vertical displacement on y = 0 varies continuously except near the surface waves. At the origin u_y varies inversely with time. At time zero this displacement is infinite as would be expected for an impulsive force concentrated at a single point.

For an actual force which must be distributed continuously over time and space, there will be no singularities in either the displacement field or the stress field.

2.6.3. The Stress Field for a Vertical Impulse

For a vertical impulse I_v, the stresses at any point are defined by the following equations:

$$\sigma_x = \mathrm{Re}\,\frac{\partial}{\partial t}\left\{\frac{I_v}{i\pi}\left(\frac{(b^{-2}-2\theta_1^2)(b^{-2}-2a^{-2}+2\theta_1^2)}{R(\theta_1^2)\delta_1'} - \frac{4\theta_2^2\sqrt{a^{-2}-\theta_2^2}\sqrt{b^{-2}-\theta_2^2}}{R(\theta_2^2)\cdot\delta_2'}\right)\right\}$$

$$\sigma_y = \mathrm{Re}\,\frac{\partial}{\partial t}\left\{\frac{I_v}{i\pi}\left(\frac{(b^{-2}-2\theta_1^2)^2}{R(\theta_1^2)\delta_1'} + \frac{4\theta_2^2\sqrt{a^{-2}-\theta_2^2}\sqrt{b^{-2}-\theta_2^2}}{R(\theta_2^2)\delta_2'}\right)\right\} \qquad (2.72)$$

$$\tau_{xy} = \mathrm{Re}\,\frac{\partial}{\partial t}\left\{\frac{I_v}{i\pi}\left(\frac{2\theta_1\sqrt{a^{-2}-\theta_1^2}(b^{-2}-2\theta_1^2)}{R(\theta_1^2)\delta_1'} - \frac{2\theta_2\sqrt{a^{-2}-\theta_2^2}(b^{-2}-2\theta_2^2)}{R(\theta_1^2)\delta_2'}\right)\right\}$$

$$\sigma_z = \mathrm{Re}\,\frac{\partial}{\partial t}\left\{\frac{I_v}{i\pi}\left(\frac{(b^{-2}-2a^{-2})(b^{-2}-2\theta_1^2)}{R(\theta_1^2)\delta_1'}\right)\right\}$$

where δ_i' is defined by Eq. (2.67).

2.6.3.1. Stresses Behind the Wave Fronts

The behavior of the stresses immediately behind the wave fronts can be determined by expanding Eqs. (2.72) asymptotically in these regions. The most rapidly varying portion of each stress near these wave fronts is given by the first term of the expansion. Each of these terms can be found directly from Eqs. (2.72).

Behind the P-wave front

$$\sigma_x \simeq \mathrm{Re}\;\frac{I_v}{\pi}\left(\frac{\sqrt{a^{-2}-\theta_0^2}(b^{-2}-2\theta_0^2)(b^{-2}-2a^{-2}+2\theta_0^2)}{R(\theta_0^2)}\cdot\frac{t}{(t^2-r^2a^{-2})^{3/2}}\right)$$

$$\sigma_y \simeq \mathrm{Re}\ \frac{I_v}{\pi}\left(\frac{(b^{-2}-2\theta_0^2)^2\sqrt{a^{-2}-\theta_0^2}}{R(\theta_0^2)}\cdot\frac{t}{(t^2-r^2a^{-2})^{3/2}}\right)$$

$$\sigma_z \simeq \mathrm{Re}\ \frac{I_v}{\pi}\left(\frac{(b^{-2}-2\theta_0^2)(b^{-2}-2a^{-2})\sqrt{a^{-2}-\theta_0^2}}{R(\theta_0^2)}\cdot\frac{t}{(t^2-r^2a^{-2})^{3/2}}\right) \qquad (2.73)$$

$$\tau_{xy} \simeq \mathrm{Re}\ \frac{I_v}{\pi}\left(\frac{2\theta_0(a^{-2}-\theta_0^2)(b^{-2}-2\theta_0^2)}{R(\theta_0^2)}\cdot\frac{t}{(t^2-r^2a^{-2})^{3/2}}\right)$$

where $\theta_0 = \frac{x}{r}\,a^{-1}$.

Behind the S-wave front

$$\sigma_x \simeq \mathrm{Re}\left\{\frac{I_v}{i\pi}\left(\frac{4\theta_0^2\sqrt{a^{-2}-\theta_0^2}\,(b^{-2}-\theta_0^2)}{R(\theta_0^2)}\cdot\frac{t}{(t^2-r^2b^{-2})^{3/2}}\right)\right\}$$

$$\sigma_y \simeq -\sigma_x \qquad (2.74)$$

$$\tau_{xy} \simeq -\mathrm{Re}\ \frac{I_v}{\pi}\left(\frac{2\theta_0\sqrt{b^{-2}-\theta_0^2}\sqrt{a^{-2}-\theta_0^2}\,(b^{-2}-2\theta_0^2)}{R(\theta_0^2)}\ \frac{t}{(t^2-r^2b^{-2})^{3/2}}\right)$$

where $\theta_0 = \frac{x}{r}\,b^{-1}$. Since there is no S-wave component of σ_z, this stress varies smoothly across the front of the S wave.

The second term in the expansion of Eqs. (2.72) gives stresses which vary as $(t - rc_i^{-1})^{1/2}$. The coefficients of these terms can be calculated straightforwardly.

It is not difficult to show that the S-wave components of the stresses behind the front of the head wave vary as the inverse of the square root of the distance behind this front.

2.6.3.2. Surface Wave Stresses

In order to determine the stresses near the position of the surface waves, Eqs. (2.72) are expanded asymptotically about either of the points $\theta = \pm c^{-1}(x_0 = \pm ct)$. Expanding the first of these equations about $\theta = c^{-1}$ results in the following series approximation of

$$\sigma_x \simeq \mathrm{Re}\left\{\frac{I_v}{i\pi}\left[\frac{A_{11}}{x_0^2(\theta_1-c^{-1})^2}+\frac{A_{12}}{x_0^2(\theta_2-c^{-1})^2}+\frac{B_{10}}{x_0^2}+\frac{B_{11}(\theta_1-c^{-1})}{x_0^2}+\frac{B_{12}(\theta_2-c^{-1})}{x_0^2}\right]\right\} \tag{2.75}$$

where $$A_{11} = \frac{(b^{-2}-2c^{-2})(b^{-2}-2a^{-2}+2c^{-2})}{c^2R'(c^{-2})}$$

$$A_{12} = -\frac{4c^{-2}\sqrt{c^{-2}-a^{-2}}\sqrt{c^{-2}-b^{-2}}}{c^2R'(c^{-2})}$$

and $$R'(c^{-2}) = \left.\frac{dR}{d\theta}\right|_{\theta=c^{-1}}$$

and the B's are all real-valued constants. The first pair of terms in each series define stresses that are singular at the position of the surface wave. These are the surface wave stresses. The remaining terms in each series are finite and can be neglected at large distances from the origin since the singular terms dominate near $\theta = c^{-1}$.

If Eq. (2.40) is used to express $\theta_i = c^{-1}$ as a function of the distance from the point $x_0 = ct$, then Eq. (2.75) can be rewritten in the form

$$\sigma_x \simeq \mathrm{Re}\left\{\frac{I_v}{i\pi}\left[\frac{A_{11}}{[-c^{-1}\xi+iy\sqrt{c^{-2}-a^{-2}}]^2}+\frac{A_{12}}{[-c^{-1}\xi+iy\sqrt{c^{-2}-b^{-2}}]^2}\right]\right\} \tag{2.76}$$

The surface wave components of the remaining stresses are computed in a similar manner. The results are

$$\begin{aligned}
\sigma_y &\simeq \mathrm{Re}\left\{\frac{I_v}{i\pi}\left[\frac{A_{21}}{[-c^{-1}\xi+iy\sqrt{c^{-2}-a^{-2}}]^2}+\frac{A_{22}}{[-c^{-1}\xi+iy\sqrt{c^{-2}-b^{-2}}]^2}\right]\right\} \\
\tau_{xy} &\simeq \mathrm{Re}\left\{\frac{I_v}{\pi}\left[\frac{A_{31}}{[-c^{-1}\xi+iy\sqrt{c^{-2}-a^{-2}}]^2}+\frac{A_{32}}{[-c^{-1}\xi+iy\sqrt{c^{-2}-b^{-2}}]^2}\right]\right\} \\
\sigma_z &\simeq \mathrm{Re}\left\{\frac{I_v}{i\pi}\frac{A_{41}}{[-c^{-1}\xi+iy\sqrt{c^{-2}-a^{-2}}]^2}\right\}
\end{aligned} \tag{2.77}$$

where

$$A_{21} = \frac{(b^{-2}-2c^{-2})^2}{c^2R'(c^{-2})} \qquad A_{22} = -A_{12}$$

$$A_{31} = -A_{32} = \frac{-2c^{-1}\sqrt{c^{-2}-a^{-2}}\,(b^{-2}-2c^{-2})}{c^2R'(c^{-2})}$$

$$A_{41} = \frac{(b^{-2}-2c^{-2})(b^{-2}-2a^{-2})}{c^2R'(c^{-2})}$$

The surface wave stresses propagate in a manner which is independent of time. Moreover, these stresses vary inversely as the square of the distance away from the surface wave along any x/y = constant plane through $x_0 = ct$ ($\theta = c^{-1}$).

The variation of these stresses along different y = constant planes is shown in Figs. 6 and 7. These curves have been non-dimensionalized by plotting

$$\frac{\sigma_x(\frac{\xi}{\epsilon}, \frac{y}{\epsilon})}{\tau_{xy}(0.0,0.1)} \quad , \quad \frac{\sigma_y(\frac{\xi}{\epsilon}, \frac{y}{\epsilon})}{\tau_{xy}(0.0,0.1)} \quad , \quad \frac{\sigma_z(\frac{\xi}{\epsilon}, \frac{y}{\epsilon})}{\tau_{xy}(0.0,0.1)} \quad ,$$

$$\text{and} \quad \frac{\tau_{xy}(\frac{\xi}{\epsilon}, \frac{y}{\epsilon})}{\tau_{xy}(0.0,0.1)} \quad \text{vs} \quad \frac{\xi}{\epsilon}$$

2.6.3.3. Stresses on the Surface of the Half Space

It is apparent from Eqs. (2.72) that σ_y and τ_{xy} are zero everywhere on the surface of the half space. Furthermore, these stresses are very small at points just below the surface except near the surface wave where their variation has already been studied.

On the $y = 0$ surface, σ_x has a non-zero value only in the region between the P and S waves. Inside the S wave the value of σ_x is zero on the surface and small at points just below the surface except in the region of the surface wave. The variation in this region was considered in the previous section.

To summarize, the stresses and displacements are continuous and finite except at the wave fronts and the two locations of the surface wave. Furthermore, at every point the stresses and displacements are homogeneous functions of degree -2 and -1 respectively.

2.7. Line Loads in an Infinite Medium

The method of self-similar solutions used in previous sections to solve half space problems can also be applied to problems involving line disturbances in an infinite, linearly elastic, homogeneous body.† To illustrate

† An alternate method of solving these problems involves the straightforward superposition of the Kelvin solution of the problem in which a time dependent load acts at a point in an infinite body. This solution is given in Ref. [1], page 304.

how this is done, consider the problem shown in Fig. 8 where a concentrated load P(t) acts vertically downward at the point x = 0, y = 0. As in previous sections, the load is assumed to act initially at t = 0. From considerations of symmetry we note the following:

$$\begin{aligned} u_x(x,0,t) &= 0 \qquad \text{for all } x \\ \sigma_y(x,0,t) &= 0 \qquad \text{for all } x \neq 0. \end{aligned} \tag{2.78}$$

It follows that the problem defined above is equivalent to the problem (see Fig. 8) in which a $y \geq 0$ half space with boundary conditions

$$\begin{aligned} \sigma_y(x,0,t) &= -\frac{P(t)}{2}\,\delta(x) \\ u_x(x,0,t) &= 0 \end{aligned} \tag{2.79}$$

is placed directly above a $y \leq 0$ half space with the boundary conditions

$$\begin{aligned} \sigma_y(x,0,t) &= \frac{P(t)}{2}\,\delta(x) \\ u_x(x,0,t) &= 0 \end{aligned} \tag{2.80}$$

It can easily be verified that these half space problems have the same shear and vertical displacement on the y = 0 surface. Consequently, the disturbance in the infinite body caused by the load P(t) can be determined by solving the half space problems defined by Eqs. (2.79) and (2.80).

2.7.1. A Line of Impulses in an Infinite Medium

The potentials which solve the two-dimensional problem in which an impulse of magnitude I_v acts vertically downward at the origin of the x,y,t space and found by solving the half space problems with the following boundary conditions:

for the $y \geq 0$ half space

$$\int_0^t \sigma_y(x,0,\tau)d\tau = -\frac{I_v}{2}\delta(x) \qquad (2.81)$$

$$u_x(x,0,t) = 0$$

and for the $y \leq 0$ half space

$$\int_0^t \sigma_y(x,0,\tau)d\tau = \frac{I_v}{2}\delta(x) \qquad (2.82)$$

$$u_x(x,0,t) = 0$$

The potentials which solve these half space problems can be determined in much the same manner as were the potentials which solve the vertical impulse problem of Sec. 2.6.1.

As in Sec. 2.6.1, the first of Eqs. (2.81) requires that

$$-\frac{I_v}{2i\mu\pi} = (b^{-2}-2\theta^2)\Phi'(\theta) - 2\theta\sqrt{b^{-2}-\theta^2}\,\Psi'(\theta) \quad \text{for} \quad y = 0. \qquad (2.83)$$

For the second of Eqs. (2.81) to be satisfied (rather than the condition that the surface of the half space be free of shear) the following equation must also be satisfied by the boundary values of the unknown potentials:

$$0 = \theta\Phi'(\theta) + (b^{-2}-\theta^2)^{1/2}\Psi'(\theta) \qquad \text{for } y = 0. \qquad (2.84)$$

It follows as in Sec. 2.5.2 that

$$\Phi' = \frac{-I_v b^2}{2i\mu\pi} \quad , \quad \Psi' = \frac{\theta_2 I_v b^2}{2i\mu\pi\sqrt{b^{-2}-\theta_2^2}} \qquad (2.85)$$

If a cut is made between $-c_i^{-1}$ and c_i^{-1} in each θ_i plane in order that the radical $\sqrt{c_i^{-2}-\theta_i^2}$ be single-valued at every point,† the potentials defined by Eq. (2.85) will also solve the $y \leq 0$ half space problem whose boundary conditions are defined by Eq. (2.81).

The stresses and displacements at any point in the infinite medium can be computed directly from Eqs. (2.44), (2.45) and (2.47).

In dealing with arbitrary loads it is convenient to have potentials corresponding to a line impulse of magnitude I_h acting in the positive x direction at the origin of the x,y,t space. These potentials are

$$\Phi'(\theta_1) = \frac{-\theta_1 I_h b^2}{2\mu i\pi\sqrt{a^{-2}-\theta_1^2}}$$

$$\Psi'(\theta_2) = \frac{I_h b^2}{2\mu i\pi} \qquad (2.86)$$

By the method of superposition solutions can be obtained from Eqs. (2.85) and (2.86) for any two-dimensional problem involving disturbances in an infinite medium.

One of the most important applications of the potentials which have been found is to the problem of a disturbance originating in the interior of a half space. The potentials calculated in this section are potentials of waves incident on the surface (incident potentials). The additional disturbances arising from the presence of the surface can be expressed in terms of a new set of self-similar potentials which might be termed "reflected potentials."

---

† This radical is specified as having negative imaginary values at all points on the real θ_i axis to the right of c_i^{-1}.

Solutions which are exact for all $t \geq 0$ have been obtained by Smirnov [21], Zvolinskii [24], and others [22,26], for problems which involve disturbances originating in the interior of a homogeneous or layered half space. It turns out that the reflection and refraction of waves at a plane boundary can be solved in a remarkably simple fashion with the use of the method of self-similar potentials.

2.8. A Generalization of the Method of Self-Similar Displacement Potentials

In this section, we show how solutions can be obtained with the aid of self-similar potentials for any problem for which the tractions are homogeneous functions of x and t of order n. These problems are solved in the same way as were the problems of Sec. 2.5.2 for which the tractions were homogeneous functions of x and t of order -2. That is, a pair of fictitious, self-similar tractions are constructed by differentiating the actual tractions n times with respect to the variable t. If the fictitious tractions are denoted by Σ_y and T_{xy}, that is

$$\Sigma_y(x,t) = \frac{\partial^n \sigma_y(x,t)}{\partial t^n} \quad , \quad T_{xy}(x,t) = \frac{\partial^n \tau_{xy}(x,t)}{\partial t^n}$$

then $$\Sigma_y^*(\theta) = \frac{\partial^n \sigma_y^*(x,t)}{\partial t^n} \quad , \quad T_{xy}^*(\theta) = \frac{\partial^n \tau_{xy}^*(x,t)}{\partial t^n} \tag{2.87}$$

and the potentials which solve the problem being considered will be defined by Eq. (2.57) for all values of n.† However, the displacements and stresses

† If n is negative, we integrate n times. Thus, for example,

$$\frac{\partial^{-1} \sigma_y(x,t)}{\partial t^{-1}} = \int_0^t \sigma_y(x,\tau)d\tau \ .$$

at any point in the half space will no longer be defined in terms of the potentials by Eqs. (2.45) and (2.47) of Sec. 2.5.1, but rather by the equations which follow:

$$u_x = -\mathrm{Re}\int_0^t\int_0^{\tau_{n+1}}\cdots\int_0^{\tau_2}\left\{\int_0^{\theta_1}\theta\cdot\Phi'd\theta + \int_0^{\theta_2}\sqrt{b^{-2}-\theta^2}\,\Psi'd\theta\right\}d\tau_1\ldots d\tau_n d\tau_{n+1}$$

$$u_y = -\mathrm{Re}\int_0^t\int_0^{\tau_{n+1}}\cdots\int_0^{\tau_2}\left\{\int_0^{\theta_1}\sqrt{a^{-2}-\theta^2}\,\Phi'd\theta - \int_0^{\theta_2}\theta\Psi'd\theta\right\}d\tau_1\ldots d\tau_n d\tau_{n+1}$$

$$\frac{\sigma_x}{\mu} = \mathrm{Re}\int_0^t\int_0^{\tau_n}\cdots\int_0^{\tau_2}\left\{\int_0^{\theta_1}(b^{-2}+2\theta^2-2a^{-2})\Phi'd\theta + \int_0^{\theta_2}2\theta\sqrt{b^{-2}-\theta^2}\,\Psi'd\theta\right\}d\tau_1\ldots d_{n-1}d\tau_n$$

$$\frac{\sigma_y}{\mu} = \mathrm{Re}\int_0^t\int_0^{\tau_n}\cdots\int_0^{\tau_2}\left\{\int_0^{\theta_1}(b^{-2}-2\theta^2)\Phi'd\theta - \int_0^{\theta_2}2\theta\sqrt{b^{-2}-\theta^2}\,\Psi'd\theta\right\}d\tau_1\ldots d\tau_{n-1}d\tau_n \qquad (2.88)$$

$$\frac{\sigma_z}{\mu} = \mathrm{Re}\int_0^t\int_0^{\tau_n}\cdots\int_0^{\tau_2}\left\{\int_0^{\theta_1}(b^{-2}-2a^{-2})\Phi'd\theta\right\}d\tau_1\ldots d\tau_{n-1}d\tau_n$$

$$\frac{\tau_{xy}}{\mu} = \mathrm{Re}\int_0^t\int_0^{\tau_n}\cdots\int_0^{\tau_2}\left\{\int_0^{\theta_1}2\theta\sqrt{a^{-2}-\theta^2}\,\Phi'd\theta + \int_0^{\theta_2}(b^{-2}-2\theta^2)\Psi'd\theta\right\}d\tau_1\ldots d\tau_{n-1}d\tau_n$$

where $\Phi'(\theta)$ and $\Psi'(\theta)$ are defined by Eqs. (2.57) and the θ_i's are defined implicitly by the equation

$$\tau_1 - \theta_i x - y\sqrt{c_i^{-2}-\theta_i^2} = 0$$

2.8.1. A Uniformly Distributed Load Acting over an Expanding Region of the Surface†

To illustrate the way in which Eqs. (2.88) are used, we consider the problem in which a uniformly distributed stress of magnitude $\Delta\sigma$ acts vertically downward over the expanding region $-\alpha t \leq x \leq \alpha t$. If the tangential traction is zero, then the boundary conditions for this problem are defined as follows:

$$\begin{aligned} \sigma_y(x,t) &= -\Delta\sigma \qquad \text{for} \quad |x| \leq \alpha t \\ &= 0 \qquad\quad \text{for} \quad |x| > \alpha t \\ \tau_{xy}(x,t) &= 0 \qquad\quad \text{for} \quad -\infty < x < +\infty \end{aligned} \tag{2.89}$$

Equations (2.89) define tractions which are homogeneous functions of x and t of order zero. Hence, this problem can be solved in terms of self-similar potentials, and the fictitious tractions defined by Eq. (2.87) are identical to the actual tractions. That is,

$$\begin{aligned} \Sigma_y(x,t) &= \sigma_y(x,t) \\ T_{xy}(x,t) &= \tau_{xy}(x,t) \end{aligned} \tag{2.90}$$

It follows that the fictitious complex valued tractions, Σ_y^* and T_{xy}^*, which are constructed from Σ_y and T_{xy} by means of Eqs. (2.58), are identical to the quantities σ_y^* and τ_{xy}^*. That is

$$\begin{aligned} \Sigma_y^*(\theta) &= \sigma_y^*(x,t) \\ T_{xy}^*(\theta) &= \tau_{xy}^*(x,t) \end{aligned} \tag{2.91}$$

where $\theta = t/x$.

---

† This problem was solved by Craggs [15] using a method which is equivalent to but less direct than that presented here.

It follows from Eqs. (2.58) that

$$\begin{aligned} \sigma_y^*(\theta) &= -\frac{\Delta\sigma}{i\pi}\log\frac{(1+\alpha\theta)}{(1-\alpha\theta)} \\ \sigma_y^{*'}(\theta) &= -\frac{\Delta\sigma}{i\pi}\,\frac{2\alpha}{1-\alpha^2\theta^2} \\ \tau_{xy}^*(\theta) &= \tau_{xy}^{*'}(\theta) = 0 \end{aligned} \tag{2.92}$$

2.8.2. Concentrated Loads Which Increase Linearly with Time

The functions $\sigma_y^*(\theta)$ and $\sigma_y^{*'}(\theta)$ for a concentrated load of magnitude Ft which acts vertically downward at the origin can be obtained directly from Eqs. (2.92) by replacing $2\Delta\sigma\alpha$ by F and then letting α tend to zero. The following results are obtained:

$$\begin{aligned} \sigma_y^*(\theta) &= -F\theta/i\pi \\ \sigma_y^{*'}(\theta) &= -F/i\pi \\ \tau_{xy}^*(\theta) &= \tau_{xy}^{*'}(\theta) = 0 \end{aligned} \tag{2.93}$$

For the problem in which a point load of magnitude Ft moves along the surface with a speed α, it is not difficult to prove that $\sigma_y^*(\theta)$ and $\sigma_y^{*'}(\theta)$ are defined as follows:†

$$\sigma_y^*(\theta) = -\frac{\theta F}{i\pi(1-\alpha\theta)} \quad , \quad \sigma_y^{*'}(\theta) = \frac{-F}{i\pi(1-\alpha\theta)^2} \tag{2.94}$$

It is obvious that Eqs. (2.93) and (2.94) are identical for $\alpha = 0$.

The stresses and displacements at any point in the half space can be determined in a straightforward manner from Eqs. (2.58) and (2.88) and

---

† This problem was solved by Payton [11] using Laplace transforms.

the equations which define $\sigma_y^{*'}(\theta)$ and $\tau_{xy}^{*'}(\theta)$ for the problem being considered.

2.8.3. Some Useful Relations for Problems with Self-Similar Tractions

For problems in which the tractions are self-similar, the velocities must also be self-similar. It follows that these velocities can be expressed in terms of complex-valued functions by equations of the form

$$\begin{aligned} v_x(x,y,t) &= \text{Re } v_x^*(\theta_1,\theta_2) \\ v_y(x,y,t) &= \text{Re } v_y^*(\theta_1,\theta_2) \end{aligned} \tag{2.95}$$

If the tangential traction is zero, it is not difficult to show that the derivatives of $\sigma_y^*(\theta)$ and $v_y^*(\theta)$ are related on the $y = 0$ surface by the equation

$$v_y^{*'}(\theta) = \frac{-(a^{-2}-\theta^2)^{1/2}\sigma_y^{*'}(\theta)}{\mu b^2 R(\theta^2)} \tag{2.96}$$

On the $y = 0$ surface $\theta = \theta_1 = \theta_2 = t/x$ as in previous sections. This relationship will be used repeatedly in Chapter 4 where solutions are obtained for various contact problems.

A number of other useful relations can be derived from the solutions obtained in Secs. 2.8.1 and 2.8.2 for problems involving uniformly distributed and concentrated loads. The validity of these relations for all problems in which the distribution of the traction is self-similar follows from the linearity of the governing differential equations.

1) The load on the surface of the half space is related to the fictitious complex-valued normal traction by the equation

$$P(t) = i\pi t\sigma_y^{*'}(0)$$

2) The function $\sigma_y^{*'}(\theta)$ is analytic at every point on the real θ axis where $\partial\sigma_y(\theta)/\partial\theta$ is zero and non-analytic at every point where $\partial\sigma_y(\theta)/\partial\theta$ is not zero.†

3) There is a simple pole in $\sigma_y^{*'}(\theta)$ at each point along the real θ axis where there is a step discontinuity in $\sigma_y(\theta)$.

4) There is a pole of order 2 in $\sigma_y^{*'}(\theta)$ at each point along the finite portion of the real θ axis where there is a vertical point load of finite magnitude.

5) On the y = 0 surface,

$$\text{Re}\,\frac{\theta}{i\pi} = t\cdot\delta(x)$$

and $\text{Re}\,\frac{\theta}{i\pi(1-\alpha\theta)} = t\cdot\delta(x-\alpha t)$, where $\delta(x)$ is the Dirac delta function. The first of these relationships will recur frequently in the work that follows.

---

† Analogous relations exist between $\sigma_x^{*'}(\theta)$ and σ_x, $v_y^{*'}(\theta)$ and v_y, etc.

3. THEORY FOR THREE-DIMENSIONAL SELF-SIMILAR PROBLEMS

3.1. General Remarks

In this chapter, a method is developed for the direct determination of solutions of a variety of three-dimensional problems. These include any traction and superseismic contact problem and any axially symmetric contact problem which has boundary conditions that are homogeneous functions of the variables of space and time. This method was developed in 1933 by Smirnov and Sobolev [6], and used by these authors to solve the three-dimensional impulse problem and certain problems involving the propagation of spherical waves in a layered medium.

The basis of the procedure is the fact that in the cases of interest a one-to-one correspondence exists between the axially symmetric problem and some fictitious two-dimensional problem. In fact, the solution of the axially symmetric problem is expressible as a simple quadrature of quantities involved in the fictitious two-dimensional problem.

If the two-dimensional problem can be solved easily, as is often the case with the aid of the Smirnov-Sobolev method, the only remaining step is to define the fictitious two-dimensional problem in terms of the actual axially symmetric problem under consideration.

If the boundary and initial conditions for the axially symmetric problem are not homogeneous functions of the variables of space and time, the corresponding conditions for the plane problem must be determined by solving an Abel integral equation which relates the boundary conditions for the two problems [24]. However, if these conditions are homogeneous, the boundary and initial conditions for the plane problem can be determined,

virtually by inspection, if one uses the method which Kostrov [9] employed in solving the problem of a slowly-indenting conical die.

The one-to-one correspondence which exists between axially symmetric and plane strain problems holds for static as well as dynamic problems. Weber [33] used this approach to solve static problems. It appears that Weber rediscovered this one-to-one correspondence independently, several years after Smirnov and Sobolev published the more general dynamic relationship.

3.2. Determination of the Correspondence Between Plane Strain and Axially Symmetric Problems

The basis for the solution of the axially symmetric problems treated in this study is the following observation. For every two-dimensional vector or scalar field $U_0(\xi,y)$, where $\xi = r\cos\omega$, it is possible to form a corresponding axially symmetric field by a "rotational superposition":

$$U_1(r,y) = \int_0^{2\pi} U_0(\xi,y)\,d\omega \tag{3.1}$$

Here ξ takes the place of x in the two-dimensional treatment of Chapter 2. If we let U_0 be a displacement field for some plane strain problem, then the U_1 field determined in accordance with Eq. (3.1) also satisfies the three-dimensional equations of elasticity, since it is the superposition of states which themselves satisfy the equations of three-dimensional elasticity.†

Not only can axially symmetric fields be found from Eq. (3.1), but, as will be shown, to every axially symmetric field there corresponds at least

---

† This follows from the equations of linear elasticity in the isotropic homogeneous case.

one two-dimensional field U_0 satisfying Eq. (3.1). With a simple restriction on the form of U_0, this correspondence between U_0 and U_1 is, in fact, one-to-one. These statements will be proved in Sec. 3.3.1.

Let u_H and u_V denote the horizontal and vertical components, respectively, for a plane strain displacement field which has no component of displacement in a direction normal to the plane along which $\omega = 0$. From Fig. 9, it can easily be seen that the radial, circumferential, and vertical components of the displacement field are defined at any point by the equations

$$\begin{aligned} u_{r0} &= \cos\omega \cdot u_H(r\cos\omega, y) \\ u_{\omega 0} &= \sin\omega \cdot u_H(r\cos\omega, y) \\ u_{y0} &= u_V(r\cos\omega, y) \end{aligned} \tag{3.2}$$

It follows from our previous remarks that the corresponding components for the axially symmetric field will be defined as follows:

$$\begin{aligned} u_{r1} &= \int_0^{2\pi} \cos\omega \cdot u_H(r\cos\omega, y)d\omega \\ u_{\omega 1} &= \int_0^{2\pi} \sin\omega \cdot u_H(r\cos\omega, y)d\omega \\ u_{y1} &= \int_0^{2\pi} u_V(r\cos\omega, y)d\omega \end{aligned} \tag{3.3}$$

Now let u_H and u_V be written as follows

$$\begin{aligned} u_H &= u_H^S + u_H^A \\ u_V &= u_V^S + u_V^A \end{aligned} \tag{3.4}$$

where u_H^S and u_V^S are the displacements which solve the symmetric portion of the plane strain problem, and u_H^A and u_V^A are the displacements which solve the antisymmetric portion of the problem. These components satisfy equations of the form

$$\begin{aligned} u_H^S(\xi,y) &= -u_H^S(-\xi,y) \\ u_V^S(\xi,y) &= u_V^S(-\xi,y) \end{aligned} \tag{3.5}$$

and

$$\begin{aligned} u_H^A(\xi,y) &= u_H^A(-\xi,y) \\ u_V^A(\xi,y) &= -u_V^A(-\xi,y) \end{aligned} \tag{3.6}$$

It can easily be verified that the rotational superposition of any antisymmetric displacement field results in zero displacements. Consequently, the axially symmetric field U_1 determined in accordance with Eq. (3.1) depends only on the symmetric portion of the plane strain displacement field U_0. In the work that follows, we restrict our attention to those symmetric two-dimensional problems whose displacements satisfy Eqs. (3.5). For any problem of this type, Eqs. (3.3) can then be simplified to the following form

$$\begin{aligned} u_r &= \int_0^{\pi} \cos\omega \cdot u_{x2}(r\cos\omega, y)\,d\omega \\ u_\omega &= 0 \\ u_y &= \int_0^{\pi} u_{y2}(r\cos\omega, y)\,d\omega \end{aligned} \tag{3.7}$$

where $u_r = u_{r1}/2$, $u_\omega = u_{\omega 1}/2 = 0$, $u_y = u_{y1}/2$, and where u_H^S and u_V^S are redefined as u_{x2} and u_{y2}, respectively.

In these equations we assume that the z axis is normal to the $\omega = 0$ plane.

For axially symmetric problems the stresses are defined in terms of the strains by the equations

$$\begin{aligned} \sigma_r &= \lambda\Delta + 2\mu\epsilon_r \\ \sigma_\omega &= \lambda\Delta + 2\mu\epsilon_\omega \\ \sigma_y &= \lambda\Delta + 2\mu\epsilon_y \\ \tau_{xy} &= \mu\gamma_{ry} \qquad \tau_{r\omega} = 0 \qquad \tau_{y\omega} = 0 \end{aligned} \tag{3.8}$$

where λ and μ are Lamé's constants, $\Delta = \epsilon_r + \epsilon_\omega + \epsilon_y$, and ϵ_r, ϵ, ϵ_y and γ_{ry} are the radial, circumferential, vertical and shear strains, respectively. These quantities are defined in terms of the displacement as follows:

$$\begin{aligned} \epsilon_r &= \frac{\partial u_r}{\partial r} \\ \epsilon_\omega &= \frac{u_r}{r} \\ \epsilon_y &= \frac{\partial u_y}{\partial y} \\ \gamma_{ry} &= \frac{\partial u_r}{\partial y} + \frac{\partial u_y}{\partial r} \end{aligned} \tag{3.9}$$

Consider the third of Eqs. (3.8). Using Eqs. (3.5), (3.7) and (3.8), we find that the vertical stress is defined in terms of the plane displacements as follows:

$$\sigma_y(r,y) = \int_0^{\pi} (\lambda(\frac{\partial u_{x2}}{\partial r} \cos\omega + \frac{u_{x2}}{r} \cos\omega + \frac{\partial u_{y2}}{\partial y}) + 2\mu \cdot \frac{\partial u_{y2}}{\partial y}) \, d\omega \tag{3.10}$$

Since $$\frac{\partial u_{x2}}{\partial r} = \frac{\partial u_{x2}}{\partial r\cos\omega} \quad \frac{\partial r\cos\omega}{\partial r} = \frac{\partial u_{x2}}{\partial x} \cos\omega \tag{3.11}$$

and $$\frac{1}{r} \int_0^{\pi} u_{x2} \cdot \cos\omega d\omega = \frac{1}{r} \cdot \sin\omega \cdot u_{x2} \Big|_0^{\pi} + \int_0^{\pi} \sin^2\omega \frac{\partial u_{x2}}{\partial x} \, d\omega \tag{3.12}$$

the integrand of Eq. (3.10) can be written in the form

$$\lambda(\frac{\partial u_{x2}}{\partial x} + \frac{\partial u_{y2}}{\partial y}) + 2\mu \frac{\partial u_{y2}}{\partial y} \, . \tag{3.13}$$

But this quantity is precisely the vertical stress σ_{y2} for the plane strain problem. Consequently, Eq. (3.10) can be written in the form

$$\sigma_y(r,y) = \int_0^{\pi} \sigma_{y2}(r\cos\omega,y) \, d\omega \tag{3.14a}$$

In an analogous manner we find that

$$\sigma_\omega = \int_0^{\pi} (\sigma_{z2} + 2\mu\epsilon_{x2} \sin^2\omega) d\omega$$

$$\sigma_r = \int_0^{\pi} (\sigma_{x2} - 2\mu\epsilon_{x2} \sin^2\omega) d\omega \tag{3.14b}$$

$$\tau_{ry} = \int_0^{\pi} \tau_{xy2} \cos\omega \, d\omega \qquad \tau_{r\omega} = \tau_{\omega y} = 0$$

where, for the plane strain problem, σ_{z2} is the stress in the z direction, σ_{x2} the stress in the x direction, τ_{xy2} the only non-zero shearing stress, and ϵ_{x2} the strain in the x direction.

When we consider the wedge and cone problems we shall require the expression for the slope of the surface of the half space. This can be determined from the following equation:

$$\frac{\partial u_y(r,0)}{\partial r} = \int_0^{\pi} \cos\omega \, \frac{\partial u_{y2}}{\partial x} (r\cos\omega, 0) d\omega \tag{3.15}$$

where $\frac{\partial u_y}{\partial r}$ and $\frac{\partial u_{y2}}{\partial x}$ denote the slope for the axially symmetric and plane strain problems, respectively. Equation (3.15) is derived in the same way as those for the stresses and displacements.

3.3. Determination of the Boundary and Initial Conditions for the Plane Strain Problem

In this section, we show how the boundary and initial conditions for the fictitious plane strain problem are determined from the analogous conditions for the particular axially symmetric problem being considered. We first consider a method which holds for both static and dynamic problems. Later we introduce a convenient method of calculation which was developed by Kostrov and can only be used for dynamic problems which have boundary and initial conditions that are homogeneous functions of the variables r and t.

3.3.1. The General Method†

To illustrate the method which holds for all axially symmetric problems, assume that the boundary and initial conditions for the problem

---

† This method appears to be due to Smirnov and Sobolev [6].

being considered are specified functions of σ_y and τ_{ry}. For such a problem, the first and fourth of Eqs. (3.14) must be solved to determine the corresponding quantities for the plane strain problem. This can be done as follows.

Let $\lambda = r\cos\omega$. Then $d\lambda = -r\sin\omega d\omega$, and with the appropriate change in the limits of integration, Eqs. (3.14) can be written in the following form:

$$\begin{aligned} \tau_{ry}(\lambda_0,y) &= -\int_{\lambda_0}^{-\lambda_0} \frac{\lambda}{\lambda_0}\,\tau_{xy2}(\lambda,y)\,\frac{d\lambda}{\sqrt{\lambda_0^2-\lambda^2}} \\ \sigma_y(\lambda_0,y) &= -\int_{\lambda_0}^{-\lambda_0} \sigma_{y2}(\lambda,y)\,\frac{d\lambda}{\sqrt{\lambda_0^2-\lambda^2}} \end{aligned} \tag{3.16}$$

where $\lambda_0 = r$. If we restrict our attention to plane strain problems whose displacement fields satisfy Eqs. (3.5), then Eqs. (3.16) can be simplified to the following:

$$\begin{aligned} \tau_{ry}(\sqrt{\xi_0},y) &= \int_0^{\xi_0} \frac{\tau_{xy2}(\sqrt{\xi},y)}{\sqrt{\xi_0}}\,\frac{d\xi}{\sqrt{\xi_0-\xi}} \\ \sigma_y(\sqrt{\xi_0},y) &= \int_0^{\xi_0} \sigma_{y2}(\sqrt{\xi},y)\,\frac{1}{\sqrt{\xi}}\,\frac{d\xi}{\sqrt{\xi_0-\xi}} \end{aligned} \tag{3.17}$$

where $\xi = \lambda^2$ and $\xi_0 = \lambda_0^2$. This transformation results in a pair of independent Abel integral equations which can be solved without difficulty. The result is

---

† See Ref. [34].

$$\tau_{xy2}(\sqrt{\xi}, y) = \sqrt{\xi_0}\,\frac{\partial}{\partial\xi}\int_0^{\xi} \tau_{ry}(\sqrt{\xi_0}, y)\,\frac{d\xi_0}{\sqrt{\xi-\xi_0}}$$

$$\sigma_{yz}(\sqrt{\xi}, y) = \sqrt{\xi}\,\frac{\partial}{\partial\xi}\int_0^{\xi} \frac{\sigma_y(\sqrt{\xi_0}, y)}{\sqrt{\xi-\xi_0}}\,d\xi_0 \qquad (3.18)$$

For y = 0, Eqs. (3.18) define the tractions for a symmetric plane strain problem which corresponds to the axially symmetric problem being considered. Since the displacement field which solves this plane problem is unique, the axially symmetric displacement field determined by the operation of rotational superposition on the plane field is also unique. Moreover, this three-dimensional field solves the problem whose tractions are determined by the rotational superposition of the tractions for the plane problem. However, the axially symmetric tractions determined in this way are identical to the tractions for the axially symmetric problem being considered. Hence, by uniqueness, the three-dimensional field determined above is the solution of the axially symmetric problem in question. It follows that every axially symmetric problem can be solved by the methods proposed in this section.

3.3.2. The Technique of Kostrov

Now let us consider axially symmetric problems having boundary and initial conditions which are homogeneous functions of the variables r and t. The analogous conditions for the corresponding plane strain problems must necessarily be homogeneous functions of the variables x and t. In Sec. 2.8 it was shown that two-dimensional problems of this type could be solved by expressing the boundary conditions in terms of complex-valued

functions of the variables θ_1 and θ_2, where both of these are equal to t/x on the y = 0 surface.

To illustrate the technique which Kostrov [9] used to solve problems of this type, assume that the boundary conditions are defined in terms of a normal and tangential traction on the surface of a half space. Moreover, assume that the functions which define these tractions are homogeneous of degree zero. It follows from our previous remarks that the axially symmetric and plane strain tractions are related by the equations

$$\begin{aligned} \sigma_y(r,t) &= \mathrm{Re} \int_0^{\pi} \sigma_y^*(\theta^2)d\omega \\ \tau_{ry}(r,t) &= \mathrm{Re} \int_0^{\pi} \cos\omega\, \tau_{xy}^*(\theta^2)d\omega \end{aligned} \tag{3.19}$$

where $\theta = \theta_1 = \theta_2 = t/x = t/r\cos\omega$. As in Chapter 2, σ_y^* and τ_{xy}^* are complex-valued functions of θ whose real parts are equal to σ_{y2} and τ_{xy2}, respectively. It is frequently more convenient to work with the time derivatives of these tractions rather than the tractions themselves. These quantities are determined from the equations

$$\begin{aligned} \dot{\sigma}_y(r,t) &= \mathrm{Re} \int_0^{\pi} \dot{\sigma}_y^*(\theta^2)d\omega \\ \dot{\tau}_{xy}(r,t) &= \mathrm{Re} \int_0^{\pi} \cos\omega\cdot\dot{\tau}_{xy}^*(\theta^2)d\omega \end{aligned} \tag{3.20}$$

If we change the variable of integration from ω to θ, the following results are obtained:

$$\dot{\sigma}_y(\theta_0) = \mathrm{Re} \int_{C_1} \frac{1}{r} \frac{\partial \sigma_y^*(\theta^2)}{\partial \theta} \frac{d\theta}{\sqrt{\theta^2-\theta_0^2}}$$

$$\dot{\tau}_{xy}(\theta_0) = \mathrm{Re} \int_{C_1} \frac{1}{r} \frac{\theta_0}{\theta} \frac{\partial \tau_{xy}^*(\theta^2)}{\partial \theta} \frac{d\theta}{\sqrt{\theta^2-\theta_0^2}} \qquad (3.21)$$

where $\theta_0 = t/r$.

Each path of integration is the contour C_1 shown in Fig. 10. This contour extends along the real θ axis from θ_0 to $+\infty$, then along a semi-circular path in a counterclockwise direction from $+\infty$ to $-\infty$, and finally along the negative portion of the real θ axis from $-\infty$ to $-\theta_0$. The radical $(\theta^2-\theta_0^2)^{+1/2}$ is specified as equal to $+i\theta_0$ at the origin and is analytic everywhere in the θ plane except across cuts outward along the real axis from $+\theta_0$ and $-\theta_0$.

Equations (3.21) can be simplified further by changing the variable of integration from θ to η where $\eta = \theta^2$. The result is

$$\dot{\sigma}_y(\eta_0) = \mathrm{Re} \int_{C_2} \frac{1}{r} \frac{\partial \sigma_y^*(\eta)}{\partial \eta} \frac{d\eta}{\sqrt{\eta-\eta_0}} \qquad (3.22a)$$

$$\dot{\tau}_{ry}(\eta_0) = \mathrm{Re} \int_{C_2} \frac{1}{r} \frac{\theta_0}{\sqrt{\eta}} \frac{\partial \tau_{xy}^*(\eta)}{\partial \eta} \frac{d\eta}{\sqrt{\eta-\eta_0}} \qquad (3.22b)$$

where $\eta_0 = \theta_0^2$, and the contour of integration is now the closed path C_2 shown in Fig. 11.

For the two-dimensional dynamic problems of Sec. 2.4 it was shown that every complex potential expressed as a function of θ_i is analytic off the real axis of the θ_i plane. Since the upper half θ plane maps into the

entire η plane, the integrands of Eqs. (3.22) must be analytic except at points or regions along the real η axis between η and $+\infty$. As a result, the contour of integration can be deformed into any curve which begins at a point just above η_0 on the real η axis, ends at a point just below η_0, and does not cross the positive real η axis between η_0 and the origin. Several curves of this type are shown in Fig. 11. The curve C_3, which is used frequently in the work that follows, lies just above the axis in passing from η_0 to the origin and just below the axis in passing from the origin back to a point directly beneath η_0.

Since the integrands of Eqs. (3.22) are functions which are analytic everywhere off the positive η axis, the value of these functions at every point in the η plane is determined completely by the non-analyticities along the axis, the behavior at infinity, and the position of the point η_0.

Using the Cauchy Integral Theorem and Morera's Theorem, we arrive at the following useful relations between the character of $\dot{\sigma}_y$ and the singularities of the integrand of Eq. (3.22a):

1) If the value of $\dot{\sigma}_y(\eta_0)$ experiences a step discontinuity at $\eta_0 = \eta_1$,† the integrand of Eq. (3.22a) is non-analytic at $\eta = \eta_1$.

2) If the value of $\dot{\sigma}_y(\eta_0)$ varies continuously in a range such as $\eta_2 < \eta_0 < \eta_3$, the integrand of Eq. (3.22a) is non-analytic in the range $\eta_2 < \eta < \eta_3$.

3) If the value of $\dot{\sigma}_y(\eta_0)$ is zero for all η_0 in the range

† It is assumed that η_1, η_2, η_3 and η_4 denote distinct, non-zero values of t/r which are points at which the function defining the axially symmetric normal traction is discontinuous.

$0 \leq \eta_0 \leq \eta_4$, both $\frac{\partial \sigma_y^*(\eta)}{\partial \eta}$ and the integrand of Eq. (3.22a) are analytic for all $0 \leq \eta \leq \eta_4$.

4) If the value of $\dot{\sigma}_y(\eta_0)$ is constant for all η_0 in the range $\eta_4 \leq \eta_0 \leq +\infty$, the integrand of Eq. (3.22a) is analytic for all $\eta_4 \leq \eta \leq +\infty$, and the value of $\dot{\sigma}_y(\eta_0)$ is equal to the value of the integral of Eq. (3.22a) taken over the portion of C_2 which forms the circle at infinity (see Fig. 11).

These relations depend on the points of non-analyticity of the integrand, not on the physical interpretation of the variables involved. Consequently, they hold whenever the integral which defines a three-dimensional quantity is of the form of Eq. (3.22a) or Eq. (3.22b).

With the aid of the four basic relations defined above, the boundary and initial conditions of the fictitious plane problem can be determined, virtually by inspection, for any axially symmetric problem which has boundary and initial conditions which are homogeneous functions of degree zero. To illustrate the process, we next consider a simple but interesting problem, which was initially solved by Craggs using a method which requires several pages of detailed calculations [18].

3.3.3. The Two-Dimensional Problem Corresponding to an Expanding, Uniformly Distributed Circular Load

Consider the axially symmetric problem in which the only load on the surface of a linearly elastic half space is a normal traction of unit magnitude acting vertically downward in the expanding circular region $r \leq \alpha t$. That is,

$$\begin{aligned} \sigma_y(r,t) &= -1 \quad \text{for } r \leq \alpha t \\ &= 0 \quad \text{for } \alpha t < r \\ \tau_{ry}(r,t) &= 0 \quad \text{for } 0 \leq r \leq \infty \end{aligned} \tag{3.23}$$

Since these conditions are homogeneous functions of degree zero they can also be expressed in the form†

$$\begin{aligned} \sigma_y(\theta_0) &= -1 \quad \text{for} \quad \theta_0 \geq \alpha^{-1} \\ &= 0 \quad \text{for} \quad \theta_0 < \alpha^{-1} \\ \tau_{ry}(\theta_0) &= 0 \quad \text{for} \quad \theta \leq \theta_0 \leq \infty \end{aligned} \tag{3.24}$$

where $\theta_0 = t/r$.

It follows directly that the first derivatives with respect to time of these tractions satisfy the conditions

$$\begin{aligned} \dot{\sigma}_y(\theta_0) &= 0 \quad \text{for all } \theta_0 \neq \alpha^{-1} \\ \dot{\tau}_{xy}(\theta_0) &= 0 \end{aligned} \tag{3.25}$$

and $$\int_{\alpha^{-1}-\epsilon}^{\alpha^{-1}+\epsilon} \frac{\partial \sigma_y(\theta^2)}{\partial \theta}\, d\theta = -1 \quad \text{for all } \epsilon > 0,$$

where the path of integration is clockwise along a semicircle with radius ϵ and center $\theta = \alpha^{-1}$.

Using the results of the previous section, we can immediately conclude that $\sigma_y^{*'}(\theta^2)$ and $\tau_{xy}^{*'}(\theta^2)$ must satisfy the following conditions:

$\tau_{xy}^{*'}(\theta^2) \equiv 0$

$\sigma_y^{*'}(\theta^2)$ is not analytic at $\theta^2 = \alpha^{-2}$

$\sigma_y^{*'}(\theta^2)$ is analytic for all $\theta^2 < \alpha^{-2}$

$\dfrac{\sigma_y^{*'}(\theta^2)}{\sqrt{\theta^2 - \theta^2}}$ is analytic for all $\alpha^{-2} < \theta_0^2 < \theta^2$ and all $\theta^2 < \theta_0^2 < \alpha^{-2}$

† The variable θ^2 is substituted for η and θ_0^2 for η_0 to facilitate certain of the computations which follow.

and $$\int_C \frac{\sigma_y^{*'}(\theta^2)d\theta^2}{\sqrt{\theta^2-\theta_0^2}} = 0 \quad ,$$

where $\sigma_y^{*'}(\theta^2) = \dfrac{\partial\sigma_y^*(\theta^2)}{\partial\theta^2}$, and C is the portion of the contour C_2 of Fig. 11 which forms a circle at infinity.

In order that $\sigma_y^{*'}(\theta^2)$ be analytic everywhere off the real $\theta^2 > 0$ axis, and that the first three of the above conditions be satisfied, $\sigma_y^{*'}(\theta^2)$ must be a function of the form

$$\sigma_y^{*'}(\theta^2) = \sum_{n=0}^{n=\infty} F_n(\theta^2)(\alpha^{-2}-\theta^2)^{-n+\frac{1}{2}} \tag{3.26}$$

where n is an integer and the $F_n(\theta^2)$ are integral (entire) functions.†

In order that there not be any singularity in load at the origin of the physical space, no essential singularity in the functions $F_n(\theta^2)$ can exist at infinity. The functions $F_n(\theta^2)$ must then be polynomials. Furthermore, F_0 and F_1 must be zero, F_2 can be constant, F_3 can be a linear expression in θ^2, etc.

It is now easy to see that the most general form of $\sigma_y^*(\theta^2)$ is

$$\sigma_y^{*'}(\theta^2) = \sum_{n=2}^{n=\infty} A_n(\alpha^{-2} - \theta^2)^{-n+\frac{1}{2}} \tag{3.27}$$

where each A_n is a constant.

Each term in this infinite series corresponds to a different axially symmetric problem. Moreover, each successive term corresponds to

† That is, functions which have no singularities or poles in the finite portion of the θ^2 plane.

a stress distribution which is more singular at the edge of the load area than the previous one. Hence, we anticipate that the first of the above functions corresponds to the axially symmetric problem whose boundary conditions satisfy Eqs. (3.24) and which has no self-equilibrating stress singularity at the edge of the expanding load. This assumption can be verified as follows.

If

$$\sigma_y^{*'}(\theta^2) = A_2(\alpha^{-2}-\theta^2)^{-3/2}$$

then

$$\sigma_y^{*}(\theta^2) = A_2[2(\alpha^{-2}-\theta^2)^{-1/2} - K] \tag{3.28}$$

where K is a constant of integration.

Equation (3.14) relating σ_y and σ_y^* could also have been written in the form

$$\sigma_y(\theta_0) = \mathrm{Re} \int_{C_2} \frac{\sigma_y^*(\theta^2)}{2} \frac{\theta_0}{\theta^2} \frac{d\theta^2}{\sqrt{\theta^2-\theta_0^2}} \tag{3.29}$$

It is apparent from Eq. (3.28) that $\sigma_y^*(\theta^2)$ must be zero at the origin in order that there be no pole at that point in the integrand. Hence, $K = 2\alpha$. It follows directly from Eqs. (3.27) and (3.28) that the traction on the boundary satisfies the conditions

$$\begin{aligned} \sigma_y(\theta_0) &= -2A_2\alpha\pi \qquad \text{for } \alpha^{-1} \le \theta_0 \\ &= 0 \qquad\quad \text{for } \theta_0 < \alpha^{-1} \end{aligned} \tag{3.30}$$

If we set $A_2 = 1/2\ \alpha\pi$, Eqs. (3.24) and (3.30) will be identical. Therefore, the normal traction for the fictitious plane problem has been determined if no self-equilibrating stress singularities are present at the edge of the

expanding surface loads. The absence of such disturbances can be verified by examining the asymptotic character of the stress field near $r = \alpha t$. The way in which this is done is described in Sec. 3.4.1.2 where the asymptotic character of the disturbances associated with a surface wave are computed.

The stress and velocity fields for the plane strain problems can be determined in a straightforward manner from the functions which define $\partial\sigma_y^{*'}/\partial\theta$ and $\partial\tau_{xy}^{*'}/\partial\theta$ and Eqs. (2.57), (2.87) and (2.88). The three-dimensional fields can then be found by substituting the corresponding plane quantities in Eqs. (3.7) and (3.14) and carrying out the required integration. No attempt is made to carry out these operations for this problem. Instead, we consider several problems involving concentrated disturbances. The fictitious tractions for these problems are determined from the results obtained in this section by the same type of limiting process that was used to determine the solution for problems involving concentrated line loads. This insures that the solutions obtained do not contain self-equilibrating stress singularities.

3.4. Dynamic Loads and Impulses Concentrated at a Point

If a normal traction of magnitude $F/\alpha^2\pi$ acts vertically downward over the expanding circular region $r \leq \alpha t$, the resultant is a vertical load of magnitude Ft^2 which acts vertically downward at the origin. The first derivative with respect to θ^2 of the boundary tractions for the fictitious plane problem can be written directly from the results of the previous section.

$$\begin{aligned} \sigma_y^{*'}(\theta^2) &= F/2\pi^2(1-\alpha^2\theta^2)^{3/2} \\ \tau_{xy}^{*'}(\theta^2) &= 0 \end{aligned} \tag{3.31}$$

The limiting value of Eqs. (3.31) as α tends to zero are the derivatives of the tractions for the plane problem which corresponds to the axially symmetric problem in which a point load of magnitude Ft^2 acts vertically downward at the origin. For this problem we find that

$$\begin{aligned} \sigma_y^{*'}(\theta^2) &= F/2\pi^2, \\ \tau_y^{*'}(\theta^2) &= 0 \end{aligned} \tag{3.32}$$

Hence,

$$\begin{aligned} \frac{\partial \sigma_y^*(\theta^2)}{\partial \theta} &= \theta F/\pi^2 \\ \frac{\partial \tau_{xy}^*(\theta^2)}{\partial \theta} &= 0 \end{aligned} \tag{3.33}$$

The self-similar potentials† which solve this fictitious plane strain problem are determined from Eqs. (2.57), (2.87), (2.88) and (3.33). We find

$$\begin{aligned} \Phi'(\theta_1) &= \frac{\theta_1(b^{-2}-2\theta_1^2)}{R(\theta_1^2)} \frac{F}{\mu\pi^2} \\ \Psi'(\theta_2) &= \frac{-2\theta_2^2(a^{-2}-\theta_2^2)^{1/2}}{R(\theta_2^2)} \frac{F}{\mu\pi^2} \end{aligned} \tag{3.34}$$

where θ_1 and θ_2 are defined implicitly by the equations

$$\delta_i = t - r\cos\omega\cdot\theta_i - y(c_i^{-2}-\theta_i^2)^{1/2} = 0 \qquad i = 1,2 \tag{3.35}$$

($r\cos\omega$ is equivalent to the x of Chapter 2.)

---

† See Sec. 2.8 for the generalization of the displacement potential method of Smirnov and Sobolev.

A relationship which will be useful later is obtained by observing that for the problems considered above, the total load on the boundary can be computed from the equation

$$P(t) = -2t^2\pi^2\sigma_y^{*'}(0) \tag{3.36}$$

It follows directly from the linearity of the wave equations that Eq. (3.36) will hold for all axially symmetric problems which have stress and velocity boundary conditions which are self-similar.

3.4.1. Derivation of the Equations Defining the Velocity and Stress Fields

The first derivative with respect to time of the velocities and stresses for the problem solved above can be found with the aid of Eqs. (2.88), (3.34), (3.7) and (3.14). The result is

$$\begin{aligned}
\frac{\partial v_y}{\partial t} &= \mathrm{Re}\int_0^{\pi}\left(\frac{(a^{-2}-\theta_1^2)^{1/2}\Phi'}{\delta_1'} - \frac{\theta_2\Psi'}{\delta_2'}\right)d\omega \\
\frac{\partial v_r}{\partial t} &= \mathrm{Re}\int_0^{\pi}\cos\omega\left(\frac{\theta_1\Phi'}{\delta_1'} + \frac{\sqrt{b^{-2}-\theta_2^2}\,\Psi'}{\delta_2'}\right)d\omega \\
\frac{\partial \sigma_y}{\partial t} &= -\mathrm{Re}\int_0^{\pi}\mu\left(\frac{(b^{-2}-2\theta_1^2)\Phi'}{\delta_1'} - \frac{2\theta_2\sqrt{b^{-2}-\theta_2^2}\,\Psi'}{\delta_2'}\right)d\omega \\
\frac{\partial \sigma_r}{\partial t} &= -\mathrm{Re}\int_0^{\pi}\mu\left(\frac{(b^{-2}-2a^{-2}+2\theta_1^2\cos^2\omega)\Phi'}{\delta_1'} + \frac{2\theta_2\sqrt{b^{-2}-\theta_2^2}\cos^2\omega\,\Psi'}{\delta_2'}\right)d\omega \\
\frac{\partial \sigma_\omega}{\partial t} &= -\mathrm{Re}\int_0^{\pi}\mu\left(\frac{(b^{-2}-2a^{-2}+2\theta_1^2\sin^2\omega)\Phi'}{\delta_1'} + \frac{2\theta_2\sqrt{b^{-2}-\theta_2^2}\sin^2\omega\,\Psi'}{\delta_2'}\right)d\omega
\end{aligned} \tag{3.37}$$

$$\frac{\partial \tau_{ry}}{\partial t} = -\mathrm{Re}\int_0^{\pi} \mu\cos\omega\left(\frac{2\theta_1\sqrt{a^{-2}-\theta_1^2}\,\Phi'}{\delta_1'} + \frac{(b^{-2}-2\theta_2^2)\Psi'}{\delta_2'}\right)d\omega$$

$$\tau_{r\omega} \equiv \tau_{y\omega} \equiv 0$$

where $\delta_i' = -r\cos\omega + \theta_i y/(c_i^{-2}-\theta_i^2)^{1/2}$, and Φ' and Ψ' are the potentials defined by Eqs. (3.34).

Since the stresses and displacements at any point can be calculated in a straightforward manner from the quantities determined in Eqs. (3.37), the problem of a point load of magnitude Ft^2 acting vertically downward at a point on the surface of a linearly elastic half space is essentially solved.

If the quantities $v_y,\ldots\ldots,\tau_{ry}$ of Eqs. (3.37) are differentiated n times with respect to t rather than just once, the resulting equations will define the relationship which exists between the velocities, stresses and potentials for axially symmetric problems whose boundary conditions are homogeneous functions of r and t of degree n-1. For such problems, Φ' and Ψ' should be interpreted as the potentials which solve the corresponding plane strain problem. Thus, the potentials defined by Eq. (3.34) can be used to determine the stress and velocity fields for any problem in which the load P(t) acting vertically downward at the origin is given by the equation

$$P(t) = \frac{\partial^{1-n}(Ft^2)}{\partial t^{1-n}} \tag{3.38}$$

For example, if n = -2, the load defined by Eq. (3.38) is an impulse of magnitude 2F which acts vertically downward at time t = 0. The stress and displacement fields for this problem (Lamb's problem [10]) can be determined without difficulty from Eqs. (3.37) with $\frac{\partial v_y}{\partial t},\ldots\ldots,\frac{\partial \tau_{ry}}{\partial t}$ replaced by

$\frac{\partial^{-2} v_y}{\partial t^{-2}}, \ldots\ldots, \frac{\partial^{-2} \tau_{ry}}{\partial t^{-2}}$, respectively. The vertical components of these fields, for example, are defined by the equations

$$u_y = \mathrm{Re}\ \frac{F}{\pi\mu}\left(\frac{\partial}{\partial t}\int_0^{\pi} \frac{\theta_1\sqrt{a^{-2}-\theta_1^2}\,(b^{-2}-2\theta_1^2)}{R(\theta_1^2)\,\delta_1'}\,d\omega + \frac{\partial}{\partial t}\int_0^{\pi} \frac{2\theta_2^3\sqrt{a^{-2}-\theta_2^2}}{R(\theta_2^2)\delta_2'}\,d\omega\right.$$

(3.39)

$$\sigma_y = -\mathrm{Re}\ \frac{F}{\pi\mu}\ \frac{\partial^2}{\partial t^2}\int_0^{\pi} \frac{\theta_1(b^{-2}-2\theta_1^2)^2}{R(\theta_1^2)\delta_1'}\,d\omega +$$

$$\frac{\partial}{\partial t^2}\int_0^{\pi} \frac{4\theta_2^3\sqrt{a^{-2}-\theta_2^2}\sqrt{b^{-2}-\theta_2^2}}{R(\theta_2^2)\ \delta_2'}\,d\omega$$

The other axially symmetric quantities can be found in the same way.

To evaluate the integrals of Eqs. (3.37) for the problem solved in Sec. 3.4, it is convenient to change the variable of integration from ω to the appropriate θ_i^2. Equations (3.37) can then be written as follows:

$$\dot{v}_y = -\mathrm{Re}\int_{C_1} \frac{\sqrt{a^{-2}-\theta_1^2}\ \Phi'}{2\theta_1 G_1}\ d\theta_1^2 + \mathrm{Re}\int_{C_2} \frac{\Psi'}{2G_2}\ d\theta_2^2$$

$$\dot{v}_r = -\mathrm{Re}\int_{C_1} \frac{\cos\omega\ \Phi'}{2G_1}\,d\theta_1^2 - \mathrm{Re}\int_{C_2} \frac{\sqrt{b^{-2}-\theta_2^2}\cos\omega\ \Psi'}{2\theta_2\ G_2}\ d\theta_2^2$$

$$\dot{\sigma}_y = \mathrm{Re}\int_{C_1} \mu\ \frac{(b^{-2}-2\theta_1^2)\Phi'}{2\theta_1 G_1}\,d\theta_1^2 - \mathrm{Re}\int_{C_2} \mu\ \frac{\sqrt{b^{-2}-\theta_2^2}}{G_2}\ \Psi'\ d\theta_2^2$$

(3.40)

$$\dot{\sigma}_r = \mathrm{Re}\int_{C_1} \mu \frac{(b^{-2}-2a^{-2}+2\theta_1^2\cos^2\omega)\Phi'}{2\theta_1 G_1}\, d\theta_1^2 + \mathrm{Re}\int_{C_2} \frac{\mu\sqrt{b^{-2}-\theta_2^2}\cos^2\omega\ \Psi'}{G_2}\, d\theta_2^2$$

$$\dot{\sigma}_\omega = \mathrm{Re}\int_{C_1} \mu \frac{(b^{-2}-2a^{-2}+2\theta_1^2\sin^2\omega)\Phi'}{2\theta_1 G_1}\, d\theta_1^2 + \mathrm{Re}\int_{C_2} \frac{\mu\sqrt{b^{-2}-\theta_2^2}\sin^2\omega\ \Psi'}{G_2}\, d\theta_2^2$$

$$\dot{\tau}_{ry} = \mathrm{Re}\int_{C_1} \mu\cos\omega\left(\frac{\sqrt{a^{-2}-\theta_1^2}\,\Phi'}{G_1}\right)d\theta_1^2 + \mathrm{Re}\int_{C_2} \frac{\mu\cos\omega(b^{-2}-2\theta_2^2)\Psi'}{2\theta_2 G_2}\, d\theta_2^2$$

where
$$G_i = r\sin\omega\cdot\theta_i = (r^2\theta_i^2 - (t - y\sqrt{c_i^{-2}-\theta_i^2}\,)^2)^{1/2}$$

$$\cos\omega = (t - y\sqrt{c_i^{-2}-\theta_i^2}\,)/r\theta_i \qquad (3.41)$$

$$\sin\omega = G_i/r\theta_i$$

and the path of each contour of integration is described later.

It is apparent from Eqs. (3.40) and (3.41) that hyperelliptic integrals must be evaluated in order to determine the axially symmetric quantities for the problem being considered. The numerical integration scheme which is used in this study to evaluate these integrals is described in detail in Chapter 5.

For the present we restrict our attention to the disturbances at points near the surface of the half space and just behind the fronts of the P, S, and head waves. It is only at points in these regions that the disturbances can be singular or discontinuous. The source of excitation is assumed to be a load of magnitude Ft^2 acting vertically downward at the origin for $t \geq 0$.

3.4.1.1. Disturbances on the Surface of the Half Space

At points on the surface of the half space the functions $G_i(\theta_i)$ can be simplified to the single expression

$$G(\theta) = r(\theta^2-\theta_0^2)^{1/2}$$

where $$\theta^2 = \theta_1^2 = \theta_2^2 = (t/r\cos\omega)^2$$

and $$\theta_0^2 = (t/r)^2.$$

Equations (3.41) can then be written more simply as follows:†

$$\dot{v}_y = \mathrm{Re}\left(\frac{F_i}{2\pi^2 r\mu}\int_C \frac{I_{11}(\theta^2)+I_{12}(\theta^2)}{R(\theta^2)\sqrt{\theta^2-\theta_0^2}}\,d\theta^2\right)$$

$$\dot{v}_r = \mathrm{Re}\left(\frac{-F}{2\pi^2 r\mu}\int_C \frac{I_{21}(\theta^2)+I_{22}(\theta^2)}{R(\theta^2)\sqrt{\theta^2-\theta_0^2}}\,d\theta^2\right)$$

$$\dot{\sigma}_r = \mathrm{Re}\left(\frac{F}{2\pi^2 r}\int_C \frac{I_{31}(\theta^2)+I_{32}(\theta^2)}{R(\theta^2)\sqrt{\theta^2-\theta_0^2}}\,d\theta^2\right) \qquad (3.42)$$

$$\dot{\sigma}_\omega = \mathrm{Re}\left(\frac{F}{2r\pi^2}\int_C \frac{I_{41}(\theta^2)+I_{42}(\theta^2)}{R(\theta^2)\sqrt{\theta^2-\theta_0^2}}\,d\theta^2\right)$$

$$\dot{\sigma}_y = \mathrm{Re}\left(\frac{F}{2r\pi^2}\int_C \frac{d\theta^2}{\sqrt{\theta^2-\theta_0^2}}\right.$$

† The first pair of Eqs. (3.42) are equivalent to the equations obtained by Pekeris [35] for the displacements on the y = 0 surface when a point load of magnitude 2F acts vertically downward at the origin for all $t \geq 0$. This problem was solved by Laplace transform methods.

$$\dot{\tau}_{ry} = \dot{\tau}_{r\omega} = \dot{\tau}_{y\omega} = 0$$

where

$$I_{11}(\theta^2) = +(b^{-2}-2\theta^2)\sqrt{\theta^2-a^{-2}} \qquad I_{12}(\theta^2) = +2\theta^2\sqrt{\theta^2-a^{-2}}$$

$$I_{21}(\theta^2) = (b^{-2}-2\theta^2)\theta\cos\omega \qquad I_{22}(\theta^2) = -2\theta\sqrt{a^{-2}-\theta^2}\sqrt{b^{-2}-\theta^2}\cos\omega$$

$$I_{31}(\theta^2) = (b^{-2}-2a^{-2}+2\theta^2\cos^2\omega)(b^{-2}-2\theta^2) \qquad (3.43)$$

$$I_{32}(\theta^2) = -4\theta^2\cos^2\omega\sqrt{a^{-2}-\theta^2}\sqrt{b^{-2}-\theta^2} \qquad \cos\omega = \frac{\theta_0}{\theta}$$

$$I_{41}(\theta^2) = (b^{-2}-2a^{-2}+2\theta^2\sin^2\omega)(b^{-2}-2\theta^2) \qquad \sin\omega = \frac{\sqrt{\theta^2-\theta_0^2}}{\theta}$$

$$I_{42}(\theta^2) = -4\theta^2\sin^2\omega\sqrt{a^{-2}-\theta^2}\sqrt{b^{-2}-\theta^2}$$

The integrand of each of these equations is analytic at every point on the real axis to the left of $\theta^2 = a^{-2}$. Consequently, the contour of integration, which begins and ends at $\theta_0^2 = (t/r)^2$, must cross the axis to the left of $\theta^2 = a^{-2}$. In the work that follows it is convenient to integrate along either one or the other of the curves C_2 and C_3 of Fig. 11.

By a straightforward but tedious calculation (see Pekeris [35]), the solution of Eqs. (3.42) can be expressed in terms of Bessel functions. However, a qualitative estimate of the disturbances and an exact determination of the surface wave disturbances can be obtained more conveniently with the aid of the results of Sec. 3.3.2. For example, if the point at which the disturbances are being calculated is on the surface between the P and S waves, the value of θ_0^2 at that point is greater than a^{-2} but less than b^{-2}. That is, $a^{-2} < \theta_0^2 < b^{-2}$. The integrands of the first four of Eqs. (3.42) are non-analytic for every value of θ^2 between a^{-2} and b^{-2}. It follows directly

from the results of Sec. 3.3.2 that the first derivatives with respect to time of v_y, v_r, σ_r and σ_ω are functions of θ_0^2 which vary continuously for all values of θ_0^2 between a^{-2} and b^{-2}. Since $\theta_0 = t/r$, these stresses and velocities at the point in question must vary continuously during the interval of time in which that point is between the P and S waves.†

For a point which lies between the surface and shear waves the value of θ_0^2 is between b^{-2} and c^{-2}. If the surface wave has passed this point, the value of θ_0^2 is greater than c^{-2}. We note that the integrands of the first four of Eqs. (3.42) have a simple pole at the point $\theta^2 = c^{-2}$ where there is a zero in the Rayleigh function. With the exception of this point, the integrand of the first of Eqs. (3.42) is analytic for all θ^2 in the range $\theta_0^2 < \theta^2 < +\infty$, and the remaining integrands are analytic if θ^2 is in the range $b^{-2} < \theta^2 < \theta_0^2 < \infty$. The following equations can be obtained without difficulty if the first integral is evaluated along the contour C_2 of Fig. 11, and the other integrals are evaluated along the contour C_3 of the same figure:

for $t > rb$, i.e., $\theta_0^2 > b^{-2}$

$$\dot{v}_y = \frac{F}{2r\mu\pi} \frac{b^{-2}}{b^{-2}-a^{-2}} + \dot{v}_y^R$$

$$\dot{v}_r = \mathrm{Re}\left(\frac{-Ft}{r^2\pi^2\mu} \int_{b^{-2}}^{a^{-2}} \frac{I_{21} + I_{22}}{R(\theta^2)\sqrt{\theta^2-\theta_0^2}}\, d\theta^2\right) + \dot{v}_r^R \qquad (3.44)$$

---

† It is not difficult to show that the variation with time of the stresses and velocities is essentially quadratic at points just behind the front of the P wave.

$$\dot{\sigma}_r = \mathrm{Re}\left(\frac{F}{\pi^2 r}\int_{b^{-2}}^{a^{-2}} \frac{I_{31}+I_{32}}{R(\theta^2)\sqrt{\theta^2-\theta_0^2}}\,d\theta^2\right) + \dot{\sigma}_r^R$$

$$\dot{\sigma}_\omega = \mathrm{Re}\left(\frac{F}{\pi^2 r}\int_{b^{-2}}^{a^{-2}} \frac{I_{41}+I_{42}}{R(\theta^2)\sqrt{\theta^2-\theta_0^2}}\right) + \dot{\sigma}_\omega^R$$

$$\dot{\sigma}_y = 0 \qquad \text{for} \quad \theta_0^2 < +\infty \qquad (r \neq 0)$$

$$\dot{\tau}_{ry} = \dot{\tau}_{r\omega} = \dot{\tau}_{y\omega} = 0$$

where $\dot{v}_y^R$, $\dot{v}_r^R$, $\dot{\sigma}_r^R$ and $\dot{\sigma}_\omega^R$ symbolically denote surface wave disturbances, the values of which are determined from the residue of the integrands at the zero point of the Rayleigh function. It can easily be verified that these disturbances are defined as follows:

$$\dot{v}_y^R = 0 \qquad \text{for } c^{-2} < \theta_0^2 \quad \text{i.e.} \quad r > ct$$

$$= \frac{F_c}{\pi\mu}\,\frac{I_{11}(c^{-2})+I_{12}(c^{-2})}{R'(c^{-2})(r^2-c^2t^2)^{1/2}} \qquad \text{for } b^{-2} < \theta_0^2 < c^{-2}$$

$$\text{i.e. } ct < r < bt$$

$$\dot{v}_r^R = 0 \qquad \text{for } b^{-2} < \theta_0^2 < c^{-2}$$

$$= \frac{-cF}{\pi\mu}\,\frac{I_{21}(c^{-2})+I_{22}(c^{-2})}{R'(c^{-2})(c^2t^2-r^2)^{1/2}} \qquad \text{for } c^{-2} < \theta_0^2 \qquad (3.45)$$

$$\dot{\sigma}_r^R = 0 \qquad \text{for } b^{-2} < \theta_0^2 < c^{-2}$$

$$= \frac{Fc}{\mu\pi}\,\frac{I_{31}(c^{-2})+I_{32}(c^{-2})}{R'(c^{-2})(c^2t^2-r^2)^{1/2}} \qquad \text{for } c^{-2} < \theta_0^2$$

$$\dot{\sigma}_{\omega}^{R} = 0 \qquad \text{for } b^{-2} < \theta_0^2 < c^{-2}$$

$$= \frac{Fc}{\mu\pi} \frac{I_{41}(c^{-2}) + I_{42}(c^{-2})}{R'(c^{-2})(c^2t^2-r^2)^{1/2}} \qquad \text{for } c^{-2} < \theta_0^2$$

where $$R'(c^{-2}) = \frac{\partial R(\theta^2)}{\partial \theta^2}\Big|_{\theta^2=c^{-2}}$$

The first term in each of Eqs. (3.44) is a smoothly varying function of θ_0^2 for all θ_0^2 greater than b^{-2}. As θ_0^2 tends to infinity, each of these functions tends to a value which is independent of time and varies inversely as the distance from the point in question to the origin.

The quantities $\dot{v}_y^R$, $\dot{v}_r^R$, and $\dot{\sigma}_r^R$ and $\dot{\sigma}_{\omega}^R$ define disturbances which are singular at the position of the surface wave. The first of these is zero for θ_0^2 greater than c^{-2} ($r < ct$), whereas $\dot{v}_r^R$, $\dot{\sigma}_r^R$, and $\dot{\sigma}_{\omega}^R$ tend to values which vary as r^{-1} for large values of θ_0^2 ($r \ll ct$).

The vertical acceleration at any point on the $y = 0$ surface has a square-root singularity immediately prior to the arrival of the surface wave at that point. In contrast, each of the remaining non-zero disturbances has a square-root singularity immediately after the surface wave passes that point.

The right-hand side of Eqs. (3.45) can also be interpreted as the surface wave velocities and stresses for the problem in which the load at the origin is defined by the equation $P(t) = -2Ft$.

By further reinterpretations (see Sec. 3.4.1) the surface wave disturbances can be computed from Eq. (3.45) for any problem involving a load

$$P(t) = \frac{\partial^{1-n}(Ft^2)}{\partial t^{1-n}} \tag{3.46}$$

acting vertically downward at the origin.

3.4.1.2. The Surface Wave Disturbances

The surface wave disturbances at points below the y = 0 surface must be computed from Eqs. (3.40) since θ_1 and θ_2 have different values if $y > 0$. To illustrate how these disturbances are computed, consider the equation which defines $\dot{v}_y$ (the first of Eqs. (3.40)). It is convenient to rewrite this equation in the form

$$\begin{aligned}
\dot{v}_y(r,y,t) = \mathrm{Re}\ & \frac{iF}{2\pi^2\mu} \int_{C_1} \left(\frac{I_{11}(\theta^2)}{R(\theta^2)G_1} - \frac{I_{11}(c^{-2})}{rR'(c^{-2})(\theta^2-c^{-2})\sqrt{(\theta-\theta_1)(\theta+\bar{\theta}_1)}} \right) d\theta^2 \\
& + \mathrm{Re}\left(\frac{iF}{2\pi^2\mu} \int_{C_1} \frac{I_{11}(c^{-2})}{rR'(c^{-2})(\theta^2-c^{-2})\sqrt{(\theta-\theta_1)(\theta+\bar{\theta}_1)}}\, d\theta^2 \right) \\
& + \mathrm{Re}\ \frac{iF}{2\pi^2\mu} \int_{C_2} \left(\frac{I_{12}(\theta^2)}{R(\theta^2)G_2} - \frac{I_{12}(c^{-2})}{rR'(c^{-2})(\theta^2-c^{-2})\sqrt{(\theta-\theta_2)(\theta+\bar{\theta}_2)}} \right) d\theta^2 \\
& + \mathrm{Re}\ \frac{iF}{2\pi^2\mu} \int_{C_2} \frac{I_{12}(c^{-2})}{rR'(c^{-2})(\theta^2-c^{-2})\sqrt{(\theta-\theta_2)(\theta+\bar{\theta}_2)}}\, d\theta^2
\end{aligned} \tag{3.47}$$

where the contour C_i $(i = 1,2)$ begins at θ_i^2, crosses the real θ_i^2 axis to the left at a^{-2}, and ends at $\bar{\theta}_i^2$. Several contours of this type for various values of θ_i^2 are shown in Fig. 12a. It can easily be verified that only the second and fourth of these integrals define disturbances which vary rapidly in the vicinity of the surface wave. Evaluating this pair of integrals gives

the following result for $\dot{v}_y^R$, the surface wave component of v_y:

$$\dot{v}_y^R = \mathrm{Re}\ \frac{\dot{F}}{\pi\mu r R(c^{-2})}\left(\frac{I_{11}(c^{-2})}{\sqrt{c^{-1}-\theta_1}\sqrt{c^{-1}+\bar{\theta}_1}} + \frac{I_{12}(c^{-2})}{\sqrt{c^{-1}-\theta^2}\sqrt{c^{-1}+\bar{\theta}_2}}\right) \tag{3.48}$$

If θ_1 and θ_2 are expressed in terms of t, y and ξ ($\xi = r - ct$), the following infinite series approximation of $\dot{v}_y^R$ is obtained:

$$\begin{aligned}\dot{v}_y^R(\xi,y,t) \simeq \mathrm{Re}\Bigg\{&\frac{F}{\sqrt{2}\,\pi\mu r^{1/2}R'(c^{-2})}\left(\frac{I_{11}(c^{-2})}{(\xi-iy\sqrt{1-c^2/a^2})^{1/2}}\right.\\ &\left.+\frac{I_{12}(c^{-2})}{(\xi-iy\sqrt{1-c^2/b^2})^{1/2}}\right) + O(\xi-iy\sqrt{1-c^2/a^2})^{1/2}\\ &+ O(\xi-iy\sqrt{1-c^2/b^2})^{1/2}\Bigg\}\end{aligned} \tag{3.49a}$$

where $\xi = r - ct$.

In a similar way it can be shown that

$$\begin{aligned}\dot{v}_r^R(\xi,y,t) \simeq \mathrm{Re}\Bigg\{&\frac{-Fc}{\sqrt{2}\,\pi\mu r^{1/2}R'(c^{-2})}\left(\frac{I_{21}(c^{-2})}{(-\xi+iy\sqrt{1-c^2/a^2})^{1/2}}\right.\\ &\left.+\frac{I_{22}(c^{-2})}{(-\xi+iy\sqrt{1-c^2/b^2})^{1/2}}\right)\\ &+ O(\xi-iy\sqrt{1-c^2/a^2})^{1/2} + O(\xi-iy\sqrt{1-c^2/b^2})^{1/2}\Bigg\}\end{aligned}$$

$$\dot{\sigma}_r^R(\xi,y,t) \simeq \mathrm{Re}\left\{\frac{Fc}{\sqrt{2}\,\mu\pi r^{1/2}R'(c^{-2})}\left(\frac{I_{31}(c^{-2})}{(-\xi+iy\sqrt{1-c^2/a^2})^{1/2}}\right.\right.$$

$$\left. + \frac{I_{32}(c^{-2})}{(-\xi+iy\sqrt{1-c^2/b^2})^{1/2}}\right)$$

$$\left. + O(\xi-iy\sqrt{1-c^2/a^2})^{1/2} + O(\xi-iy\sqrt{1-c^2/b^2})^{1/2}\right\}$$

$$\dot{\sigma}_\omega^R(\xi,y,t) \simeq \mathrm{Re}\left\{\frac{Fc}{\sqrt{2}\,\mu\pi r^{1/2}R'(c^{-2})}\left(\frac{I_{41}(c^{-2})}{(-\xi+iy\sqrt{1-c^2/a^2})^{1/2}}\right.\right.$$

$$\left. + \frac{I_{42}(c^{-2})}{(-\xi+iy\sqrt{1-c^2/b^2})^{1/2}}\right)$$

$$\left. + O(\xi-iy\sqrt{1-c^2/a^2})^{1/2} + O(\xi-iy\sqrt{1-c^2/b^2})^{1/2}\right\} \qquad (3.49b)$$

$$\dot{\sigma}_y^R(\xi,y,t) \simeq \mathrm{Re}\left\{\frac{F\quad(b^{-2}-2c^{-2})}{\sqrt{2}\,\mu\pi r^{1/2}R'(c^{-2})}\left(\frac{1}{(-\xi+iy\sqrt{1-c^2/a^2})^{1/2}}\right.\right.$$

$$\left. + \frac{1}{(-\xi+iy\sqrt{1-c^2/b^2})^{1/2}}\right)$$

$$\left. + O(\xi-iy\sqrt{1-c^2/a^2})^{1/2} + O(\xi-iy\sqrt{1-c^2/b^2})^{1/2}\right\}$$

$$\dot{\tau}_{ry}^R(\xi,y,t) \simeq \mathrm{Re}\left\{\frac{-\sqrt{2}\,Fc^{-1}(b^{-2}-2c^{-2})(c^{-2}-a^{-2})^{1/2}}{\mu\pi r^{1/2}R'(c^{-2})}\left(\frac{1}{(\xi-iy\sqrt{1-c^2/a^2})^{1/2}}\right.\right.$$

$$\left. - \frac{1}{(\xi-iy\sqrt{1-c^2/b^2})^{1/2}}\right)$$

$$+ O(\xi - iy\sqrt{1-c^2/b^2})^{1/2} + O(\xi - iy\sqrt{1-c^2/b^2})^{1/2}\Big\}$$

For points on the y = 0 surface, Eqs. (3.49) simplify to Eqs. (3.45).

It is apparent from Eqs. (3.49) that the magnitude of the disturbance in the vicinity of the surface wave depends on three factors. These are

1) the distance of the surface wave from the origin (the $r^{1/2}$ term),

2) the distance of the point in question from the location of the surface wave (the $(\xi - iy(1-c^2/c_i^2)^{1/2})^{1/2}$ term), and

3) the relative values of ξ and y.

At any given time, the magnitude of the disturbances at points along a ξ/y = constant ray through the surface wave vary inversely as the square root of the distance from the surface wave.

The variation of the accelerations along y = constant planes is shown in Figs. 13. The variation of the time derivative of the stresses along the same planes is shown in Figs. 14 and 15. These curves have been non-dimensionalized by plotting

$$\frac{\dot{v}_y^R(\frac{\xi}{\epsilon}, \frac{y}{\epsilon})}{|\dot{v}_r^R(0.0,0.1)|}, \quad \frac{\dot{v}_r^R(\frac{\xi}{\epsilon}, \frac{y}{\epsilon})}{|\dot{v}_r^R(0.0,0.1)|}, \quad \frac{\dot{\sigma}_r^R(\frac{\xi}{\epsilon}, \frac{y}{\epsilon})}{|\dot{\sigma}_r^R(0.0,0.1)|},$$

$$\frac{\dot{\sigma}_\omega^R(\frac{\xi}{\epsilon}, \frac{y}{\epsilon})}{|\dot{\sigma}_r^R(0.0,0.1)|}, \quad \frac{\dot{\sigma}_y^R(\frac{\xi}{\epsilon}, \frac{y}{\epsilon})}{|\dot{\sigma}_r^R(0.0,0.1)|}, \quad \frac{\dot{\tau}_{ry}(\frac{\xi}{\epsilon}, \frac{y}{\epsilon})}{|\dot{\sigma}_r^R(0.0,0.1)|}$$

vs ξ/ϵ, where ϵ is a fixed distance below the surface wave. These curves have been drawn assuming a value of Poisson's ratio equal to 0.25, for which $\lambda = \mu$, $b^{-2} = 3a^{-2}$ and $c^{-2} = ((3 + 3^{1/2})/4)b^{-2}$.

The curves of Fig. 13 can obviously be reinterpreted as

1) the velocities associated with a load $2Ft(t \geq 0)$,

2) the displacement associated with a load $2F(t \geq 0)$, or

3) the integral with respect to time of the displacements associated with an impulse 2F acting vertically downward at t = 0.

The curves of Figs. 14 and 15 can be reinterpreted in an analogous manner.

3.4.1.3. Disturbances Near the Front of the P Wave†

The stresses and velocities at points near the front of the P wave are calculated from the first integral of each of Eqs. (3.40). For each of these integrals the ends of the contour of integration are determined from the following equations:

$$\theta_{11}^2 = \bar{\theta}_{11}^2 = \left(\frac{rt - y\sqrt{((r^2+y^2)/a^2 - t^2)}}{r^2 + y^2}\right)^2 \qquad \text{for } t \leq t_p$$

$$\theta_{11}^2 = \bar{\theta}_{11}^2 = \frac{a^{-2}r^2}{(r^2 + y^2)} \qquad \text{for } t = t_p \qquad (3.50)$$

$$\theta_{11}^2 = \left(\frac{rt + iy\sqrt{((r^2+y^2)/a^2) - t^2}}{r^2 + y^2}\right)^2 \qquad \text{for } t \geq t_p$$

where t_p is the time at which the P wave reaches the point in question, and θ_{11} and $\bar{\theta}_{11}$ are the upper and lower limits of integration, respectively.

For the work that follows it is convenient to rewrite the final equation in the following form:

---

† It appears that Zvolinskii [24] was the first to show that the asymptotic character of the stress field near the wave fronts could be computed without difficulty using self-similar methods. The approach used in Secs. 3.4.1.3 and 3.4.1.4 is equivalent to but slightly more direct than employed by the above author.

$$\theta_{11}^2 = \left(\theta_p + \frac{r\Delta t + iy\sqrt{2t_p\cdot\Delta t+\Delta t^2}}{r^2 + y^2}\right)^2 \tag{3.51}$$

where $\theta_p = \theta_{11} = \overline{\theta}_{11}$ at time $t = t_p$ and $\Delta t = t - t_p$.

From Eq. (3.51) and the second of Eqs. (3.50) we note the following. If Δt is sufficiently small, and the point in question is below the surface of the half space, the straight line which joins θ_{11}^2 and $\overline{\theta}_{11}^2$ will cross the real θ_1^2 axis to the left of the point $\theta_1^2 = a^{-2}$. (See Fig. 12a.) Since each integrand† is analytic on the real θ_1^2 axis to the left of $\theta_1^2 = a^{-2}$, the straight line joining θ_{11}^2 and $\overline{\theta}_{11}^2$ is a suitable contour of integration for each of the integrals being considered. These integrals are hyperelliptic, and it is inconvenient, in general, to express the solutions in closed form. However, if the integrands are approximated by the particular infinite series which are derived in the work that follows, the value of each of the integrals can be determined to any specified degree of accuracy.

Consider, for example, the integral which defines the P-wave component of the vertical acceleration. The $(a^{-2}-\theta^2)^{1/2}\Phi'/2\theta_1$ portion of the integrand of that integral is a function which is real-valued and analytic at every point on the real axis to the left of $\theta_1^2 = a^{-2}$. If this function is expanded in a Taylor series about the point $\theta_1^2 = \theta_p^2$, the following infinite series is obtained:

$$A(\theta_1^2) \simeq A_0 + A_1(\theta_1^2-\theta_p^2) + A_2(\theta_1^2-\theta_p^2)^2 + \ldots \tag{3.52}$$

where

$$A(\theta_1^2) = (a^{-2}-\theta_1^2)^{1/2}\Phi'/2\theta_1 \ , \ A_0 = A(\theta_1^2)\Big|_{\theta_1^2=\theta_p^2} \tag{3.53}$$

---

† That is, the integrand of the first integral of each of Eqs. (3.40).

$$A_1(\theta) = \left.\frac{dA(\theta_1^2)}{d\theta_1^2}\right|_{\theta_1^2=\theta_p^2} \quad , \qquad A_2 = \frac{1}{2!}\left.\frac{d^2A(\theta_1^2)}{d(\theta_1^2)^2}\right|_{\theta_1^2=\theta_p^2}$$

and so on.

Now consider the function $G_1(\theta_1)$ which is defined by Eq. (3.41). It is not difficult to show that this function can be rewritten in the form

$$G_1(\theta_1) = (r^2+y^2)^{1/2}(\sqrt{a^{-2}-\theta_{11}^2} - \sqrt{a^{-2}-\theta_1^2})^{1/2}(\sqrt{a^{-2}-\theta_1^2} - \sqrt{a^{-2}-\bar{\theta}_{11}^2})^{1/2} \tag{3.54}$$

It is apparent from Eq. (3.54) that $G_1(\theta_1)$ is zero at points where $(a^{-2}-\theta_1^2)^{1/2} = (a^{-2}-\theta_{11}^2)^{1/2}$ and where $(a^{-2}-\theta_1^2)^{1/2} = (a^{-2}-\bar{\theta}_{11}^2)^{1/2}$, i.e. at the points $\theta_1^2 = \theta_{11}^2$ and $\theta_1^2 = \bar{\theta}_{11}^2$. Expansion of the first of the two $(a^{-2}-\theta_1^2)^{1/2}$ radicals about the point θ_{11}^2 and the second about the point $\bar{\theta}_{11}^2$ results in the following expressions:

$$G_1(\theta_1) \simeq \frac{((\theta_{11}^2-\theta_1^2)(\theta_1^2-\bar{\theta}_{11}^2))^{1/2}(r^2+y^2)^{1/2}}{2((a^{-2}-\theta_{11}^2)(a^{-2}-\bar{\theta}_{11}^2))^{1/4}} \times \left[1 + \frac{1}{4}\frac{\theta_1^2-\theta_{11}^2}{a^{-2}-\theta_{11}^2} + \frac{1}{4}\frac{\theta_1^2-\bar{\theta}_{11}^2}{a^{-2}-\bar{\theta}_{11}^2} + \cdots\right]^{1/2} \tag{3.55}$$

The infinite series approximation of the vertical acceleration near the wave front can now be determined by a term-by-term integration of the infinite series approximation of the function $A(\theta_1^2)/G_1(\theta_1^2)$. The following result is obtained:†

† Here, and in the work which follows, the superscripts P and S denote, respectively, the P- and S-wave components of the particular quantity being considered. Hence,

$$v_y = v_y^P + v_y^S \ , \quad \sigma_r = \sigma_r^P + \sigma_r^S \ , \text{ etc.}$$

$$\frac{\partial v_y^P}{\partial t} = 0 \qquad \text{for } t < t_p$$

$$\simeq \frac{2((a^{-2}-\theta_{11}^2)(a^{-2}-\bar{\theta}_{11}^2))^{1/4}}{(r^2+y^2)^{1/2}} \quad x \qquad (3.56)$$

$$\left[A_0\pi + A_1\pi \frac{\theta_{11}^2 + \bar{\theta}_{11}^2 - 2\theta_p^2}{2} + O(\bar{\theta}_{11}^2-\theta_{11}^2)^2\right] \quad \text{for } t_p \leq t$$

To determine the variation with time of the vertical acceleration, Eqs. (3.50) are used to express θ_{11}^2 and $\bar{\theta}_{11}^2$ as functions of r, y, t and t_p. The final result of this operation is the equation

$$\frac{\partial v_y^P}{\partial t} = 0 \qquad \text{for } t < t_p$$

$$\simeq \frac{2y\pi}{a(r^2+y^2)}\left[A_0 + O(t-t_p)\right] \qquad \text{for } t \geq t_p \qquad (3.57)$$

where $$A_0 = \frac{(a^{-2}-\theta_p^2)^{1/2}\Phi'(\theta_p)}{2\theta_p} = \frac{F(a^{-2}-\theta_p^2)^{1/2}(b^{-2}-2\theta_p^2)}{2\mu\pi^2 R(\theta_p^2)}$$

The coefficients of the time dependent terms in Eq. (3.57) can be determined in a straightforward manner from Eqs. (3.50) and (3.56).

It follows from Eq. (3.57) that the vertical components of the velocity and displacement vectors are approximated near the front of the P wave by the equations

$$v_y^P = u_y^P = 0 \qquad \text{for} \qquad t < t_p$$

$$v_y^P \simeq \frac{2y\, A_0\pi(t-t_p)}{a(r^2+y^2)} + O(t-t_p)^2 \qquad (3.58)$$

$$u_y^P \simeq \frac{y A_0 \pi (t-t_p)^2}{a(r^2+y^2)} + O(t-t_p)^3$$

With the same method that was used to determine Eqs. (3.57) and (3.58), we obtain the following series approximations for the stresses, radial velocity and radial displacement at points near the front of the P wave.

$$v_r^P = u_r^P = \sigma_r^P = \sigma_y^P = \sigma_\omega^P = \tau_{ry}^P \qquad \text{for } t < t_p$$

$$v_r^P \simeq \frac{y\pi}{a(r^2+y^2)} \Phi'(\theta_p)(t-t_p) + O(t-t_p)^2$$

$$u_r^P \simeq \frac{y\pi}{2a(r^2+y^2)} \Phi'(\theta_p)(t-t_p)^2 + O(t-t_p)^3 \qquad (3.59)$$

$$\sigma_y^P \simeq \frac{-y\pi\mu}{a(r^2+y^2)} \frac{(b^{-2}-2\theta_p^2)}{\theta_p} \Phi'(\theta_p)(t-t_p) + O(t-t_p)^2$$

$$\sigma_r^P \simeq \frac{-y\pi\mu}{a(r^2+y^2)} \frac{(b^{-2}-2a^{-2}+2\theta_p^2)}{\theta_p} \Phi'(\theta_p)(t-t_p) + O(t-t_p)^2$$

$$\sigma_\omega^P \simeq \frac{-y\pi\mu}{a(r^2+y^2)} \frac{(b^{-2}-2a^{-2})}{\theta_p} \Phi'(\theta_p)(t-t_p) + O(t-t_p)^2$$

$$\tau_{ry}^P = \frac{-y\pi\mu}{a(r^2+y^2)} (a^{-2}-\theta_p^2)^{1/2} \Phi'(\theta_p)(t-t_p) + O(t-t_p)^2$$

It is apparent that the first term of each of the above series can be obtained without computation once the potentials which defines the corresponding two-dimensional disturbance have been determined.

The character of the disturbances at points near the front of the P wave can be summarized as follows:

1) Once the P wave passes any point, the stresses and velocities at that point increase linearly from zero with time. The displacements at a point just behind the front are proportional to the square of the time which has elapsed since the arrival of the P wave at that point.

2) At a point which is just behind the front, the rate at which the stresses, velocities, and displacements increase with time is inversely proportional to the distance of that point from the origin.

3) The first derivative with respect to time of the velocities and stresses are functions which are zero beyond the front of the P wave, experience a step discontinuity right at the front, and are essentially constant at points which are just behind the front.

3.4.1.4. Disturbances Near the Fronts of the Head and S Waves

For the half space problem being considered, the front of the equivoluminal component of the disturbances is defined at any time by the equations

$$\begin{aligned} r^2 + y^2 &= b^2 t^2 \quad \text{for} \quad \frac{r}{y} > \frac{b}{\sqrt{a^{-2}-b^{-2}}} \\ r a^{-1} + y\sqrt{b^{-2}-a^{-2}} &= t \quad \text{for} \quad \frac{r}{y} < \frac{b}{\sqrt{a^{-2}-b^{-2}}} \end{aligned} \tag{3.60}$$

The first of these equations defines the front of the S wave; the second defines the front of the head wave. The position of these fronts relative to each other is shown schematically in Fig. 18.

The equivoluminal components of the stresses and velocities at any point in the half space are calculated from the second integral of each of Eqs. (3.40). For these integrals, the ends of the contour of integration are defined by the following equations:

$$\theta_{22}^2 = \overline{\theta}_{22}^2 = \left(\frac{rt - y\sqrt{(r^2+y^2)^3/b^2-t^2}}{r^2+y^2}\right)^2 \qquad \text{for } t \leq t_s$$

$$\theta_{22}^2 = \overline{\theta}_{22}^2 = \frac{b^{-2}r^2}{(r^2+y^2)} \qquad \text{for } t = t_s \tag{3.61}$$

$$\theta_{22}^2 = \left(\theta_s + \frac{r\Delta t + iy\sqrt{2t_s\Delta t+(\Delta t)^2}}{r^2+y^2}\right)^2 \qquad \text{for } t > t_s$$

where $\overline{\theta}_{22}^2$ and θ_{22}^2 are the upper and lower limits of integration, respectively; t_s is the time at which the S wave reaches the point in question; $\Delta t = t - t_s$; and $\theta_s = \theta_{22} = \overline{\theta}_{22}$ at $t = t_s$. With the exception of points on the surface of the half space, the value of θ_s^2 is always less than b^{-2}. It can easily be shown that the value of θ_s^2 will be greater than a^{-2} if a head wave passes through the point in question, and less than a^{-2} if no head wave passes through that point.

If no head wave passes through the point being considered,† the straight line joining θ_{22}^2 and $\overline{\theta}_{22}^2$ will lie to the left of $\theta_2^2 = a^{-2}$ for sufficiently small values of Δt. For these problems, the shear wave component of the stresses, velocities and displacements near the front of the S wave can be calculated by the same method which was used to calculate the disturbances behindthe front of the P wave. The following results are obtained:

---

† Any point, where the ratio of r to y is less than $b/(a^2-b^2)^{1/2}$.

$$
\begin{aligned}
v_y^s &\simeq \frac{-y\pi}{b(r^2+y^2)}\,\Psi'(\theta_s)(t-t_s) + O(t-t_s)^2 \\
u_y^s &\simeq \frac{-y\pi}{2b(r^2+y^2)}\,\Psi'(\theta_s)(t-t_s)^2 + O(t-t_s)^3 \\
v_r^s &\simeq \frac{y\pi}{b(r^2+y^2)}\,\frac{\sqrt{b^{-2}-\theta_s^2}}{\theta_s}\,\Psi'(\theta_s)(t-t_s) + O(t-t_s)^2 \\
u_r^s &\simeq \frac{y\pi}{2b(r^2+y^2)}\,\frac{\sqrt{b^{-2}-\theta_s^2}}{\theta_s}\,\Psi'(\theta_s)(t-t_s)^2 + O(t-t_s)^3 \\
\sigma_y^s &\simeq \frac{2y\pi\mu}{b(r^2+y^2)}\,\sqrt{b^{-2}-\theta_s^2}\;\Psi'(\theta_s)(t-t_s) + O(t-t_s)^2 \\
\sigma_r^s &\simeq \frac{-2y\pi\mu}{b(f^2+y^2)}\,\sqrt{b^{-2}-\theta_s^2}\;\Psi'(\theta_s)(t-t_s) + O(t-t_s)^2 \\
\sigma_\omega^s &\simeq 0 + O(t-t_s)^2 \\
\tau_{ry}^s &\simeq \frac{-y\pi\mu}{b(r^2+y^2)}\,\frac{b^{-2}-2\theta_s^2}{\theta_s}\,\Psi'(\theta_s)(t-t_s) + O(t-t_s)^2
\end{aligned}
\tag{3.62}
$$

If a head wave passes through the point being considered, it will do so before the arrival of the S wave at that point (see Figs. 16 and 17). During the interval of time when the point is behind the front of the head wave but beyond the front of the S wave, the end points of the contour of integration are real, equal and lie on the real axis between a^{-2} and θ_s^2. That is, $a^{-2} < \theta_{22}^2 = \bar{\theta}_{22}^2 < \theta_s^2$, where θ_{22}^2 and $\bar{\theta}_{22}^2$ are defined by the first of Eqs. (3.61).

Since the integrands from which the disturbances are being calculated are not analytic on the real θ_2^2 axis between a^{-2} and b^{-2}, the contour of integration must not cross the axis to the right of $\theta_2^2 = a^{-2}$.

It is convenient to select the contour of integration C_5 which is shown in Figs. 12a. This contour lies just above the real θ_2^2 axis in passing from θ_{22}^2 to a^{-2}, and just below the real axis in passing from a^{-2} to $\overline{\theta}_{22}^2$. Near the point a^{-2} the contour is deformed into the "almost-closed" circle shown in Fig. 12a.

The radical $(a^{-2} - \theta_2^2)^{1/2}$, which occurs in each of the integrands being considered, has negative imaginary values on the portion of the contour above the real axis, and positive imaginary values on the contour below the real axis. Since this term forms part of the Rayleigh function,† this function is complex-valued in the range $a^{-2} < \theta_2^2 < b^{-2}$.

For the calculations that follow, it is convenient to rationalize the denominator of each integrand by multiplying both the numerator and denominator by the conjugate of the Rayleigh function. Then the head wave component of the vertical acceleration, for example, is defined by the integral

$$\dot{v}_y^s = -\frac{F}{\mu\pi^2}\int_{C_5} \frac{2\theta_2^2(b^{-2}-2\theta_2^2)^2\sqrt{a^{-2}-\theta_2^2}}{R(\theta_2^2)\,\overline{R(\theta_2^2)}\,G_2(\theta_2)}\,d\theta_2^2 - \int_{C_5} \frac{8\theta_2^4(a^{-2}-\theta_2^2)\sqrt{b^{-2}-\theta_2^2}}{R(\theta_2^2)\,\overline{R(\theta_2^2)}\,G_2(\theta_2)}\,d\theta_2^2 \tag{3.63}$$

where $G_2(\theta_2)$ denotes the function defined by Eq. (3.41).

The integrand of the second integral is analytic at every point on the real axis to the left of θ_{22}^2. Consequently, the value of this integral

† $R(\theta^2) = (b^{-2}-2\theta^2)^2 + 4\theta^2(a^{-2}-\theta^2)^{1/2}(b^{-2}-\theta^2)^{1/2}$

is zero. It follows that the head wave component of the vertical acceleration is completely defined by the first of the integrals of Eq. (3.63).

To determine the character of $\dot{v}_y^S$ at points near the front of the head wave, we approximate the integrand of the first integral of Eq. (3.63) by a series and then integrate this series term-by-term. The asymptotic expansion of $G_2(\theta_2)$ about the point $\theta_2^2 = \theta_{22}^2$ results in the following infinite series:

$$G_2(\theta_2) \simeq i((r^2+y^2)(\theta_{22}^2-\theta_2^2))^{1/2}\, B_0[1 + B_1(\theta_2^2-\theta_{22}^2) + \ldots]$$

where $$i = (-1)^{1/2}, \quad B_0 = \left(1 - \frac{ty}{(r^2+y^2)\sqrt{b^{-2}-\theta_{22}^2}}\right)^{1/2} \tag{3.64}$$

and $$B_1 = -\frac{1}{8}\,\frac{ty}{(b^{-2}-\theta_{22}^2)((r^2+y^2)\sqrt{b^{-2}-\theta_{22}^2} - ty))}$$

Consequently, the integrand being considered can now be written in the form

$$\frac{(a^{-2}-\theta_2^2)^{1/2}}{i(\theta_{22}^2-\theta_2^2)^{1/2}}\,\frac{A(\theta_2^2)}{(B_0+B_1(\theta_2^2-\theta_{22}^2)+\ldots..)(r^2+y^2)^{1/2}} \tag{3.65}$$

where $A(\theta_2^2)$ denotes the infinite series obtained by expanding

$$\frac{2\theta_2^2(b^{-2}-2\theta_2^2)^2}{R(\theta_2^2)\,\overline{R(\theta_2^2)}}$$

about the point $\theta_2^2 = a^{-2}$. That is,

$$A(\theta_2^2) = \frac{2a^{-2}}{(b^{-2}-2a^{-2})^2} + O(\theta_2^2 - a^{-2})$$

If the right-hand side of Eq. (3.63) is multiplied by 2, the contour of integration can be reduced from C_5 to the straight line which joins θ_{22}^2 and a^{-2} and lies just above the real axis, i.e., the line along which $(a^{-2}-\theta_2^2)^{1/2}$ has negative imaginary values. When the integration is carried out, the following result is obtained:

$$\dot{v}_y^s \simeq - \frac{2a^{-2}F_\mu}{B_0(b^{-2}-2a^{-2})^2\pi} \frac{(\theta_{22}^2-a^{-2})}{(r^2+y^2)^{1/2}} + O(\theta_{22}^2-a^{-2})^2 \qquad (3.66)$$

Using Eq. (3.61), we obtain the following approximation of $\theta_{22}^2 - a^{-2}$ in the region near the front of the head wave:

$$\theta_{22}^2 - a^{-2} \simeq \frac{2(t-t_H)}{a} \frac{\sqrt{b^{-2}-a^{-2}}}{-\sqrt{b^{-2}-a^{-2}}\, x + ya^{-1}} + O(t-t_H)^2 \qquad (3.67)$$

where t_H is the time of arrival of the head wave at the point in question.

It follows from Eq. (3.66) and (3.67) that the dependence on time of the head wave component of the vertical acceleration at a point near the front of the head wave is defined by the equations

$$\begin{aligned} \dot{v}_y^s &= 0 \qquad \text{for } t < t_H \\ &\simeq + C_0 \frac{(t-t_H)}{(r^2+y^2)^{1/2}} + O(t-t_H)^2 \qquad \text{for } t \geq t_H \end{aligned} \qquad (3.68)$$

where $$C_0 = \left[\frac{4Fa^{-1}\mu}{\pi B_0(b^{-2}-2a^{-2})} \frac{\sqrt{b^{-2}-a^{-2}}}{(-\sqrt{b^{-2}-a^{-2}}\, x + ya^{-1})}\right]$$

Hence, the velocity and displacement are defined by the equations

$$v_y = + \frac{(t-t_H)^2}{(r^2+y^2)^{1/2}} \frac{C_0}{2} + O(t-t_H)^3$$

$$u_y = + \frac{(t-t_H)^3}{(r^2+y^2)^{1/2}} \frac{C_0}{6} + O(t-t_H)^4 \qquad (6.69)$$

It is apparent that the head wave component of the stresses, radial velocity and radial displacement can be found by computations which are similar to those used to obtain Eqs. (3.68) and (3.69).

3.5. Dynamic Disturbances in an Infinite Body†

Three-dimensional problems involving disturbances in an infinite medium are solved in the same manner as the corresponding two-dimensional problems solved in Sec. 2.7. That is, the infinite medium is divided into two half spaces on whose surfaces the boundary conditions can be determined from considerations of symmetry.

Consider, for example, the problem in which a load Ft^2 acts vertically downward at $r = 0$, $y = 0$ for all $t \geq 0$. It can easily be verified that this problem is equivalent to the superimposed half space problems for which the boundary conditions on the $y = 0$ surface are defined as follows:

---

† The problem of a time-dependent load concentrated at a point in an infinite body was solved initially by Kelvin (see Ref. [1], page 304).

1) for the $y \geq 0$ half space

$$u_r(r,0,t) = 0 \qquad \text{for} \quad 0 < r < \infty$$

$$\sigma_y(r,0,t) = 0 \qquad \text{for} \quad r > 0 \tag{3.70}$$

$$2\pi \int_0^{\epsilon} r\sigma_y(r,0,t)dr = -\frac{Ft^2}{2} \qquad \text{for} \quad \text{any } \epsilon > 0$$

2) for the $y \leq 0$ half space

$$u_r(r,0,t) = 0 \qquad \text{for } 0 < r < \infty$$

$$\sigma_y(r,0,t) = 0 \qquad \text{for } r > 0 \tag{3.71}$$

$$2\pi \int_0^{\epsilon} r\sigma_y(r,0,t)dr = \frac{Ft^2}{2}$$

It follows directly from the work of previous sections that the boundary conditions defined above will be satisfied if the self-similar potentials which solve the corresponding two-dimensional problem are defined on the $y = 0$ surface by the equations

$$\frac{\theta F}{2\pi^2} = \mu\left[(b^{-2}-2\theta^2)\Phi'(\theta) - 2\theta(b^{-2}-\theta^2)^{1/2}\Psi'(\theta)\right]$$
$$0 = \theta\Phi'(\theta) + (b^{-2}-\theta^2)^{1/2}\Psi'(\theta) \tag{3.72}$$

Solving Eqs. (3.72) gives

$$\Phi'(\theta_1) = \frac{\theta_1 Fb^2}{2\pi^2\mu}$$

$$\Psi'(\theta_2) = -\theta_2^2\, Fb^2/(2\pi^2\mu(b^{-2}-\theta_2^2)^{1/2})$$

The time rate of change of the stresses and velocities for this problem can be found directly from Eqs. (3.72) and (3.40). From these results the stress and velocity fields for the problem involving an impulse of magnitude 2F acting vertically downward at time t = 0 can be found by the method described in Sec. 3.4.1. Then, by superposition, the stress and displacement fields can be computed for any problem involving an arbitrarily distributed load in an infinite body.

4. DYNAMIC CONTACT PROBLEMS

4.1. Indentation by a Rigid Wedge-Shaped Die

4.1.1. General Remarks

In this section, self-similar solutions are obtained for the frictionless contact problem in which a rigid wedge-shaped die indents a homogeneous, linearly elastic half space at a constant rate. The die is assumed to be shallow enough that the usual assumptions of the small displacement theory of elasticity are satisfied. Moreover, it is assumed that displacements and velocities normal to the surface of the die are essentially normal to the original location of the $y = 0$ surface. Then, the condition of no friction between the die and the half space is expressed by the relation $\tau_{xy} = 0$ on $y = 0$.

Figure 16a shows the die at time $t = 0$ when it begins to indent the half space. The position of the die, the deformed shape of the $y = 0$ surface, and the location of the various wave fronts at some later time are shown schematically in Fig. 16b. The vertical scale has been greatly exaggerated for clarity.

If a wedge is pressed into the half space slowly enough, the speed α at which the boundary of the contact region moves outward along the $y = 0$ surface will be less than the speed of the Rayleigh wave, i.e. $\alpha < c$. For problems of this type, the wedge will be said to be indenting "slowly," or α will be said to lie in the slow range of contact speeds.

If the wedge indents the half space rapidly enough, the speed α will exceed the speed of the P wave, i.e. $\alpha > a$. For these problems, the wedge will be said to indent "superseismically." It will be seen later that

two intermediate possibilities must be considered separately for values of α in the range $c < \alpha < a$. If the boundary of the contact region is between the surface wave and the S wave, i.e. if $c < \alpha < b$, α will be said to be in the "first intermediate" range of contact speeds;† if the boundary of the contact region is between the S and P waves, i.e. $b < \alpha < a$, α will be said to be in the "second intermediate" range of contact speeds.

In the work that follows it will be shown that the distribution of the stress near the edge of the region of contact is significantly different for the four ranges of contact speed defined above.

It will also be shown that shock fronts are formed if the edge of the region of contact moves along the surface more rapidly than the S wave. If α is in the second intermediate range, i.e. $b < \alpha < a$, a single shock front, which is also associated with singularities in both the stress and velocity fields, is developed at each edge of the contact region. This front, which is shown in Fig. 18, propagates into the half space just like a Mach front with the same speed as the S wave. If the contact is superseismic, i.e. if $\alpha > a$, two shock fronts are developed at each edge of contact. One front is tangent to the front of the P wave; the second is tangent to the S wave. The first of these propagates with the speed of the P wave and the second with the speed of the S wave. These fronts are shown in Fig. 19.

It will be seen that the classical theory of elasticity predicts that the stresses will be singular beneath the apex of the die, along one of the Mach fronts mentioned above, and (for the two intermediate ranges of

---

† This range of speeds is quite small since the ratio c/b varies between 0.874 when Poisson's ratio is 0.0 and 0.955 when Poisson's ratio is 0.5.

contact speed) at the edge of the region of contract. The non-linear behavior of the half space in the regions near stress singularities is not considered in this study.

For static and dynamic contact problems, the deformations of the bodies as they come together must be considered in determining the location of the contact surface between them. This fact was overlooked by Kostrov [9] in treating the slowly indenting wedge and cone problems.†

It was incorrectly assumed in [9] that any point on the surface of the wedge (or cone) would come in contact with the half space at the instant at which it crossed the original position of the $y = 0$ surface. As a consequence of this assumption, Kostrov supposed that the boundary of the expanding region of contact would move along the $y = 0$ surface with a constant speed α which is related to the indentation velocity V and the apex angle of the die γ, by the incorrect equation

$$V = \alpha \tan \frac{(\pi - \gamma)}{2} \tag{4.1}$$

However, for subseismic contact problems, i.e. problems for which $\alpha < a$, points on the $y = 0$ surface generally have non-zero vertical displacements at the instant at which they come in contact with the die (see Figs. 16b, 17 and 18). As a result, the quantities V, γ and α are not related by Eq. (4.1). It turns out that Kostrov's results [9] are interpretable in the slow range as the correct solutions for wedges or cones with some different apex angle. In other words, the indentation velocity cannot be found from

---

† The problem in which a rigid, axially symmetric conical die is pressed without friction and at a constant rate into a half space is solved in Sec. 4.2.

Eq. (4.1). The relation between the correct indentation velocity and that calculated from Eq. (4.1) is shown in Fig. 24.

The method which Kostrov used in [9] to determine the contact stress beneath a slowly indenting wedge depended on the assumption that α would not vary with time. When the correct boundary condition is applied in the work that follows it is verified that α is constant for a constant velocity of indentation. Kostrov's method turns out to be applicable directly in the slow range and is easily extended to the three other ranges, in which Kostrov claimed no solution exists.

4.1.2. The Boundary and Initial Conditions

The elastic half space is assumed to be completely free of stress until $t = 0$. Thus, for $t < 0$

$$u_x = u_y = v_x = v_y = 0 \tag{4.2}$$

For $t > 0$, when the die is in contact with the half space, the only region of non-zero traction on the $y = 0$ surface is the normally stressed zone of contact beneath the wedge. Each of the surface points in this region has the same downward velocity as the wedge. Moreover, the slope of the $y = 0$ surface at each point in the region of contact is identical to the slope of that face of the wedge which is in contact with the point in question. Consequently, if γ, V and α denote, respectively, the apex angle of the die, the indentation velocity, and the speed of the boundary of the region of contact, the boundary conditions for this problem are defined as follows:

$$\begin{aligned}
\tau_{xy}(x,t) &= 0 \quad \text{for} \quad -\infty \leq x \leq +\infty \quad (-\infty \leq \theta_0 \leq +\infty) \\
\sigma_y(x,t) &= 0 \quad \text{for} \quad \alpha t < |x| \leq +\infty \quad (0 \leq |\theta_0| < \alpha^{-1}) \\
u_y(x,t) &= Vt - |x| \tan \frac{\pi-\gamma}{2} \quad \text{for} \quad |x| \leq \alpha t \quad (|\theta_0| \geq \alpha^{-1})
\end{aligned} \tag{4.3}$$

where α is as yet unknown and $\theta_0 = t/x$ as in previous chapters.

It follows from the initial conditions and Eqs. (4.3) that for subseismic problems ($\alpha < a$)

$$u_y(x,t) = 0 \qquad \text{for} \qquad at \leq |x| \quad (|\theta_0| \leq a^{-1}) \tag{4.4}$$

and for superseismic problems ($\alpha > a$)

$$u_y(x,t) = 0 \qquad \text{for} \qquad \alpha t \leq |x| \quad (|\theta_0| \leq \alpha^{-1}) \tag{4.5}$$

4.1.3. Additional Conditions Satisfied by the Solution of the Wedge Problem

In addition to causing Eqs. (4.3) to be satisfied, the normal traction $\sigma_y(x,t)$ must be such that

1) the deformed position of the $y = 0$ surface lies below the surface of the die at every point beyond the region of contact,
2) the stress field in the half space contains no singularity which is associated with a self-equilibrating disturbance, and
3) the force required to press the die into the half space be finite.

Moreover, if there is no bond developed between the die and the half space, then the normal traction must be compressive at every point of contact between the two bodies.

We will satisfy the second and third of the conditions listed above by requiring that the stress beneath the wedge be nowhere more singular than the stress at a point directly beneath a concentrated load of finite magnitude.

4.1.4. The Fundamental Integral Equations for the Solution of the Wedge Problem

Since the vertical displacement on the y = 0 surface is a homogeneous function of degree +1 of x and t, the stresses and velocities at every point in the half space must be homogeneous functions of degree 0 of x, y, and t.† Consequently, the complex-valued quantities σ_x^*, σ_y^*, σ_z^*, τ_{xy}^*, v_x^* and v_y^*, whose real parts are equal to the actual stresses and velocities, are self-similar functions of θ_1 and θ_2. Moreover, for the boundary conditions defined by Eqs. (4.3) to be satisfied, σ_y^*, τ_{xy}^*, and v_y^* must satisfy the following conditions:

$$\tau_{xy} = \text{Re}\ \tau_{xy}^*(\theta_0) = 0 \qquad \text{for} \quad -\infty \leq \theta_0 < +\infty \quad (-\infty < x < +\infty)$$

$$\sigma_y = \text{Re}\ \sigma_y^*(\theta_0) = 0 \qquad \text{for} \quad |\theta_0| < \alpha^{-1} \quad (x > \alpha t) \tag{4.6}$$

$$u_y = \text{Re} \int_0^t v_y^*(\theta)d\tau = Vt - |x| \tan\frac{\pi - \gamma}{2} \quad \text{for} \quad |\theta_0| \geq \alpha^{-1} \quad (x \leq \alpha t)$$

where $\vartheta_0 = \vartheta_1 = \vartheta_2 = t/x$ on y = 0 and $\vartheta = \tau/x$.

For the first condition to be satisfied, $\tau_{xy}^*(\vartheta_0)$ must be identically equal to zero, i.e. $\tau_{xy}^*(\theta_0) = 0$

As a consequence of the absence of shear on the boundary, the derivatives of σ_y^* and v_y^* are related by the equation (Eq. 2.96 of Sec. 2.8)

$$v_y^{*\prime}(\theta_0) = -\frac{\sqrt{a^{-2}-\theta_0^2}\ \sigma_y^{*\prime}(\theta_0)}{\mu b^2 R(\theta_0^2)} \tag{4.7}$$

† This follows from the work of Sec. 2.8.

Hence, it is convenient to rewrite the second and third of Eqs. (4.3) in the form

$$\sigma_y = \mathrm{Re}\int_0^{\theta_0} \sigma_y^{*'}(\theta)d\theta = 0 \qquad \text{for} \quad |\theta_0| < \alpha^{-1} \tag{4.8}$$

$$u_y = -\mathrm{Re}\int_0^t\int_0^{\theta} \frac{\sqrt{a^{-2}-\theta^2}\ \sigma_y^{*'}(\theta)}{\mu b^2 R(\theta^2)}\, d\theta dt = Vt - |x| \tan\frac{\pi-\gamma}{2} \quad \text{for} \quad |\theta_0| \geq \alpha^{-1} \tag{4.9}$$

The coupled integral equations defined by (4.8) and (4.9) are the fundamental integral equations for the problem being considered. It is apparent that the solution of these equations is facilitated by differentiating Eq. (4.9) once with respect to time. The result is

$$v_y = -\mathrm{Re}\int_0^{\theta_0} \frac{\sqrt{a^{-2}-\theta^2}\ \sigma_y^{*'}(\theta)}{\mu b^2 R(\theta^2)}\, d\theta = V \qquad \text{for} \quad |\theta_0| \geq \alpha^{-1} \tag{4.10}$$

At first sight it would appear that the specification of the vertical velocity at every point in the region of contact would be sufficient to guarantee that the displacements in this region be wedge-shaped. This is not the case since the vertical displacement of each surface point prior to the instant of contact with the die plays as important a rule in determining the total displacement of the y = 0 surface as does the displacement experienced by that point after contact. Thus, there may be several distributions of normal traction which satisfy the conditions of 4.1.3 and cause every surface point in the $|x| < \alpha t$ region to move vertically downward with the same velocity V. Consequently, if the wedge problem is solved in terms

of σ_y and v_y, rather than σ_y and u_y, the condition that the displacement in the region of contact be wedge-shaped must also be satisfied. That is, that

$$u_y(x,t) = Vt - |x| \tan \frac{\pi - \gamma}{2} \qquad \text{for } |x| < \alpha t \qquad (|\theta| > \alpha^{-1}) \qquad (4.11)$$

At this point, the results of Sec. 2.8 are applied to Eqs. (4.8) and (4.10) to determine certain properties of $\sigma_y^{*'}(\theta)$ which hold for all ranges of contact speed. These are

1) that $\sigma_y^{*'}(\theta)$ must be analytic for $|\theta| < \alpha^{-1}$ if $\sigma_y(\theta_0)$ is zero for $|\theta_0| > \alpha^{-1}$, and
2) that $(a^{-2}-\theta^2)^{1/2}\sigma_y^{*'}(\theta)/R(\theta^2)$, i.e. $v_y^{*'}(\theta)$, must be analytic for $|\theta| > \alpha^{-1}$ if $v_y(\theta_0)$ is constant for $|\theta_0| < \alpha^{-1}$.

Furthermore, for the conditions defined by Eqs. (4.4) and (4.5) to be satisfied, $v_y^{*'}(\theta)$ must be analytic for all $|\theta| < a^{-1}$ if $\alpha < a$ and analytic for all $|\theta| < \alpha^{-1}$ if $a < \alpha$. Consequently, the only possible non-analyticities of $\sigma_y^{*'}$ and $v_y^{*'}$ are at points of on the segements of the real θ axis denoted by the wide lines in Figs. 20 and 21.

4.1.4.1. A Slowly Indenting Wedge†

Since the Rayleigh function is analytic for all $|\theta| > c^{-1}$, the stress and velocity boundary conditions for a slowly indenting wedge ($c^{-1} < \alpha^{-1}$) will be satisfied if

1) $\sigma_y^{*'}(\theta)$ is analytic for all $|\theta| < \alpha^{-1}$, and if
2) the function $(a^{-2}-\theta^2)^{1/2}\sigma_y^{*'}(\theta)$ is analytic for all $|\theta| > \alpha^{-1}$. (See Fig. 20a.)

---

† This problem, which is shown schematically in Fig. 16b, was solved in a slightly different manner by Kostrov [9].

For these conditions to be satisfied, $\sigma_y^{*'}(\theta)$ must be a function of the form

$$\sigma_y^{*'}(\theta) = \sum_{n=-\infty}^{n=+\infty} F_n(\theta)(\alpha^{-2}-\theta^2)^{n+1/2} \tag{4.12}$$

where n is the integer and the $F_n(\theta)$'s are integral (entire) functions.

In order that the stresses be nowhere more singular than under a concentrated load of finite magnitude (see the second condition listed in Sec. 4.1.3), the highest allowable singularity in $\sigma_y^{*'}(\theta)$ at a point in the finite portion of the θ plane is a pole of order 2.† Moreover, as θ tends to infinity, the Laurent series expansion of $\sigma_y^{*'}(\theta)$ must be of the form

$$\lim_{\theta \to \infty} \sigma_y^{*'}(\theta) = C_0 + C_1\theta^{-1} + C_2\theta^{-2} + \ldots. \tag{4.13}$$

where the C_i's are constants. It follows from Eq. (4.13) and these additional restrictions that $\sigma_y^{*'}(\theta)$ must be a function of the form

$$\begin{aligned}\sigma_y^{*'}(\theta) = {} & iA_1/(\alpha^{-2}-\theta^2)^{1/2} + iA_2/(\alpha^{-2}-\theta^2)^{3/2} \\ & + iA_3\theta/(\alpha^{-2}-\theta^2)^{1/2} + iA_4\theta/(\alpha^{-2}-\theta^2)^{3/2}\end{aligned} \tag{4.14}$$

where the A_j's are constants and i has been introduced to simplify the calculations which follow.

---

† The function $\sigma_y^{*'}(\theta)$ for the problem in which a point load of magnitude Ft acts vertically downward at $x = \alpha t$ was found in Chapter 2 to be

$$\sigma_y^{*'}(\theta) = -F/(i\pi(1 - \alpha\theta)^2) \quad \text{for } \alpha \neq 0$$

$$= -F/i\pi \quad \text{for } \alpha = 0$$

The constants of Eq. (4.14) must be real-valued in order that the value of σ_y defined by Eq. (4.8) be zero for $|\theta_0| < \alpha^{-1}$, i.e. at points beyond the region of contact, and non-zero and varying for $|\theta_0| > \alpha^{-1}$, i.e. at points within the region of contact. It follows that the final pair of terms of Eq. (4.14) define tractions which are antisymmetric functions of θ (or x). Hence, A_3 and A_4 must be identically zero for the symmetric wedge problems being considered.

Then, from Eqs. (4.8) and (4.14), we find that

$$\begin{aligned} \sigma_y(x,t) &= 0 \qquad \text{for} \qquad |x| > \alpha t \\ &= -A_1 \cosh^{-1}\frac{\alpha t}{|x|} - A_2 \frac{\alpha^3 t}{(\alpha^2 t^2 - x^2)^{1/2}} \quad \text{for} \quad |x| < \alpha t \end{aligned} \tag{4.15}$$

Since each of the terms of Eq. (4.15) corresponds to a finite total force acting downward over the region of contact, only two conditions remain with which to evaluate A_1 and A_2.† These are the conditions which requires that the displacement be wedge-shaped in the region of contact, and the condition which requires that every point on the surface beyond the region of contact lie below the face of the indenting die.

The slope at any point on the surface of the half space resulting from the traction defined by Eq. (4.15) can be determined from the following equation:

$$\frac{\partial u_y}{\partial x} = \int_0^t \frac{\partial v_y(\theta)}{\partial x}\, dt = \mathrm{Re} \int_{-\theta_0}^{\theta_0} \frac{\theta(a^{-2}-\theta^2)^{1/2}\sigma_y^{*\prime}(\theta)}{2R(\theta^2)\mu b^2}\, d\theta \tag{4.16}$$

---

† It was incorrectly reasoned in [9] that infinite power would be required to impose the traction $\alpha^3 A_2 t/(\alpha^2 t^2 - x^2)^{1/2}$. Hence, Kostrov set $A_2 = 0$. This turns out to be correct for a slowly indenting wedge, but not for the reason stated by Kostrov.

where $\theta_0 = t/x$ and where the contour joining $-\theta_0$ and θ_0 lies entirely in the upper half of the complex θ plane. If $|\theta_0| > \alpha^{-1}$, i.e. for points in the region of contact, it is convenient to integrate along the contour shown in Fig. 10. This contour is formed by the semicircle at infinity and straight lines which lie just above the $|\theta| > |\theta_0|$ portions of the real θ axis. The following result is obtained:

$$\frac{\partial u_y(x,t)}{\partial x} = \frac{A_1 \pi}{4\mu(1-b^2/a^2)} \qquad \text{for} \quad |x| < \alpha t \tag{4.17}$$

irrespective of the value of A_2. Therefore,

$$A_1 = \frac{4\mu(1-b^2/a^2)\tan\frac{\pi - \gamma}{2}}{\pi} \tag{4.18}$$

Hence, the first stress distribution of Eq. (4.15) is compressive at each point in the region of contact and causes the wedge-shaped displacement shown in Fig. 22a. It also follows from Eq. (4.17) that the second stress distribution of Eq. (4.15) is associated with a displacement of the $y = 0$ surface which does not have a cusp at the origin, i.e. an expanding punch-like displacement of the type shown in Fig. 22b. It is apparent from these figures that any superposition of the two stress distributions in such a way that $\sigma_y \leq 0$ at every point will result in a deformation which violates the condition that the $y = 0$ surface lie below the face of the die at every point beyond the region of contact. Hence, $A_2 = 0$, and the contact stress beneath a slowly indenting wedge is defined by the equation

$$\sigma_y(x,t) = -\frac{4\mu}{\pi}(1-b^2/a^2)\tan\frac{\pi - \gamma}{2}\cosh^{-1}\frac{\alpha t}{|x|} \qquad \text{for} \quad |x| \leq \alpha t \tag{4.19}$$

The relationship which exists between α, V, γ, μ and b^2/a^2 is determined in Sec. 4.1.5.

The slowly indenting wedge problem is essentially solved since the stresses and velocities at any point in the half space can be determined in a straightforward manner from Eqs. (4.14) and (4.18) of this section and Eqs. (2.57), (2.87) and (2.88). Certain features of these disturbances are considered in Chapter 6.

In the following subsections, solutions which satisfy all the physical conditions of the wedge problem are obtained for the three ranges of contact speeds where Kostrov claimed solutions did not exist.

4.1.4.2. A Wedge Indenting in the First Intermediate Range of Contact Speeds

When the indentation velocity of the wedge is such that the contact speed is in the first intermediate range, i.e. $c < \alpha < b$, the vertical velocity is the same at every surface point in the region $0 \leq |x| < \alpha t$. It follows that $v_y^{*'}(\theta)$, i.e. $-(a^{-2}-\theta^2)^{1/2}\sigma_y^{*'}(\theta)/R(\theta^2)\mu b^2$, must be analytic for all θ in the range $|\theta| \geq \alpha^{-1}$, including the points $\theta = \pm c^{-1}$ where the Rayleigh function is zero (see Fig. 20b). For this to be so, $\sigma_y^{*'}(\theta)$ must be zero at $\theta = \pm c^{-1}$, i.e.

$$\sigma_y^{*'}(\theta)_{\theta=\pm c^{-1}} = 0 \tag{4.20}$$

This condition must be satisfied by the function which defines $\sigma_y^{*'}(\theta)$, in addition to all the conditions which applied for the slowly indenting wedge problem. It follows that

$$\sigma_y^{*'}(\theta) = iA_1/(\alpha^{-2}-\theta^2)^{1/2} + iA_2/(\alpha^{-2}-\theta^2)^{3/2} \tag{4.21}$$

where A_1 is defined by Eq. (4.18) and A_2 is chosen in such a way that (4.20) is satisfied. That is,

$$A_2 = -A_1(\alpha^{-2} - c^{-2})$$

It follows that the contact stress for this problem is defined by the equation

$$\sigma_y(x,t) = \frac{-4\mu}{\pi}(1-b^2/a^2)\tan\frac{\pi - \gamma}{2}\left(\cosh^{-1}\frac{\alpha t}{|x|} + \frac{\alpha^3 t\,(c^{-2}-\alpha^{-2})}{(\alpha^2 t^2 - x^2)^{1/2}}\right) \qquad (4.22)$$

The deformed shape of the y = 0 surface is shown in Fig. 17. The condition that each point beyond the region of contact lie below the face of the indenting die is obviously satisfied.

It is instructive to rewrite Eq. (4.21) in the form

$$\sigma_y^{*'}(\theta) = (iA_1/(\alpha^{-2}-\theta^2)^{1/2})\{(c^{-2}-\theta^2)/(\alpha^{-2}-\theta^2)\} \qquad (4.23)$$

The function within the braces can be considered as a correction factor needed to extend the solution for the slowly indenting wedge into the first intermediate range of contact speeds. This correction factor has two important properties. These are

1) a zero at the point at which the Rayleigh function is zero, and

2) a value which tends asymptotically to +1 as θ tends to infinity.

These properties extend the region of analyticity of $v_y^{*'}(\theta)$ without changing the slope of the y = 0 surface in the region of contact. Thus, Eqs. (4.19) and (4.22) define contact stresses for the same wedge. Only the speed of indentation and the speed of the boundary of the region of contact differ for the two problems.

4.1.4.3. A Wedge Indenting in the Second Intermediate Range of Contact Speeds

It follows from the remarks of the previous section that the contact stress beneath a wedge with apex angle γ, having a contact speed in the second intermediate range, i.e. $b < \alpha < a$, will be determined from a function of the form

$$\sigma_y^{*'}(\theta) = (iA_1(c^{-2}-\theta^2)/(\alpha^{-2}-\theta^2)^{3/2})F_{\alpha b}(\theta) \tag{4.24}$$

if a function $F_{\alpha b}(\theta)$ exists which is uniquely determined by the conditions

1) that $F_{\alpha b}(\theta)/R(\theta^2)$ be analytic for all real values of θ in the range $\alpha^{-1} \leq |\theta| \leq b^{-1}$,

2) that $F_{\alpha b}(\theta)$ be analytic except for real values of θ in the range $\alpha^{-1} \leq |\theta| < b^{-1}$, and

3) that $\lim_{\theta \to \infty} F_{\alpha b}(\theta) = 1$.

If the first condition is satisfied, $v_y^{*'}(\theta)$ will be analytic for all $|\theta| > \alpha^{-1}$ as required to ensure the constancy of v_y in the contact zone (see Fig. 21a). If the second condition is satisfied, $\sigma_y^{*'}(\theta)$ will be analytic for all $|\theta| < \alpha^{-1}$, and there will be no traction beyond the contact area. Finally, if the last condition is satisfied, the deflection of the surface of the solid will match the shape of the wedge.

The three conditions defined above are sufficient to determine uniquely the following relationship for $F_{\alpha b}(\theta)$ (see Appendix A):

$$F_{\alpha b}(\theta) = \exp \int_{\alpha^{-2}}^{b^{-2}} \frac{\beta(\lambda^2)}{\pi(\lambda^2-\theta^2)}\, d\lambda^2 \tag{4.25}$$

where $\beta(\lambda^2)$ is the argument of the Rayleigh function. The argument β is not zero since $R(\lambda^2)$ is complex-valued for all λ^2 in the range $a^{-2} < \lambda^2 < b^{-2}$. Straightforward computation gives

$$\beta(\lambda^2) = -\tan^{-1}\left\{\frac{4\lambda^2(\lambda^2-a^{-2})^{1/2}(b^{-2}-\lambda^2)^{1/2}}{(b^{-2}-2\lambda^2)^2}\right\} \tag{4.26}$$

It was not found convenient to try to express either the function $\sigma_y^{*'}(\theta)$ or the function which defines the contact stress in closed form. However, the distribution of σ_y has been determined numerically and is shown in Fig. 23c.

4.1.4.4. A Wedge Indenting Superseismically

For superseismic contact problems, i.e. problems for which $\alpha > 0$, no disturbances propagate along the surface more rapidly than the boundary of the region of contact. Hence, every point on the surface of the die which has crossed the original position of the $y = 0$ surface is in contact with the half space. It follows that points on the boundary experience a step discontinuity in the vertical velocity at the instant of contact. That is,

$$\begin{aligned} v_y(x,t) &= 0 \quad \text{for} \quad |x| > \alpha t \\ &= V \quad \text{for} \quad |x| < \alpha t \end{aligned} \tag{4.27}$$

It follows directly from Eq. (4.27) and the relations derived in Sec. 2.8 that $v_y^*(\theta)$ is analytic except at $\theta = \pm \alpha^{-1}$, where it has simple poles. (See Fig. 21b.) It can easily be verified that

$$v_y^{*'}(\theta) = \frac{2\alpha^{-1} V}{i\pi(\alpha^{-2}-\theta^2)} \tag{4.28}$$

and

$$\sigma_y^{*'}(\theta) = -\frac{\mu b^2 R(\theta^2) v_y^{*'}(\theta)}{(a^{-2}-\theta^2)^{1/2}} \tag{4.29}$$

For superseismic problems the indentation velocity, speed of the contact region, and apex angle are related by the equation†

$$V = \alpha \tan \frac{\pi - \gamma}{2}$$

Consequently, Eq. (4.29) can be rewritten as

$$\sigma_y^{*'}(\theta) = -\frac{R(\theta^2)}{i(a^{-2}-\theta^2)^{1/2}(\alpha^{-2}-\theta^2)} \times \frac{A_1}{2(b^{-2}-a^{-2})} \tag{4.30}$$

Hence,

$$\sigma_y(x,t) = 0 \qquad \text{for} \quad |x| > \alpha t \tag{4.31a}$$

$$= -\frac{A_1 R(\alpha^{-2})}{(a^{-2}-\alpha^{-2})^{1/2}} \frac{\pi}{4\alpha^{-1}(b^{-2}-a^{-2})} \quad \text{for} \quad at < |x| < \alpha t$$

$$\sigma_y(x,t) = \frac{-A_1}{2(b^{-2}-a^{-2})} \left\{ 4(b^{-2}-\alpha^{-2}) \cosh^{-1}\left(\frac{\theta}{a^{-1}}\right) - 2\theta\sqrt{\theta^2-a^{-2}} \right.$$

$$- 2a^{-2}\cosh^{-1}\left(\frac{\theta}{a^{-1}}\right)$$

$$+ \frac{(b^{-2}-2\alpha^{-2})^2}{\alpha^{-1}\sqrt{a^{-2}-\alpha^{-2}}} \operatorname{arctg} \frac{\theta\sqrt{a^{-2}-\alpha^{-2}}}{\alpha^{-1}\sqrt{\theta^2-a^{-2}}}$$

$$\left. + 4\alpha^{-1}\sqrt{b^{-2}-\alpha^{-2}} \cdot \frac{\pi}{2} \right\} \quad \text{for } bt < |x| < at$$

† This is the relationship which Kostrov assumed would hold for the slowly indenting wedge problem.

$$\sigma_y(x,t) = \frac{-A_1}{2(b^{-2}-a^{-2})}\left\{(4b^{-2}-4\alpha^{-2}-2a^{-2})\cosh^{-1}\left(\frac{\theta}{a^{-1}}\right)\right. \tag{4.31b}$$

$$+ 2\theta\left(\sqrt{\theta^2-b^{-2}} - \sqrt{\theta^2-a^{-2}}\right)$$

$$+ (4\alpha^{-2}-2b^{-2})\cosh^{-1}\left(\frac{\theta}{b^{-1}}\right)$$

$$+ \frac{(b^{-2}-2\alpha^{-2})^2}{\alpha^{-1}\sqrt{a^{-2}-\alpha^{-2}}}\operatorname{arctg}\frac{\theta\sqrt{a^{-2}-\alpha^{-2}}}{\alpha^{-1}\sqrt{\theta^2-a^{-2}}}$$

$$\left. + 4\alpha^{-1}\sqrt{b^{-2}-\alpha^{-2}}\operatorname{arctg}\frac{\theta\sqrt{b^{-2}-\alpha^{-2}}}{\alpha^{-1}\sqrt{\theta^2-b^{-2}}}\right\}$$

$$\text{for} \quad 0 < |x| < bt$$

where $\theta = t/x$.

It is apparent from Eq. (4.31) that points on the boundary experience a step discontinuity in σ_y at the instant at which they come in contact with the die. The magnitude of the normal stress remains constant at these points until the front of the P wave reaches them. Thereafter, the stresses vary continuously in the manner shown in Fig. 23d.

The four cases considered above completely solve the problem of a rigid wedge indenting a linearly elastic, homogeneous half space. The stresses and velocities at any point can be determined in a straightforward manner from Eqs. (2.57), (2.87) and (2.88), and the equation which defines $\sigma_y^{*\prime}(\theta)$ for the wedge problem being considered. A description of the stress and velocity fields for the four ranges of contact speed is presented in Chapter 6. The relationship between the force, the indentation velocity and the speed of the boundary of the contact region is considered in Secs. 4.1.5 and 4.1.6.

4.1.5. The Dependence of the Contact Speed on the Indentation Velocity

To determine the dependence of α on V, use is made of the second of Eqs. (2.88) which defines the vertical displacement at any point in the half space. This equation can be simplified to the following for a point which is directly beneath the apex of the die:

$$v_y(0,0,t) = -\mathrm{Re}\int_0^\infty \frac{i(a^{-2}+\lambda^2)^{1/2}\sigma_y^{*'}(i\lambda)}{\mu b^2\, R(-\lambda^2)}\, d\lambda \qquad (4.32)$$

where, to facilitate the computations, $i\lambda$ has been substituted for the dummy variable θ of Eq. (2.88).

Since $\sigma_y^{*'}$ is a function of α and V is equal to $v_y(0,0,t)$, Eq. (4.32) can be used to determine the relationship between V and α. This relationship is shown in non-dimensional form ($\frac{\alpha}{b}$ vs $\frac{\mu V}{A_1 b}$) in Fig. 24 for a material having a Poisson's ratio equal to 0.285.†

For superseismic problems ($\alpha > a$), the relationship between V and α is linear since, for these problems, $V = \alpha \tan\frac{\pi - \gamma}{2}$. Kostrov assumed that this relationship would hold for all values of α. This linear relationship is shown in non-dimensional form by the dashed line in Fig. 24. It is apparent from this figure that the greatest difference between the actual dependence of α on V and the linear dependence assumed by Kostrov occurs when the contact speed is in the slow range.

It follows from Eq. (4.32) and the equations which define $\sigma_y^{*'}$ that α is a monotonically increasing function of V. This result, which is

---

† This choice of Poisson's ratio follows from the assumption that the linearly elastic material being considered is steel or an alloy steel. The value of Poisson's ratio for these materials ranges between 0.26 and 0.30.

apparent from Fig. 24, is used in the following section where, among other things, the stability of the indenting wedge is considered.

4.1.6. The Force Required to Indent the Wedge

The force required to press the wedge into the half space in any range of contact speed can be determined from the following formula which was derived in Sec. 2.8:

$$P(t) = i\pi t\sigma_y^{*'}(0) \tag{4.33}$$

Hence, the indentation force for the wedge is defined as follows:

$$\begin{aligned} P(t) &= -\pi t A_1 \alpha && \text{for } \alpha < c \\ &= -\pi t A_1 \alpha^3/c^2 && \text{for } c < \alpha < b \\ &= -\pi t A_1 \alpha^3 F_{\alpha b}(0)/c^2 && \text{for } b < \alpha < a \\ &= -\pi t A_1 \frac{a\,\alpha^2}{2(1-b^2/a^2)b^2} && \text{for } a < \alpha \end{aligned} \tag{4.34}$$

where $A_1 = 4\mu(1-b^2/a^2)\tan\frac{\pi-\gamma}{2} / \pi$ and $F_{\alpha b}(0)$ can be determined from Eq. (4.25).

The indentation force increases linearly with time for all $t \geq 0$. The dependence of the rate of increase of this force, i.e. $\frac{\partial P}{\partial t}$, on the shape, shear modulus and contact speed is shown in non-dimensional form in Fig. 25.

$$\left(\frac{\partial P/\partial t}{A_1 \pi} \text{ vs } \frac{\alpha}{b}\right) \tag{4.35}$$

The relationship between V and α determined in the previous section is then

used to determine the dependence of $\partial P/\partial t$ on the indentation velocity. This is shown in non-dimensional form in Fig. 26

$$\left(\frac{\partial P/\partial t}{A_1 \pi} \quad \text{vs.} \quad \frac{\mu V}{A_1 b}\right). \tag{4.36}$$

It can easily be verified from Eqs. (4.33) and the equation defining $F_{\alpha b}(\theta)$ that P is a monotonically increasing function of α. Consequently, P is a monotonically increasing function of V since $\frac{\partial P}{\partial V} = \frac{\partial P}{\partial \alpha} \frac{\partial \alpha}{\partial V}$ and $\frac{\partial \alpha}{\partial V} > 0$. Hence, the operation of pressing a rigid wedge into a half space at a constant rate is stable; that is to say, a greater rate of penetration can be achieved only by an increase in the rate at which the force is applied to the wedge.

4.2. Indentation by a Rigid Conical Die

4.2.1. General Remarks

In this section, self-similar solutions are obtained for the frictionless contact problem in which a rigid, axially symmetric conical die is pressed at a constant rate into a homogeneous, linearly elastic half space. In every respect this problem is the three-dimensional analogue of the wedge problem solved in the previous section.

The cone problem is solved by determining, for each of the four ranges of contact speeds, the unique distribution of normal traction for which the boundary conditions and the additional physical constraints of the contact problem (see Sec. 4.1.3) are satisfied.

The method used by Kostrov [9] to solve the problem of a slowly indenting cone can be applied directly in the remaining ranges of contact

speed, i.e. in the ranges where Kostrov claimed solutions do not exist. As a result of the same misinterpretation of the boundary conditions that was made for the wedge problem (see Sec. 4.1.1), the solution obtained in [9] is valid for a cone having a different apex angle than assumed by Kostrov.

4.2.2. Boundary and Initial Conditions

If the conical die begins to indent the half space at t = 0, the boundary and initial conditions will be defined as follows:

$$\text{for } t < 0 \qquad u_r = u_y = v_r = v_y = 0$$

$$\text{and for } t \geq 0$$

$$\begin{aligned} &\tau_{ry}(r,t) = 0 && \text{for } 0 \leq r \leq \infty \\ &\sigma_y(r,t) = 0 && \text{for } \alpha t < r \leq \infty \\ &u_y(r,t) = Vt - r \tan \frac{\pi - \gamma}{2} && \text{for } 0 \leq r \leq \alpha t \end{aligned} \tag{4.37}$$

where V, γ and α are the indentation velocity, vertex angle of the cone, and speed of the boundary of contact, respectively.

It follows from the boundary and initial conditions that for subseismic problems ($\alpha < a$)

$$u_y(r,t) = 0 \qquad \text{for} \quad r > at, \tag{4.38}$$

and for superseismic problems ($\alpha > a$)

$$u_y(r,t) = 0 \qquad \text{for } r > \alpha t \tag{4.39}$$

Since the boundary conditions are self-similar, the cone problem can be solved in terms of a fictitious plane strain problem which has

self-similar stresses and velocities.† To determine the boundary conditions for the fictitious problem, we must solve the dual integral equations

$$\sigma_y = \mathrm{Re}\int_C \theta_0 \frac{\sigma_y^*(\theta^2)}{2\theta^2}\frac{d\theta^2}{\sqrt{\theta^2-\theta_0^2}} = 0 \qquad \text{for } r > \alpha t$$

$$u_y = \mathrm{Re}\int_0^t dt \int_C \theta_0 \frac{v_y^*(\theta^2)}{2\theta^2}\frac{d\theta^2}{\sqrt{\theta^2-\theta_0^2}} = Vt - r\tan\frac{\pi-\gamma}{2} \qquad \text{for } 0 \le r \le \alpha t \tag{4.40}$$

where $\theta_0 = t/r$, $\sigma_y^*(\theta^2)$ is the fictitious normal traction, $v_y^*(\theta^2)$ is the fictitious normal velocity, and C is any contour of the type shown in Fig. 11.

To facilitate the solution of Eqs. (4.40) the first of these equations is differentiated once with respect to time, and the second is differentiated twice with respect to time. The final result is

$$r\dot{\sigma}_y(\theta_0) = \mathrm{Re}\int_C \frac{\sigma_y^{*'}(\theta^2)d\theta^2}{\sqrt{\theta^2-\theta_0^2}} = 0 \qquad \text{for } r > \alpha t \quad (\theta_0 < \alpha^{-1})$$

$$r\dot{v}_y(\theta_0) = -\mathrm{Re}\int_C (a^{-2}-\theta^2)^{1/2}\sigma_y^{*'}(\theta^2)/\mu b^2 R(\theta^2)\frac{d\theta^2}{\sqrt{\theta^2-\theta_0^2}} \qquad \text{for } r \le \alpha t \quad (\theta_0 \ge \alpha^{-1}) \tag{4.41}$$

where C is any of the contours of Fig. 11 and $\sigma_y^{*'}(\theta^2) = \dfrac{d\sigma_y^{*'}(\vartheta^2)}{d\theta^2}$

† See the work of Sec. 3.3.2.

In differentiating Eqs. (4.40), the condition that the deformation of the boundary be conical has been lost. Hence, from the set of fictitious tractions which solve Eq. (4.41), we must select the single distribution of traction which causes a conical deformation and which satisfies the additional conditions listed in Sec. 4.1.3.

4.2.3. A Slowly Indenting Cone

The function $\sigma_y^{*'}$ from which the complete solution of the slowly indenting cone problem ($\alpha < C$) can be obtained is determined in the following manner. Using the relations of Sec. 3.3.2 and the boundary conditions of Eqs. (4.41), we find that $\sigma_y^{*'}(\theta^2)$ must be analytic for all $\theta^2 > \alpha^{-2}$ and for all $\theta^2 < \alpha^{-2}$. Hence, $\sigma_y^{*'}(\theta^2)$ must be a function, or linear superposition of functions, of the form $F_n(\theta^2)/(\alpha^{-2}-\theta^2)^n$ where n is a positive integer and $F_n(\theta^2)$ is a function which is analytic everywhere with the possible exception of the point at infinity.

Let us investigate whether the least singular of these functions is the solution for the problem being considered. That is, we determine the problem solved by

$$\sigma_y^{*'}(\theta^2) = A_1/(\alpha^{-2} - \theta^2) \tag{4.43}$$

where A_1 is a non-zero constant. The following result is obtained when the first of Eqs. (4.41) is integrated along the contour C_3 of Fig. 11:

$$\begin{aligned} r\dot{\sigma}_y(r,t) &= 0 && \text{for } \theta_0^2 < \alpha^{-2} \\ & && \text{i.e. for } \alpha t < r \\ &= -2\pi A_1/(\theta_0^2 - \alpha^{-2})^{1/2} && \text{for } \theta_0^2 > \alpha^{-2} \\ & && \text{i.e. for } \alpha t > r \end{aligned} \tag{4.44}$$

Hence $$\sigma_y(r,t) = 0 \qquad \text{for } \alpha t < r$$
$$= -2\pi A_1 \cosh^{-1}\frac{\alpha t}{r} \qquad \text{for } \alpha t > r \tag{4.45}$$

The slope of points on the y = 0 surface which results from this distribution of traction can be determined from the equation†

$$\frac{\partial u_y(x,y,t)}{\partial r} = -\,\mathrm{Re}\int_C \frac{\sqrt{\theta^2-\theta_0^2}\sqrt{a^{-2}-\theta^2}}{\mu b^2\, R(\theta^2)}\,\sigma_y^{*\prime}\,d\theta^2 \tag{4.46}$$

where C is any of the contours of Fig. 10. For points in the region of contact (where $\theta_0^2 > \alpha^{-2}$) integration along a contour such as C_1 of Fig. 10 gives the following result:

$$\frac{\partial u_y(r,0,t)}{\partial r} = -\frac{A_1\pi}{\mu(1-b^2/a^2)} \qquad \text{for } \theta_0^2 > \alpha^{-2} \quad (r < \alpha t) \tag{4.47}$$

Hence, the traction defined by Eq. (4.45) causes a conical deformation in the region of contact. Moreover, the deformed shape will match that of the rigid die, i.e. the second of Eqs. (4.40) will be satisfied, if A_1 is defined by the equation

$$A_1 = \frac{\mu}{\pi}(1 - b^2/a^2)\tan\left(\frac{\pi - \gamma}{2}\right) \tag{4.48}$$

Therefore,

$$\sigma_y(r,t) = -2\mu(1 - b^2/a^2)\tan\left(\frac{\pi - \gamma}{2}\right)\cosh^{-1}\frac{\alpha t}{r} \qquad \text{for } r \le \alpha t \tag{4.49}$$

---

† This equation is obtained by integrating Eq. (3.15) by parts and then changing the variable of integration from ω to θ^2.

It is not difficult to show that the deformed shape of the y = 0 surface lies beneath the surface of the cone at every point beyond the region of contact. Furthermore, the traction is compressive at every point in the region of contact and is nowhere more singular than at the vertex, where a logarithmic type of singularity occurs.† Thus, the additional conditions of 4.1.3 are satisfied and the problem of a slowly indenting cone is solved.

4.2.4. Solutions for the Remaining Ranges of Contact Speed

The solution for the remaining ranges of contact speed can be determined by modifying $\sigma_y^{*'}(\theta^2)$ by the same correction factors which were used in Sec. 4.1.4 to extend the solution for the slowly indenting wedge. The final result is

$$\begin{aligned}
\sigma_y^{*'}(\theta^2) &= A_1(c^{-2}-\theta^2)/(\alpha^{-2}-\theta^2)^2 && \text{for } c < \alpha < b \\
&= A_1(c^{-2}-\theta^2)/(\alpha^{-2}-\theta^2)^2 F_{\alpha b}(\theta) && \text{for } b < \alpha < a \\
&= \frac{A_1 R(\theta^2)}{2(b^{-2}-a^{-2})(\alpha^{-2}-\theta^2)^{3/2}(a^{-2}-\theta^2)^{1/2}} && \text{for } a < \alpha
\end{aligned} \tag{4.50}$$

where A_1 and $F_{\alpha b}(\theta)$ are defined by Eqs. (4.48) and (4.25), respectively.

The contact stress for a cone indenting in the first intermediate range of contact speeds is given by the equation

---

† For small values of r, $\cosh^{-1}\frac{\alpha t}{r}$ varies in the same manner as $\log\frac{\alpha t}{r}$.

$$\sigma_y = -2\mu(1-b^2/a^2)\tan\frac{\pi-\gamma}{2}\left(\cosh^{-1}\frac{\alpha t}{r} + \frac{c^{-2}-\alpha^{-2}}{2}\frac{t\alpha^3}{\sqrt{\alpha^2t^2-r^2}}\right)$$

$$\text{for } r < \alpha t \qquad (4.51)$$

$$= 0 \qquad \text{for } r > \alpha t$$

The contact stresses for the remaining two ranges of speed are not conveniently expressed in closed form. However, the variation of the contact stress near the edge of the region of contact is determined in Sec. 6.2.

The stress and velocity fields for this problem can be determined directly from the equations defining $\partial\sigma_y^*/\partial\theta$ and Eqs. (2.57), (2.87), (2.88) and (3.40). A description of these fields is presented in Chapter 6. The relationship between the force, the indentation velocity and the speed of the boundary of the contact region is considered in Secs. 4.2.5 and 4.2.6.

4.2.5. The Dependence of the Contact Speed on the Indentation Velocity

It follows from Eq. (2.57) and the first of Eqs. (3.40) that the vertical acceleration at any point on the x = 0 plane is defined by the equation

$$\frac{\partial v_y}{\partial t}(0,y,t) = \frac{2\pi(b^{-2}-2\theta_1^2)(a^{-2}-\theta_1^2)}{yR(\theta_1^2)}\sigma_y^{*\prime}(\theta_1^2)$$

$$+ \frac{4\pi\theta_2^2\sqrt{a^{-2}-\theta_2^2}\sqrt{b^{-2}-\theta_2^2}}{yR(\theta_2^2)}\sigma_y^{*\prime}(\theta_2^2) \qquad (4.52)$$

where $\quad t - y\sqrt{c_i^{-2}-\theta_i^2} = 0$

The relationship between V and α can be determined simply by integrating Eq. (4.52) with respect to time for a value of y which in the limit tends to 0. It is not difficult to verify that the following result is obtained:

$$V = v_y(0,0,t) = \frac{2\pi}{\mu b^2} \int_0^\infty \frac{\sqrt{a^{-2}+\lambda^2}}{R(-\lambda^2)} \sigma_y^{*'}(-\lambda^2)\lambda d\lambda \tag{4.53}$$

The dependence of α on v_y determined by integrating Eq. (4.53) numerically is shown in non-dimensional form in Fig. 24 by plotting α/b vs $\mu V/4A_1 b$. As in the wedge problem, the value of ν for the half space is taken as .285 so that the results obtained will be applicable to problems in which the linearly elastic material is a steel or an alloy steel.

It is apparent from Fig. 24 that the difference between the actual dependence of α on V and the linear dependence assumed by Kostrov is smaller for the cone problem than for the wedge problem. It appears from Fig. 24 that $\partial\alpha/\partial V > 0$ for all α. The verification of this observation follows without difficulty from Eq. (4.53) and the equations which define $\sigma_y^{*'}$ for the four ranges of contact speeds.

4.2.6. The Vertical Force Required to Indent the Cone

The force required to press the cone into the half space in any range of contact speed can be found from the relation between P(t) and $\sigma_y^{*'}(0)$ which was noted in Sec. 3.4, i.e. from the formula

$$P(t) = -2\pi^2 t^2 \sigma_y^{*'}(0) \tag{4.54}$$

Therefore,

$$
\begin{aligned}
P(t) &= -2A_1\pi^2t^2\alpha^2 && \text{for } \alpha < c \\
&= -2A_1\pi^2t^2\alpha^4/c^2 && \text{for } c < \alpha < b \\
&= -2A_1\pi^2t^2(\alpha^4/c^2)F_{\alpha b}(0) && \text{for } b < \alpha < a \\
&= -A_1\pi^2t^2\alpha^3 a/b^2(1-b^2/a^2) && \text{for } a < \alpha
\end{aligned}
\tag{4.55}
$$

where A_1 is defined by Eq. (4.48) and $F_{\alpha b}(0)$ can be computed from Eq. (4.25). The indentation force increases quadratically with time for all $t \geq 0$. The dependence of $\ddot{P}(\ddot{P} = \frac{\partial^2 P(t)}{\partial t^2})$ on the shape, shear modulus and rate of penetration is shown in non-dimensional form in Figs. 25 and 26. In the first figure, $\frac{\ddot{P}}{4A_1\pi^2}$ is plotted against α/b; in the second, $\frac{\ddot{P}}{4A_1\pi^2}$ is plotted against $\frac{\mu V}{4A_1 b}$.

It is not difficult to prove that P(t) defined by Eq. (4.55) is a monotonically increasing function of α. Consequently, P increases monotonically with V since $\frac{\partial P}{\partial V} = \frac{\partial P}{\partial \alpha} \cdot \frac{\partial \alpha}{\partial V}$ and $\frac{\partial \alpha}{\partial V} > 0$. Hence, the operation of pressing a rigid conical die into a half space at a constant rate is a stable process.

4.3. Arbitrarily Shaped Rigid Dies Indenting Superseismically

4.3.1. General Remarks

In this section, a method is described for the solution of problems in which rigid dies of arbitrary shape are pressed into a linearly elastic half space rapidly enough to cause the contact to be superseismic. For these problems, no disturbance propagates along the surface of the half space more rapidly than the boundary of the region of contact. Consequently, there

will be no deformation of the y = 0 surface at points beyond the region of contact. Moreover, the deformation of the surface within the contact zone is completely defined by the portion of the rigid die which has crossed the original position of the y = 0 surface.

It follows from the work of Secs. 4.1 and 4.2 that the rate of penetration must exceed a certain value for the contact between a half space and a die with a cusp at the point of initial contact to be superseismic. However, the situation is quite different if the die is smooth in the region of contact. For problems of this type, it can be easily be verified that the contact will always be superseismic for a finite interval of time. Moreover, the length of this interval of time can easily be computed for the shape and indentation velocity of the die and the velocity of the P wave in the half space.

4.3.2. Two-Dimensional Problems

For plane strain contact problems, it is convenient to denote the vertical displacement symbolically as U(x,t). If the contact is frictionless, the boundary conditions defined below are sufficient to completely determine the stress and displacement fields at every point in the half space:

$$\begin{aligned} u_y(x,t) &= U(x,t) \\ \tau_{xy}(x,t) &= 0 \end{aligned} \tag{4.56}$$

If U(x,t) is a homogeneous function of x and t, the problem can be solved readily with the aid of the method of self-similar potentials described in Chapter 2.

When U(x,t) is not a homogeneous function of x and t, the vertical displacement can always be expressed as the superposition of homogeneous

functions in the following manner:

$$U(x,t) = \int_0^t \int_{-\infty}^{\infty} U(\xi,t_0) u_y^0(x-\xi,t-t_0)\,d\xi\,dt_0 \tag{4.57}$$

where $u_y^0(x-\xi,t-t_0)$ is a vertical displacement which satisfies the conditions

$$u_y^0(x-\xi,t-t_0) = 0 \qquad \text{for } \xi \neq x \text{ or } t \neq t_0$$

$$\int_0^t \int_{-\infty}^{\infty} u_y^0(x-\xi,t-t_0)\,d\xi\,dt_0 = 1 \tag{4.58}$$

That is,

$$u_y^0(x-\xi,t-t_0) = \delta(x-\xi)\delta(t-t_0)$$

where δ is the Dirac delta function. It is apparent that u_y^0 is the displacement equivalent of a vertical impulse. That is, the relationship between u_y^0 and a "distributed displacement" $U(x,t)$ is completely analogous to the relationship between an impulse of unit magnitude and a distributed load $\sigma(x,t)$.

From Eqs. (4.58), it is apparent that u_y^0 is a homogeneous function of $(x-\xi)$ and $(t-t_0)$. Thus, the solution of this problem can be expressed in terms of self-similar potentials by the method described in Sec. 2.8 of Chapter 2. Only the principal steps in this calculation are outlined here.

1) The displacement u_y^0 is integrated twice with respect to time in order to construct a fictitious displacement u_F which is a homogeneous function of degree zero. That is,

$$u_F = \int_0^t \int_0^{t_1} u_y^0(x,t_0)\,dt_0\,dt_1 \qquad \dagger$$

$$= \int_0^t \int_0^{t_1} \delta(x)\delta(t_0)\,dt_0\,dt_1 \tag{4.59}$$

$$= t\cdot\delta(x) \qquad \text{for } t > 0$$

2) The Cauchy integral formula for the half plane is used to construct a complex valued function u_F^* whose real part is identical to u_F.

$$u_F^* = -\frac{1}{i\pi}\int_{-\infty}^{\infty} \frac{u_F(\xi,t)}{\xi - x}\,d\xi$$

$$= -\frac{1}{i\pi}\int_{-\infty}^{\infty} \frac{t\cdot\delta(\xi)}{\xi - x}\,d\xi \tag{4.60}$$

$$= \frac{t}{i\pi x} = \frac{\theta}{i\pi}\,. \qquad \dagger\dagger$$

3) On the y = 0 surface, the self-similar potentials which solve this problem are related to u_F^* by the equation

$$\frac{\partial u_F^*}{\partial\theta} = -(a^{-2}-\theta^2)^{1/2}\Phi'(\theta) + \theta\Psi'(\theta) \tag{4.61}$$

For the tangential traction to be zero, the potentials must

---

† For convenience, the impulsive displacement is assumed to occur at x = y = t = 0.

†† We note, as in Sec. 2.8.3, that the simple pole at x = 0 is the singularity associated with $\delta(x)$. It is apparent that Eq. (4.60) contains no extraneous singularities at x = 0.

also satisfy the equation

$$0 = 2\theta(a^{-2}-\theta^2)^{1/2}\Phi'(\theta) + (b^{-2}-2\theta^2)\Psi'(\theta) \tag{4.62}$$

4) The potentials which solve the impulsive displacement problem are found by solving Eqs. (4.61) and (4.62) and replacing θ by the appropriate θ_i. The result is

$$\Phi'(\theta_1) = -\frac{(b^{-2}-2\theta_1^2)b^2}{i\pi(a^{-2}-\theta_1^2)^{1/2}}$$

$$\Psi'(\theta_2) = \frac{2\theta_2 b^2}{i\pi} \tag{4.63}$$

The stress and velocity fields can now be found from Eqs. (3.40). The normal traction, for example, is defined by the equation

$$\sigma_y^0(x,t) = -\mathrm{Re}\left(\frac{\mu b^2}{i\pi x}\,\frac{\partial^2}{\partial t^2}\,\frac{R(\theta^2)}{\sqrt{a^{-2}-\theta^2}}\right) \tag{4.64}$$

where $\theta = \frac{t}{x}$. It follows that the normal traction required to cause any deformation $U(x,t)$ of the $y = 0$ surface is determined by the equation

$$\sigma_y(x,t) = \mathrm{Re}\int_{-\infty}^{\infty}\int_{0}^{t} U(\xi,t-\tau)\sigma_y^0(x-\xi,\tau)\,d\tau\,d\xi$$

$$= -\mathrm{Re}\left(\frac{\mu b^2}{i\pi}\int_{-\infty}^{\infty}\int_{0}^{t}\frac{U(\xi,t-\tau)}{x-\xi}\,\frac{\partial^2}{\partial\tau^2}\,\frac{R(\theta^2)}{(a^{-2}-\theta^2)^{1/2}}\,d\tau\,d\xi\right) \tag{4.65}$$

where $\theta = \frac{\tau}{x-\xi}$ and $\tau = t - t_0$.

Equation (4.65) determines the contact stress beneath a rigid die only as long as the contact remains superseismic. Once the contact becomes subseismic, the displacement is no longer completely known at every point on the surface. That is, the quantity $U(x,t)$ can no longer be determined solely from the known shape and velocity of the rigid die.

For computational purposes, it is convenient to reduce the singularity in the σ_y^0 term of the integrand by integrating by parts. The first of Eqs. (4.65) can than be rewritten as

$$\sigma_y(x,t) = \int_{-\infty}^{\infty} \left(u(\xi,t-\tau)\sigma_y^1\Big|_0^t - V(\xi,t-\tau)\sigma_y^2\Big|_0^t + \int_0^t A(\xi,t-\tau)\sigma_y^2 d\tau\right)d\xi \tag{4.66}$$

where

$$\sigma_y'(x-\xi,\tau) = \int_0^\tau \sigma_y^0(x-\xi,\tau_1)d\tau_1 = -\mathrm{Re}\left(\frac{\mu b^2}{i\pi(x-\xi)} \frac{\partial}{\partial\tau} \frac{R(\theta^2)}{\sqrt{a^{-2}-\theta^2}}\right)$$

$$\sigma_y^2(x-\xi,\tau) = \int_0^\tau \sigma_y^1(x-\xi,\tau_1)d\tau_1 = -\mathrm{Re}\left(\frac{\mu b^2}{i\pi(x-\xi)} \frac{R(\theta^2)}{\sqrt{a^{-2}-\theta^2}}\right) \tag{4.67}$$

$$V(\xi,t-\tau) = \frac{\partial}{\partial\tau} U(\xi,t-\tau)$$

$$A(\xi,t-\tau) = \frac{\partial}{\partial\tau} V(\xi,t-\tau)$$

The tractions defined by σ_y^1 and σ_y^2 are the tractions required to cause the vertical displacements $u_y = \delta(x)$ and $u_y = t\cdot\delta(x)$, respectively. The terms $V(\xi,t-\tau)$ and $A(\xi,t-\tau)$ are the velocity and acceleration, respectively, at every point on the $y = 0$ surface.

If the velocity of the rigid die varies continuously, it can be shown that the final integral of Eq. (4.66) is the only non-zero term of that equation. Moreover, the $A(\xi,t-\tau)$ term will be identically zero at any point until that point comes in contact with the die. The instantaneous increase in velocity (from zero to the velocity of the die at that instant) can be treated as a delta function type of acceleration. That is, $A(\xi,t-\tau)$ can be written in the form

$$A(\xi,t-\tau) = V_D(t_c(\xi))\cdot\delta(t-\tau-t_c(\xi)) + \bar{A}(\xi,t-\tau) \qquad (4.68$$

where $V_D(t_c(\xi))$ is the velocity of the die at the instant when the die first comes in contact with the half space at the point ξ. The term $\bar{A}(\xi,t-\tau)$ denotes the acceleration at the point ξ, exclusive of the infinite acceleration which, at the instant of contact, causes the jump in the velocity at ξ.

4.3.2.1. The Superseismic Wedge

To illustrate the way in which the contact stress is calculated for a superseismic contact problem, we compute the stress beneath the surface of a rigid wedge-shaped die with an apex angle $\gamma = \pi - 2\tan^{-1}\frac{\alpha}{V_D}$, where V_D denotes the indentation velocity of the die. This problem was solved by a different method in Sec. 4.1.4.4.

The displacement of points on the $y = 0$ surface is defined by the equations

$$\begin{aligned} u_y &= V_D(t - |x|\alpha^{-1}) && \text{for} \quad |x| \leq \alpha t \\ &= 0 && \text{for} \quad \alpha t < |x| \end{aligned} \qquad (4.69)$$

It follows that the velocity and acceleration of points on the surface are defined by the equations

$$v_y = V_D \cdot H(t - |x|\alpha^{-1}) \qquad \text{and}$$
$$a_y = V_D \cdot \delta(t - |x|\alpha^{-1}) \tag{4.70}$$

where H and δ are the Heaviside step function and the Dirac delta function, respectively.

It follows directly from Eqs. (4.66), (4.67) and (4.70) that the contact stress is defined by the equation

$$\sigma_y(x,t) = -\mathrm{Re} \int_{-\infty}^{\infty} \frac{\mu b^2}{i\pi} \int_0^t V_D \frac{R(\theta^2)}{\sqrt{a^{-2}-\theta^2}} \frac{\delta(t-\tau-|\xi|\alpha^{-1})}{x-\xi} \, d\tau d\xi \tag{4.71}$$

where $\theta = \frac{\tau}{x-\xi}$.

With the aid of the properties of the delta function, Eqs. (4.71) can be simplified to the form

$$\sigma_y(x,t) = -\mathrm{Re} \int_{-\infty}^{0} \frac{\mu b^2}{i\pi} V_D \frac{R(\theta^2)}{\sqrt{a^{-2}-\theta^2}} \frac{d\xi}{x-\xi}$$
$$-\mathrm{Re} \int_0^{\infty} \frac{\mu b^2}{i\pi} V_D \frac{R(\theta^2)}{\sqrt{a^{-2}-\theta^2}} \frac{d\xi}{x-\xi} \tag{4.72}$$

where $\theta = \frac{t + \alpha^{-1}\xi}{x - \xi}$ in the first integrand, and $\theta = \frac{t - \alpha^{-1}\xi}{x - \xi}$ in the second integrand. By an appropriate change in the variable in integration, Eq. (4.72) can be written as

$$\sigma(x,t) = -\mathrm{Re}\ \frac{\mu b^2}{i\pi}\left(\int_{-\alpha^{-1}}^{\theta_0} \frac{R(\theta^2)}{\sqrt{a^{-2}-\theta^2}}\, V_D\, \frac{d\theta}{\alpha^{-1}+\theta}\right.$$

$$\left. + \int_{\theta_0}^{\alpha^{-1}} \frac{R(\theta^2)}{\sqrt{a^{-2}-\theta^2}}\, V_D\, \frac{d\theta}{(-\alpha^{-1}-\theta)}\right) \qquad (4.73)$$

where $\theta_0 = \frac{t}{x}$. It is apparent that $\sigma(x,t)$ is a function of θ_0. If both sides of Eq. (4.73) are differentiated with respect to θ_0, the following result is obtained:

$$\frac{\partial\, y(x,t)}{\partial\theta_0} = -\mathrm{Re}\ \frac{\mu b^2 R(\theta_0^2) 2\alpha^{-1} V_D}{i\pi\sqrt{a^{-2}-\theta_0^2}\,(\alpha^{-2}-\theta_0^2)} \qquad (4.74)$$

Equation (4.74) gives the derivative with respect to t/x of the contact stress beneath the rigid die if the edge of the contact moves superseismically, i.e. if $\alpha^{-1} < a^{-1}$. Exactly the same result was obtained by a different approach in Sec. 4.1.4.4.

4.3.3. Three-Dimensional Problems

It follows directly from the work of the previous section that the contact stress for any three-dimensional superseismic contact problem is defined by the equation

$$\sigma_y(r,\omega,t) = \int_0^{\infty}\int_0^{t}\int_0^{2\pi} U(r_0,\omega_0,t-\tau)\,\sigma_y^0(r-r_0,\omega-\omega_0\tau)\,r_0\,d\omega\,d\tau\,dr_0 \qquad (4.75)$$

where

1) $U(r_0,\omega_0,t_0)$ defines the vertical displacement at every point on the y = 0 surface during the interval of time in which the contact is superseismic, and

2) $\sigma_y^0(r-r_0,\omega-\omega_0,\tau)$ defines the normal traction required to force a vertical impulsive displacement of unit magnitude at $r = r_0$, $\omega = \omega_0$ and $\tau = 0$. This impulsive displacement satisfies the equation

$$u_y^0(r-r_0,\omega-\omega_0,\tau) = \delta(r-r_0)\cdot\delta(\omega-\omega_0)\cdot\delta(t-t_0) \qquad (4.76)$$

It can be shown without difficulty that the stress σ_y^0 is defined by the equation

$$\sigma_y^0(r-r_0,\omega-\omega_0,\tau) = -\mathrm{Re}\left(\frac{\mu b^2}{2\pi^2}\frac{\partial^3}{\partial\tau^3}\int_C \frac{R(\theta^2)\,d\theta^2}{r_1\sqrt{a^{-2}-\theta^2}\sqrt{\theta^2-\theta_0^2}}\right) \qquad (4.77)$$

where r_1 is the distance between the point r,ω and the point r_0,ω_0, $\theta_0^2 = (\tau/r_1)^2$, and C is the contour of integration shown by the curve C_3 of Fig. 11. This contour begins and ends at θ_0^2 and crosses the real θ^2 axis to the left of $\theta^2 = a^{-2}$.

Just as with two-dimensional problems, Eq. (4.75) is integrated by parts to reduce the singularity in the σ_y^0 term of the integrand. The following result is obtained:

$$\sigma_y(r,\omega,t) = \int_0^\infty\int_0^{2\pi}\left(U\sigma_y^1\Big|_0^t - V\sigma_y^2\Big|_0^t + \int_0^t A\sigma_y^2\,d\tau\right)d\omega dr_0 \qquad (4.78)$$

where $A = \dfrac{\partial V(t-\tau)}{\partial\tau}$, $V = \dfrac{\partial U(t-\tau)}{\partial\tau} = \dfrac{\partial U(r_0,\omega_0,t-\tau)}{\partial\tau}$,

$$\sigma_y^1(r-r_0,\omega-\omega_0,\tau) = \int_0^\tau \sigma_y^0(r-r_0,\omega-\omega_0,\tau_1)d\tau_1$$

and $$\sigma_y^2(r-r_0,\omega-\omega_0,\tau) = \int_0^\tau \sigma_y^1(r-r_0,\omega-\omega_0,\tau_1)d\tau_1 \qquad (4.79)$$

It should be emphasized that Eq. (4.79) holds for the superseismic indentation of any three-dimensional die, not just axially symmetric ones.

4.3.4. The Force Required to Indent a Rigid Die Superseismically

In the previous section, the distribution of the contact stress for the impulsive displacement defined by Eq. (4.76) was used as an influence function in computing the contact stress beneath a rigid die indenting superseismically. In this section, a similar procedure is used to compute the force required to press the die into the elastic half space.

The relationship Eq. (3.36) can be used to compute the force on the boundary from $\sigma_y^{*'}$ if the stresses and velocities are self-similar. We shall construct a problem having self-similar stresses and velocities, a vertical displacement at the origin, and no vertical displacement at any other point on the y = 0 surface. From the force on the boundary for this problem, we shall derive the influence function needed to obtain the force required to indent any die superseismically.

Consider initially the problem in which the normal velocity is zero except in a uniformly expanding circular region $r \leq \alpha t$. That is, consider the problem having the boundary conditions

$$\begin{aligned} v_y &= \Delta \quad \text{for} \quad 0 \leq r < \alpha t \\ &= 0 \quad \text{for} \quad \alpha t < r \\ \tau_{ry} &= 0 \quad \text{for} \quad 0 \leq r \leq \infty \end{aligned} \qquad (4.80)$$

Computations similar to those used in Sec. 3.3.3 to solve the analogous traction problem give the following expression for $v_y^{*'}$:

$$v_y^{*'} = - \frac{\alpha^2 \Delta}{2\pi(1 - \alpha^2\theta^2)^{3/2}} \tag{4.81}$$

The solution of the problem in which v_y is given by an equation

$$v_y = t^2 \cdot \delta(r) \quad \text{for} \quad 0 \leq r \leq \infty \tag{4.82}$$

is obtained from Eqs. (4.80) and (4.81) by setting $\Delta = \frac{1}{\alpha^2\pi}$ and then taking the limit of Eq. (4.81) as α tends to zero. This yields

$$v_y^{*'} = - \frac{1}{2\pi^2} \tag{4.83}$$

With the aid of Eqs. (4.42) and (3.36), we obtain the following for $\sigma_y^{*'}$ and P(t):

$$\sigma_y^{*'}(\theta^2) = \mu b^2 \frac{R(\theta^2}{\sqrt{a^{-2} - \theta^2}} \frac{1}{2\pi^2} \tag{4.84}$$

$$P(t) = -\mu b^{-2} a t^2 \tag{4.85}$$

It follows from Eqs. (4.83) and (4.85) that a force

$$\begin{aligned} P(t) &= -\mu b^{-2} a \\ &= -\rho a \end{aligned} \tag{4.86}$$

is required for the problem whose boundary conditions are

$$\begin{aligned} v_y &= \delta(r) \quad \text{for} \quad \delta \leq r \leq \infty \\ \tau_{ry} &= 0 \quad \text{for} \quad 0 \leq r \leq \infty \end{aligned} \tag{4.87}$$

If the velocity of the point r = 0 has an arbitrary time history denoted by V(t), the following expression for the variation of the surface force with time is obtained from Eq. (4.86) by superposition:

$$P(t) = - \rho a V(t) \tag{4.88}$$

When a rigid die indents a half space superseismically, the force required to indent a small region of the contact zone with a velocity V(t) is given by the equation

$$dP(t) = - \rho a V(t) dA \tag{4.89}$$

The total force is computed as follows:

$$P(t) = - \int_{A(t)} \rho a V(t) dA \tag{4.90}$$

where A(t) denotes the area of contact between the die and the half space at time t. Because the die is rigid, each point in contact with the die moves downward with the same velocity at any time. Hence, Eq. (4.90) can be rewritten as

$$P(t) = -\rho a V(t) \int_{A(t)} dA = -\rho a V(t) A(t) \tag{4.91}$$

The extremely simple relationship defined by Eq. (4.91) holds for rigid dies of any shape with any time variation of the indentation velocity, as long as the contact remains superseismic. Moreover, Eq. (4.91) indicates that the force at any time depends only on the area of contact between the die and the half space and the indentation velocity at that instant of time.

That is, the instantaneous force P(t) does not depend on the time histories of either the area of contact or the indentation velocity prior to the instant of time being considered.

5. THE NUMERICAL INTEGRATION PROCEDURES FOR THE WEDGE AND CONE PROBLEMS

5.1. General Remarks on the Calculations for the Wedge Problem

The stresses and velocities for the wedge problem solved in Sec. 4.1 are expressed in most instances as integrals which are hyperelliptic. An asymptotic approximation of these integrals is easily obtained for points which are near the various wave fronts.† However, in general it is more convenient to evaluate these integrals numerically than to try to express their values in closed form. To illustrate the numerical integration scheme used in this study, the computations necessary to determine σ_y are described in detail. Similar computations are used to determine the other disturbances. The results obtained are discussed in Chapter 6.

5.2. The Numerical Integration Scheme for the Wedge Problem

The vertical stress at any point in the $y \geq 0$ half space is defined by the equation

$$\sigma_y(x,y,t) = \mathrm{Re}\int_0^{\theta_1} \frac{(b^{-2}-2\theta^2)^2\sigma_y^{*'}(\theta)}{R(\theta^2)\mu b^2}\,d\theta + \mathrm{Re}\int_0^{\theta_2} \frac{4\theta^2(a^{-2}-\theta^2)^{1/2}(b^{-2}-\theta^2)^{1/2}\sigma_y^{*'}(\theta)}{R(\theta^2)\mu b^2}\,d\theta \tag{5.1}$$

where $\sigma_y^{*'}(\theta)$ is the function which solves the wedge problem being considered

† See Sec. 2.6.3.1.

and θ_1 and θ_2 are defined, as in Sec. 4.1, by the equations

$$t - \theta_i x - y\sqrt{c_i^{-2} - \theta_i^2} = 0 \qquad i = 1,2 \ . \tag{5.2}$$

5.2.1. The P-Wave Disturbance

The time history of σ_y at a fixed point $P_0(x_0,y_0)$ can be determined by evaluating the first integral of Eq. (5.1) along the contour traced out in the complex θ_1 plane as θ_1 varies with time. If t_1 denotes the time at which the P-wave reaches $P_0(x_0,y_0)$,† the portion of the contour traced out during the interval $0 < t < t_1$ will lie along the real axis between $\theta_1 = 0$ and $\theta_1 = x_0/r_0 a$, where $r_0^2 = x_0^2 + y_0^2$. For $t > t_1$, the curve traced out by θ_1 is defined by the equation

$$\theta_1 = \frac{x_0}{ar_0}\frac{t}{t_1} + \frac{iy_0}{ar_0}\left(2\frac{(t-t_1)}{t_1} + \frac{(t-t_1)^2}{t_1^2}\right)^{1/2} \tag{5.3}$$

It is apparent that the curves defined by Eq. (5.3) for different ratios of x_0 to y_0 lie entirely in the upper half plane for $t > t_1$ and $y > 0$. Typical curves of this type are shown in Fig. 27a.

Since the character of the curves changes at $t = t_1$, it is convenient for computational purposes to write the equation defining the P-wave component in the form

$$\sigma_y^P(x_0,y_0,t) = \mathrm{Re}\int_0^{\theta_1(t)} I_1(\theta)d\theta \qquad \text{for } t < t_1$$

---

† For convenience x_0 is assumed to be positive.

$$= \mathrm{Re}\int_{0}^{\theta_1(t_1)} I_1(\theta)d\theta + \mathrm{Re}\int_{\theta_1(t_1)}^{\theta_1(t)} I_1(\theta)d\theta \quad \text{for } t > t_1 \tag{5.4}$$

where $I_1(\theta)$ symbolically denotes the integrand of the first integral of Eq. (5.1). In order to compute the value of σ_y^P at times $t_1 + n\Delta t$, the second of Eqs. (5.4) is rewritten as follows:

$$\sigma_y^P(x_0,y_0,t_1 + n\Delta t) = \mathrm{Re}\int_{0}^{\theta_1(t_1)} I_1(\theta)d\theta + \sum_{j=0}^{j=n-1} \mathrm{Re}\int_{\theta_1^j}^{\theta_1^{j+1}} I_1(\theta)d\theta \tag{5.5}$$

where Δt is a positive increment of time, n is an integer, and θ_1^j is defined by the equation

$$\theta_1^j(x_0,y_0,t_1+j\Delta t) = \frac{x_0}{ar_0}\left[1 + j\,\frac{\Delta t}{t_1}\right] + \frac{iy_0}{ar_0}\left[\frac{2j\Delta t}{t_1} + \left(\frac{j\Delta t}{t_1}\right)^2\right]^{1/2} \tag{5.6}$$

It is apparent that the points defined by Eq. (5.6) for j = 0,1,2,3..... lie on the curve of Eq. (5.3), i.e. that

$$\theta_1(x_0,y_0,t) = \theta_1^j(x_0,y_0,t_1 + j\Delta t) \tag{5.7}$$

for each $t = t_1 + j\Delta t$ $\qquad$ $j = 0,1,2,3$ .....

Since $I_1(\theta)$ is analytic for all θ in the upper half plane, the contour of integration between each pair of successive points can be deformed into the straight line joining these points (see Fig. 27b). Moreover, if $\Delta t/t_1$ is sufficiently small, $I_1(\theta)$ can be accurately approximated by a quadratic function between θ_1^j and θ_1^{j+1}. Hence, the value of σ_y^P can be computed from the following equations:

$$\sigma_y^P(x_0,y_0,t) = \mathrm{Re}\int_0^{\theta_1(t)} I_1(\theta)d\theta \qquad \text{for } t < t_1 \tag{5.8}$$

$$\sigma_y^P(x_0,y_0,t_1+n\Delta t) \simeq \mathrm{Re}\sum_{j=0}^{j=n-1}\left(I_1(\theta_1^i) + 4I_1\left(\frac{\theta_1^j+\theta_1^{j+1}}{2}\right)\right.$$

$$\left. + I_1(\theta_1^{j+1})\right)\frac{\theta_1^{j+1}-\theta_1^j}{6}$$

$$+ \mathrm{Re}\int_0^{\theta_1(t_1)} I_1(\theta)d\theta \qquad \text{for } t > t_1$$

Since the maximum value of $\theta_1(t_1)$ is a^{-1}, σ_y^P will be zero for all $t < t_1$ unless $I_1(\theta)$ is real-valued for some $\theta < a^{-1}$. This will occur only if the contact is superseismic, i.e. if $\alpha > a$. For these problems

$$I_1(\theta) = \frac{2\alpha^{-1}\mu V(b^{-2}-2\theta^2)^2}{(i\pi(a^{-2}-\theta^2)^{1/2}(\alpha^{-2}-\theta^2))} \tag{5.9}$$

where V is the indentation velocity of the wedge. We note that $I_1(\theta)$ is imaginary for all $0 < \theta < a^{-1}$ with the exception of the point $\theta = \alpha^{-1}$ where there is a simple pole. It follows that

$$\begin{aligned}\sigma_y^P(x_0,y_0,t) &= 0 \qquad \text{for} \quad 0 < \theta_1(t) < \alpha^{-1} \\ &= \frac{-b^2\mu V(b^{-2}-2\alpha^{-2})^2}{(a^{-2}-\alpha^{-2})^{1/2}} \quad \text{for } a^{-1} < \theta_1(t) \le \theta_1(t_1)\end{aligned} \tag{5.10}$$

It follows that the plane on which $\theta_1 = \alpha^{-1}$ is a shock front in the x,y,t space. This Mach front (see Fig. 19) is defined by the equation

$$t - x\alpha^{-1} - y\sqrt{a^{-2}-\alpha^{-2}} = 0 \qquad (5.11)$$

It can easily be verified that the value of σ_y^P is constant in the regions bounded by the front of the P-wave, the P shock waves and the y = 0 surface (see Fig. 19).

5.2.2. The S-Wave Disturbances

By a method which is completely analogous to that used in the previous section, we find that the S-wave component of σ_y is given by the equations

$$\sigma_y^S(x_0,y_0,t) = \mathrm{Re}\int_0^{\theta_2(t)} I_2(\theta)d\theta \qquad \text{for} \quad t < t_2 \qquad (5.12)$$

$$\sigma_y^S(x_0,y_0,t_2+n\Delta t) \simeq \mathrm{Re}\int_0^{\theta_2(t_2)} I_2(\theta)d\theta + \mathrm{Re}\sum_{j=0}^{j=n-1}\left(I_2(\theta_2^j) + 4I_2\left(\frac{\theta_2^j+\theta^{j+1}}{2}\right) + I_2(\theta_2^{j+1})\right)\frac{(\theta_2^{j+1}-\theta_2^j)}{6} \qquad (5.13)$$

where t_2 denotes the time at which the S wave reaches P_0,

$$I_2(\theta) = \frac{4\theta^2(a^{-2}-\theta^2)^{1/2}(b^{-2}-\theta^2)^{1/2}\sigma_y^{*\prime}(\theta)}{R(\theta^2)} \quad , \qquad (5.14)$$

$$\theta_2 = \frac{x_0}{r_0^2}\,t - \frac{y_0}{r_0^2}\,(r_0^2/b^2 - t^2)^{1/2} \qquad \text{for} \quad t < t_2 \ , \qquad (5.15)$$

and $$\theta_2^j = \frac{x_0}{br_0}\left[1 + j\,\frac{\Delta t}{t_2}\right] + \frac{iy_0}{r_0 b}\left(2j\,\frac{\Delta t}{t_2} + \left(j\,\frac{\Delta t}{t_2}\right)^2\right)^{1/2} \qquad (5.16)$$

$$\text{for } t > t_2$$

As in Sec. 5.2.1 Δt is a positive increment of time.

The integral of Eq. (5.12) determines the value of any equivoluminal disturbance which occurs at $P_0(x_0,y_0)$ prior to the arrival of the cylindrical front of the S wave. The method used to evaluate this integral depends on the character of the non-analyticities in $I_2(\theta)$ along the contour of integration. This contour lies just above the real θ axis between $\theta = 0$ and $\theta = \theta_2(t_2)$, where $\theta_2(t_2) = x_0/r_0 b$. Hence, we must determine the non-analyticities in $I_2(\theta)$ along the real axis between 0 and b^{-1}. We consider separately the four ranges of contact speed.

The Superseismic Range

If the wedge indents superseismically ($\alpha > a$) the function $I_2(\theta)$ is defined by the equation

$$I_2(\theta) = -\frac{4\theta^2\sqrt{b^{-2}-\theta^2}\;\mu b^2 2\alpha^{-1}V}{i\pi(\alpha^{-2}-\theta^2)} \qquad (5.17)$$

The only non-analyticity in I_2 between 0 and b^{-1} is at $\theta = \alpha^{-1}$ where there is a simple pole. It can easily be verified that

$$\sigma_y^S = \mathrm{Re}\int_0^{\theta_2(t)} I_2(\theta)\,d\theta = 0 \qquad \text{for } 0 < \theta_2(t) < \alpha^{-1}$$

$$= -4\mu b^2 V^{-2}(b^{-2}-\alpha^{-2})^{1/2} \qquad \text{for } \alpha^{-1} < \theta_2(t) < \theta_2(t_2) \qquad (5.18)$$

It is not difficult to show that the value of σ_y^S is constant in the regions of the x,y,t space bounded by the y = 0 surface, the front of the S wave, and the planes along which $|\theta_2| = \alpha^{-1}$ (see Fig. 17a). Thus, the planes along which $|\theta_2| = \alpha^{-1}$ must be Mach fronts for the equivoluminal component of the disturbance. The location of these moving fronts can be determined from the equation

$$t - x\alpha^{-1} - y\sqrt{b^{-2}-\alpha^{-2}} = 0 \qquad \text{for } \frac{x}{y} > \frac{b}{(\alpha^2-b^2)^{1/2}} \tag{5.19}$$

The Slow Range

If the wedge indents slowly, i. e. if $\alpha < c$,

$$I_2(\theta) = \frac{iA_1 4\theta^2(a^{-2}-\theta^2)^{1/2}(b^{-2}-\theta^2)^{1/2}}{(R(\theta^2)(\alpha^{-2}-\theta^2)^{1/2})} \tag{5.20}$$

where A_1 is the constant defined by Eq. (4.48) of Sec. 4.1.4.1, and where $R(\theta^2)$ denotes the Rayleigh function, defined previously. It is apparent from Eq. (5.20) that I_2 is imaginary and analytic for all $0 < \theta < a^{-1}$. Therefore,

$$\sigma_y^S = \mathrm{Re}\int_0^{\theta_2(t)} I_2(\theta) = 0 \qquad \text{for } 0 < \theta_2(t) < a^{-1} \tag{5.21}$$

Equation (5.21) merely proves that there is no equivoluminal disturbance beyond the region bounded by the head waves and the front of the S wave (see Fig. 16a).

For $a^{-1} < \theta < b^{-1}$, $I_2(\theta)$ is complex-valued since $R(\theta^2)$ is complex-valued in this range. It is convenient to separate the real and

imaginary parts of $I_2(\theta)$ by rationalizing the denominator of Eq. (5.20). The following result is obtained:

$$I_2(\theta) = (\theta - a^{-1})^{1/2} I_{21}(\theta) + iI_{22}(\theta) \tag{5.22}$$

where $$I_{21}(\theta) = \frac{A_1 4\theta^2 \sqrt{a^{-1}+\theta^2}\sqrt{b^{-2}-\theta^2}\,(b^{-2}-2\theta^2)^2}{(\alpha^{-2}-\theta^2)^{1/2} R(\theta^2)\,\overline{R(\theta^2)}} \tag{5.23}$$

and $$I_{22}(\theta) = -\frac{A_1 16\theta^4 (a^{-2}-\theta^2)(b^{-2}-\theta^2)}{(\alpha^{-2}-\theta^2)^{1/2} R(\theta^2)\,\overline{R(\theta^2)}} \tag{5.24}$$

$R(\theta^2)\overline{R(\theta^2)}$ simplifies to $-16(b^{-2}-a^{-2})\theta^6 + b^{-2}(24b^{-2}-16a^{-2})\theta^4 - 8b^{-6}\theta^2 + b^{-8}$.

The function in the denominator of each of the above expressions has three zeros in the θ^2 plane. Obviously, one of these zeros is at $\theta^2 = c^{-2}$ (the zero point of the Rayleigh function). It can easily be verified that the remaining zeros do not lie on the real θ^2 axis between a^{-2} and b^{-2}. Consequently, Eq. (5.21) can be simplified as follows:

$$\sigma_y^S = \mathrm{Re}\int_{a^{-1}}^{\theta_2(t)} I_2(\theta) = \int_{a^{-1}}^{\theta_2(t)} (\theta - a^{-1})^{1/2} I_{21}(\theta)\,d\theta \quad \text{for } a^{-1} \le \theta_2(t) \le \theta_2(t_2) \tag{5.25}$$

Since I_{21} is analytic between a^{-1} and b^{-1}, this function can be approximated by a linearly varying function over a sufficiently small increment $\Delta\theta$. As a result, an accurate numerical evaluation of the integration of $(\theta - a^{-1})^{1/2} I_{21}(\theta)$ over the interval $\Delta\theta$ can be obtained by multiplying the values of $I_{21}(\theta)$ at the end points of this interval by weighting factors which take account of the rapid variation of $(\theta - a^{-1})^{1/2}$ near a^{-1}. In

essence, what is done is to use an integration formula which would be exact for a function of the form $(\theta-a^{-1})^{1/2}[A + B(\theta-a^{-1})]$.

If the integrand is approximated in the manner described above and if the interval between a^{-1} and $\theta_2(t_2)$ is divided into n sufficiently small increments, it is not difficult to show that an accurate approximation of σ_y^S at an intermediate point is given by the formula,†

$$\sigma_y^S(a^{-1}+m\Delta\theta) \simeq (\Delta\theta)^{3/2} \sum_{j=0}^{j=m-1} B_1(j)I_{21}(a^{-1}+j\Delta\theta) + B_2(j)I_{21}(a^{-1}+(j+1)\Delta\theta) \tag{5.26}$$

where
$$B_1(j) = \frac{2}{3}\left((j+1)^{3/2} - j^{3/2}\right) - \frac{2}{5}\left((j+1)^{5/2} - j^{5/2}\right) \tag{5.27}$$

$$B_2(j) = \frac{2}{5}\left((j+1)^{5/2} - j^{5/2}\right)$$

and $0 \leq m \leq n$ so that $a^{-1} \leq a^{-1} + m\Delta\theta \leq \theta_2(t_2)$. The relationship between t and $m\Delta\theta$ is computed from the equation

$$t - x_0(a^{-1}+m\Delta\theta) - y_0(b^{-1} - (a^{-1} + m\Delta\theta)^2)^{1/2} = 0 \tag{5.28}$$

Equation (5.28) defines the moving plane in the half space which is tangent to the front of the S wave and intersects the y = 0 surface along the line $x = t/(a^{-1}+m\Delta\theta)$. Consequently, the value of σ_y^S calculated by Eq. (5.26) is the same at every point on this plane. These planes lie in the region of the x,y,t space bounded by the front of the S wave, the y = 0 surface, and the front of the head wave (see Fig. 28).

---

† This integration technique is similar to that used by Jeffreys and Jeffreys [36] and by Paul [37].

The First Intermediate Range

If the contact speed is in the first intermediate range of contact speeds, i.e. if $c < \alpha < b$, the integrand $I_2(\theta)$ of Eq. (5.21) will be defined as follows

$$I_2(\theta) = \frac{iA_1 4\theta^2(a^{-2}-\theta^2)^{1/2}(b^{-2}-\theta^2)^{1/2}(c^{-2}-\theta^2)}{R(\theta^2)(\alpha^{-2}-\theta^2)^{3/2}} \tag{5.29}$$

It is not difficult to show that the character of this function between a^{-1} and b^{-1} is essentially the same as that of the function which defines $I_2(\theta)$ for a slowly indenting wedge. Consequently, the value of σ_y^S corresponding to points for which $\theta_2(t)$ is between a^{-1} and $\theta_2(t_2)$ can be determined by the method described in the previous subsection.

The Second Intermediate Range

If the contact speed is in the second intermediate range of contact speeds, i.e. if $b < \alpha < c$, the integrand $I_2(\theta)$ of Eqs. (5.21) will be defined as follows:

$$I_2(\theta) = \frac{iA_1 4\theta^2(a^{-2}-\theta^2)^{1/2}(b^{-2}-\theta^2)^{1/2}(c^{-2}-\theta^2)}{R(\theta^2)(\alpha^{-2}-\theta^2)^{3/2}} \; F_{\alpha b}(\theta) \tag{5.30}$$

where $$F_{\alpha b}(\theta) = \exp \int_{\alpha^{-2}}^{b^{-2}} \frac{\beta(\lambda^2)}{\pi(\lambda^2-\theta^2)} \, d\lambda^2 \tag{5.31}$$

and $$\beta(\lambda^2) = -\tan^{-1} \frac{4\lambda^2(\lambda^2-a^{-2})^{1/2}(b^{-2}-\lambda^2)^{1/2}}{(b^{-2}-2\lambda^2)^2} \tag{5.32}$$

The function† $F_{\alpha b}(\theta)$ is real-valued and analytic for all $\theta^2 > b^{-2}$ and $\theta^2 < \alpha^{-2}$. However, in the vicinity of α^{-1}, $F_{\alpha b}(\theta^2)$ varies in the same manner as $C_0(\alpha^{-2}-\theta^2)^{-\beta(\alpha^{-2})/\pi}$, where C_0 is the real-valued constant defined by Eq. (A.13) of Appendix A.

It follows that $I_2(\theta)$ has a non-integrable singularity at $\theta = \alpha^{-1}$. However, this singularity presents no computational difficulties as we now show.

The method described in the two previous subsections can be used to evaluate σ_y^S for $\theta_2(t) < \alpha^{-1}$ if $\theta_2(t)$ is not too close to α^{-1}.†† If $\theta_2(t)$ is greater than α^{-1}, the contour of integration can be deformed around the singular point in the manner shown in Fig. 29. Since $I_2(\theta)$ is analytic at every point in the upper half plane, the integration along these contours can be carried out numerically without any difficulty.

At points near α^{-1}, the singular component of σ_y^S can be determined by expanding $I_2(\theta)$ asymptotically about $\theta = \alpha^{-1}$ and then integrating the first term of the series. The following result is obtained:

$$\sigma_y^S \simeq \mathrm{Re}\ \frac{D_0 C_0}{(2\alpha^{-1})^{3/2+\beta(\alpha^{-2})/\pi}\left(\frac{1}{2}+\frac{\beta(\alpha^{-2})}{\pi}\right)(\alpha^{-1}-\theta)^{1/2+\beta(\alpha^{-2})/\pi}} \quad \text{for } \theta_2 \simeq \alpha^{-1} \tag{5.33}$$

where D_0 is the complex-valued constant

$$D_0 = \frac{4A_1\alpha^{-2}(a^{-1}+\alpha^{-1})^{1/2}(b^{-2}-\alpha^{-2})^{1/2}(c^{-2}-\alpha^{-2})}{R(\alpha^{-2})} \tag{5.34}$$

---

† A form of this function which is convenient for computational purposes is given in Appendix A.

†† If $\theta_2(t)$ is close to α^{-1}, the approximation of the real part of $I_2(\theta)$ in the manner described previously will not be accurate.

and C_0 is the complex-valued constant defined by Eq. (A.13) of Appendix A.

The planes in the x,y,t space along which $\theta_2 = \pm \alpha^{-1}$ are shown in Fig. 18. These planes are tangent to the front of the S wave and intersect the y = 0 surface at each boundary of the region of contact.

The integration procedures used to evaluate σ_y^P and σ_y^S must be modified slightly if the point in question lies on the surface of the half space. When $y_0 = 0$ the contour of integration lies along the real axis between $\theta_i = 0$ and $\theta_i = t/x$. Special consideration must be given to the rapidly varying character of the integrands at points on the real axis near $\theta = a^{-1}$ (where $(a^{-2}-\theta^2)^{1/2}$ varies rapidly), near $\theta = b^{-1}$ (where $(b^{-2}-\theta^2)^{1/2}$ varies rapidly), near $\theta = \alpha^{-1}$ (where the function $\sigma_y^{*'}(\theta)$ is singular), and near $\theta = c^{-1}$ (where there is a simple pole in $1/R(\theta^2)$). Near these points, the integrals can be evaluated by methods which are similar to those already described in this section.

The following remarks can be made regarding the integration procedures described in Secs. 5.21 and 5.22.

1) Equations (5.6) and (5.8) have been formulated in such a way that the time variation of σ_y^P can be computed by a simple step-by-step operation.

2) Equations (5.13), (5.16), (5.26) and (5.28) have been formulated in such a way that the time variation of σ_y^S can be computed by simple ste-by-step operations for problems in which $\alpha < b$ or $\alpha > a$. For problems in which $b < \alpha < a$, these equations can be used to compute σ_y^S except when the value of $\theta_2(t)$ is close to α^{-1}. Near this point the value of σ_y^S is given by Eq. (5.33).

3) The self-similar results determined from the equations mentioned above can also be interpreted as the variation of σ_y along the plane $x/y = x_0/y_0$ for a specified instant of time. This follows from the fact that the θ_i's are homogeneous functions of x,y, and t of degree zero, i.e. that

$$\theta_i(\lambda x,\lambda y,t) = \theta_i(x,y,t/\lambda) \tag{5.35}$$

where λ is any scalar constant.

The procedure used to determine σ_y can also be applied for the calculation of the velocities and the remaining stresses. These operations were programmed for the IBM 360-50 computer at the University of Illinois. The results obtained are discussed in Chapter 6.

5.3. General Remarks on the Calculations for the Cone Problem

The first derivative with respect to time of the velocities and stresses which solve the cone problem are expressed in terms of convolution integrals which, in most cases, are hyperelliptic.† As a result, it is not possible to express the value of these integrals in terms of elementary functions. Moreover, it is not possible to formulate a step-by-step integration procedure as was done for the wedge problem considered in Secs. 5.1 and 5.2, because, unlike the two-dimensional case, the end points occur in the integrand.

The numerical integration procedure which is used to evaluate $\dot{\sigma}_y$ and σ_y is described in the following section. The other stresses and velocities can be computed in a similar manner.

---

† See Sec. 3.4.1.

5.4. The Numerical Integration Scheme for the Cone Problem

5.4.1. Evaluation of the Time Derivatives of the Vertical Stress

The value of $\dot{\sigma}_y$ at any point in the half space can be calculated from the following equation (Eq. (3.37) of Sec. 3.4.1):

$$\dot{\sigma}_y(t,r,y) = -\mathrm{Re}\int_0^{\pi} 2\theta_1 \frac{I_1(\theta_1^2)}{\delta_1'}\,d\omega - \mathrm{Re}\int_0^{\pi} 2\theta_2 \frac{I_2(\theta_2^2)}{\delta_2'}\,d\omega \tag{5.36}$$

where $$\delta_i' = -r\cos\omega + \frac{y\theta_i}{(c_i^{-2}-\theta_i^2)^{1/2}}\,, \tag{5.37}$$

$$I_1(\theta_1^2) = \frac{(b^{-2}-2\theta_1^2)^2\sigma_y^{*'}(\theta_2)}{R(\theta_1^2)}\,, \tag{5.38}$$

and $$I_2(\theta_2^2) = \frac{4\theta_2^2(a^{-2}-\theta_2^2)^{1/2}(b^{-2}-\theta_2^2)^{1/2}\sigma_y^{*'}(\theta_2)}{R(\theta_2^2)}\,. \tag{5.39}$$

In Eqs. (5.38), $\sigma_y^{*'}(\theta)$ is the function which solves the cone problem being considered (see Eqs. (4.43) and (4.50)).

The P-wave component of $\dot{\sigma}_y$, which we denote by $\dot{\sigma}_y^P$, is defined by the first integral of Eq. (5.36). This integral can be written in the following form if the variable of integration is changed from ω to θ_1^2:

$$\dot{\sigma}_y^P = \mathrm{Re}\int_{\theta_{11}^2}^{\bar{\theta}_{11}^2} \frac{I_1}{G_1}\,d\theta_1^2 \tag{5.40}$$

where

$$G_1(\theta) = (r^2+y^2)^{1/2}((a^{-2}-\theta_{11}^2)^{1/2}-(a^{-2}-\theta_1^2)^{1/2})^{1/2}((a^{-2}-\theta_1^2)^{1/2}-(a^{-2}-\bar{\theta}_{11}^2)^{1/2})^{1/2} \tag{5.41}$$

and where θ_{11} is defined implicitly by the equation

$$t - \theta_{11} r - y(a^{-2} - \theta_{11}^2)^{1/2} = 0 \qquad (5.42)$$

It can easily be verified that the integrand of Eq. (5.40) has a wquare-root singularity at each end of the contour of integration. However, the remaining portion of the contour of integration must lie in a region of the θ_1^2 plane where the function I_1/G_1 is analytic.† Moreover, this contour must cross the real θ_1^2 axis to the left of any non-analyticities in I_1.

In order to compute the value of $\dot{\sigma}_y^P$ numerically, it is convenient to choose a contour which is made up of straight line segments. Contours of this type for various values of θ_{11}^2 are shown in Fig. 12b. The wide lines in this figure indicate the branch cuts of I_1 and G_1 for a problem in which the cone indents superseismically. For this problem, I_1 is non-analytic for all real values of θ_1^2 in the range $\theta_1^2 \geq \alpha^{-2}$.

An accurate approximation of $\dot{\sigma}_y^P$ can be obtained if a numerical integration scheme analogous to the one used to compute the head wave disturbances in Sec. 5.2.2 is employed over small intervals at each end of the contour of integration. It should be noted that, in this case, this is not merely a refinement; it is an absolute necessity because the integrand is singular at each end of the contour of integration. Simpson's Rule can be used along the remainder of the contour. In this way $\dot{\sigma}_y^P$ can be computed without difficulty for any point in the elastic half space. Similar calculations can be used to determine the value of $\dot{\sigma}_y^S$, the S-wave component of $\dot{\sigma}_y$.

---

† See the work of Sec. 3.4.1.2.

It should be noted that the volume of calculation is considerably greater in the cone problem than for the wedge, because no step-by-step solution is possible.

5.4.2. Evaluation of the Vertical Stress

It still remains to consider the method which is used to compute σ_y^P and σ_y^S once the time derivatives of these quantities are known.

The P-Wave Component

To illustrate how this is done, consider initially the way in which σ_y^P is computed for a problem in which the contact speed is subseismic and the point at which σ_y^P is being computed lies below the y = 0 surface. It follows from the work of Sec. 3.4.1.3 that $\dot{\sigma}_y^P$ will vary smoothly with time for all $t > t_1$, where t_1 denotes the time at which the front of the P wave reaches the point in question. Moreover, the magnitude of the step discontinuity in $\dot{\sigma}_y^P$ which occurs at $t = t_1$ can be computed analytically by the method described in Sec. 3.4.1.3. It follows that an accurate approximation of σ_y^P at times $t_1 + 2n\Delta t$ can be found from the equation

$$\sigma_y^P(t_1+2n\Delta t) \simeq Re \sum_{j=0}^{j=n-1} (\dot{\sigma}_y^P(t_1+2j\Delta t) + 4\dot{\sigma}_y^P(t_1 + (2j+1)\Delta t) + \dot{\sigma}_y^P(t_1 + (2j+2)\Delta t)) \frac{\Delta t}{3} \qquad (5.43)$$

In Eq. (5.43), n is an integer, Δt is a positive increment of time, and the value of $\dot{\sigma}_y^P$ for times $t > t_1$ is computed numerically by the methods described previously.

Equation (5.43) is also used to compute the value of σ_y^P at points which experience no shock wave disturbance for problems in which the cone

indents superseismically. It can easily be verified that the ratio of r to y for these points is less than $a/(\alpha^2-a^2)^{1/2}$. At points where $r/y > a/(\alpha^2-a^2)^{1/2}$, the value of σ_y^P is computed from the following equation:

$$\sigma_y^P(t_{PM}+2n\Delta t) \simeq \sigma_y^P(t_{PM}) + \mathrm{Re} \sum_{j=0}^{j=n-1} (\dot{\sigma}_y^P(t_{PM}+2j\Delta t) + 4\dot{\sigma}_y^P(t_{PM}+(2j+1)\Delta t) + \dot{\sigma}_y(t_{PM}+(2j+2)\Delta t)) \frac{\Delta t}{3} \tag{5.44}$$

where t_{PM} is the time at which the Mach front associated with the P wave shock wave passes through the point in question and $\sigma_y^P(t_{PM})$ is the magnitude of the step discontinuity in σ_y^P across the shock front.

Since $\theta_1 = \alpha^{-1}$ on the shock front, t_{PM} can be determined from the equation,

$$t_{PM} = r\alpha^{-1} + y(a^{-2}-\alpha^{-2})^{1/2} \tag{5.45}$$

Equation (5.45) defines the Mach cone (see Fig. 19) which is tangent to the spherical front of the P wave and cuts the y = 0 surface at the edge of the region of contact, i.e. at $r = \alpha t$.

The magnitude of $\sigma_y^P(t_{PM})$ and of $\dot{\sigma}_y^P(t_{PM})$ must be computed analytically. This is done in Appendix B. The following result is obtained for the step discontinuity in $\sigma_y^P(t_{PM})$ at the shock front:

$$\sigma_y^P(r,y,t_{PM}) = -\frac{\pi A_1}{(b^{-2}-a^{-2})} \frac{(b^{-2}-2\alpha^{-2})^2}{(a^{-2}-\alpha^{-2})^{1/2}} \times \frac{t_{PM} - ya^{-2}/(a^{-2}-\alpha^{-2})^{1/2}}{\alpha^{-2}(r^2+y^2-t_{PM}y/(a^{-2}-\alpha^{-2})^{1/2})^{1/2}} \tag{5.46}$$

The magnitude of Δt in (5.44) should be chosen in such a way that for some integral value of n,

$$t_{PM} + 2n\Delta t = t_1 \tag{5.47}$$

This is necessary since $\dot{\sigma}_y^P$ varies smoothly in front of the P wave and behind this wave but not across its surface. That is, $\dot{\sigma}_y^P$ is continuous across the front of the P wave, but all the derivatives with respect to time of $\dot{\sigma}_y^P$ are discontinuous there. Hence, $\dot{\sigma}_y^P$ should not be approximated across this surface by a quadratic functions.

If Δt is chosen in the manner described above, Eq. (5.44) will accurately approximate the value of σ_y^P at all times $t_{PM} + 2n\Delta t$, including those times when the point in question is in the vicinity of the front of the P wave.

Reasoning in the same manner as above, we find that the value of σ_y^S at a point below the y = 0 surface will be approximated accurately at times $t_2^* + 2n\Delta t$ by the equation

$$\sigma_y^S(t_2^* + 2n\Delta t) \simeq \sigma_y^S(t_2^*) + \mathrm{Re} \sum_{j=0}^{j=n-1} (\dot{\sigma}_y^S(t_2^* + 2j\Delta t) + 4\dot{\sigma}_y^S(t_2^* + (2j+1)\Delta t + \dot{\sigma}_y^S(t_2^* + (2j+2)\Delta t)) \frac{\Delta t}{3} \tag{5.48}$$

In the above equation, t_2^* denotes the time at which the initial equivoluminal disturbance reaches the point in question, and $\sigma_y^S(t_2^*)$ denotes the magnitude of any step discontinuity in σ_y^S which occurs at that instant. It can easily be verified that $\sigma_y^S(t_2^*)$ is zero except for problems in which the cone indents superseismically and a Mach front associated with the S wave passes through

the point at which σ_y^S is being computed. This shock front is defined by the equation

$$t_2^* - \alpha^{-1}r - y(b^{-2}-\alpha^{-2})^{1/2} = 0 \tag{5.49}$$

This front is shown schematically in Fig. 19. The magnitude of σ_y^S across this front is given by Eq. (B.12) of Appendix B, i.e.

$$\sigma_y^S(r,y,t_{SM}) = -\frac{4\pi A_1(b^{-2}-\alpha^{-2})^{1/2}}{(b^{-2}-a^{-2})} \frac{(t_{SM}-yb^{-2}/(b^{-2}-\alpha^{-2})^{1/2})}{(r^2+y^2-t_{SM}y/(b^{-2}-\alpha^{-2})^{1/2})^{1/2}} \tag{5.50}$$

If a shock wave or a head wave passes through the point in question, the magnitude of Δt should be chosen in such a way that for some n,

$$t_2^* + 2n\Delta t = t_2 \tag{5.51}$$

where t_2 denotes the time at which the S wave reaches the point being considered. This is done so that no attempt will be made to approximate $\dot{\sigma}_y^S$ by a quadratic function across the front of the S wave. (All the derivatives with respect to time of $\dot{\sigma}_y^S$ are discontinuous when $t = t_2$.)

Equation (5.48) must be modified somewhat if α is in the second intermediate range of contact speeds and if the front shown schematically in Fig. 18 passes through the point in question. It can easily be verified that this will only occur if $r/y > b/(\alpha^{-2}-b^2)^{1/2}$ or, what is equivalent, if $\theta_2(t_2) < \alpha^{-1}$.

The front mentioned above is a conical surface which is tangent to the spherical front of the S wave and cuts the $y = 0$ surface at the edge of the region of contact, i.e. at $r = \alpha t$. The time at which the front reaches the point in question can be determined from the equation

$$t = r\alpha^{-1} + y(b^{-2}-\alpha^{-2})^{1/2} \tag{5.52}$$

It is not difficult to show (see Appendix C) that the value of $\dot{\sigma}_y^S$ near the front is given by an infinite series of the form

$$\dot{\sigma}_y^S \simeq \left\{\frac{B_0 + B_1(\alpha^{-2}-\theta_2^2) + B_2(\alpha^{-2}-\theta_2^2)\log(\alpha^{-2}-\theta_2^2) + \ldots.}{(\alpha^{-2}-\theta_2^2)^{3/2} + \beta(\alpha^{-2})/\pi}\right\} + \text{Re } A(\theta) \tag{5.53}$$

where $A(\theta)$ is the smoothly varying function defined by the first integral of Eq. (C.5), $\beta(\alpha^{-2})$ is the argument of the Rayleigh function at α^{-2}, and θ_2 is defined implicitly by the equation

$$t - \theta_2 r - y(b^{-2}-\theta_2^2)^{1/2} = 0 \tag{5.54}$$

The method used to compute the B_i's is described in Appendix C.

For computational purposes the infinite series of Eq. (5.53) is truncated after a finite number of terms. Using this finite series approximation of $\dot{\sigma}_y^S$, we compute the value of σ_y^S from the following equation when the point in question is near the front shown in Fig. 18:

$$\begin{aligned}\sigma_y^S(t) \simeq \text{Re} \sum_{j=0}^{j=m-1} &(\dot{\sigma}_y^S(t_2^*+2j\Delta t) + 4\dot{\sigma}_y^S(t_2^* + (2j+1)\Delta t) \\ &+ \dot{\sigma}_y^S(t_2^* + (2j+2)\Delta t))\,\frac{\Delta t}{3} \\ + \text{Re} \int_{\theta_2(t_2^*+2m\Delta t)}^{\theta_2^2(t)} &\dot{\sigma}_y^S\,\frac{\partial t}{\partial \theta^2}\,d\theta^2\end{aligned} \tag{5.55}$$

The values of m and Δt in Eq. (5.55) are chosen in such a way that

1) $\dot{\sigma}_y^S$ is accurately approximated by the above-mentioned finite series during the interval of time $t_2^* + 2m\Delta t$ to t, and

2) $\dot{\sigma}_y^S$ is accurately approximated by a quadratic function during the interval of time $t_2^* + (2m-2)\Delta t$ to $t_2^* + 2m\Delta t$.

The integrand of the integral of Eq. (5.55) is singular at $\theta^2 = \alpha^{-2}$ but is analytic at every point above the real θ axis. Consequently, if $\theta_2(t) > \alpha^{-1}$, it is convenient to deform the contour of integration into a curve which, except for the end points, lies entirely in the upper half of the θ^2 plane (see Fig. 29). If the deformed contour is made up of straight line segments, the integral can be evaluated very easily by means of Simpson's Rule. Thus, it is not difficult to compute the value of σ_y^S at a point during a short interval of time following the arrival of the front on which σ_y^S is singular. The value of σ_y^S at greater times is computed from the equation

$$\sigma_y^S(t_2^*+2n\Delta t) \simeq \sigma_y^S(t_2^*+2k\Delta t) + \mathrm{Re} \sum_{j=k}^{j=n-1} (\dot{\sigma}_y^S(t_2^*+2j\Delta t) + 4\dot{\sigma}_y^S(t_2^* + (2j+1)\Delta t) + \dot{\sigma}_y^S(t_2^* + (2j+2)\Delta t) \frac{\Delta t}{3} \qquad (5.56)$$

where $\sigma_y^S(t_2^*+2k\Delta t)$ is the value of σ_y^S at a point shortly after the arrival of the front on which σ_y^S is singular.

It is not difficult to show that equations similar to (5.44), (5.48), (5.55) and (5.56) can be used to compute the value of σ_y^S and σ_y^P when the point in question is on the surface of the half space. For these

problems the value of σ_y^P and σ_y^S must be computed analytically when the edge of the region of contact is near the point being considered since $\dot{\sigma}_y^P$ and $\dot{\sigma}_y^S$ become singular as the edge of contact passes over the point in question.

The following remarks summarize the integration procedures described in Secs. 5.4.1 and 5.4.2.:

1) The time variation of $\dot{\sigma}_y^P$ and $\dot{\sigma}_y^S$ cannot be computed by a step-by-step procedure. However, the value of these quantities at any given time can be computed without difficulty. (See Sec. 5.4.1.)

2) The equations of Sec. 5.4.2 have been formulated in the natural way, so that the variation with time of σ_y^P and σ_y^S at a fixed point is found by a step-by-step procedure after the values of $\dot{\sigma}_y^P$ and $\dot{\sigma}_y^S$ are determined.

3) Since σ_y is a homogeneous function of degree zero of t, r and y, the results obtained from Eqs. (5.43), (5.44), (5.48), (5.55) and (5.56) can also be interpreted as the variation of σ_y along a "r/y = constant" ray at a specified instant of time. This follows since

$$\sigma_y(r,y,\lambda t) = \sigma_y(r/\lambda, y/\lambda, t) \tag{5.57}$$

where λ is any positive constant.

The procedure used to evaluate σ_y is typical of the way in which the velocities and remaining stresses are computed. The results obtained are discussed in Chapter 6.

6. THE STRESS AND VELOCITY FIELDS FOR THE WEDGE AND CONE PROBLEMS

6.1. The Wedge Problem

6.1.1. Stresses near the Contact Zone

The results obtained in Sec. 4.1 for the distribution of the contact stress σ_y beneath a wedge are plotted in Fig. 23 for a value of α in each range of contact speed.† From this figure it can be seen that the stress is singular beneath the apex of the die. For contact speeds in the first and second intermediate range, another singularity is present at the edge of the contact zone. Between the apex of the die and the edge of the contact zone, $\sigma_y(x,0,t)$ is finite and continuous with a minimum value at $|x| = ct$ for all but the slow range of contact speeds.

The asymptotic character of the stress near the apex and the edge of the region of contact can be determined in a straightforward manner from the function which solves the wedge problem, i.e. from the function $\sigma_y^{*'}(\theta)$ which is defined as follows:

$$\begin{aligned}
\sigma_y^{*'}(\theta) &= \frac{iA_1}{(\alpha^{-2}-\theta^2)^{1/2}} && \text{for } \alpha \leq c \\
&= \frac{iA_1}{(\alpha^{-2}-\theta^2)^{1/2}} + \frac{iA_1(c^{-2}-\alpha^{-2})}{(\alpha^{-2}-\theta^2)^{3/2}} && \text{for } c \leq \alpha \leq b \\
&= \frac{iA_1 F_{\alpha b}(\theta)}{(\alpha^{-2}-\theta^2)^{1/2}} + \frac{iA_1(c^{-2}-\alpha^{-2})F_{\alpha b}(\theta)}{(\alpha^{-2}-\theta^2)^{3/2}} && \text{for } b \leq \alpha \leq a
\end{aligned} \tag{6.1}$$

† The four ranges of contact speeds are defined in Sec. 1.2.

$$= \frac{iA_1}{2(b^{-2}-a^{-2})} \frac{R(\theta^2)}{(a^{-2}-\theta^2)^{1/2}(\alpha^{-2}-\theta^2)} \qquad \text{for } \alpha > a$$

where $F_{\alpha b}(\theta)$ is the function defined by Eq. (4.25) of Sec. 4.1.4.3, and

$$A_1 = \frac{4\mu}{\pi}\left(1 - \frac{b^2}{a^2}\right) \tan \frac{\pi - \gamma}{2} \tag{6.2}$$

At points near the apex of the die, each of the above equations is accurately approximated in the following manner:

$$\sigma_y^{*'}(\theta) \simeq \frac{A_1}{\theta} \tag{6.3}$$

Hence $\sigma_y^*(\theta)$ and $\sigma_y(x,0,t)$ are approximated by the equations

$$\sigma_y^*(\theta) \simeq A_1 \log \theta \tag{6.4}$$

$$\sigma_y(x,0,t) = A_1 \log \frac{t}{|x|}$$

It is apparent from Eqs. (6.2) and (6.4) that the logarithmic singularity in the contact stress beneath the apex of the die depends only on the shape of the die and the elastic properties of the half space. As in the static case (see Ref. [38], page 43) a logarithmic singularity is associated with a sudden change of slope.

The character of the contact stress near the edge of the contact zone is found by integrating termwise the asymptotic expansion of $\sigma_y^{*'}(\theta)$ about $\theta = \alpha^{-1}$ and then taking the real part of the resulting expression. This yields

$$\sigma_y \simeq -\sqrt{2}\,\frac{A_1 \xi^{1/2}}{x^{1/2}} + O(\xi^{3/2}) \qquad \text{for } \alpha \leq c$$

$$\sigma_y \simeq -\frac{A_1\alpha^2(c^{-2}-\alpha^{-2})x^{1/2}}{\sqrt{2}\ \xi^{1/2}} + O(\xi^{1/2}) \qquad \text{for } c \leq \alpha \leq b$$

$$\simeq -\frac{A_1 B_0(c^{-2}-\alpha^{-2})x^{1/2+\beta/\pi}}{\xi^{1/2+\beta(\alpha^{-2})/\pi}}\cos\beta + O(\xi^{1/2-\beta(\alpha^{-2})/\pi}) \qquad (6.5)$$

$$\text{for } b \leq \alpha \leq a$$

$$\simeq -\frac{A_1\pi\alpha R(\alpha^{-2})H(\alpha t-x)}{4(b^{-2}-a^{-2})(a^{-2}-\alpha^{-2})^{1/2}} \qquad \text{for } \alpha > a$$

where $B_0 = C_0 \cdot \alpha^{2+2\beta/\pi}\Big/(1/2+\beta/\pi)2^{3/2+\beta/\pi}$, and C_0 is the constant defined by Eq. (A.13); and where $\xi = \alpha t - x$ and H is the Heaviside step function. (The results of Appendix A have been used in obtaining the expansion of $\sigma_y^{*'}(\theta)$ about α^{-1} for the case in which $b \leq \alpha \leq c$.)

Since the value of $\beta(\alpha^{-2})/\pi$ is between 0 and -1/2, the singularity in the contact stress for α in the second intermediate range is of lower order that the square-root singularity which occurs for contact speeds in the first intermediate range. It might be noted that a square-root singularity is present in the static contact problem for a rectangular punch [38].

At first glance it would appear from Eqs. (6.1) that the distribution of the contact stress is significantly different for values of α just above and just below c. Note, however, that the first term in the second of Eqs. (6.1) is multiplied by a factor $c^{-2}-\alpha^{-2}$. Consequently, if α is only slightly greater than c, the component of the stress associated with this term will be small except near the edge of the region of contact. Hence, the transition between the slow and first intermediate ranges of contact speeds is a smooth process. In a similar manner, it can be shown that the transition

is smooth between the first and second intermediate ranges and between the second intermediate and superseismic ranges.

It is of interest to consider the asymptotic character of the stress field near the edge of the region of contact, not only at the surface, but also a small distance below. This can be done using a method which is essentially the same as that just used to determine the behavior of the stress on the surface. It can easily be verified that the vertical stress, for example, is approximated near the edge of the contact zone by the equations

$$\sigma_y(\xi,y,t) \simeq \mathrm{Re}\left(\frac{-\sqrt{2}\,A_1}{x^{1/2}}\left[B_1\xi_1^{1/2} + B_2\xi_2^{1/2}\right]\right) \qquad \text{for } \alpha \le c$$

$$\simeq \mathrm{Re}\left(\frac{-A_1\alpha^2(c^{-2}-\alpha^{-2})x^{1/2}}{\sqrt{2}}\left[\frac{B_1}{\xi_1^{1/2}} + \frac{B_2}{\xi_2^{1/2}}\right]\right) \qquad \text{for } c \le \alpha \le b$$

$$\simeq \mathrm{Re}\left(-A_1B_0(c^{-2}-\alpha^{-2})x^{1/2+\beta/\pi}\left[\frac{iB_1}{(-\xi_1)^{1/2+\beta/\pi}} \quad \frac{iB_2}{(-\xi_2)^{1/2+\beta/\pi}}\right]\right)$$

$$\text{for } b < \alpha < a$$

$$= -\frac{A_1\pi}{4(b^{-2}-a^{-2})}\left[\frac{(b^{-2}-2\alpha^{-2})^2}{(a^{-2}-\alpha^{-2})^{1/2}}\,H(t-\alpha^{-1}x - y\sqrt{a^{-2}-\alpha^{-2}}\right.$$

$$\left. + 4\alpha^{-2}\sqrt{b^{-2}-\alpha^{-2}}\,H(t-\alpha^{-1}x - y\sqrt{b^{-2}-\alpha^{-2}})\right]$$

$$\text{for } \alpha > a \qquad (6.6)$$

where $B_1 = \dfrac{(b^{-2}-2\alpha^{-2})^2}{R(\alpha^{-2})}$, $B_2 = \dfrac{4\alpha^{-2}\sqrt{a^{-2}-\alpha^{-2}}\sqrt{b^{-2}-\alpha^{-2}}}{R(\alpha^{-2})}$

and $\xi_i = \xi + iy\sqrt{1-\alpha^2/c_i^2}$ $\qquad i = 1,2.$

The second of Eqs. (6.6) is plotted in Fig. 30 for the case in which $\alpha = 0.95b$. The curves in this figure illustrate the variation of (ξ,y,t) along the portion of several y = constant planes just below the edge of the region of contact. These results have been non-dimensionalized by plotting

$$\frac{\sigma_y(\frac{\xi}{\alpha t}, \frac{y}{\alpha t})}{|\sigma_y(\frac{\xi}{\alpha t}, 0.1)|} \quad \text{vs} \quad \frac{\xi}{\alpha t} .$$

6.1.2. The Stress and Velocity Fields in the Half Space

The stress and velocity fields for the wedge problem have been determined using the numerical integration procedure described in Chapter 5. This procedure gives the time history of the stresses and velocities at pre-selected points in the half space.

Figures 31, 32 and 33 show the results obtained for the problem in which a wedge indents slowly with a value of α equal to $0.25b$. The curves in these figures give the variation with time of stresses and velocities at points on rays in the z = 0 plane which pass through the origin and make angles of 0°, 15°, 30° and 90° with the surface of the half space. The shape of the curves for the 15°, 30° and 90° rays for times following the arrival of the S wave is essentially the same for all values of α. However, for times up to an immediately following the arrival of the S wave, the shape of a curve for values of α in the different ranges of contact will depend on whether or not a Mach front passes the point for which the curve is drawn. These disturbances occur at certain points in the half space when the contact speed is in the second intermediate and superseismic ranges. Figures 34a and

34b show how such disturbances influence the vertical velocity and stress at a point on the ray making an angle of 30° with the surface.

6.2. The Cone Problem

6.2.1. Stresses Near the Contact Zone

The distribution of the contact stress σ_y beneath a rigid cone is shown in Fig. 35 for a value of α in each range of contact speed. The curves for the slow and first intermediate ranges are plots of the equations (Eqs. (4.49) and (4.51) of Sec. 4.2)

$$\sigma_y(r,0,t) = -\frac{A_1}{2}\pi \cosh^{-1}\frac{\alpha t}{r} \qquad \text{for } \alpha \leq c$$

$$= -\frac{A_1}{2}\pi\left(\cosh^{-1}\frac{\alpha t}{r} + \frac{1}{2}\frac{(c^{-2}-\alpha^{-2})t\alpha^3}{\sqrt{\alpha^2t^2-r^2}}\right), \qquad \text{for } \alpha \geq c \tag{6.7}$$

where $$A_1 = 4\frac{\mu}{\pi}\tan\frac{\pi-\gamma}{2}\cdot\left(1-\frac{b^2}{a^2}\right), \tag{6.8}$$

as in Sec. 6.1.1. The curves of Fig. 35 for the second intermediate and superseismic ranges were determined using the numerical integration procedure described in Chapter 5.

It follows from Eqs. (6.7) that the contact stress near the vertex of the die is given for $\alpha \leq b$ by the equation

$$\sigma_y(r,0,t) \simeq \frac{A_1}{2}\log\frac{1}{r} \tag{6.9}$$

It is not difficult to verify that Eq. (6.9) holds for all values of α.

For static contact problems, there is also a stress singularity in the contact stress at points where the slope of the surface is discontinuous (see Ref. [38], page 188).

From Eqs. (6.4) and (6.9), it can be seen that the logarithmic singularity beneath the tip of a wedge with apex angle γ has twice the intensity of the logarithmic singularity beneath the vertex of a cone with the same angle γ.

The variation of the stress and velocity fields in the half space near the edge of the region of contact can be computed by an asymptotic method very similar to that used in Sec. 3.4.1.2 to determine the surface wave stresses and velocities for the problem involving a concentrated load at the origin. These computations give the following result for the vertical stress:

$$\sigma_y(\xi,y,t) \simeq \mathrm{Re}\left(-\frac{A_1\pi}{\sqrt{2}\,r^{1/2}}\left(\frac{B_1}{\xi_1^{1/2}}+\frac{B_2}{\xi_2^{1/2}}\right)\right) \qquad \text{for } \alpha \le c$$

$$\simeq \mathrm{Re}\left(-\frac{A_1\pi r^{1/2}}{4\sqrt{2}}\left(\frac{B_1}{\xi_1^{1/2}}+\frac{B_2}{\xi_2^{1/2}}\right)\right) \qquad \text{for } c \le \alpha \le b \quad (6.10)$$

$$\simeq \mathrm{Re}\left(-\frac{A_1B_3r^{1/2+\beta/\pi}}{4}\left(\frac{iB_1}{(-\xi_1)^{1/2+\beta/\pi}}+\frac{iB_2}{(-\xi_2)^{1/2+\beta/\pi}}\right)\right)$$

$$\text{for } b \le \alpha \le a$$

$$\simeq -\frac{A_1\pi}{4(b^{-2}-a^{-2})}\left(\frac{(b^{-2}-2\alpha^{-2})^2}{(a^{-2}-\alpha^{-2})^{1/2}}\,H(t-\alpha^{-1}r-y\sqrt{\alpha^{-2}-a^{-2}}\right.$$

$$\left.+\,4\alpha^{-2}\sqrt{b^{-2}-\alpha^{-2}}\,H(t-\alpha^{-1}r-y\sqrt{\alpha^{-2}-b^{-2}})\right)$$

$$\text{for } \alpha \ge a$$

where B_1 and B_2 are defined as in Eqs. (6.6),

$$\xi = \alpha t - r \quad , \quad \xi_i = \xi + iy\sqrt{1 - \alpha^2/c^2} \quad ,$$

$$B_3 = \frac{C_0(\alpha^{2+2B/\pi})(c^{-2}-\alpha^{-2})}{(1 + \beta/\pi)(2^{1/2+\beta/\pi})} \cdot \mathrm{Re}\int_0^1 \frac{id\lambda}{(\lambda^{1+\beta/\pi})(1 - \lambda)^{1/2}} \quad ,$$

C_0 is defined by (A.13), and $\lambda = (\alpha^{-2}-\theta^2)/(\alpha^{-2}-\theta_0^2)$. The values of λ are computed assuming that θ^2 lies on a contour which joins α^{-2} and θ_0^2 and which is just above the real θ^2 axis.

For $y = 0$, $\xi_1 = \xi_2 = \alpha t - r$ and Eqs. (6.10) give the asymptotic character of the contact stress near the edge of the contact zone.

A comparison of Eqs. (6.7) and (6.10) indicates that the cominant terms in the asymptotic expansion of $\sigma_y(\xi,y,t)$ for the wedge and cone problems are identical for $\alpha > a$ and differ only by a scale factor for $\alpha < a$. That is,

$$\frac{\sigma_y^c(\xi,y,t)}{\sigma_y^w(\xi,y,t)} = \frac{\pi}{2} \qquad \text{for } \alpha \leq c$$

$$= \frac{\pi}{4} \qquad \text{for } c \leq \alpha \leq b \qquad (6.11)$$

$$= \frac{(\frac{1}{2} + \frac{\beta}{\pi})\ \mathrm{Re}\int_0^1 \frac{i\ d}{\lambda^{1+\ B/\pi}\sqrt{1-\lambda}}}{2(1 + \beta/\pi)} \qquad \text{for } b \leq \alpha \leq a$$

$$= 1 \qquad \text{for } \alpha \geq a$$

where σ_y^c and σ_y^w are the first term on the right-hand side of Eqs. (6.10) and (6.6), respectively. The result obtained for the superseismic case is to be expected since the initial disturbance experienced by a point on the surface would appear to be the same for the two problems.

The smoothness of the transition from one range of speeds to the next can be proved in the same way as for the wedge problem.

Since σ_y^w and σ_y^c differ only by a scale factor the ratios of

$\frac{\sigma_y^c(\frac{\xi}{\alpha t}, \frac{y}{\alpha t})}{|\sigma_y^c(0,0.1)|}$ and $\frac{\sigma_y^w(\frac{\xi}{\alpha t}, \frac{y}{\alpha t})}{|\sigma_y^w(0,0.1)|}$ are equal. Hence, the non-dimensionalized curves of Fig. 30 define the variation of both σ_y^w and σ_y^c in the neighborhood of the edge of the region of contact for problems in which the contact speed of a wedge or cone is equal to 0.95b.

6.2.2. Stresses and Velocities in the Half Space

The stress and velocity fields for the cone problem can be evaluated using the numerical integration techniques described in Sec. 5.4. Figures 36 and 37 show the results obtained for the vertical component of these fields for the problem in which a cone indents with a contact speed in the slow range ($\alpha = 0.25b$). The curves of these figures illustrate the time variation for the vertical stress and velocity at points on rays which pass through the origin and make angles of 0°, 15°, 30° and 90° with the surface of the half space.

The way in which the arrival of a Mach front influences the vertical stress and velocity is shown in Fig. 38. The curves in this figure are drawn for a point on a ray which makes an angle of 30° with the surface of the half space.

6.3. A Comparison of Analytical and Numerical Results

It follows from the work of Sec. 2.6.3.1 that, for the wedge problem, the asymptotic character of the P, S and head wave components of σ_y at points

just behind the various wave fronts is given by equations of the form

$$\begin{aligned} \sigma_y^P &\simeq \epsilon^{1/2}[A_0 + A_1\epsilon + \ldots] \\ \sigma_y^S &\simeq \epsilon^{1/2}[B_0 + B_1\epsilon + \ldots] \\ \sigma_y^H &\simeq \epsilon^{3/2}[C_0 + C_1\epsilon + \ldots] \end{aligned} \tag{6.12}$$

In Eqs. (6.12) the P, S and head wave components of σ_y are denoted by σ_y^P, σ_y^S and σ_y^H, respectively; ϵ is a small distance behind the front being considered; and the A's, B's and C's are real constants, the value of which can be determined in the manner described in Sec. 2.6.3.1.

The asymptotic character of σ_y^P, σ_y^S and σ_y^H for the cone problem can be determined by the method described in Secs. 3.4.1.3 and 3.4.1.4. The result is equations of the form

$$\begin{aligned} \sigma_y^P &\simeq D_0\epsilon + D_1\epsilon^2 + \ldots \\ \sigma_y^S &\simeq E_0\epsilon + E_1\epsilon^2 + \ldots \\ \sigma_y^H &\simeq F_0\epsilon^2 + F_1\epsilon^3 + \ldots \end{aligned} \tag{6.13}$$

where the D's, E's and F's are real constants determined in the manner indicated in the sections mentioned above.

It can easily be verified that the P, S and head wave components of the remaining stresses and velocities are defined by equations which are similar in form to Eqs. (6.12) and (6.13).

In each of the problems considered in this study, it has been found that the results obtained numerically are in excellent agreement with the results predicted by Eqs. (6.12) and (6.13). Figure 39 shows the agreement

between these results for the problem in which a wedge indents slowly with $\alpha = 0.1b$. The results for the corresponding cone problem are given in Fig. 40.†

6.4. The Stress Field for Slowly Indenting Dies

It is to be expected that the stress field associated with a die which indents very slowly will be virtually the same, except near the origin, as the stress field associated with a load of equal intensity concentrated at the origin, i.e. with a concentrated load which has the same magnitude at each instant of time as the force pressing the die into the half space. Results obtained numerically (see Figs. 41 and 42) indicate that for values of α/b as large as 0.1, the stress fields for these problems are almost identical at points further from the origin than one-third of the distance to the front of the S wave.

The similarity in the stress fields results from the fact that the functions solving the die and concentrated load problems are virtually the same for small α, except at points near the origin. This will now be explained in detail.

It can easily be verified that the functions which solve the wedge and cone problems are accurately approximated away from the origin by the series:

$$\frac{\partial \sigma_y^*}{\partial \theta} \simeq i\alpha A_1 + \frac{i\alpha^3 A_1 \theta^2}{2} + O(\alpha^5 \theta^4) \qquad (6.14)$$

for the wedge and

† In plotting Eqs. (6.12) and (6.13), terms of order ϵ^3 and higher have been neglected.

$$\frac{\partial \sigma_y^*}{\partial \theta^2} \simeq A_1\alpha^2 + A_1\alpha^2\theta^2 + O(\alpha^6\theta^4)$$

for the cone. For these contact problems, the net force on the surface of the half space is given by the equations

$$P(t) = \alpha A_1 \pi t \tag{6.15a}$$

for the wedge and

$$P(t) = \alpha A_1 \pi^2 t^2 \tag{6.15b}$$

for the cone.

It follows directly from the work of Secs. 2.6.1 and 3.4 that the functions given below solve the problems in which loads defined by Eqs. (6.16) are concentrated at the origin:

$$\frac{\partial \sigma_y^*}{\partial \theta} = i\alpha A_1$$

for the two-dimensional problem and (6.16)

$$\frac{\partial \sigma_y^*}{\partial \theta^2} = \alpha^2 A_1$$

for the axially symmetric problem.

It is apparent that the values of the functions defined by Eqs. (6.14) are accurately approximated by the values of Eqs. (6.16) if α is sufficiently small and θ is finite. Hence, the stress fields for the die and concentrated load problems are virtually the same, except near the origin of the half space.

7. SUMMARY AND RECOMMENDATIONS FOR FURTHER STUDY

7.1. The Method of Solution

In this study, it has been found that a wide variety of two-dimensional and axially symmetric three-dimensional wave propagation problems can be solved without difficulty by the method of self-similar solutions developed by Smirnov and Sobolev [5,6]. The form of any solutions obtained by this method is such that the position of the fronts of the various waves and other singularities at any time can be determined virtually by inspection. Moreover, the stresses and displacements at any point can be determined by a simple quadrature. The asymptotic behavior of the stresses and displacements near fronts can be extracted especially simply.

7.2. Results Obtained for the Contact Problems Studied

The following results have been obtained using the method of self-similar solutions for contact problems involving the penetration of a homogeneous, isotropic, linearly elastic half space by a rigid die:

1) If the die penetrates the half space superseismically,† the magnitude of the force applied to the half space by the die is given by the following equation:

$$P(t) = - a\rho A(t)V(t)$$

where $P(t)$, $A(t)$ and $V(t)$ denote, respectively, the force, area of contact and indentation velocity of the die at any instant; a is the speed of the P wave; and ρ is the density of the elastic half space (Sec. 4.3.4).

† The contact is said to be superseismic if every point on the boundary of the expanding region of contact moves outward at least as rapidly as the P wave disturbances in the half space.

2) The force required to press a wedge or cone into a half space with constant speed is a monotonically increasing function of the rate of penetration. Thus, to achieve an increase in the rate of penetration, it is only necessary to apply a greater force to the indenting die (Secs. 4.1.6 and 4.2.6).

3) For all ranges of contact speeds,† the contact stress varies as $\log |\epsilon|$ at points near the apex of the die, where ϵ denotes the distance from the apex to the point in question. Near the edge of the region of contact, this stress varies for the slow, first intermediate and second intermediate ranges of contact speeds as $\epsilon^{1/2}$, $\epsilon^{-1/2}$, and $\epsilon^{-\gamma}$, respectively, where ϵ now denotes the distance from the point in question to the edge of the region of contact, and γ is a function of the contact speed. The value of γ ranges between 0 and 1/2. If the contact speed is superseismic, there is a step discontinuity in the stress at the edge of the region of contact (Secs. 5.2.1 and 5.4.2).

4) Singularities in the stress field at points below the surface occur only for problems in which the contact speed is in the second intermediate range. For these problems the equivoluminal component of the stress field is singular on the Mach surface which is tangent to the front of the S wave and meets the surface of the half space at the edge of the region of

---

† These ranges are defined in Sec. 1.2.

contact. (See Figs. 18 and 19.) The singular portion of the stress field varies at $\epsilon^{-\gamma}$ at points a distance ϵ on either side of this moving surface (Secs. 5.2.2 and 5.4.2).

5) Mach fronts are formed, as expected, when the contact speed is superseismic. (See Fig. 19.) The arrival at a point of the Mach front associated with the P wave results in an instantaneous jump in the stresses at that point by a stress state which is irrotational.

A second Mach front propagates at the same rate as the S wave. The arrival of this front at a point results instantly in a set of finite stresses which have no irrotational component. These stresses must be added to those arising from any other wave which has passed this point to determine the total stress at the point.

6) A head wave disturbance occurs, as expected, for any problem which has a subseismic contact speed. This equivoluminal disturbance is present at every point in the region bounded by the front of the S wave, the surface of the half space, and the head wave (see Figs. 16, 17 and 18).

In a short interval of time following the arrival of the head wave at any point, the equivoluminal component of the stress field varies as $\epsilon^{3/2}$ for the wedge problem and as ϵ^{2} for the cone problem, where ϵ denotes the distance from the point to the head wave (Secs. 6.3).

7) The arrival of the P wave at a point gives rise to irrotational stresses, which for wedge and cone problems vary as $\epsilon^{1/2}$ and ϵ respectively. As before, ϵ is the distance from a point just

behind the front to the front. The S wave causes equivoluminal stresses which for wedge and cone problems vary as $\epsilon^{1/2}$ and ϵ, respectively, at points which are a distance ϵ behind the front of the S wave (Sec. 6.3).

The total stress at any point is the algebraic sum of the stresses caused by each of the waves which has passed through the point in question.

8) The stress field associated with a die which indents very slowly is virtually the same, except at points near the origin, as the stress field associated with a concentrated load which acts vertically downward at the origin and which is equal in magnitude to the force pressing the die into the half space (Sec. 6.4).

7.3. Recommendations for Further Study

This section contains a brief description of some further problems which might conveniently be solved by the method of self-similar solutions.

The axially symmetric problems considered in this study were solved by a "rotational superposition" of plane strain problems around a vertical axis (Chapter 3). Further study is necessary to determine whether three-dimensional wave propagation problems which lack axial symmetry might readily be solved by superimposing plane strain problems which are weighted by factors which are functions of the angle of rotation about the vertical axis. This method of solving three-dimensional static problems has been proposed by Aleksandrov [39].

The problems treated in this study involved a rigid wedge or cone indenting an elastic half space. The case of collisions of two elastic wedges

or cones† presents additional complications unless the wave speeds in the two bodies are identical. If they are not identical, the "indentation" in one body may occur in a different range of contact speed than in the other body. Treatment of this problem may well require considerable extension of the method used.

Of course, the region of contact between two bodies of general shape can be computed from the initial geometry and the known impact velocity as long as the contact remains superseismic, i.e. as long as each point on the boundary of the expanding region of contact moves outward at least as rapidly as the faster of the two P waves in the dissimilar bodies. As long as the contact is superseismic, the integral equation from which the location of the surface is determined can be formulated by a simple extension of the methods used in Sec. 4.3 to solve problems involving the superseismic penetration of an elastic half space by a rigid die.

Finally, it is noted that the solution obtained analytically for times when the contact is superseismic could be taken as the initial data for a numerical scheme used to extend the solution to times when the contact is no longer superseismic.

---

† These dies must have a very shallow apex angle if small displacement theory is used to determine the contact stress.

LIST OF REFERENCES

1. Love, A. E. H. A Treatise on the Mathematical Theory of Elasticity. Fourth edition. Dover, New York, 1944.

2. Riney, T. D. Depth of penetration of hypervelocity projectiles. A.I.A.A. J. 3 (1965), 52-60.

3. Rakhmatulin, Kh. A. and Dem'yanov, Yu A. Strength Under High Transient Loads. Israel Program for Scientific Translation, Jerusalem, 1966.

4. Frank, Ph. and von Mises R. Differential and Integral Equations of Mathematical Physics. Chapter XII, by S. L. Sobolev. (Russian edition only†) ONTI, Moscow-Leningrad, 1937.

5. Smirnov, V. I. and Sobolev, S. L. Sur une méthode nouvelle dans le problème plan des vibrations élastiques. Trud. Inst. Seism. Akad. Nauk SSSR 20 (1932).

6. Smirnov, V. I. and Sobolev, S. L. On the application of a new method of investigation of the elastic vibrations in the space with axial symmetry. Trud. Inst. Seism. Akad. Nauk SSSR 29 (1933).

7. Cagniard, L. Reflection and Refraction of Progressive Seismic Waves. International Series in the Earth Sciences, McGraw-Hill, New York, 1962.

8. Ewing, W. N., Jardetzky, W. S. and Press, F. Elastic Waves in a Layered Medium. McGraw-Hill Series in the Geological Sciences, McGraw-Hill, New York, 1957.

9. Kostrov, B. V. Self-similar dynamic problems of pressing of a rigid die into an elastic half space. (In Russian.) Mekhanika I Mashinostroenie 4 (1964), 54.

10. Lamb, H. On the propagation of tremors over the surface of an elastic solid. Phil. Trans. Royal Soc. A, 203 (1904), 1-42.

11. Payton, R. G. Transient motion of an elastic half-space due to a moving surface line load. Int. J. Engng. Sci. 5 (1967), 49-79.

12. Dix, C. H. The reflected seismic pulse. J. Geophys. Research 66 (1961), 227-234.

13. Lamé, M. G. Lecons sur la théorie mathématique de l'élasticité des corps solides. Second edition. Gauthier Villars, Paris, 1866.

---

† The only copy of this reference that could be located in North America is at Brown University in Providence, R.I.

14. Sommerfeld, A. Partial Differential Equations in Physics. Volume 1. Academic Press, New York, 1949.

15. Craggs, J. W. Two-dimensional waves in an elastic half-space. Proc. Cambridge Philos. Soc. 56 (1960), 269-285.

16. Craggs, J. W. On axially symmetric waves. I. Linearized compressible flow with axial boundary conditions. Proc. Cambridge Philos. Soc. 59 (1963), 637-654.

17. Craggs, J. W. On axially symmetric waves. II. The treatment of a plane boundary. Proc. Cambridge Philos. Soc. 59 (1963), 655-667.

18. Craggs, J. W. On axially symmetric waves. III. Elastic waves in a half-space. Proc. Cambridge Philos. Soc. 59 (1963), 803-809.

19. Kostrov, B. V. The axisymmetric problem of propagation of a tension crack. Prikladnaia Matematika i Mekhanika 28 (1964), 793.

20. Kostrov, B. V. Selfsimilar problems of propagation of shear cracks. Prikladnaia Matematika i Mekhanika 28 (1964), 1077.

21. Smirnov, V. I. A Course of Higher Mathematics. Volume III, Part 2, Sections 52-55. Addison-Wesley, Reading, Mass., 1964.

22. Pod"Yapol'ski, G. S. I. The propagation of elastic waves in a layered medium. Bulletin of the Academy of Sciences of the U.S.S.R., Geophysics Series (translation of Izv. Akad. Nauk SSSR ser. goefiz.) 1959, No. 8, 788-793.

23. Filippov, A. F. Some problems of diffractions of plane elastic waves. (In Russian.) Prikladnaia Matematika i Mekhanika 20 (1956), 688.

24. Zvolinskii, N. V. Reflected and head waves emerging at a plane interface of two elastic media I. Bulletin of the Academy of Sciences of the U.S.S.R., Geophysics Series. 1957, No. 10, 1-21.

25. Pariiskaya, G. N. and Kuhn, V. V. The relative intensity of head waves propagated in media with vertical interfaces. Bull. Acad. Sci. U.S.S.R., Geophysics Series. 1960, No. 5, 480.

26. Pod"Yapol'ski, G. S. and Vassil'ev, Yu. I. A Rayleigh-type wave at a non-free surface. Bull. Acad. Sci. U.S.S.R., Geophysics Series. 1960, No. 9, 859.

27. Duhem, P. Sur l'integrale des equations des petits mouvements d'un solide isotrope. Mem. Soc. Sci. Bordeaux Ser. V, 3 (1898), 317-329.

28. Sternberg, E. On the integration of the equations of motion in the classical theory of elasticity. Arch. Rational Mech. Anal. 6 (1960), 34-50.

29. Duff, G. F. D. Partial Differential Equations. University of Toronto Press, Toronto, 1956.

30. Ward, G. N. The Linearized Theory of Steady High-Speed Flow. Chapter VIII. Cambridge, 1955.

31. Churchill, R. V. Complex Variables and Applications. Second edition. McGraw-Hill, New York, 1960.

32. Hille, E. Analytic Function Theory. Volume I. Ginn, New York, 1959.

33. Weber, C. Zur Umwandlung von rotationssymmetrischen Problemen in zweidimensionale und umgekehrt. Z. angew. Math. Mech. 20 (1940), 117-118.

34. Hamel, G. Integralgleichungen. Springer-Verlag, Berlin, 1949.

35. Pekeris, C. L. The seismic surface pulse. Proc. N.A.S. 41 (1955), 469-480.

36. Jeffreys, H. and Jeffreys, B. S. Methods of Mathematical Physics. Third edition. Cambridge: Cambridge University Press, 1956.

37. Paul, S. Interaction of Plane Elastic Waves with a Cylindrical Cavity. Doctoral thesis, University of Illinois, 1963.

38. Shtaerman, I. Ya. The Contact Problem of the Theory of Elasticity. (In Russian.) GITTL, Moscow-Leningrad, 1949.

39. Aleksandrov, A. Ya. Applications of the Theory of Functions in Continuum Mechanics. Proc. Int. Symp. of IUTAM, Tiflis, (Sept. 1963), "Nauka," Moscow, 1965.

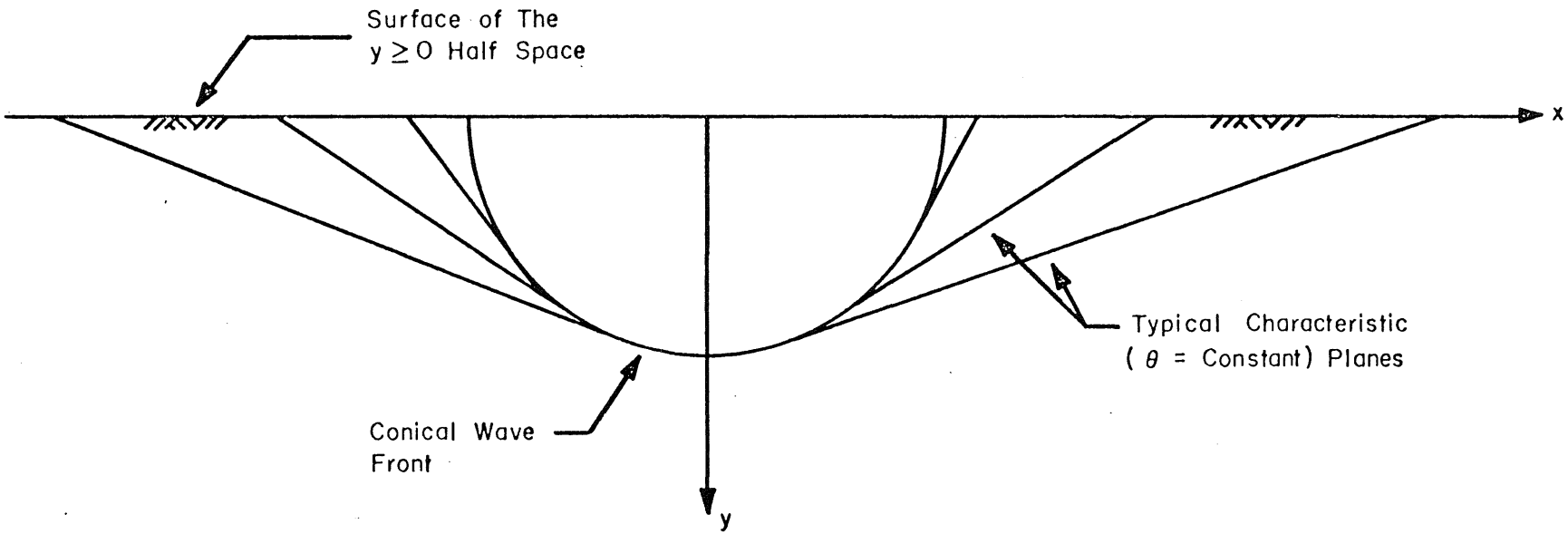

FIG. 1. INTERSECTION OF THE CONE AND TYPICAL CHARACTERISTIC PLANES WITH THE t = 1 PLANE

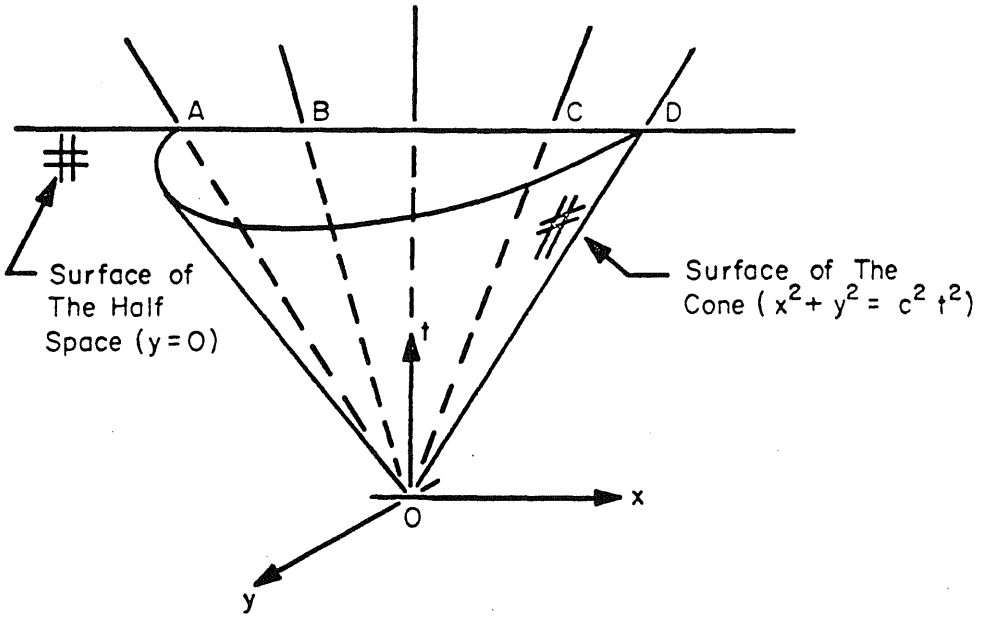

(a) θ = CONSTANT RAYS IN THE y = 0 PLANE

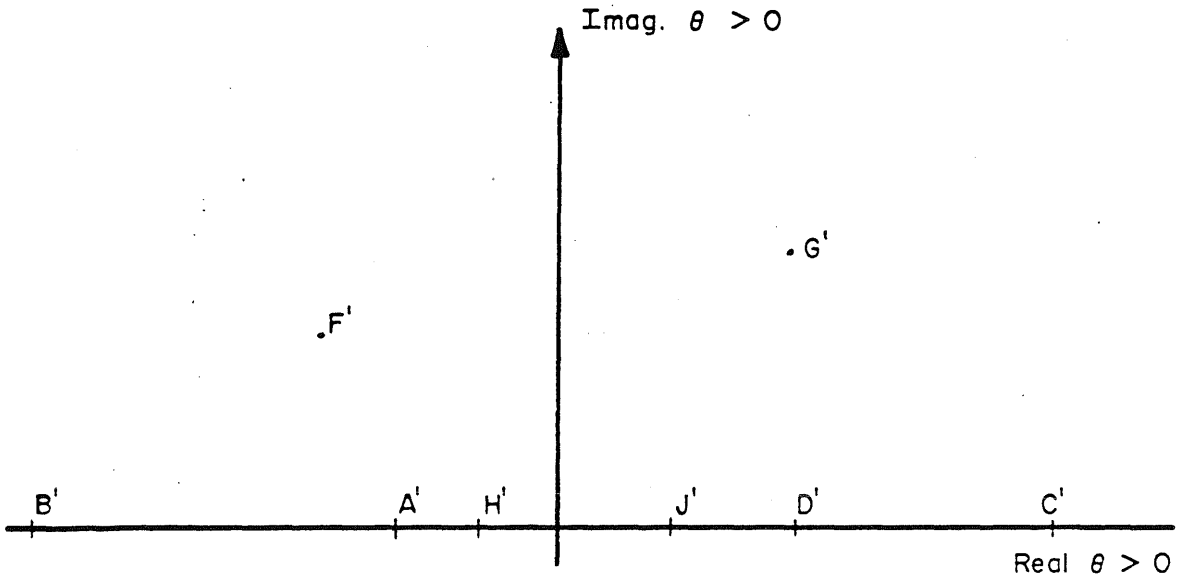

(b) THE UPPER HALF OF THE COMPLEX θ PLANE

FIG. 2. THE MAPPING OF THE $y \geq 0$ HALF SPACE INTO THE COMPLEX θ PLANE

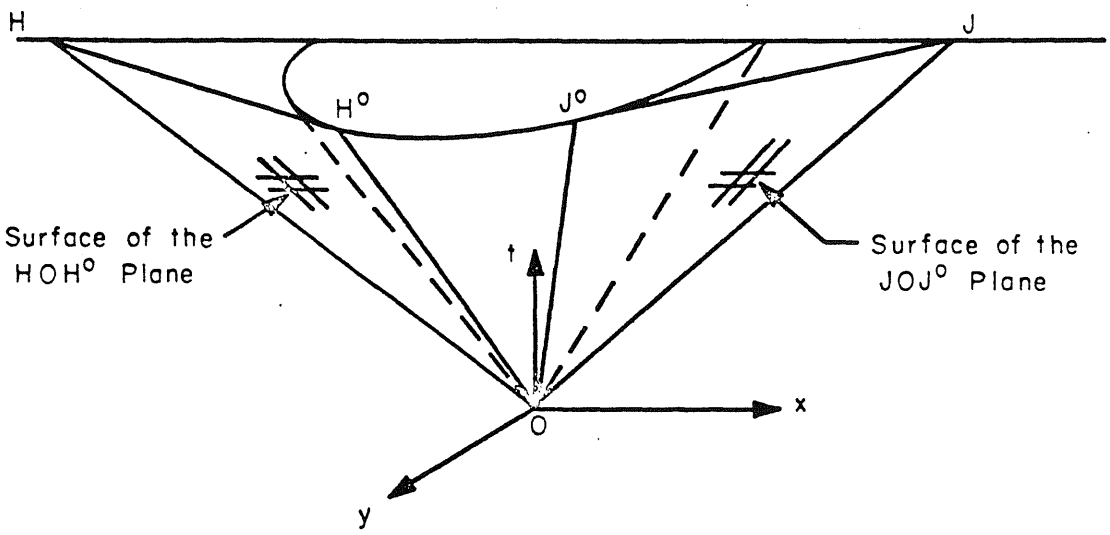

(a) θ = CONSTANT PLANES TANGENT TO THE CONE

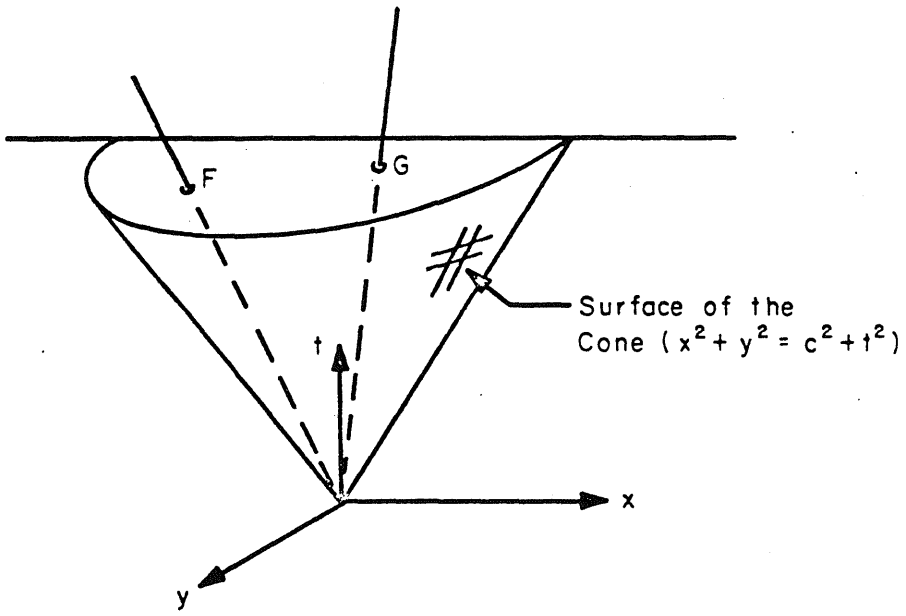

(b) θ = CONSTANT RAYS IN THE INTERIOR OF THE CONE

FIG. 3. TYPICAL θ = CONSTANT RAYS AND PLANES

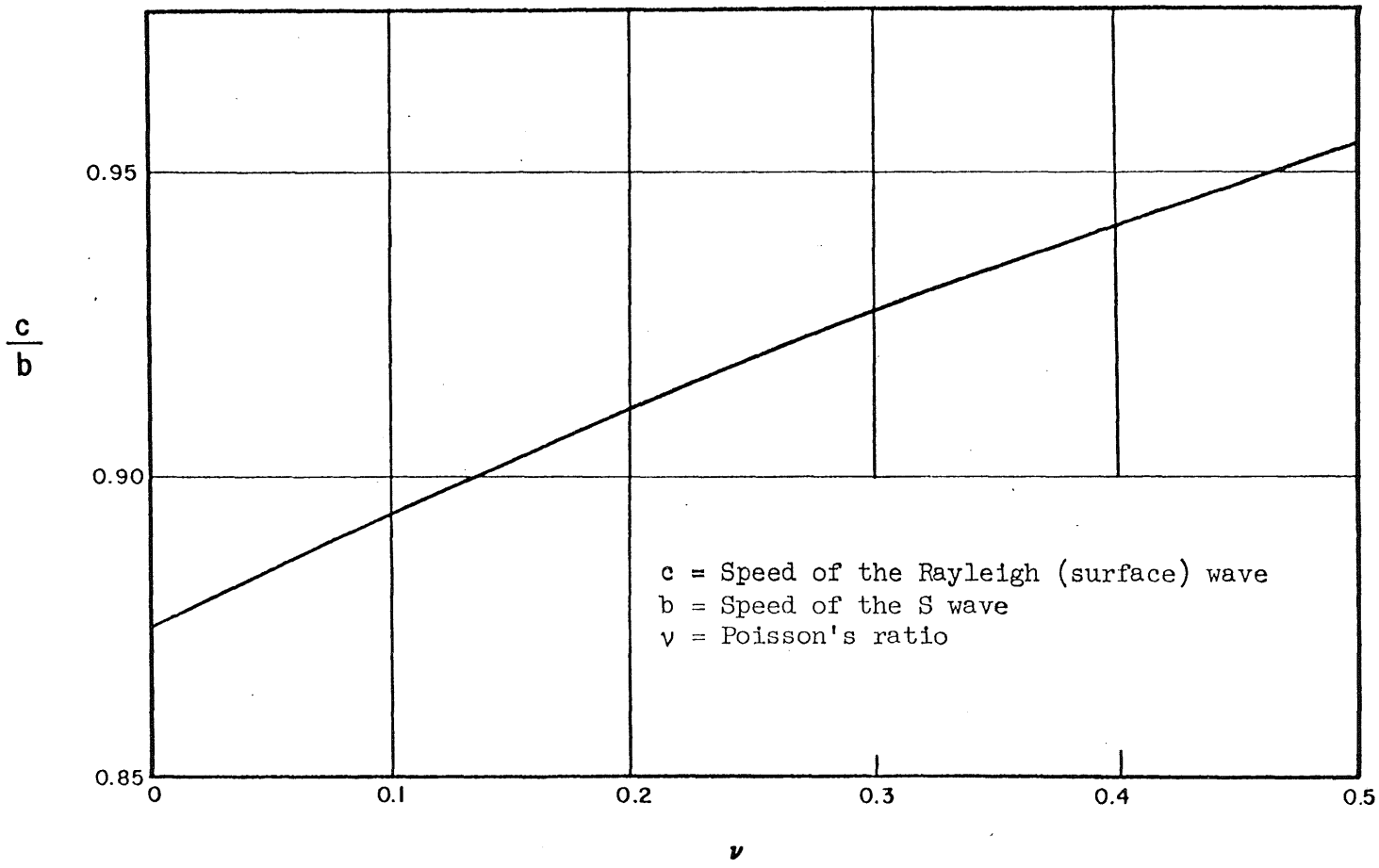

FIG. 4. DEPENDENCE OF THE SPEED OF THE RAYLEIGH WAVE ON POISSON'S RATIO

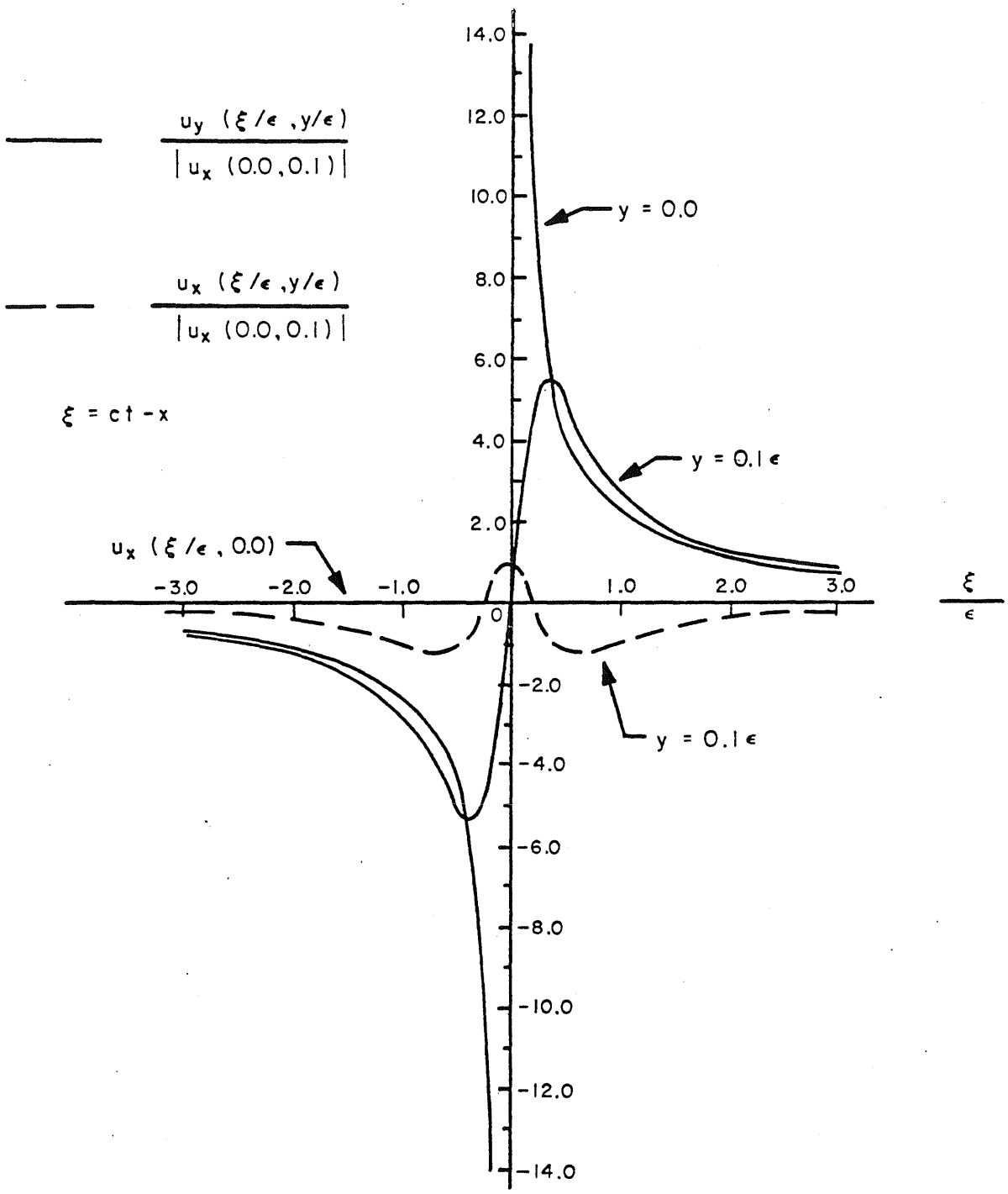

FIG. 5. SURFACE WAVE DISPLACEMENTS FOR A LINE OF IMPULSES

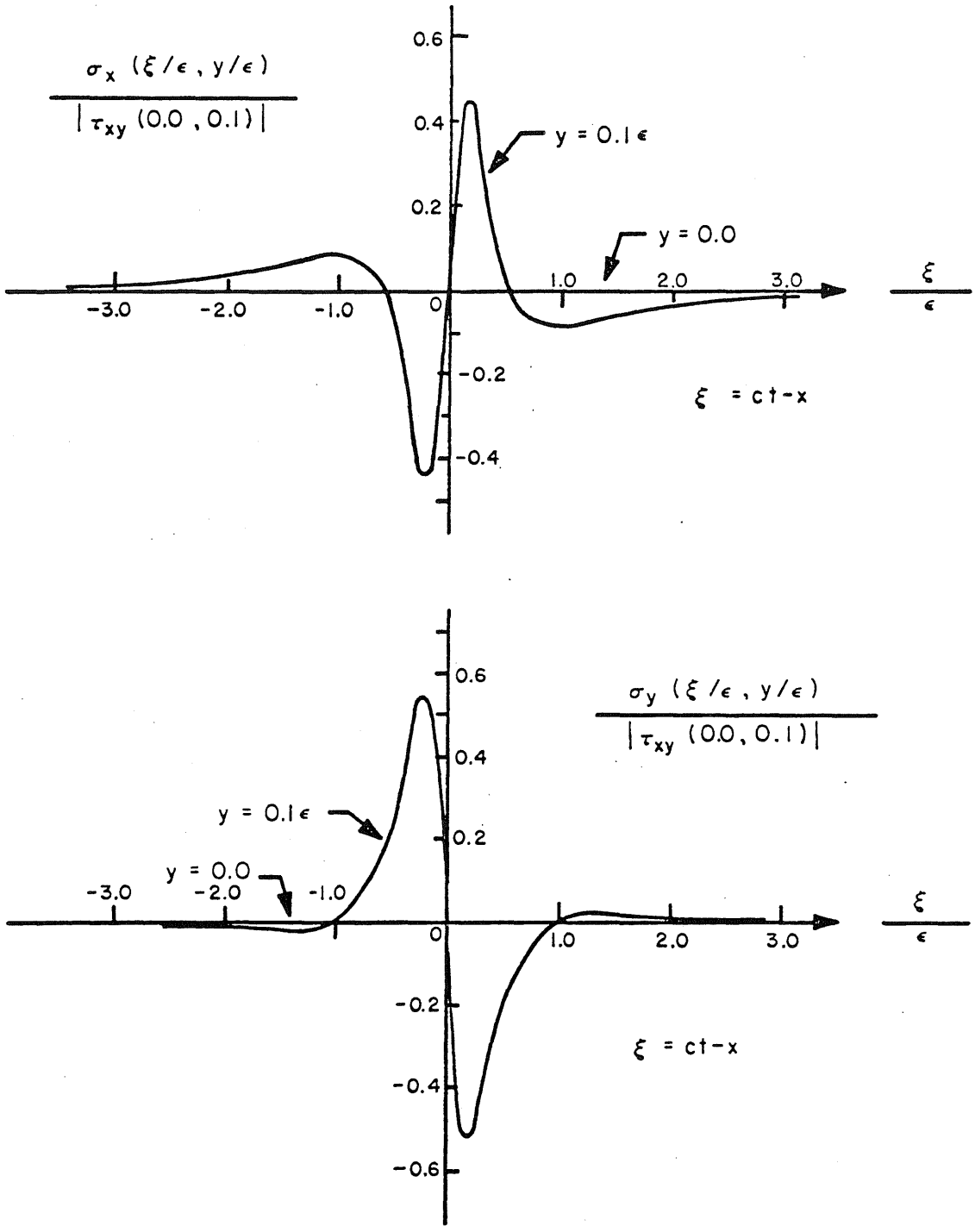

FIG. 6. SURFACE WAVE COMPONENTS OF σ_x AND σ_y FOR A LINE OF IMPULSES

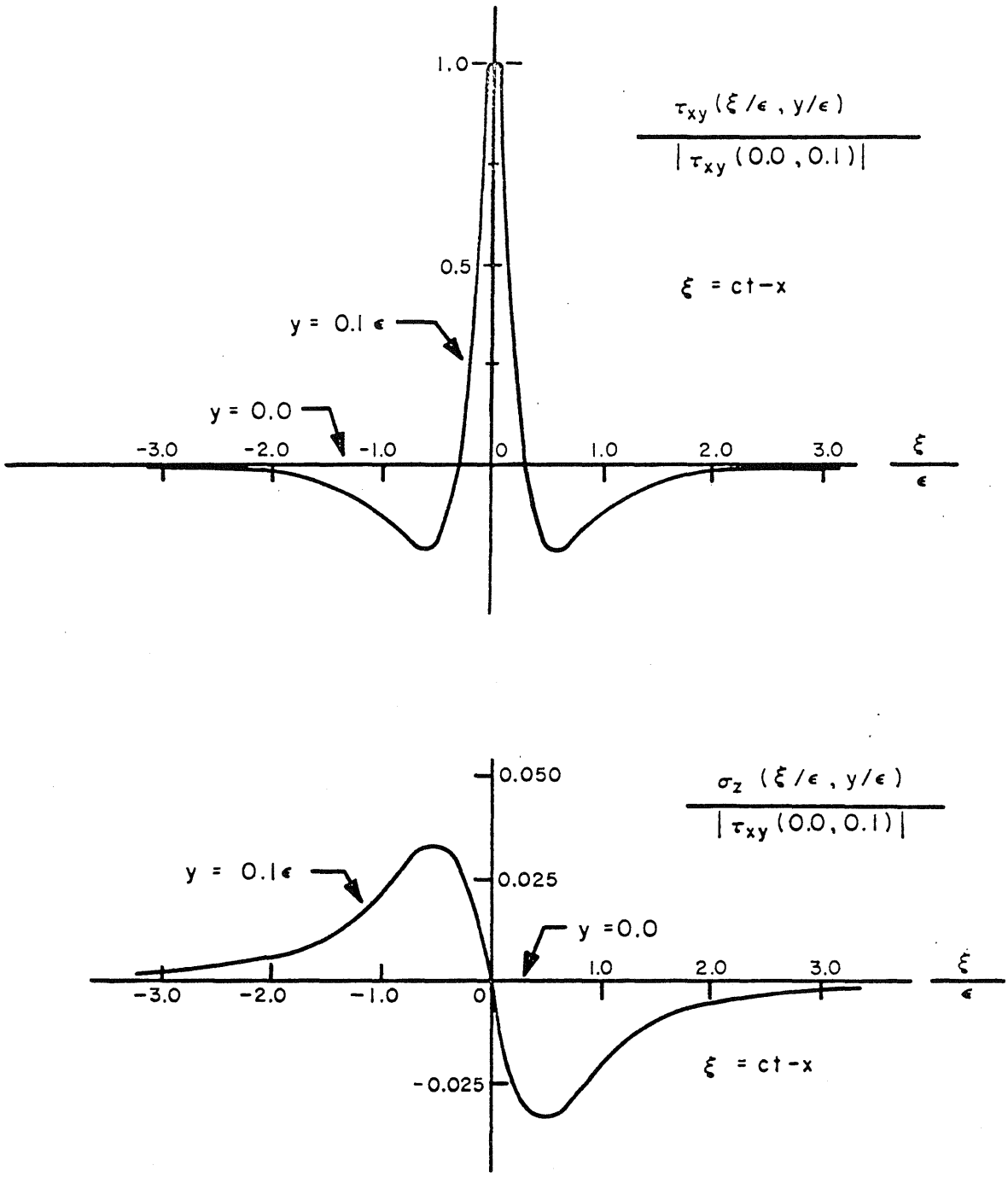

FIG. 7. SURFACE WAVE COMPONENTS OF τ_{xy} AND σ_z FOR A LINE OF IMPULSES

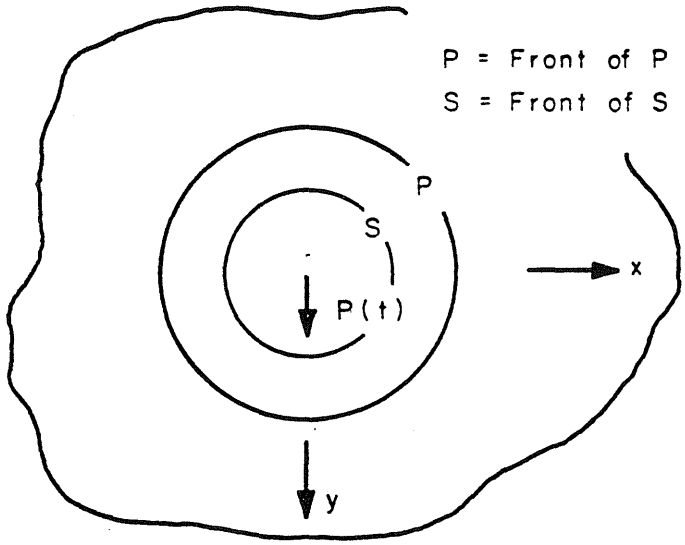

(a) LOAD P(t) IN AN INFINITE BODY

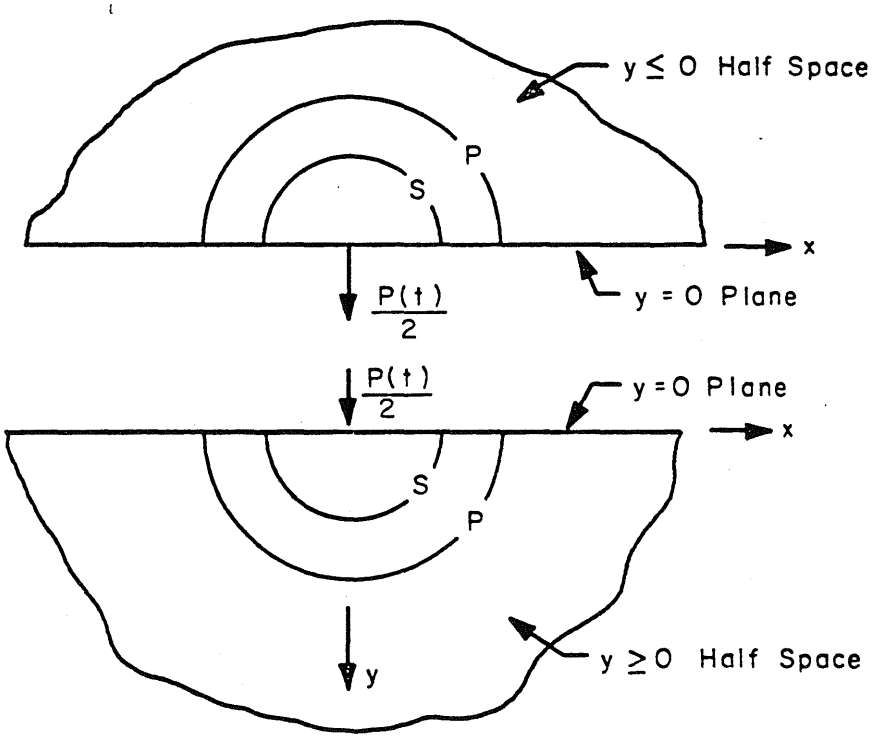

(b) LOADS P(t)/2 ON THE SURFACE OF THE HALF SPACES

FIG. 8. THE INFINITE BODY AND EQUIVALENT HALF SPACE PROBLEMS

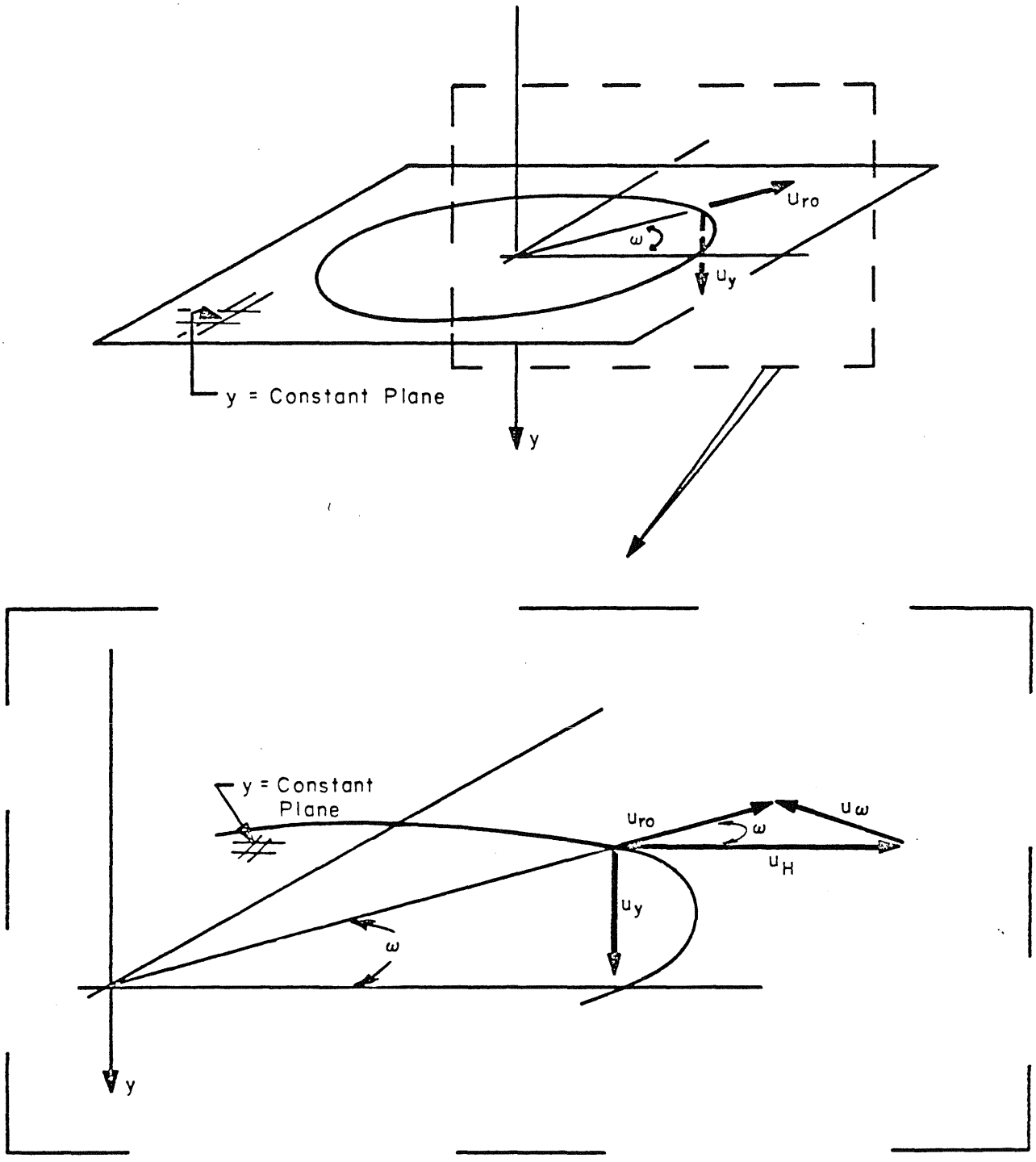

FIG. 9. RADIAL, CIRCUMFERENTIAL AND VERTICAL COMPONENTS OF THE DISPLACEMENTS

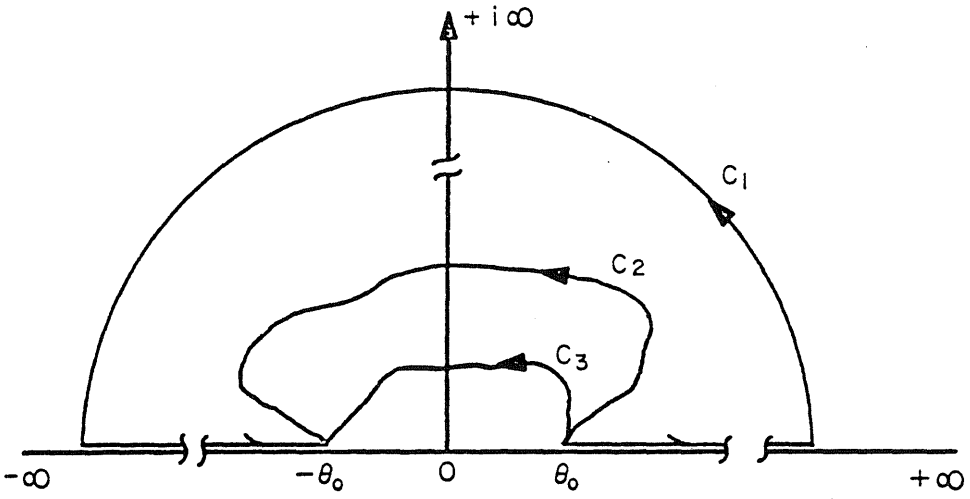

FIG. 10. POSSIBLE CONTOURS OF INTEGRATION IN THE θ PLANE FOR A POINT ON THE y = 0 SURFACE

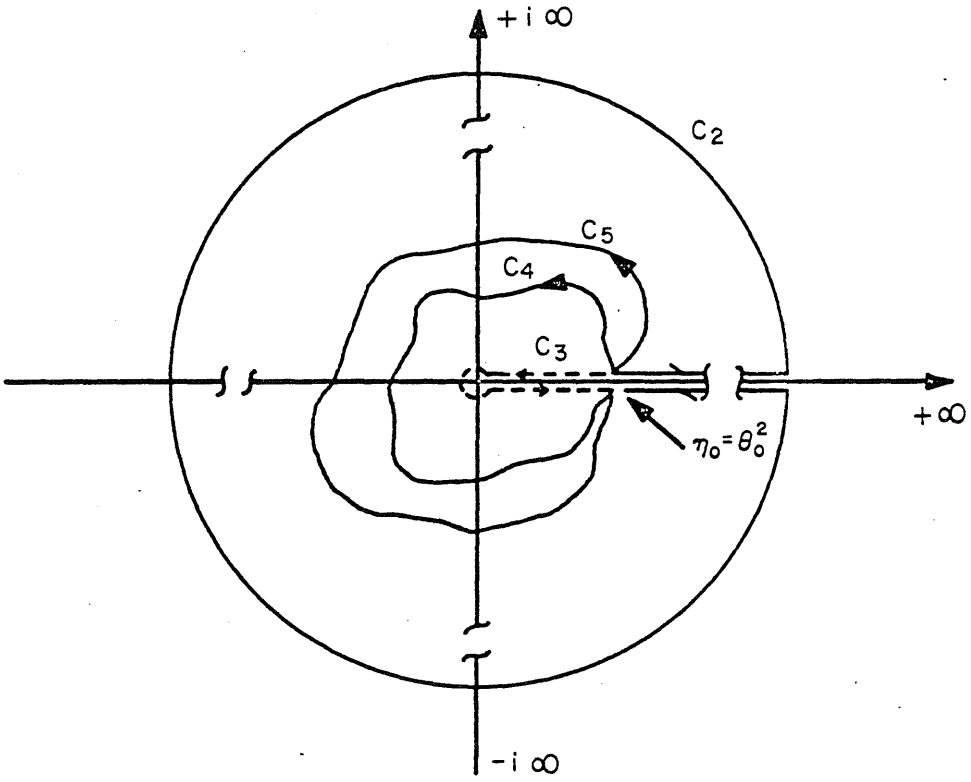

FIG. 11. POSSIBLE CONTOURS OF INTEGRATION IN THE $\eta = \theta^2$ PLANE FOR A POINT ON THE y = 0 SURFACE

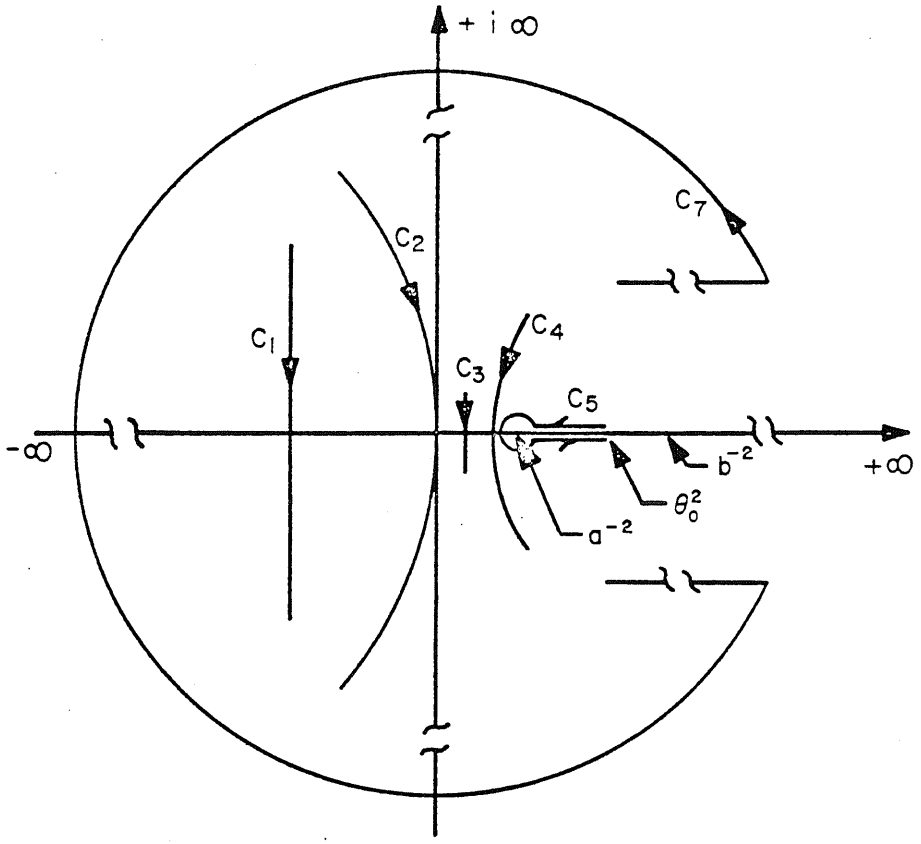

FIG. 12a. TYPICAL CONTOURS OF INTEGRATION IN THE θ^2 PLANE FOR POINTS IN THE INTERIOR OF THE HALF SPACE

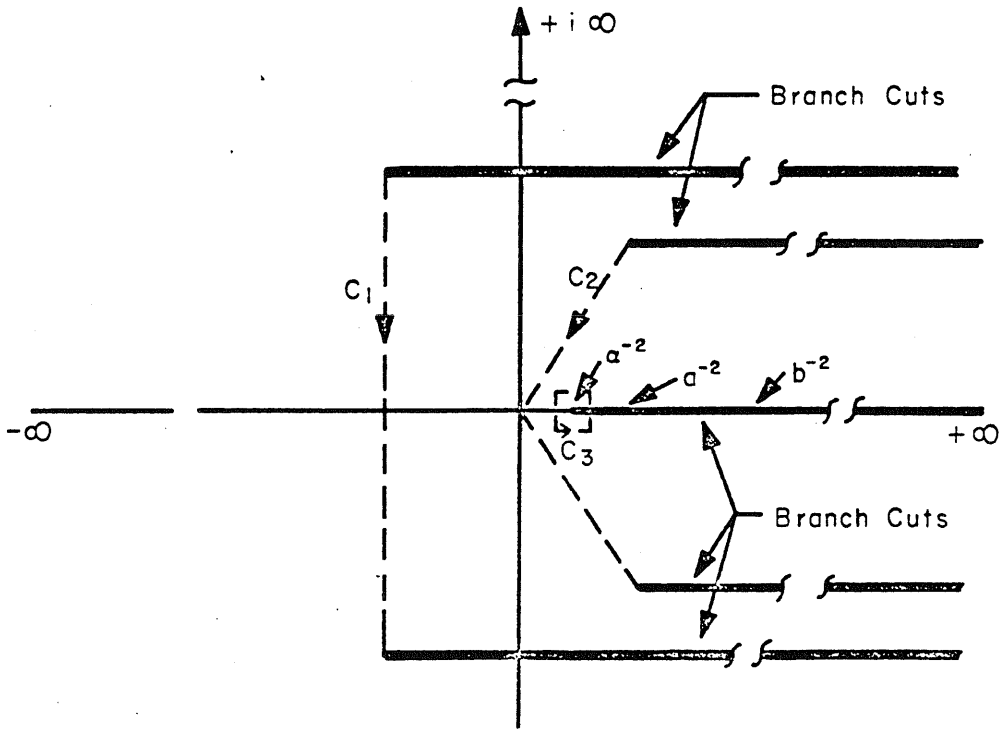

FIG. 12b. TYPICAL CONTOURS OF INTEGRATION FOR THE PROBLEM OF A CONE INDENTING SUPERSEISMICALLY

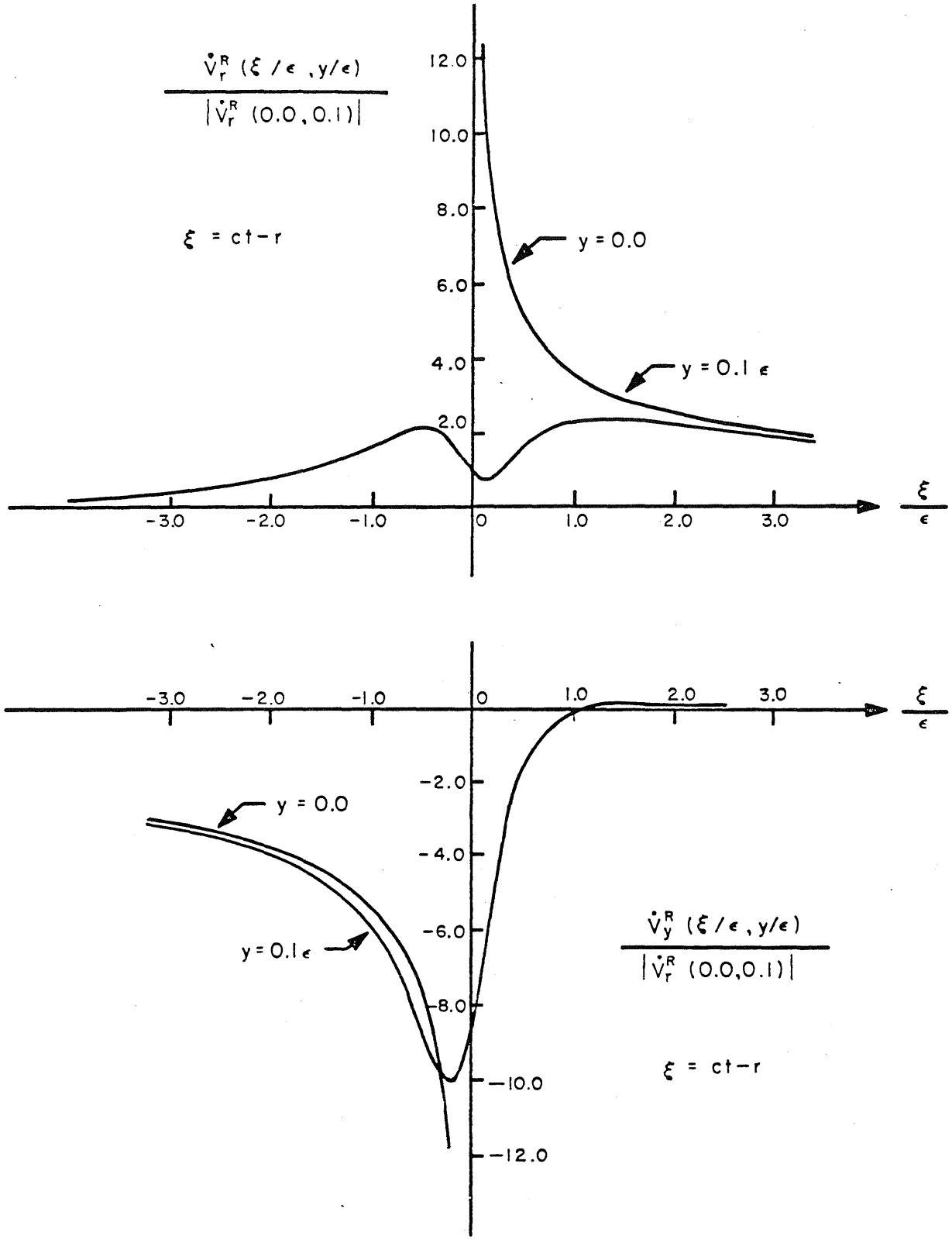

FIG. 13. SURFACE WAVE COMPONENTS OF $\dot{v}_r$ AND $\dot{v}_y$ FOR THE POINT LOAD OF SEC. 3.4.1.2

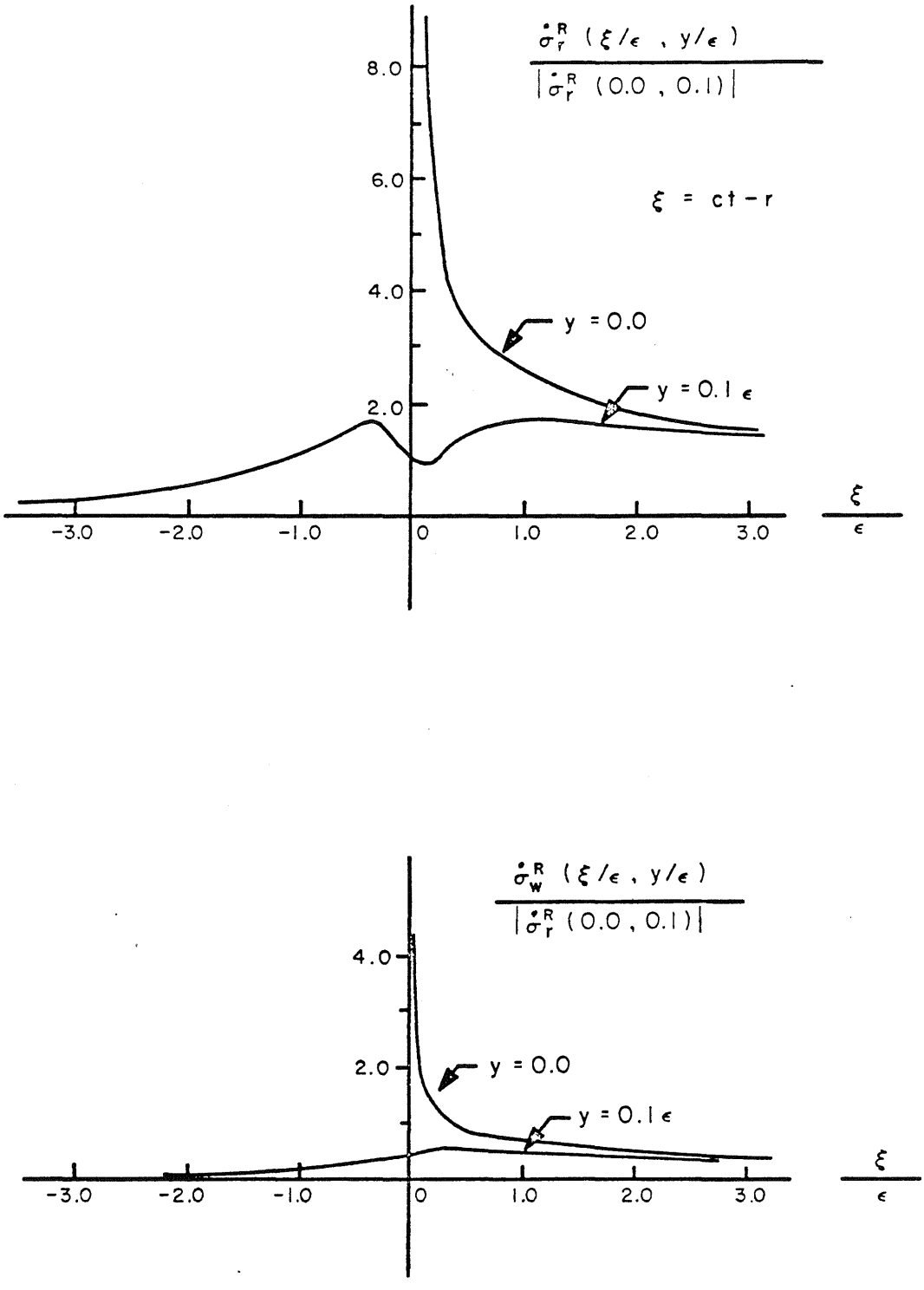

FIG. 14. SURFACE WAVE COMPONENTS OF $\dot{\sigma}_r$ AND $\dot{\sigma}_w$ FOR THE POINT LOAD OF SEC. 3.4.1.2

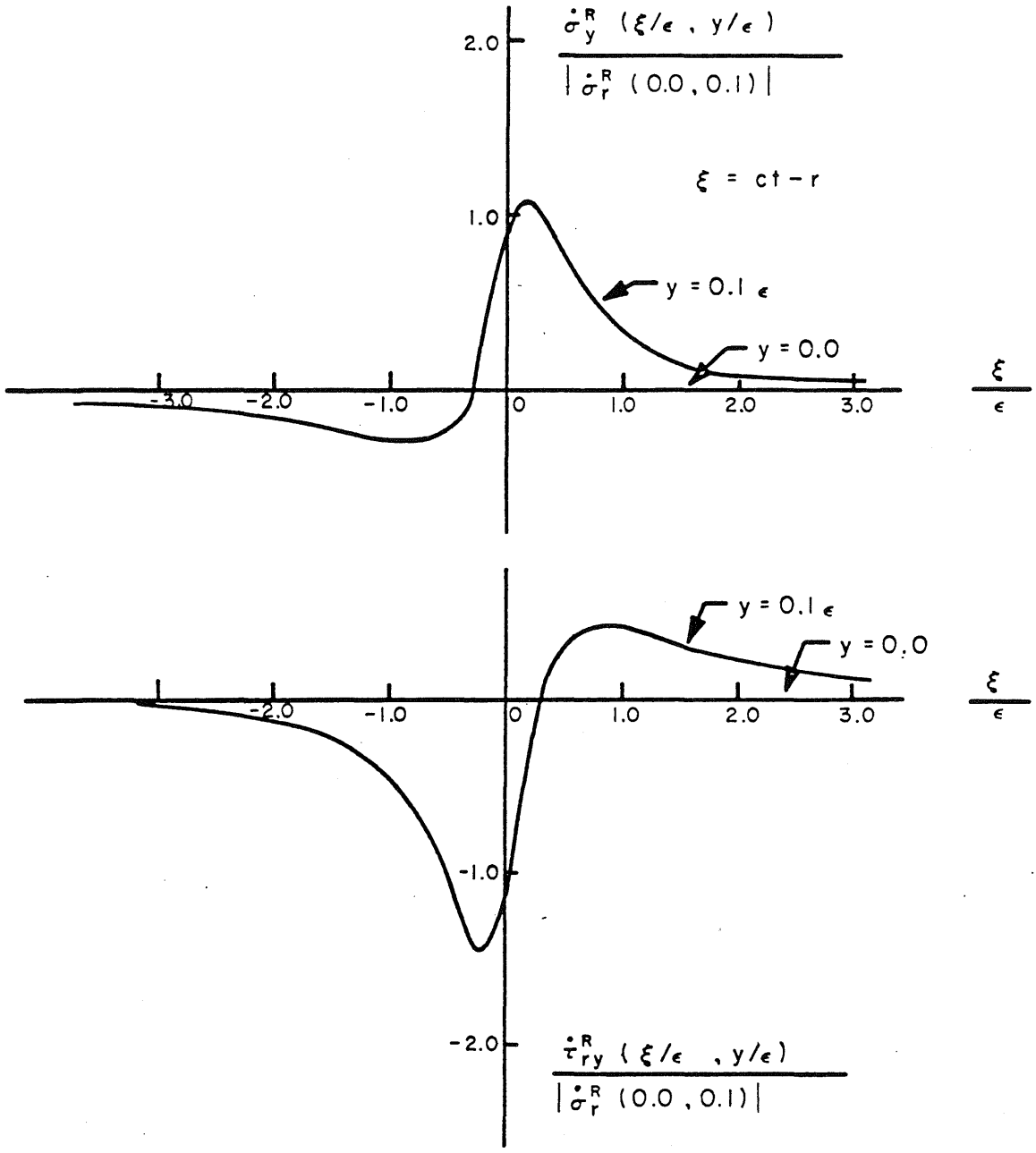

FIG. 15. SURFACE WAVE COMPONENTS OF $\dot{\sigma}_y$ AND $\dot{\tau}_{ry}$ FOR THE POINT LOAD OF SEC. 3.4.1.2

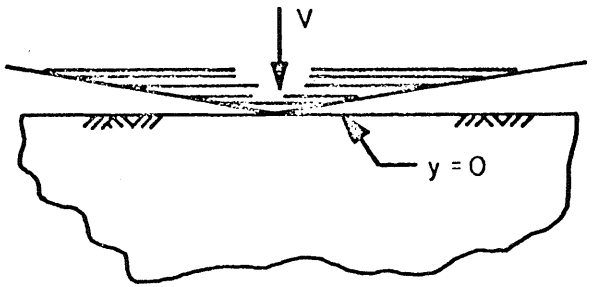

FIG. 16a. THE POSITION OF THE DIE AT t = 0

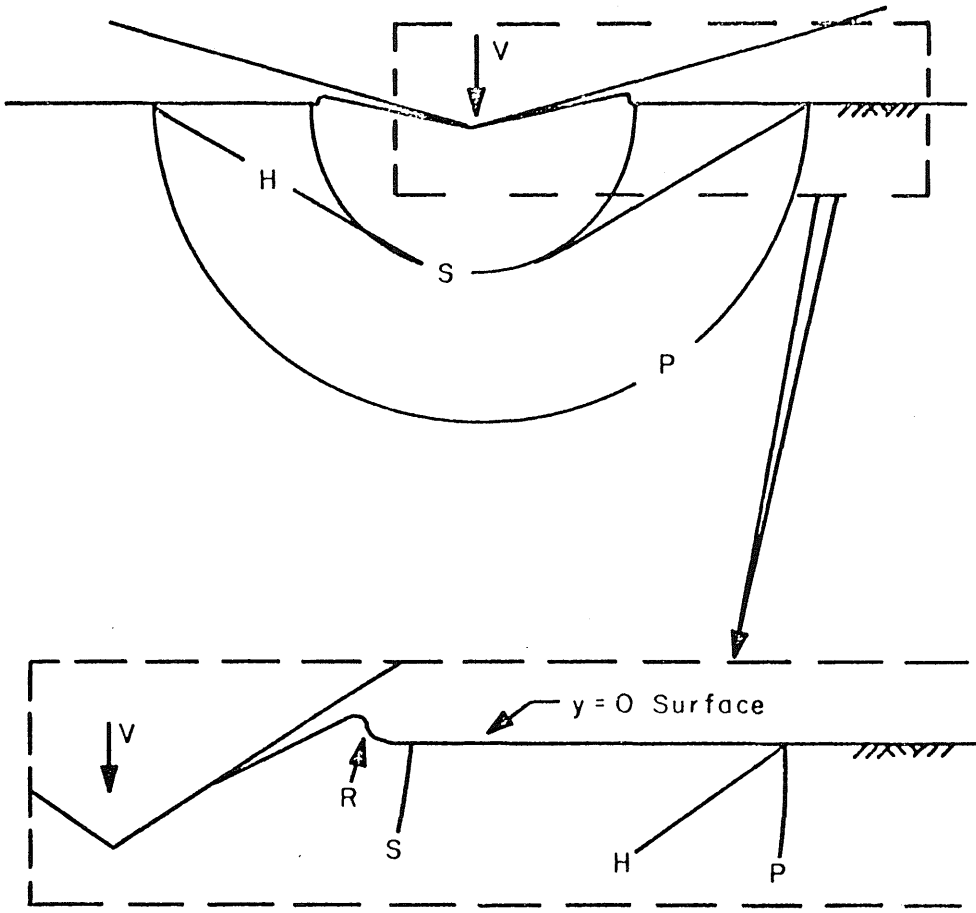

P = Front of P Wave

S = Front of S Wave

H = Front of Head Wave

R = Location of Rayleigh Wave

FIG. 16b. LOCATION OF THE WAVE FRONTS AND DEFORMATION OF THE y = 0 SURFACE FOR A CONTACT SPEED IN THE SLOW RANGE

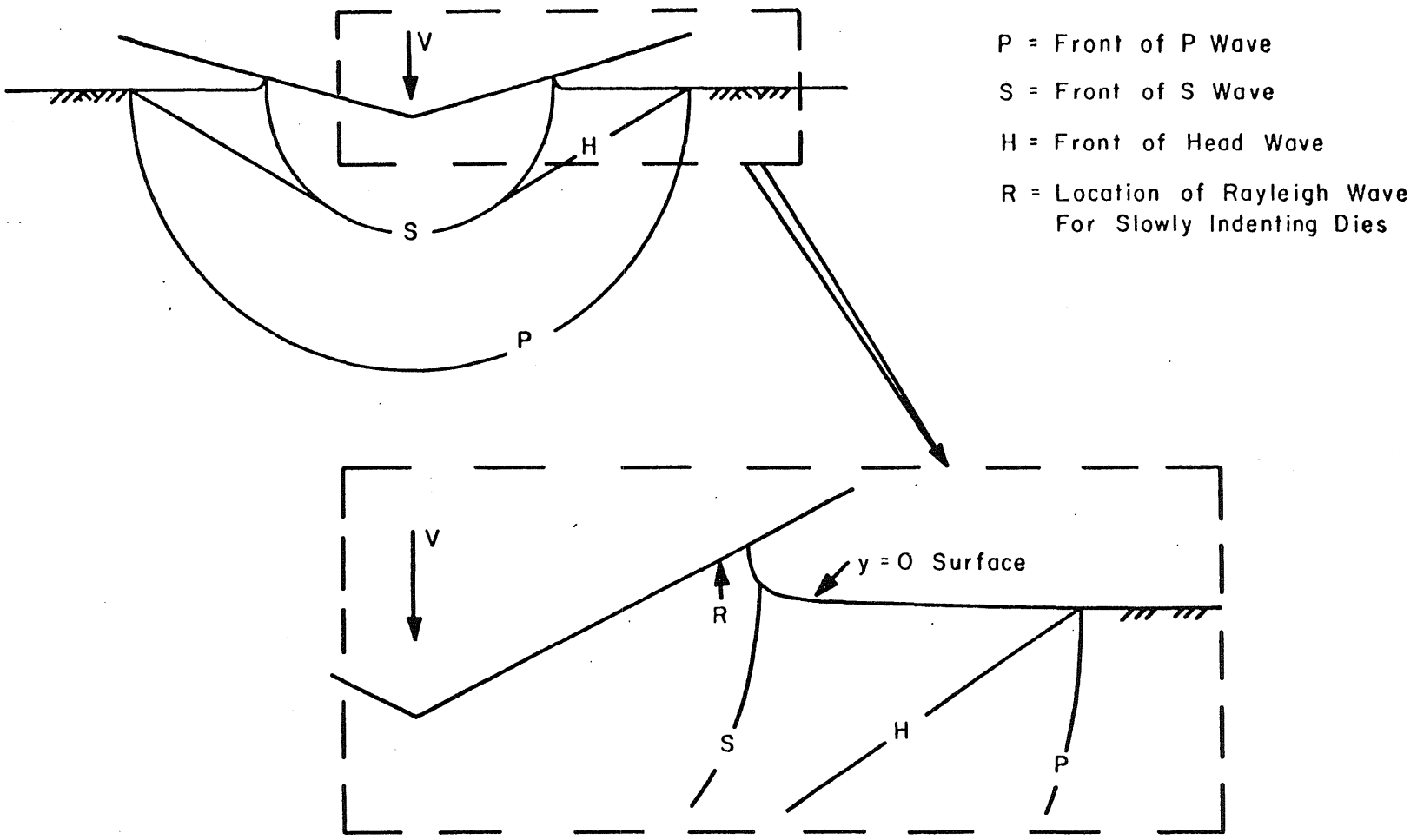

FIG. 17. LOCATION OF THE WAVE FRONTS AND DEFORMATION OF THE y = 0 SURFACE FOR A CONTACT SPEED IN THE FIRST INTERMEDIATE RANGE

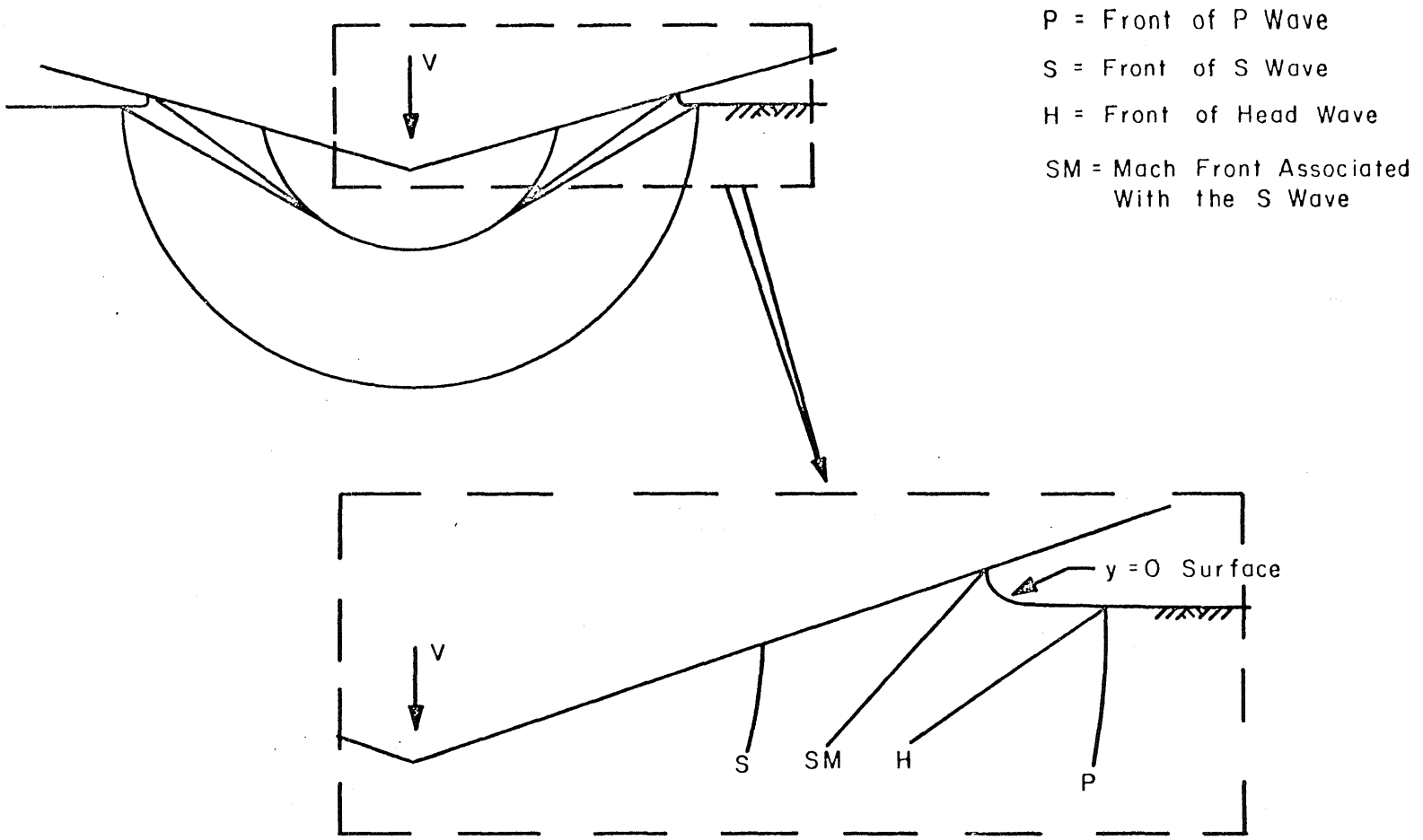

FIG. 18. LOCATION OF THE WAVE FRONTS AND DEFORMATION OF THE y = 0 SURFACE FOR A CONTACT SPEED IN THE SECOND INTERMEDIATE RANGE

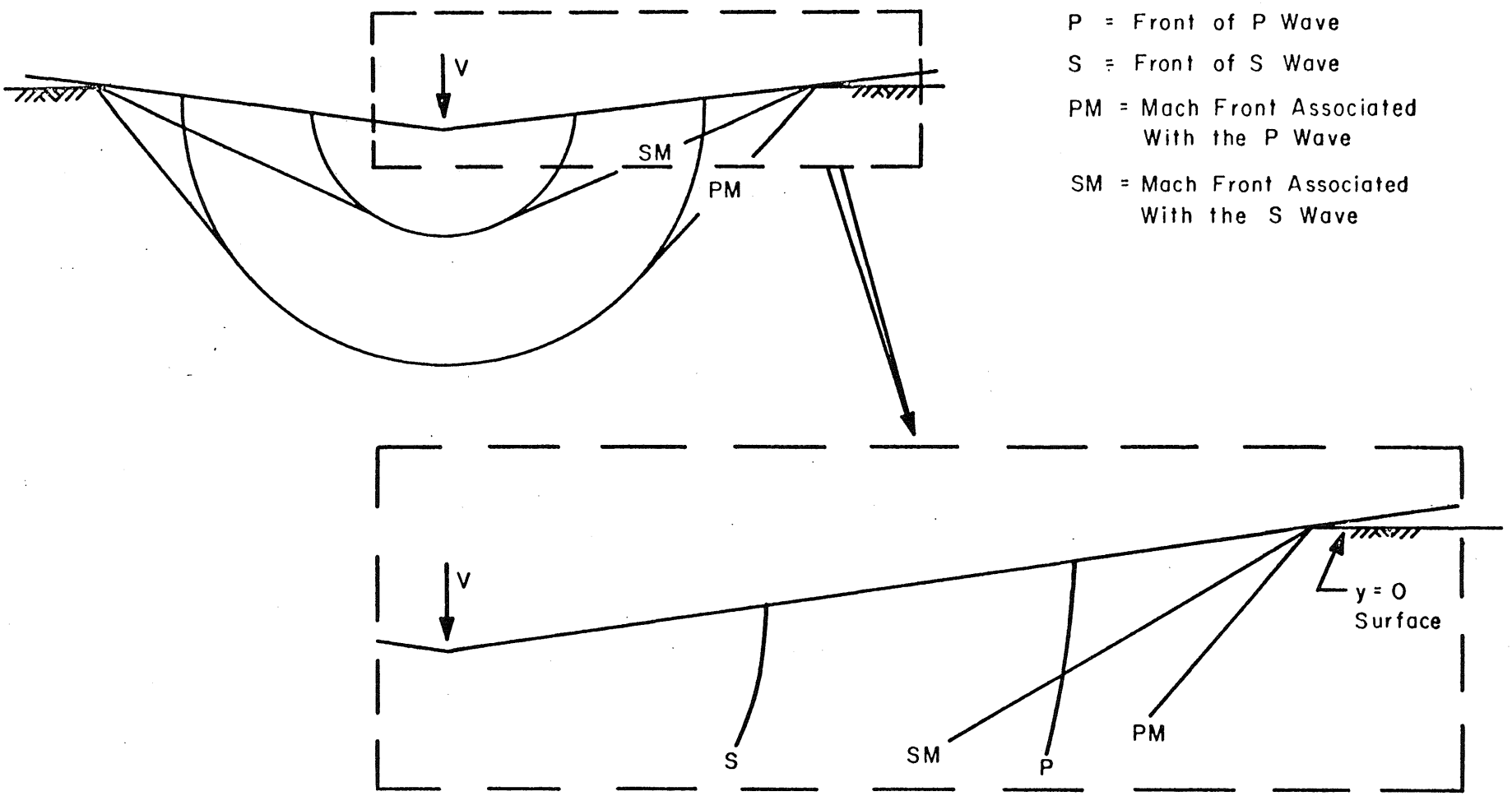

FIG. 19. LOCATION OF THE WAVE FRONTS AND DEFORMATION OF THE y = 0 SURFACE FOR A CONTACT SPEED IN THE SUPERSEISMIC RANGE

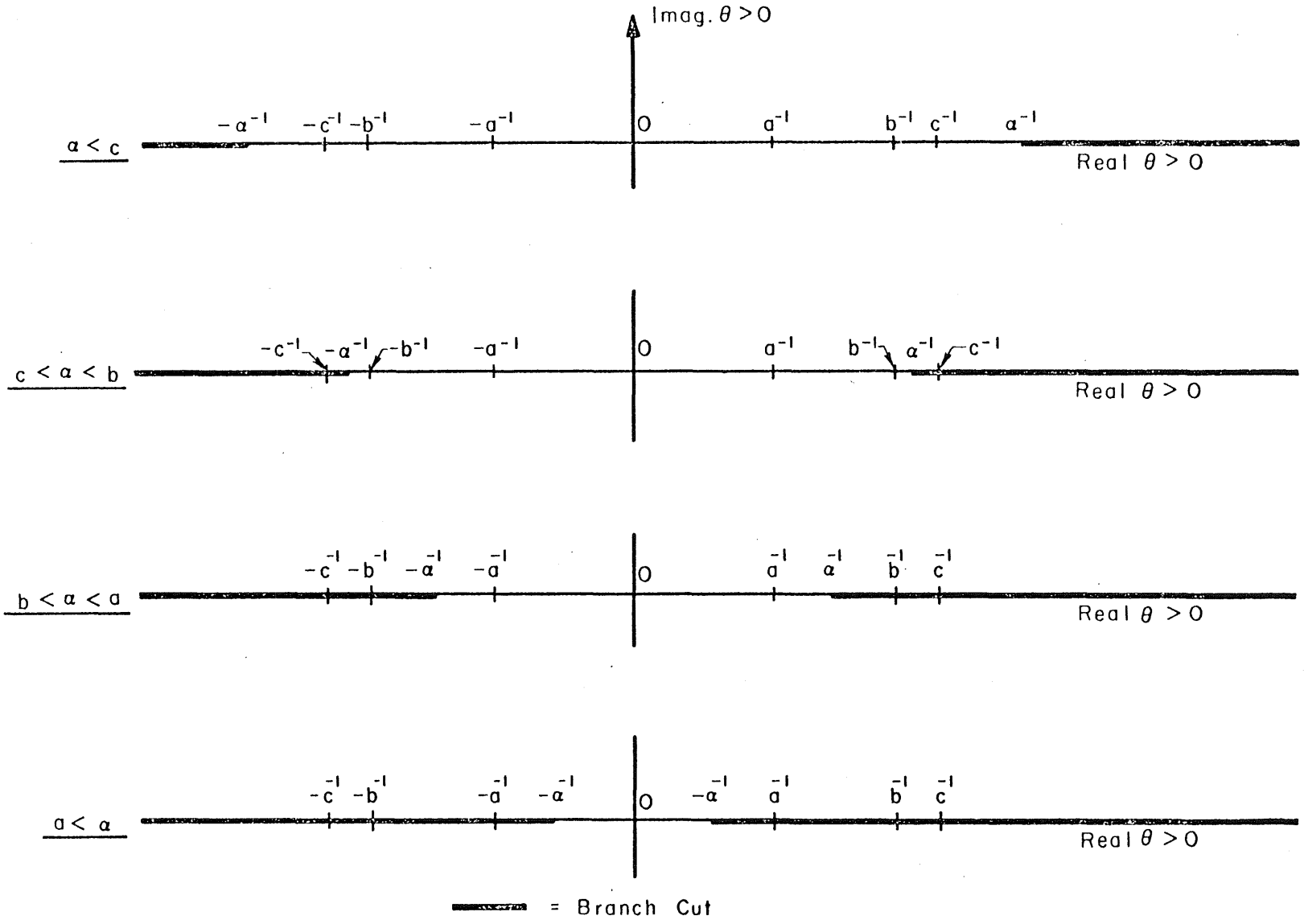

FIG. 20. POSSIBLE NON-ANALYTICITIES IN $\sigma_y^{*\prime}$ FOR THE FOUR RANGES OF CONTACT SPEEDS

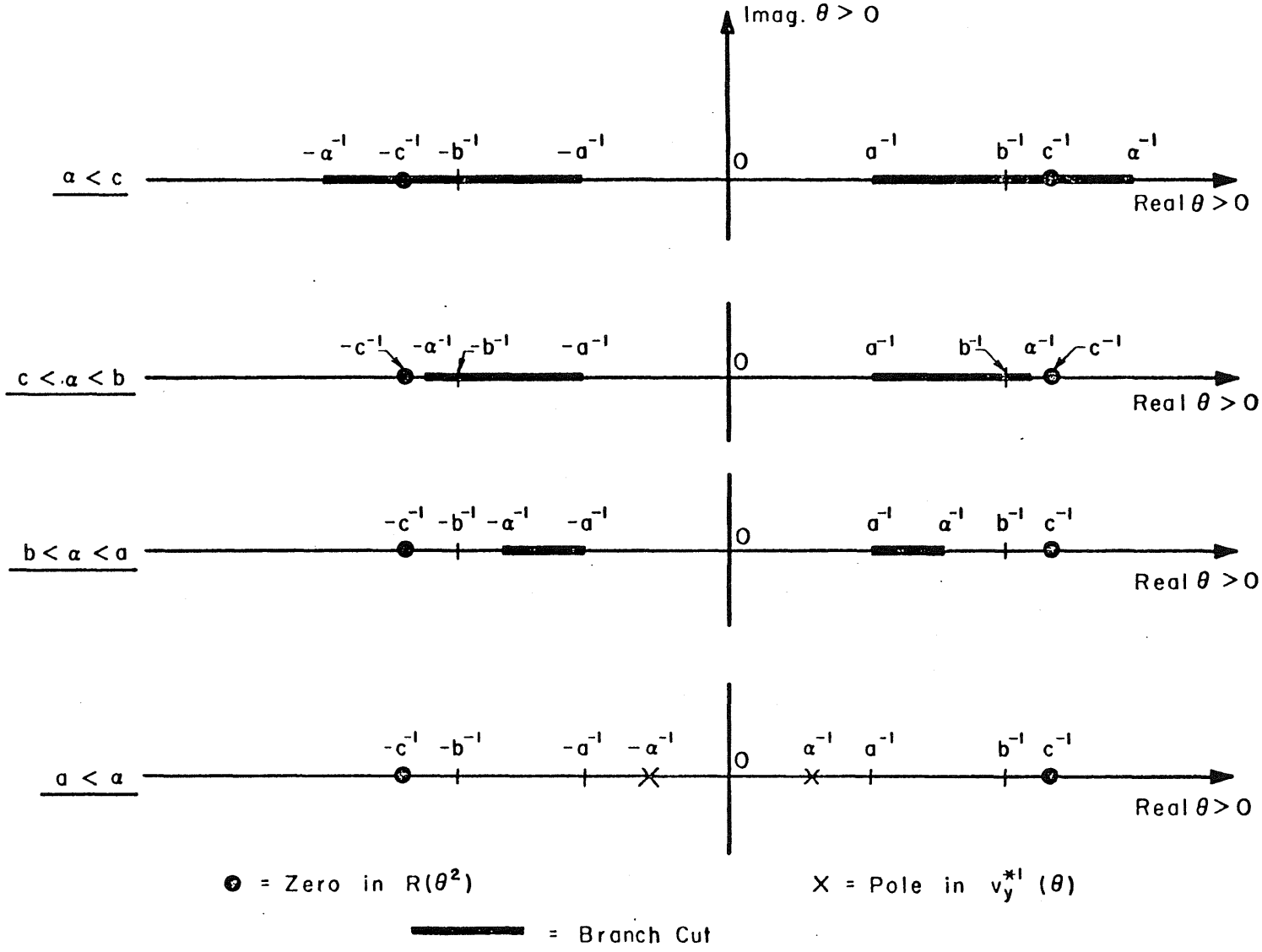

FIG. 21. POSSIBLE NON-ANALYTICITIES IN $v_y^{*'}$ FOR THE FOUR RANGES OF CONTACT SPEEDS

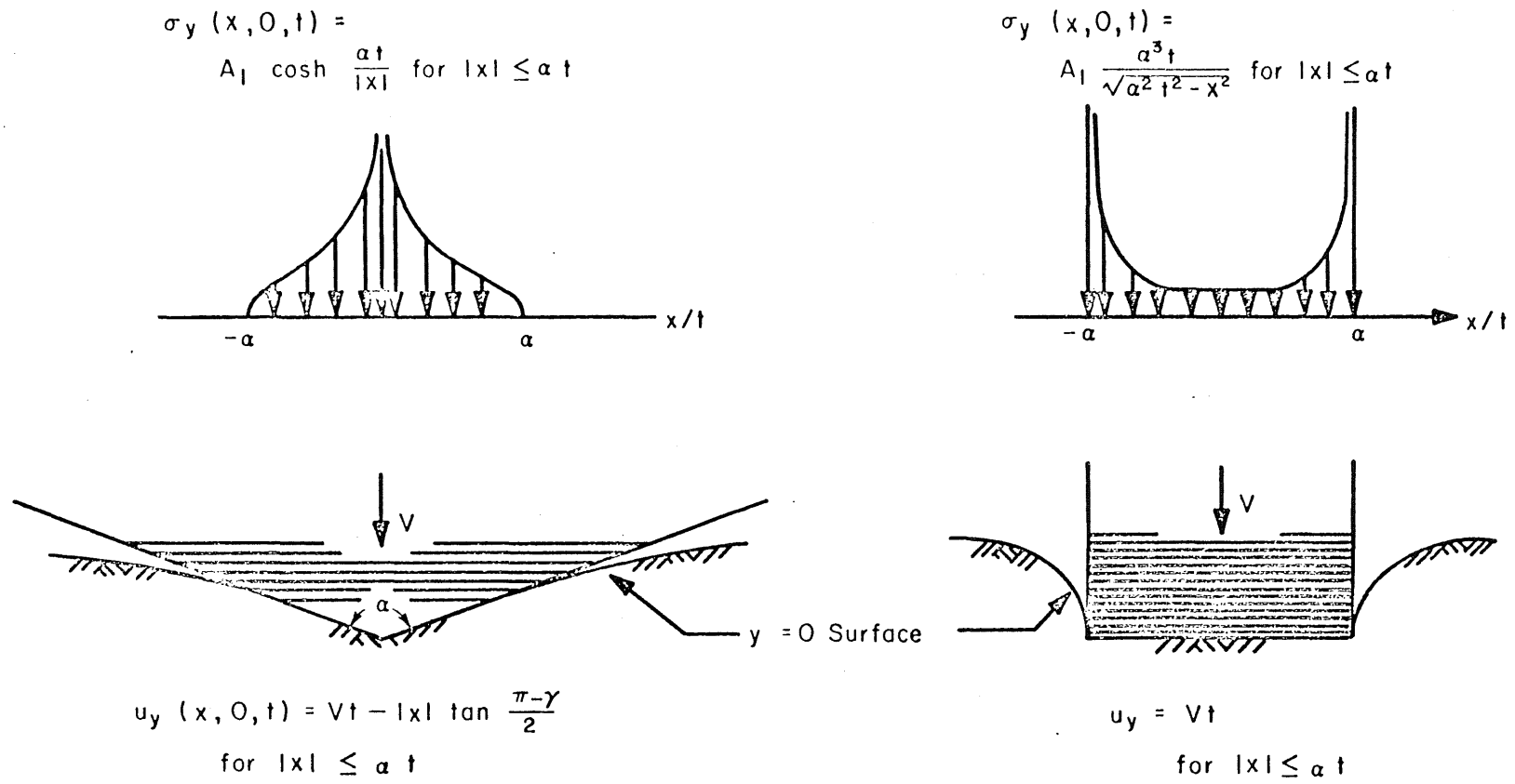

FIG. 22. DEFORMATION OF THE SURFACE RESULTING FROM THE CONTACT STRESS DISTRIBUTIONS OF EQ. (4.15)

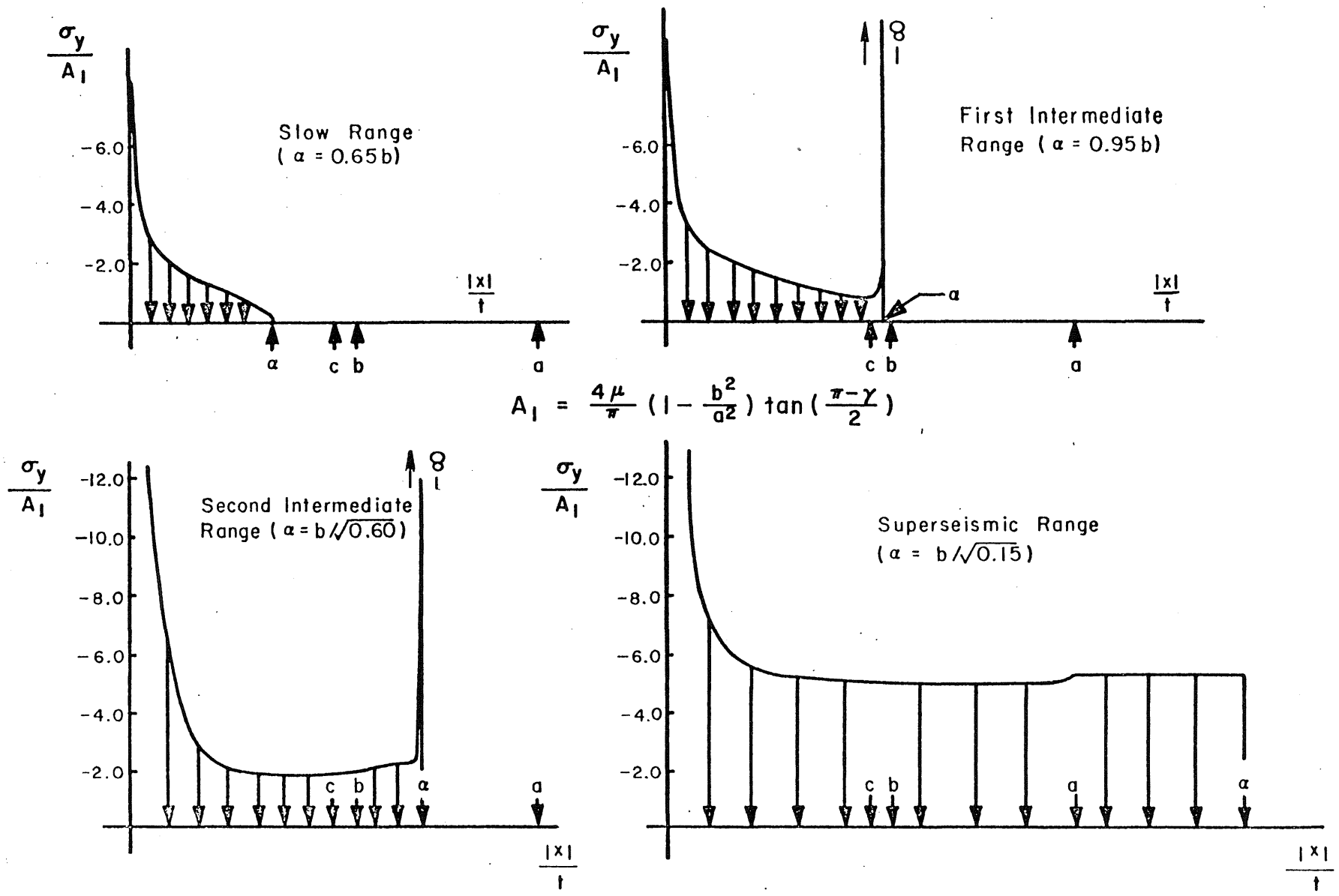

$$A_1 = \frac{4\mu}{\pi}\left(1 - \frac{b^2}{a^2}\right)\tan\left(\frac{\pi-\gamma}{2}\right)$$

FIG. 23. DISTRIBUTION OF THE CONTACT STRESS FOR THE WEDGE PROBLEM ($\nu = 0.285$)

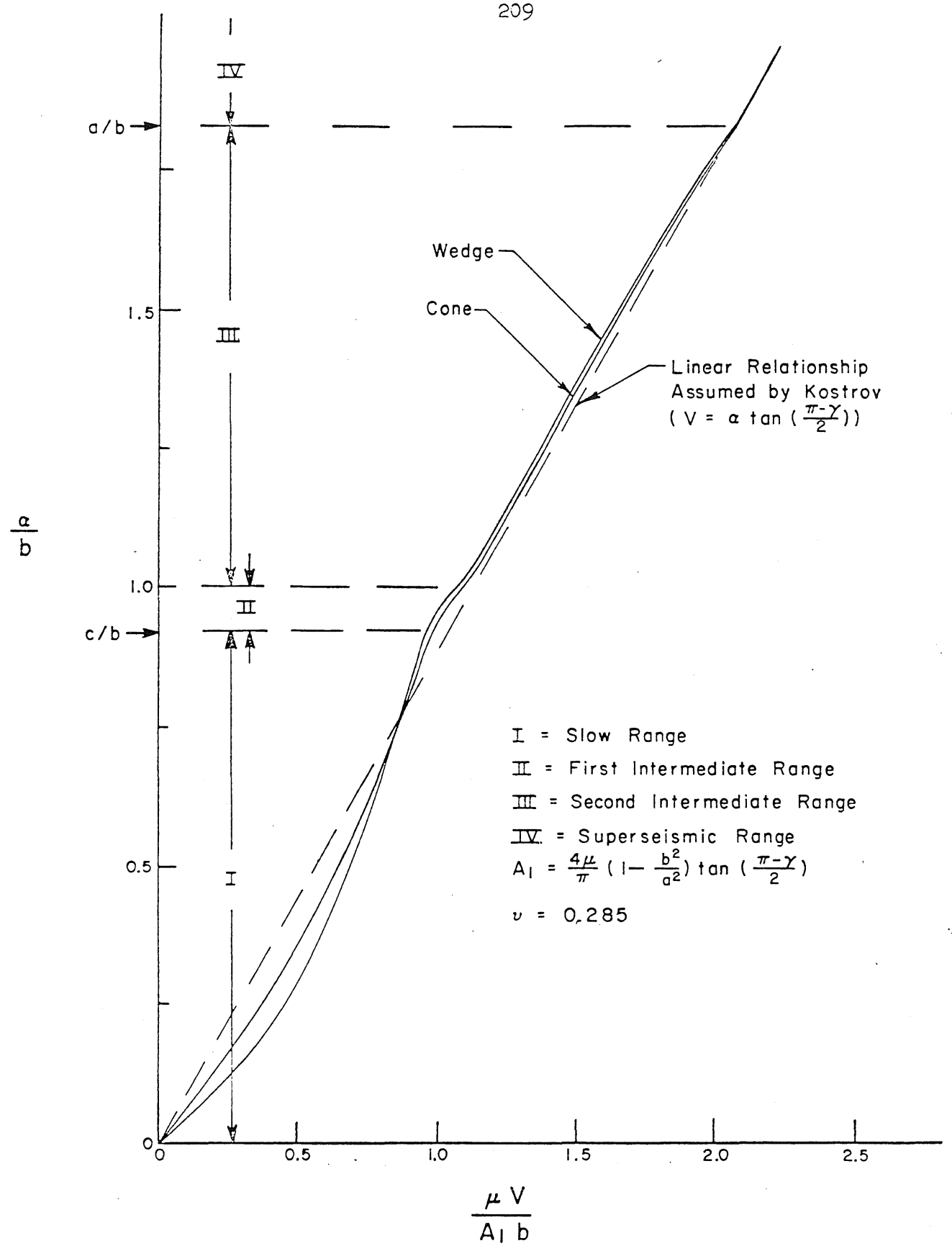

FIG. 24. DEPENDENCE OF THE CONTACT SPEED ON THE INDENTATION VELOCITY OF THE DIE

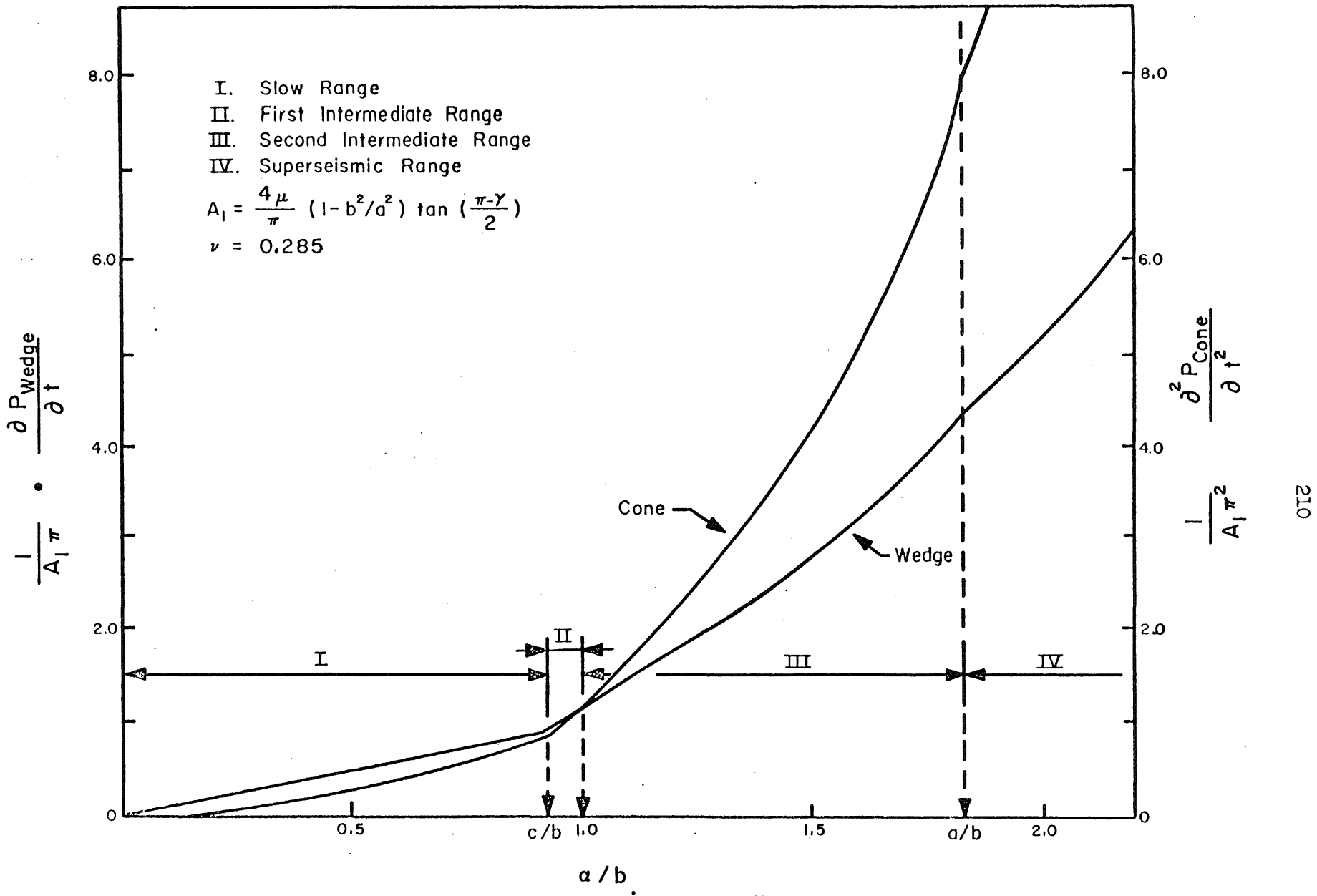

FIG. 25. DEPENDENCE OF $\dot{P}_{Wedge}$ AND $\ddot{P}_{Cone}$ ON α/b

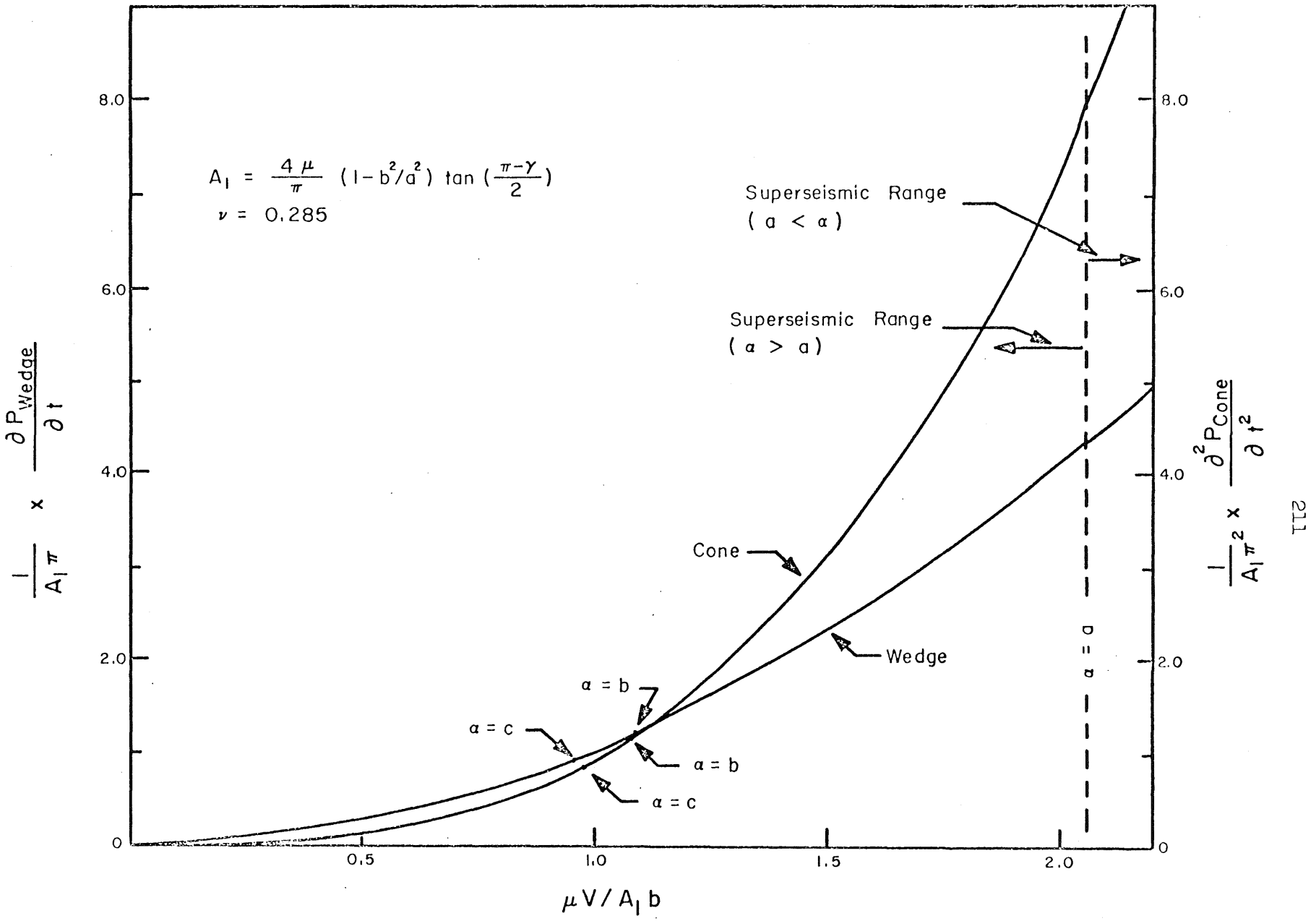

FIG. 26. DEPENDENCE OF $\dot{P}_{Wedge}$ AND $\ddot{P}_{Cone}$ ON $\mu V/A_1 b$

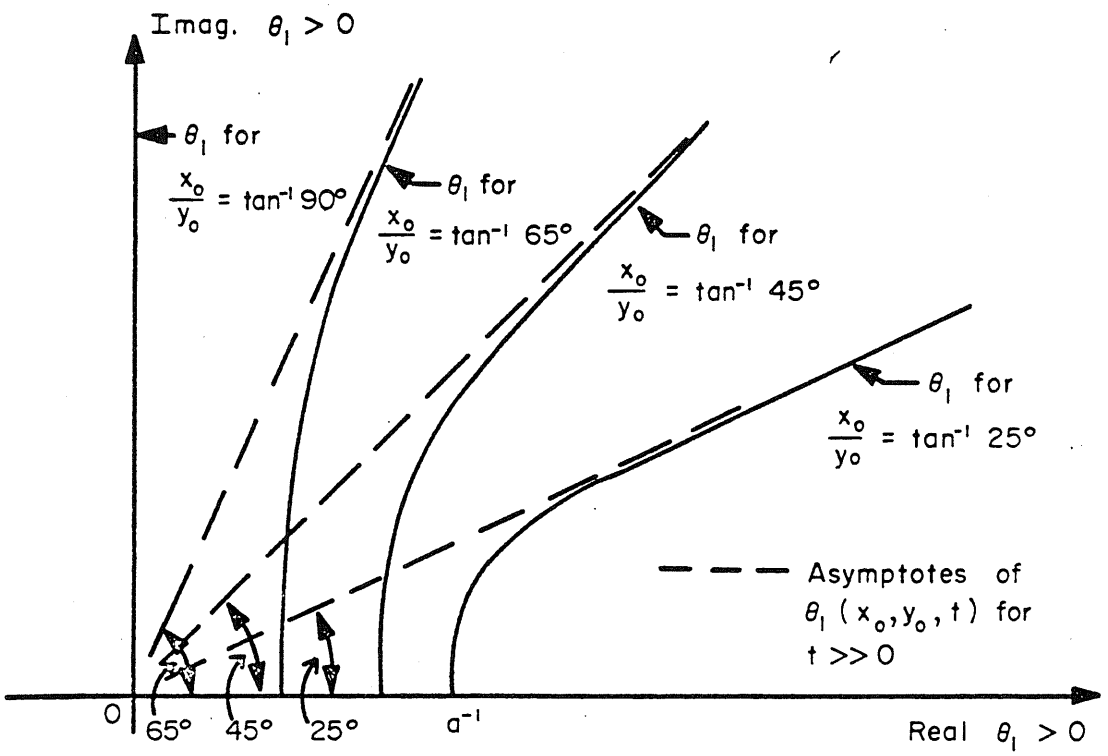

(a) $\theta_1(x_0,y_0,t)$ FOR TYPICAL RATIOS OF x_0/y_0

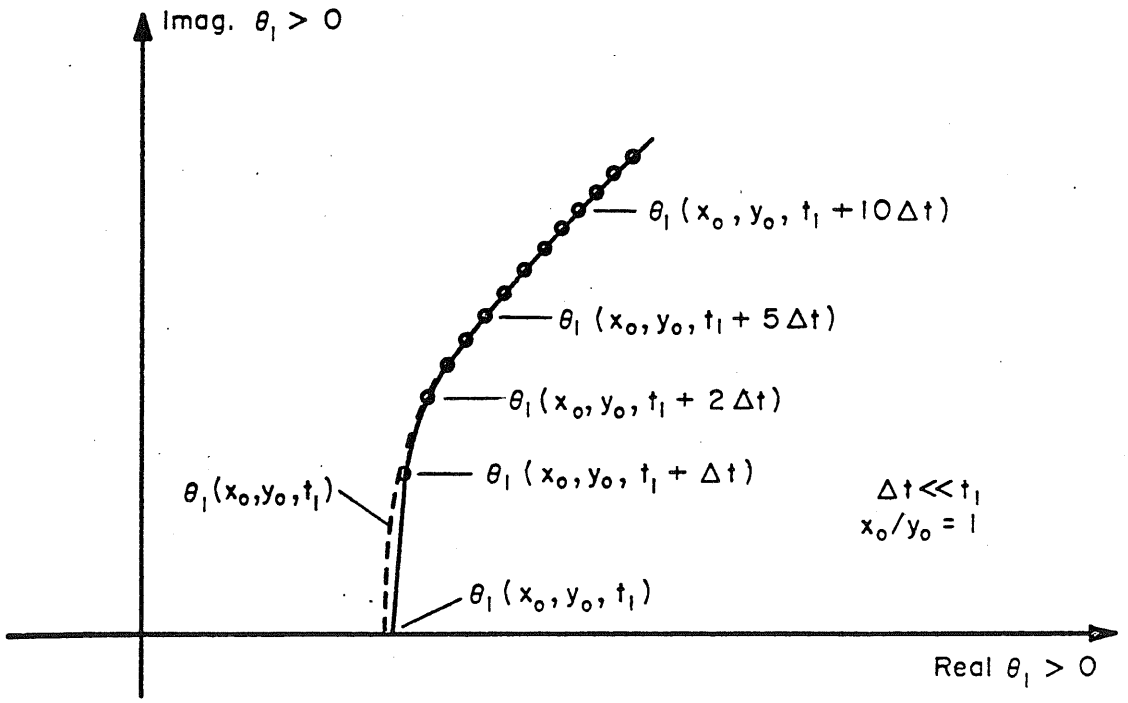

(b) DEFORMED CONTOUR FOR THE NUMERICAL INTEGRATION PROCEDURE

FIG. 27. TRACES OF $\theta_1(x_0,y_0,t)$ IN THE COMPLEX θ PLANE

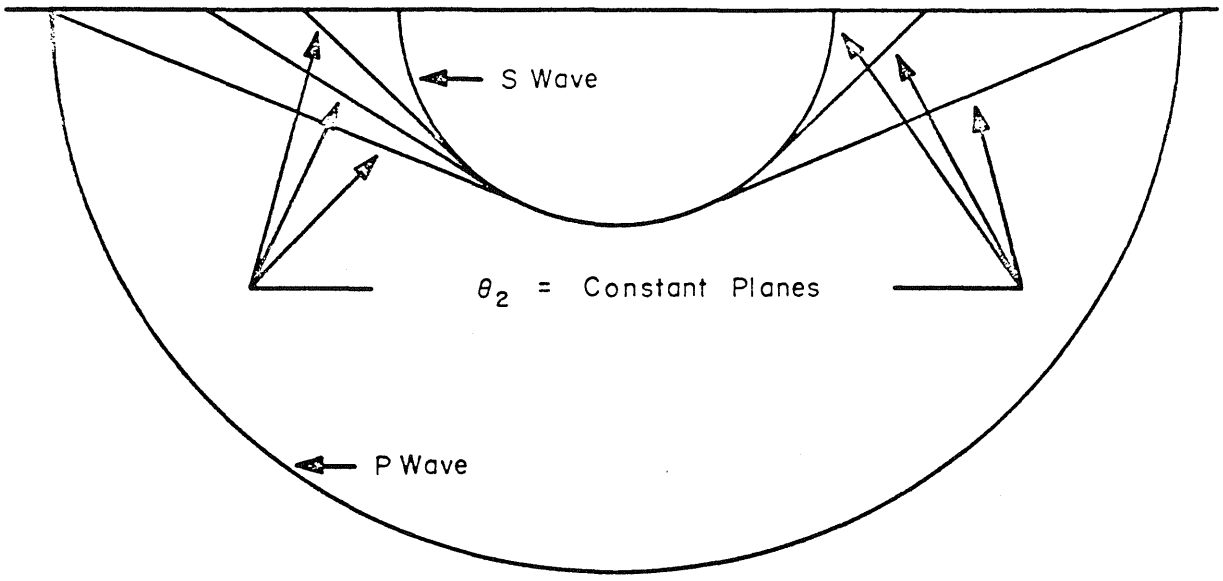

FIG. 28. TYPICAL θ_2 = CONSTANT PLANES IN THE REGION OF HEAD WAVE DISTURBANCES

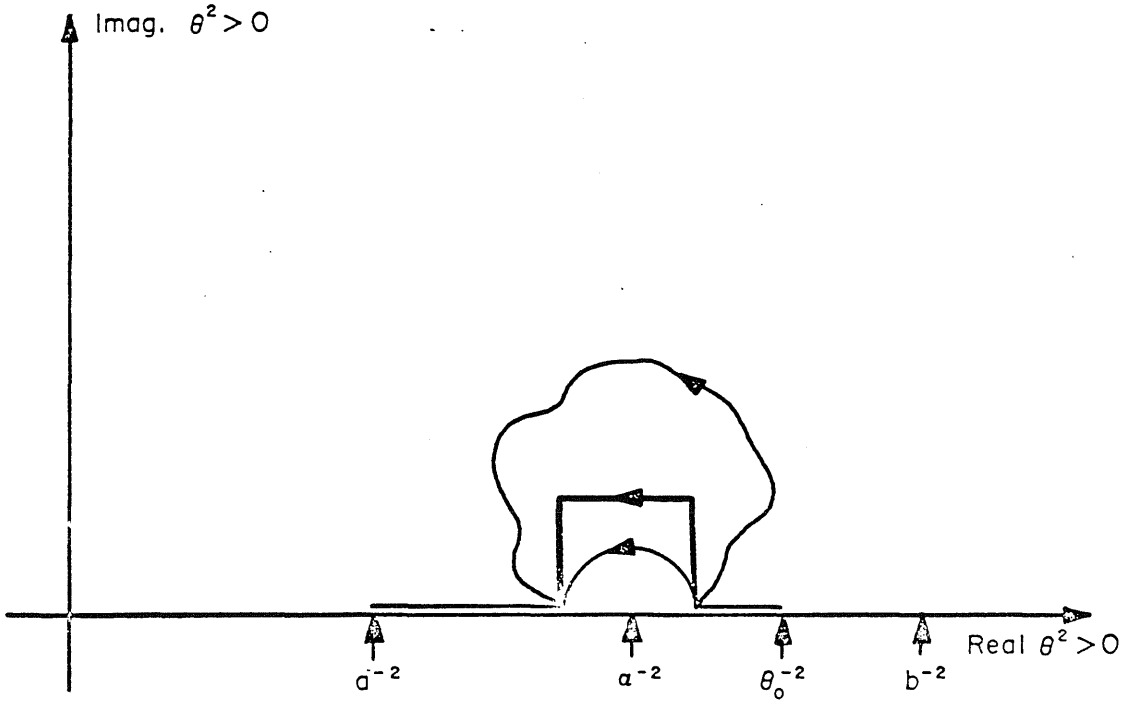

FIG. 29. POSSIBLE INTEGRATION CONTOURS AROUND $\theta^2 = \alpha^{-2}$

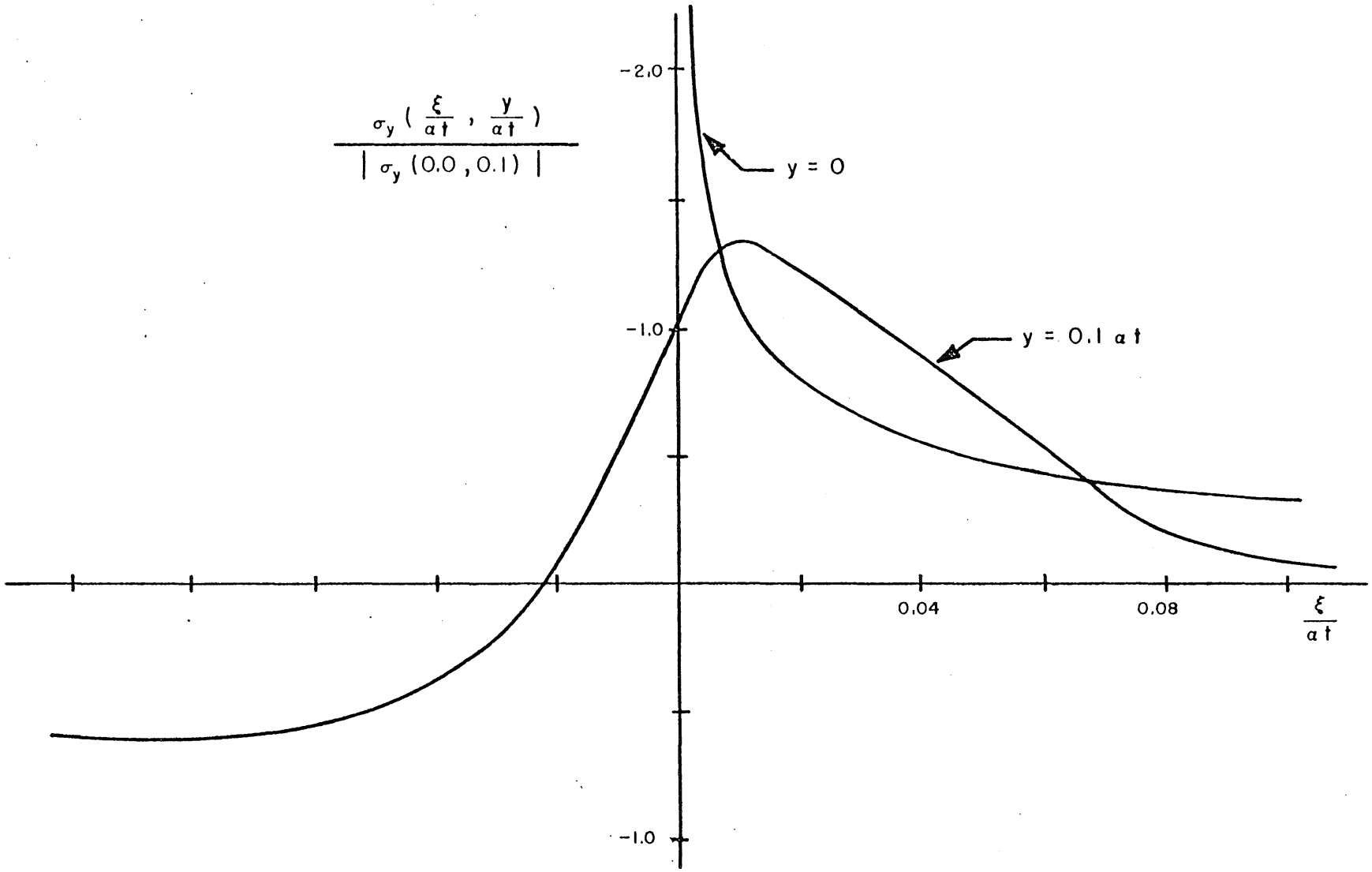

FIG. 30. ASYMPTOTIC CHARACTER OF σ_y NEAR THE EDGE OF THE CONTACT ZONE FOR $\alpha = 0.95b$

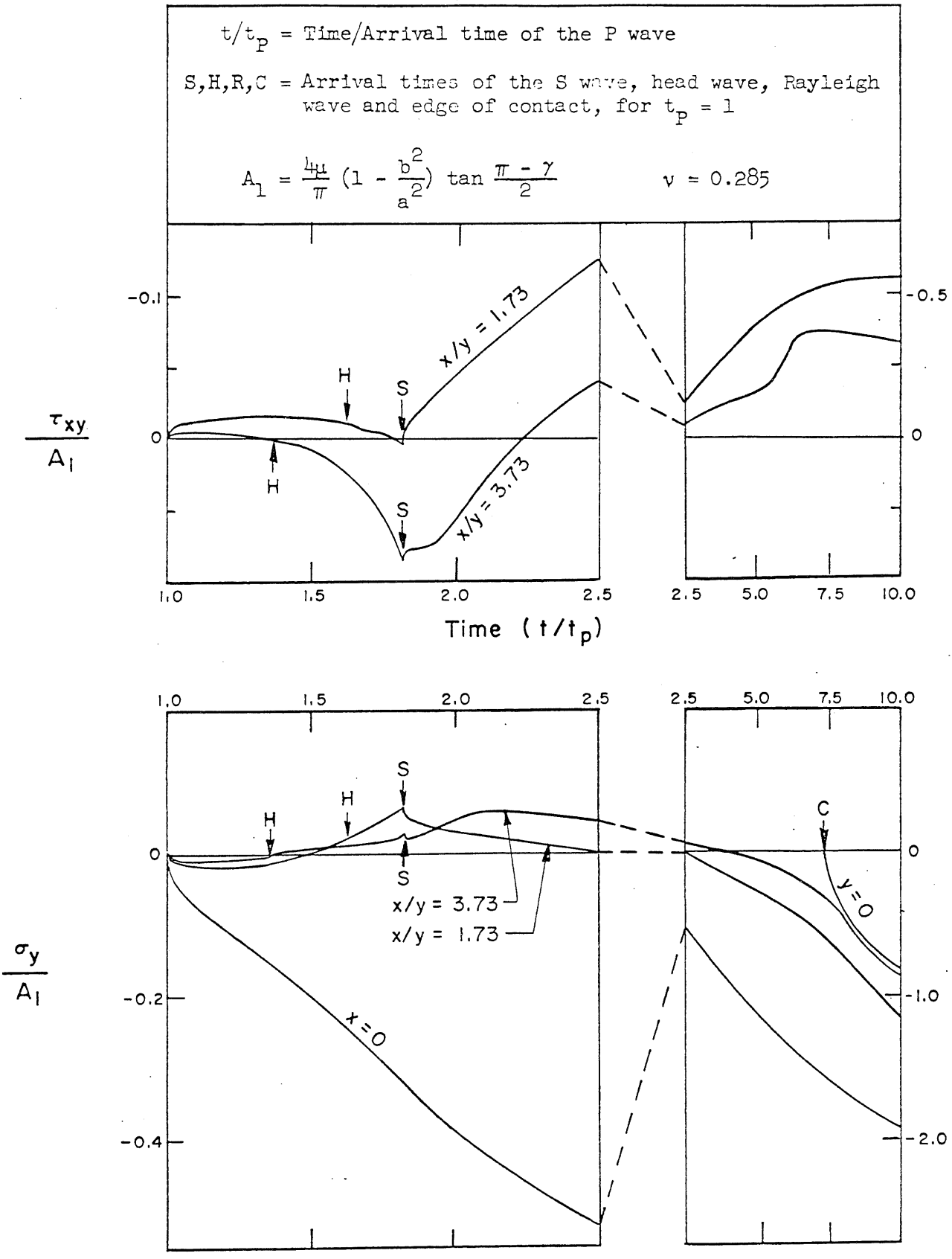

FIG. 31. TIME HISTORY OF τ_{xy} and σ_y FOR A SLOWLY INDENTING WEDGE PROBLEM ($\alpha = 0.25b$)

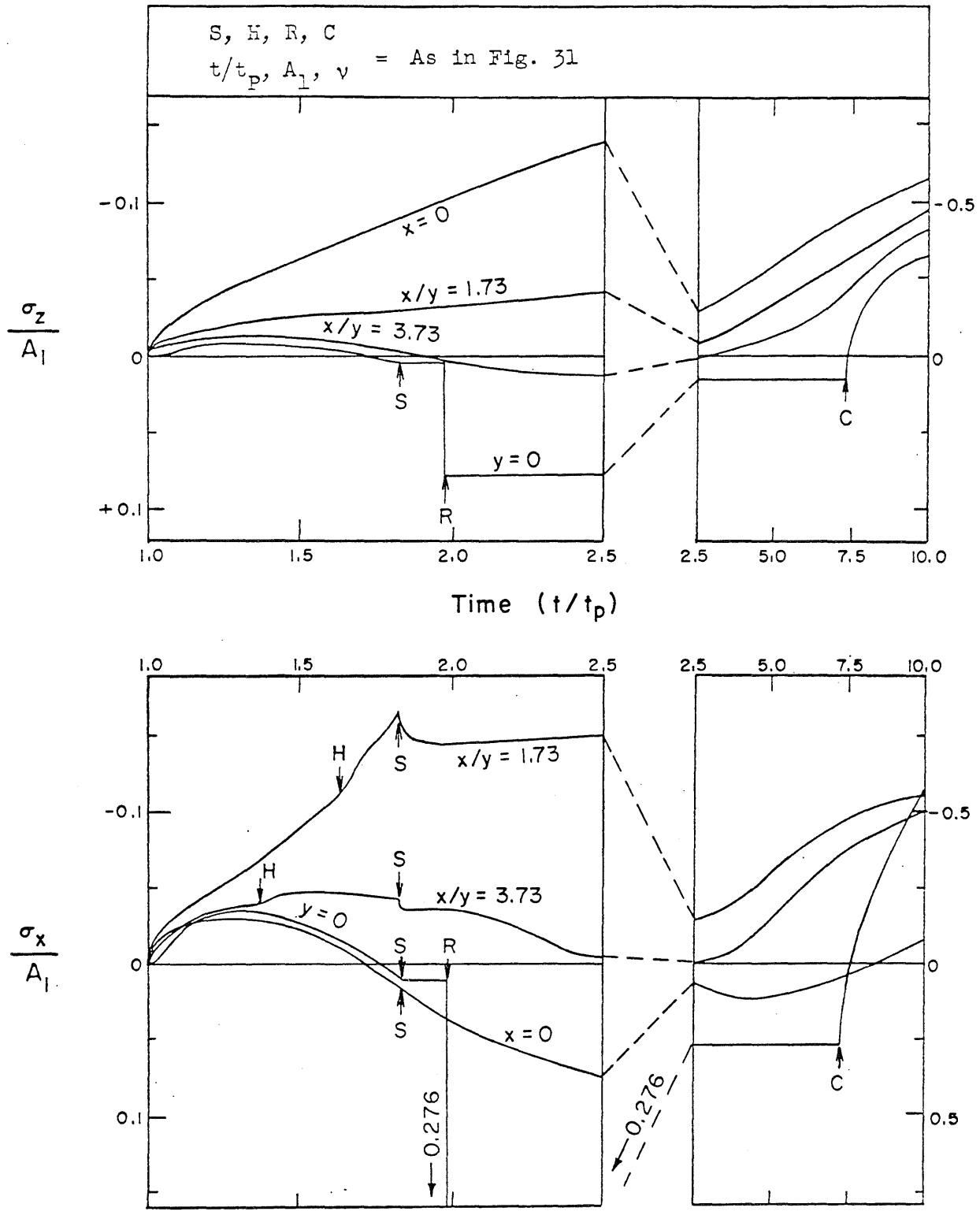

FIG. 32. TIME HISTORY OF σ_z AND σ_x FOR A SLOWLY INDENTING WEDGE PROBLEM (α = 0.25b)

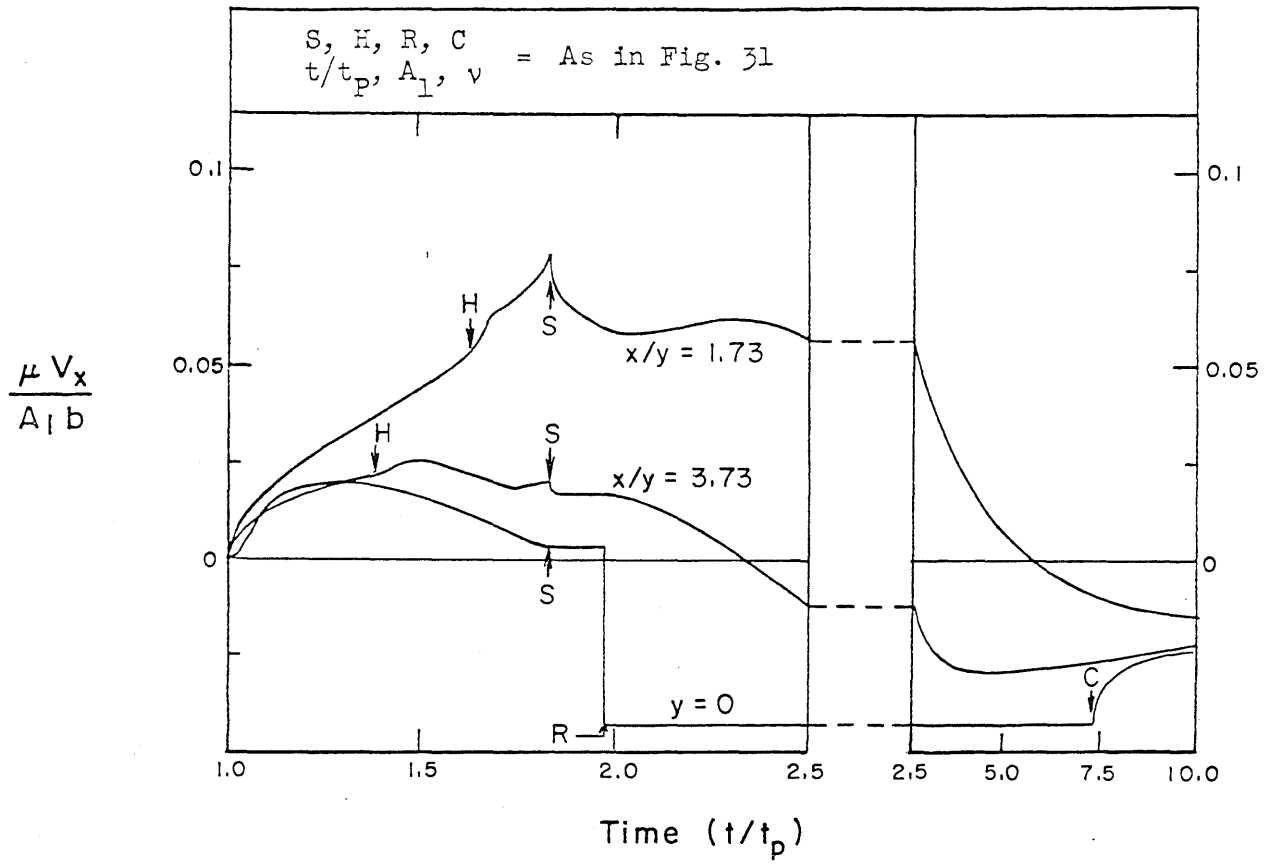

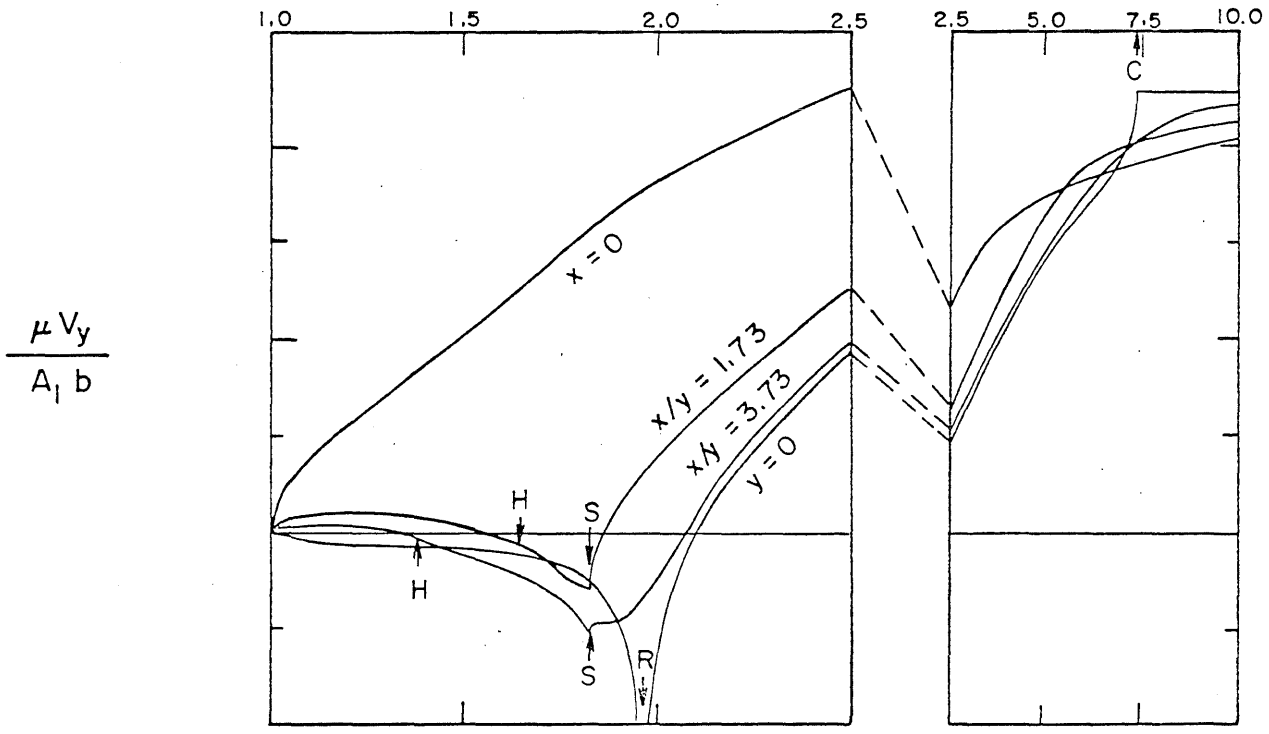

FIG. 33. TIME HISTORY OF v_x AND v_y FOR A SLOWLY INDENTING WEDGE PROBLEM (α = 0.25b)

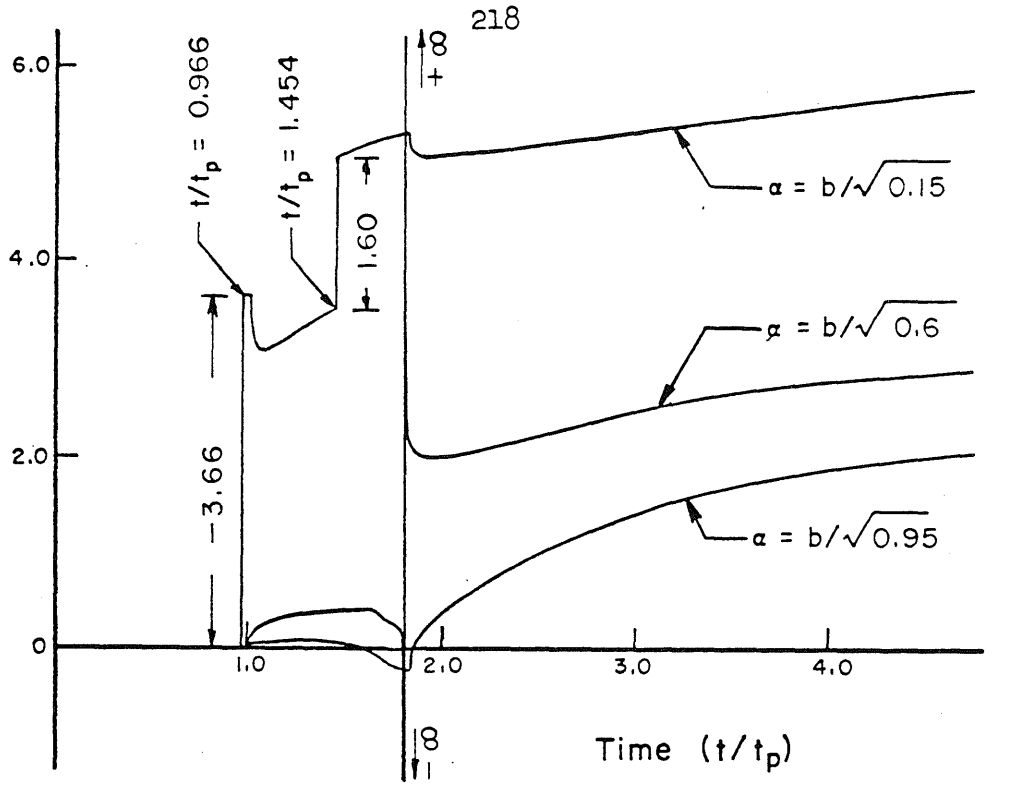

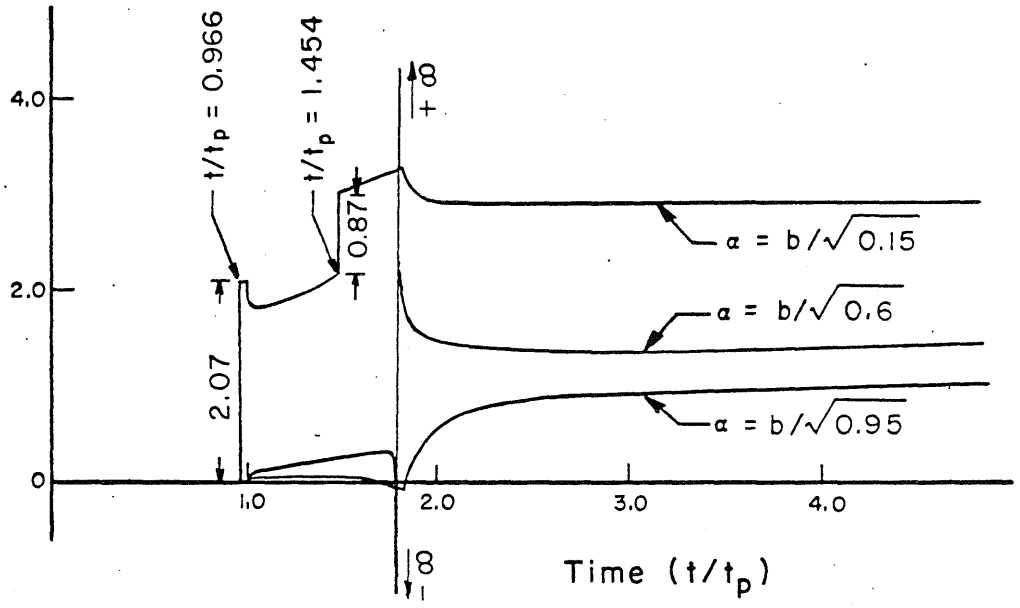

t/t_p, A_1, ν = As in Fig. 31

FIG. 34. DEPENDENCE OF σ_y and v_y on α FOR THE WEDGE PROBLEM ($x/y = 1.73$)

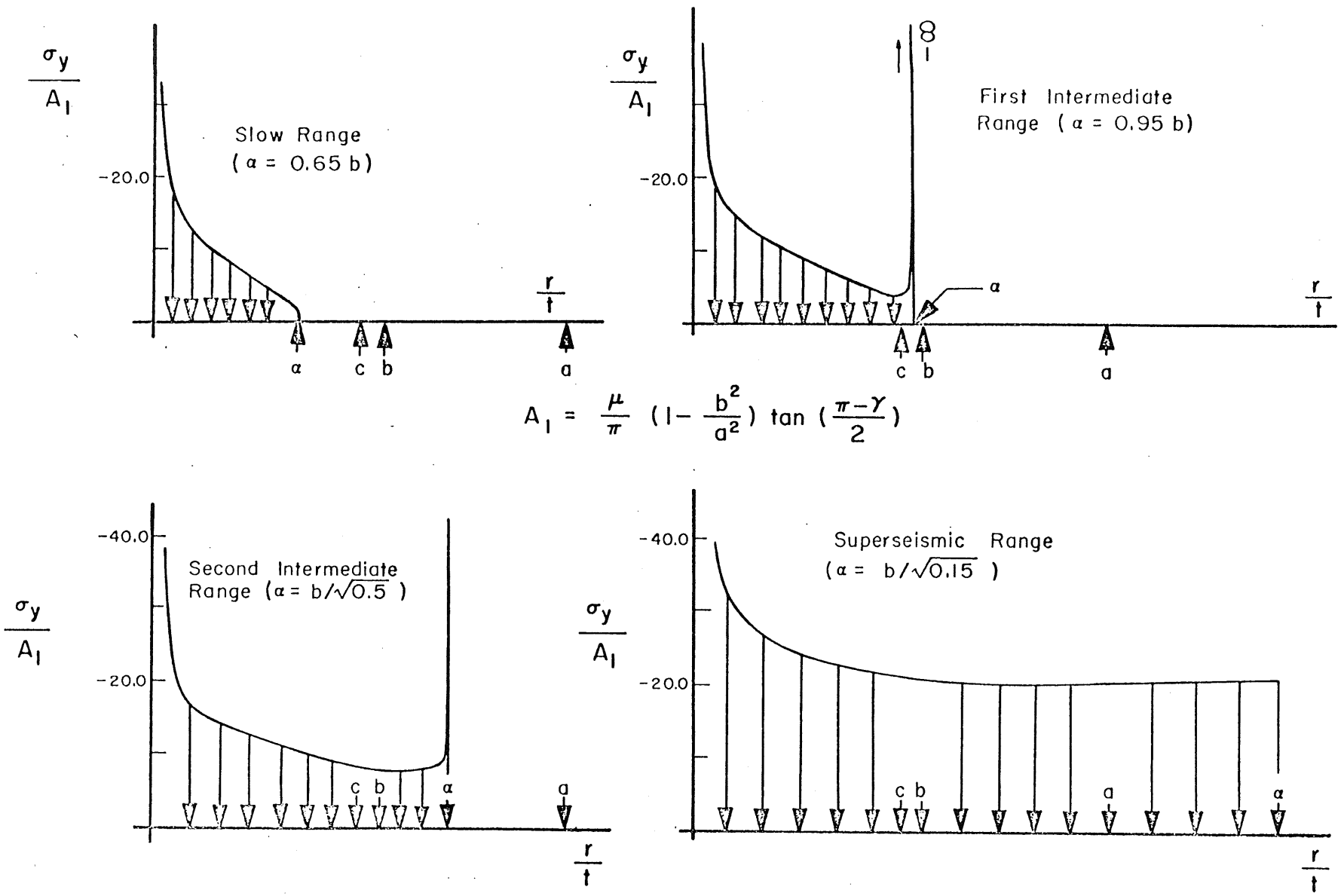

FIG. 35. DISTRIBUTION OF THE CONTACT STRESS FOR THE CONE PROBLEM ($\nu = 0.285$)

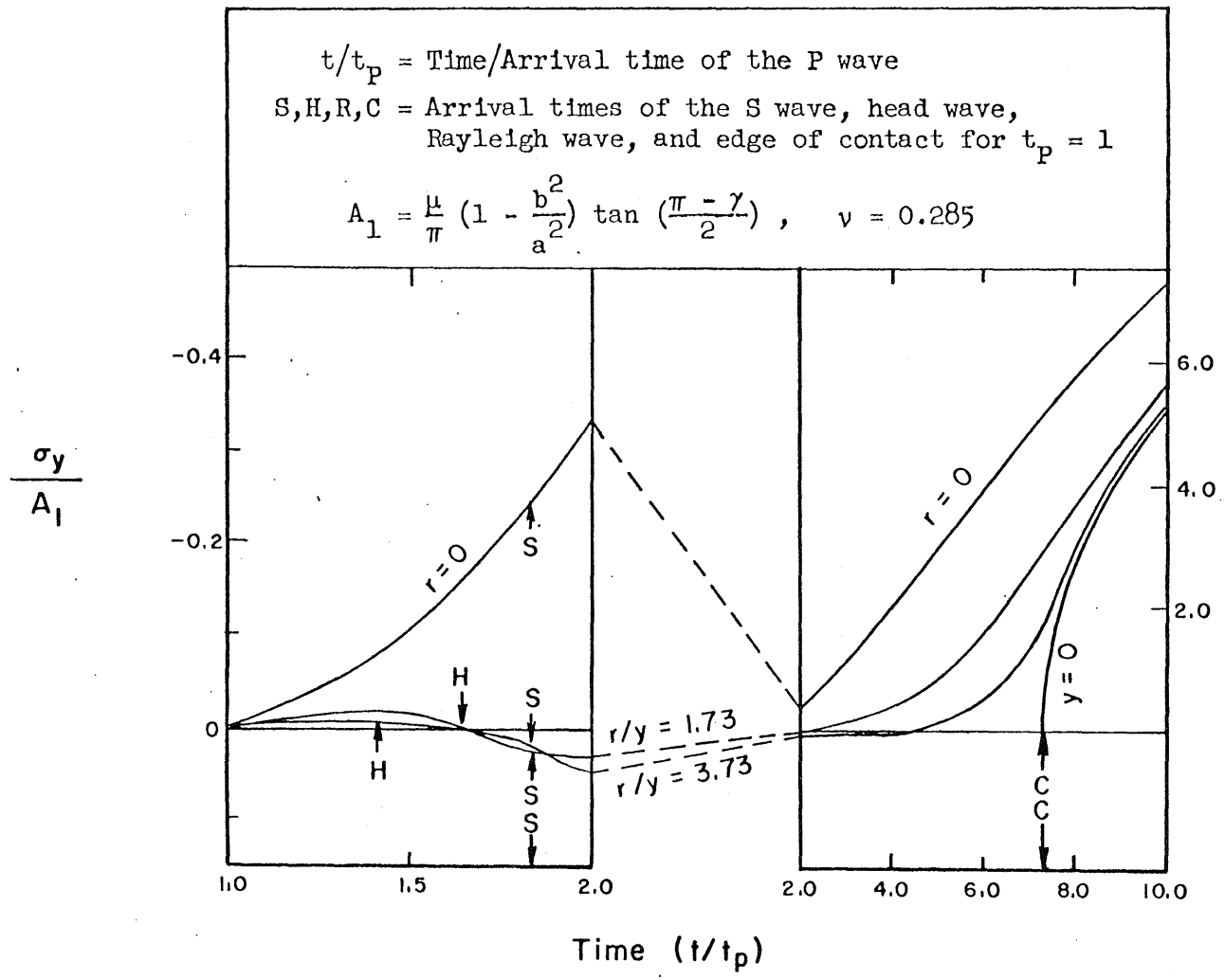

FIG. 36. TIME HISTORY OF σ_y FOR A SLOWLY INDENTING CONE PROBLEM ($\alpha = 0.25b$)

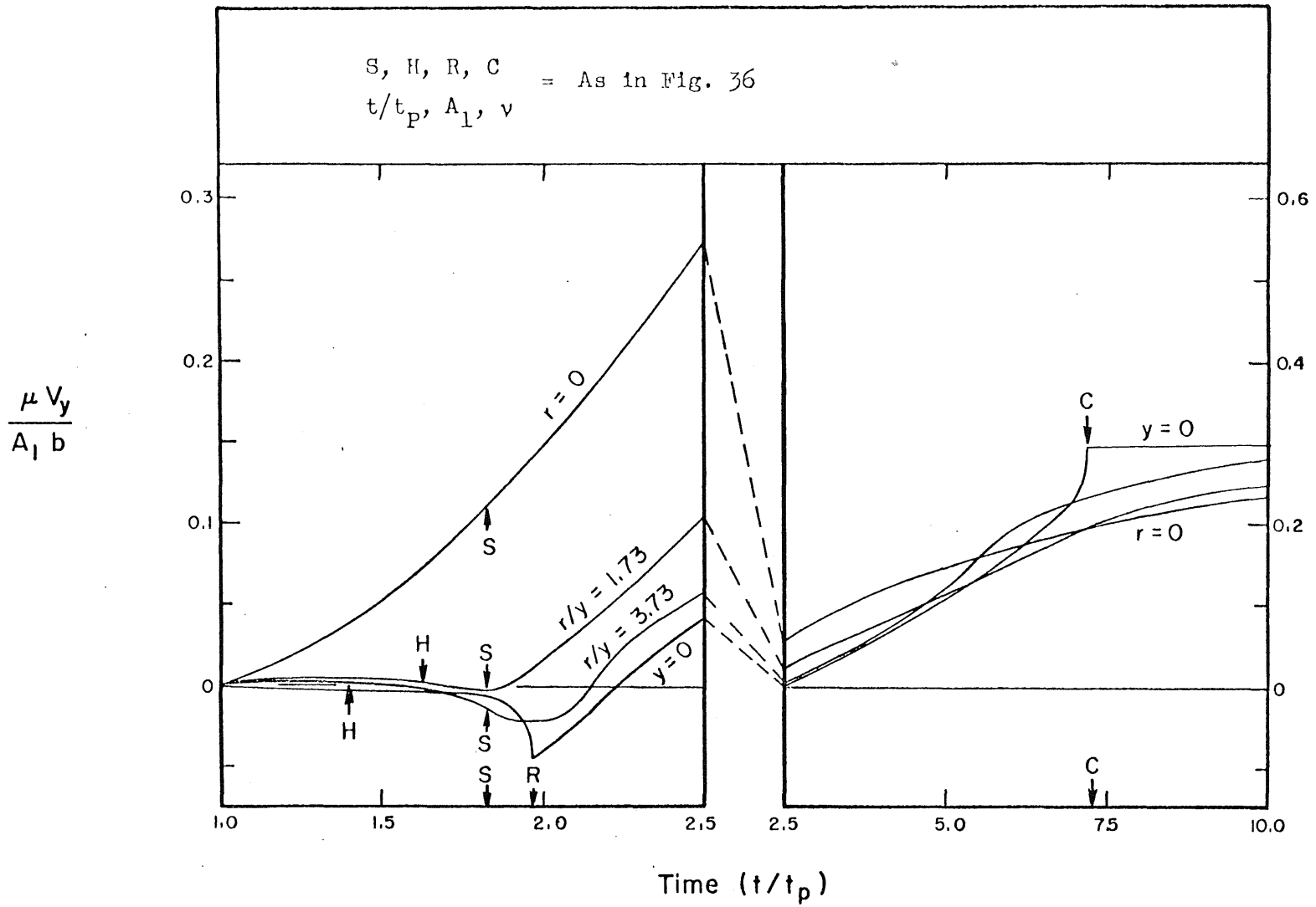

FIG. 37. TIME HISTORY OF v_y FOR A SLOWLY INDENTING CONE PROBLEM ($\alpha = 0.25b$)

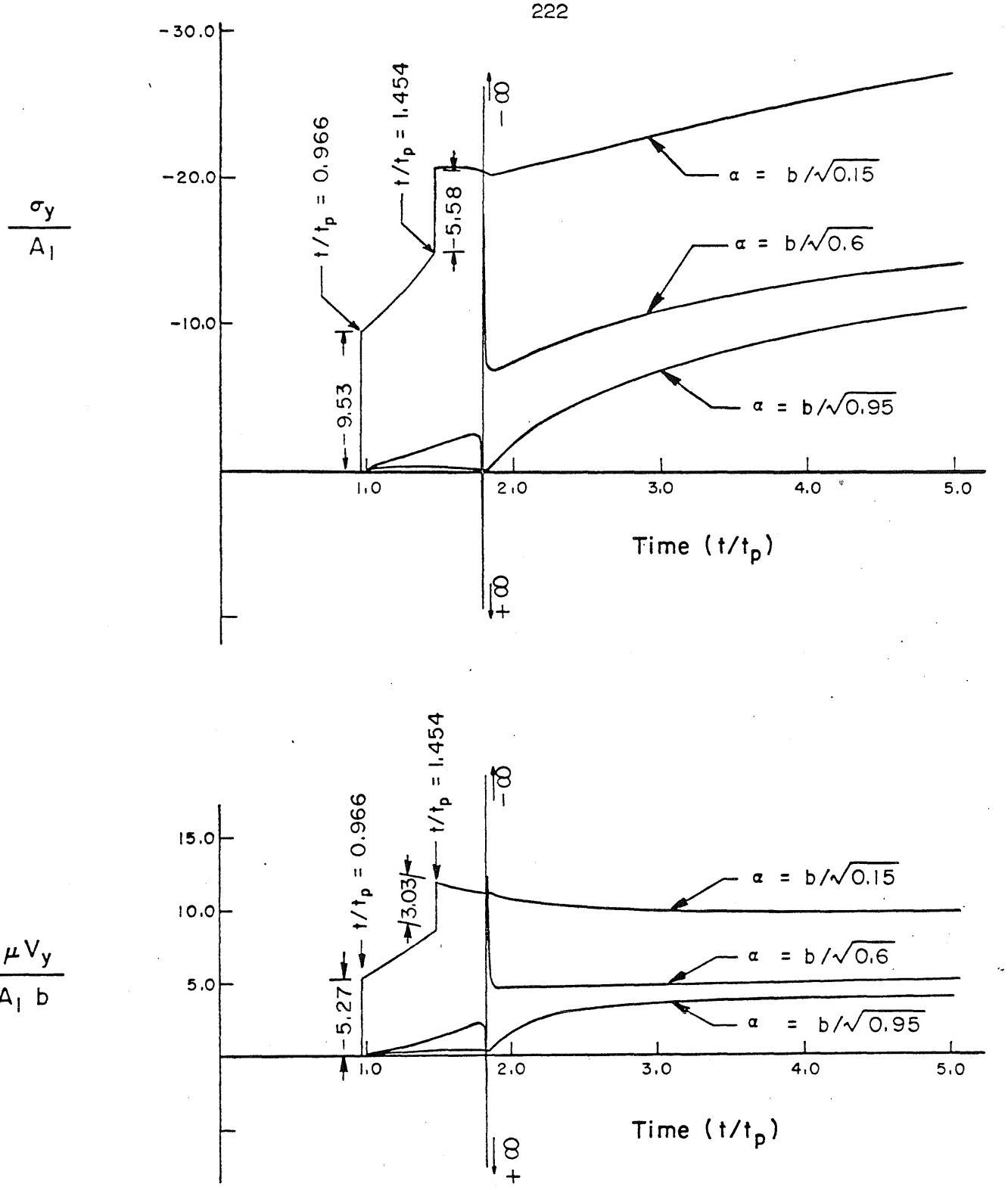

t/t_p, A_1, ν = As in Fig. 36

FIG. 38. DEPENDENCE OF σ_y AND v_y ON α FOR THE CONE PROBLEM ($r/y = 1.73$)

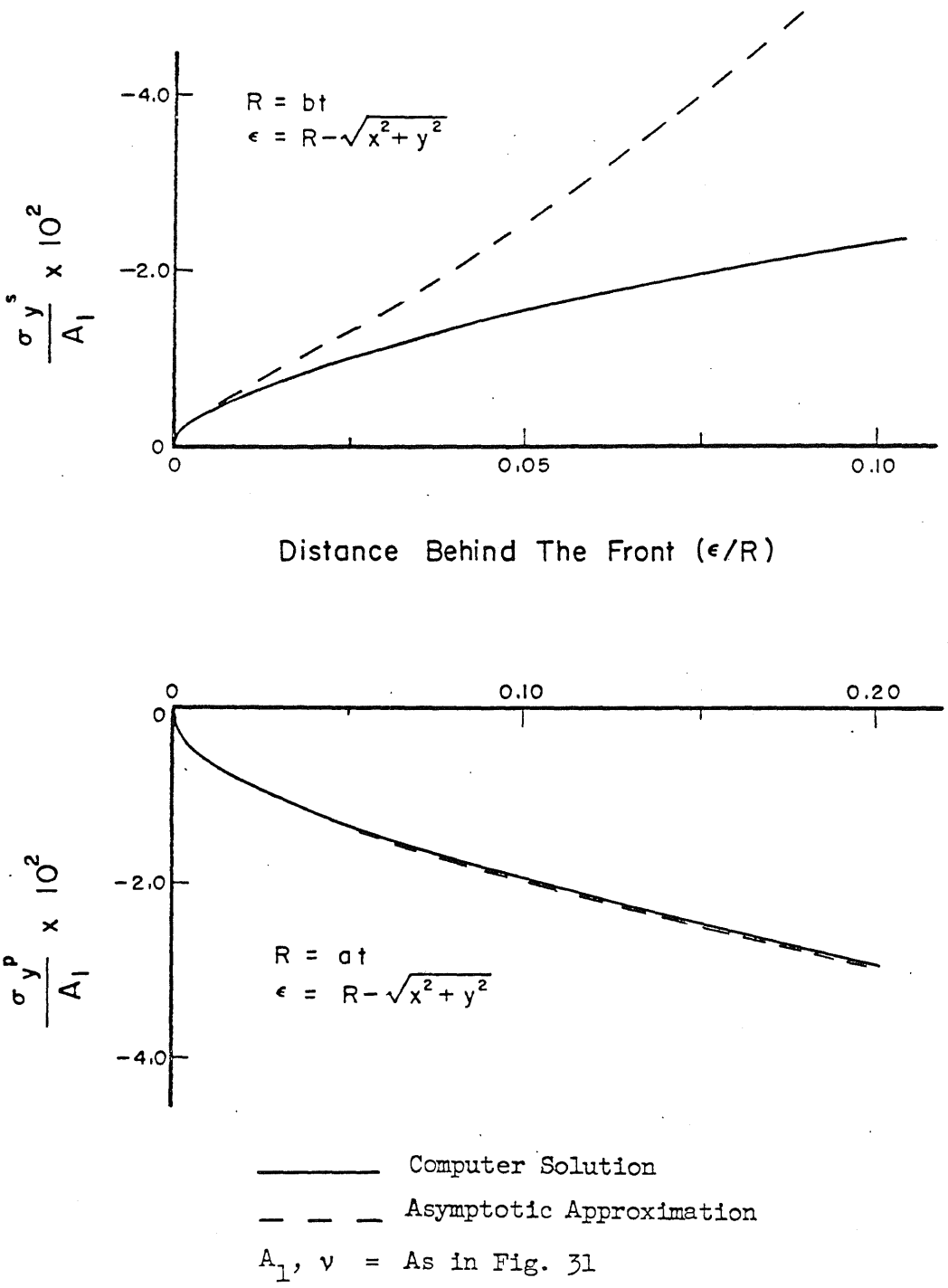

FIG. 39. ASYMPTOTIC APPROXIMATIONS OF σ_y^S AND σ_y^P NEAR THE WAVE FRONTS FOR THE WEDGE PROBLEM ($\alpha = 0.1b$, $x/y = 1/\sqrt{3}$)

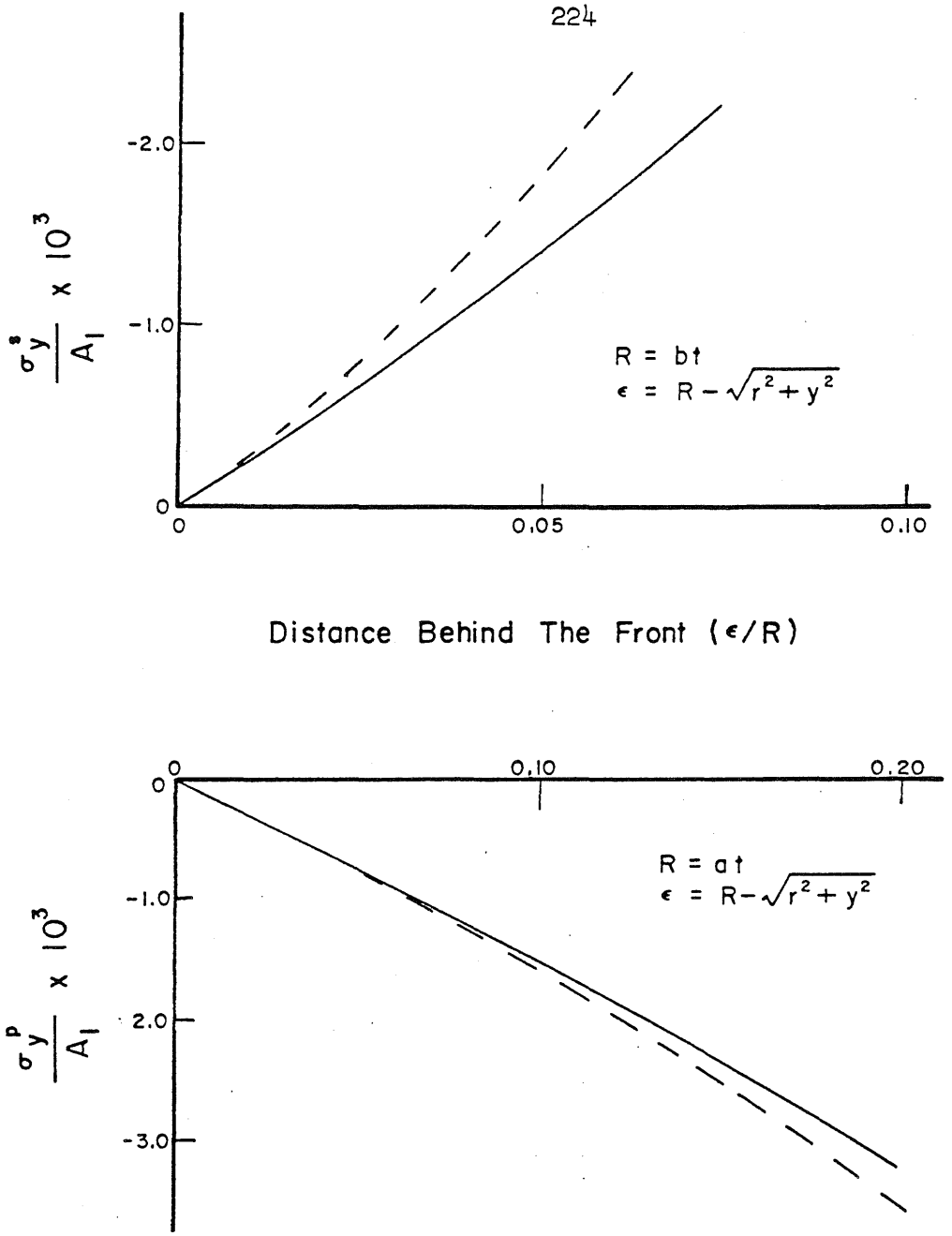

FIG. 40. ASYMPTOTIC APPROXIMATIONS OF σ_y^S AND σ_y^P NEAR THE WAVE FRONTS FOR THE CONE PROBLEM (α = 0.1b, $r/y = 1/\sqrt{3}$)

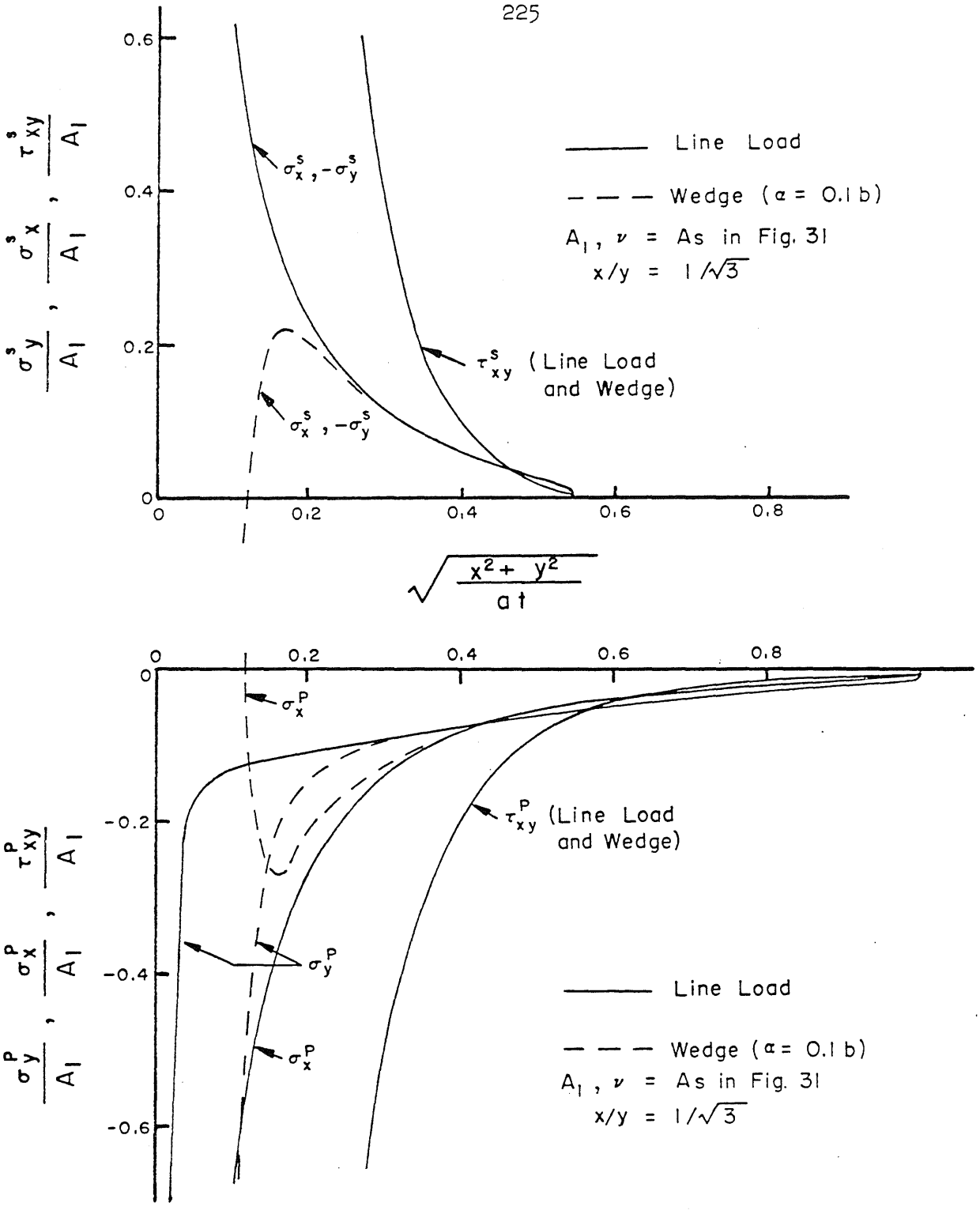

FIG. 41. P- AND S-WAVE COMPONENTS OF THE STRESSES FOR SLOWLY INDENTING WEDGE AND LINE LOAD PROBLEMS WITH EQUAL VERTICAL LOADS APPLIED TO THE HALF SPACE

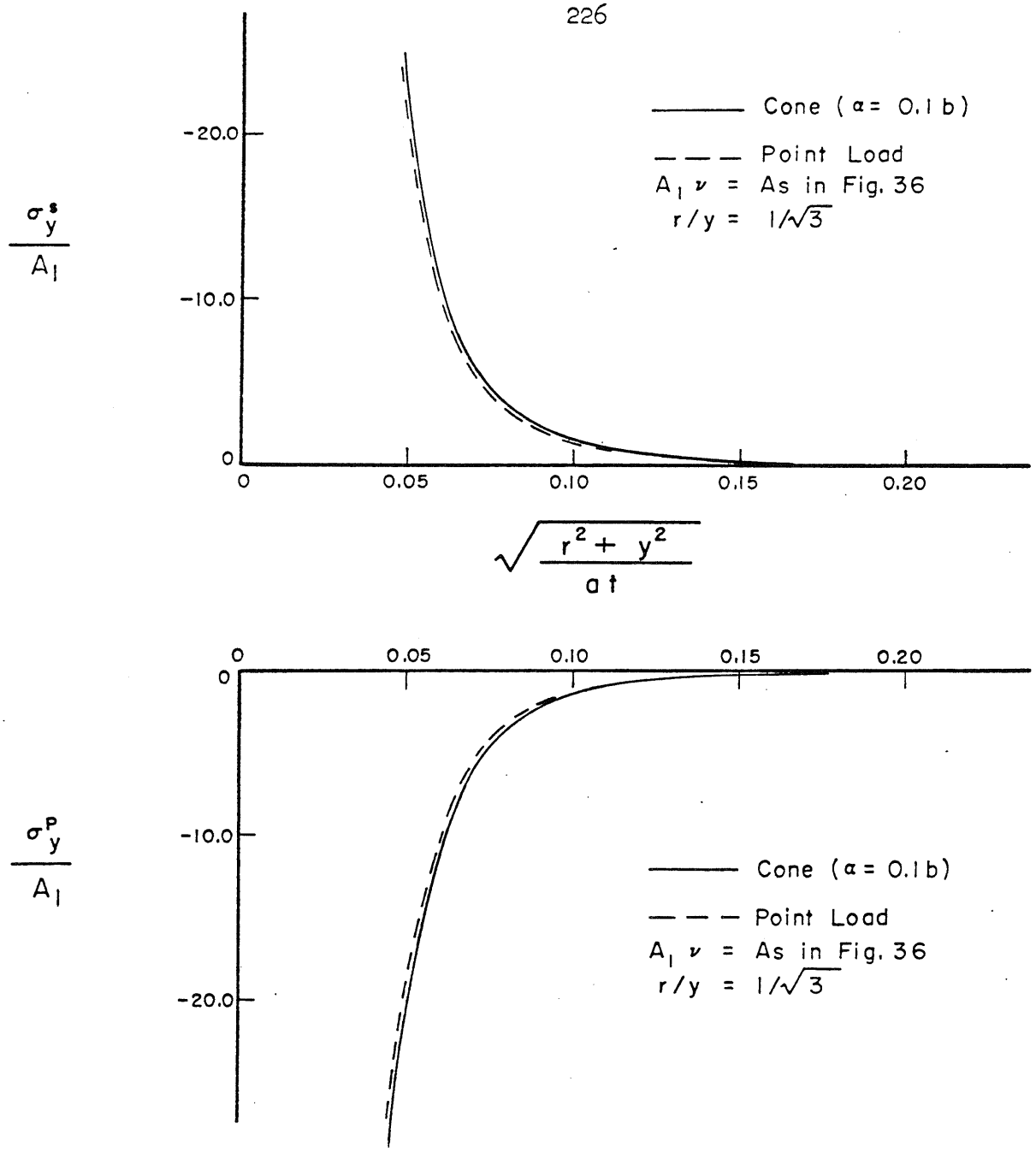

FIG. 42. P- AND S-WAVE COMPONENTS OF σ_y FOR SLOWLY INDENTING CONE AND POINT LOAD PROBLEMS WITH EQUAL VERTICAL LOADS APPLIED TO THE HALF SPACE

APPENDIX A. THE FUNCTION $F_{\alpha b}(\theta)$ OF SEC. 4.1.4.3

A.1. Derivation of $F_{\alpha b}(\theta)$

In Chapters 4 and 5, frequent mention is made of the function $F_{\alpha b}(\theta)$ which arises in connection with problems involving wedges and cones which indent in such a way that $b < \alpha < a$, i.e. in the second intermediate range of contact speeds. The conditions which this function must satisfy are specified in Sec. 4.1.4.3. These are

1) that $F_{\alpha b}(\theta)/R(\theta^2)$ be analytic for all real values of θ in the range $\alpha^{-1} \leq |\theta| \leq b^{-1}$,

2) that $F_{\alpha b}(\theta)$ be analytic everywhere except for real values of θ in the range $\alpha^{-1} \leq |\theta| \leq b^{-1}$, and

3) that $\lim_{\theta \to \infty} F_{\alpha b}(\theta) = 1$.

For the first condition to be satisfied, the argument of $F_{\alpha b}(\theta)$ (and, therefore, the imaginary part of $\log F_{\alpha b}(\theta)$) must be equal to the argument of $R(\theta^2)$ in the range $\alpha^{-1} \leq |\theta| \leq b^{-1}$. We note that the imaginary part of $\log F_{\alpha b}(\theta)$ will be zero on the remaining portion of the real θ axis if $\log F_{\alpha b}(\theta)$ is analytic at every point outside of the range $\alpha^{-1} \leq |\theta| \leq b^{-1}$. However, this requires that $F_{\alpha b}(\theta)$ be nowhere equal to zero. We now show that such a function exists and that, in fact, it is the only function satisfying the conditions listed above.

The Cauchy integral theorem for the half plane can be used to determine the unique function which defines $\log F_{\alpha b}(\theta)$ and which satisfies the following conditions on the real θ axis and at infinity:

$$\text{Im } (\log F_{\alpha b}(\theta)) = \beta(\theta) \quad \text{for } \alpha^{-1} \leq |\theta| \leq b^{-1}$$

$$= 0 \quad \text{for } |\theta| < \alpha^{-1} \text{ and } b^{-1} < |\theta|$$

$$\lim_{\theta \to \infty} (\log F_{\alpha b}(\theta)) = 0$$

where $\beta(\theta)$ is the argument of $R(\theta^2)$. That is,

$$\beta(\theta) = \text{Im } (\log R(\theta^2)) \tag{A.1}$$

The calculation gives

$$\log F_{\alpha b}(\theta) = \frac{1}{\pi}\int_{\alpha^{-1}}^{b^{-1}} \frac{\beta(\lambda)}{\lambda - \theta}\, d\lambda + \frac{1}{\pi}\int_{-b^{-1}}^{-\alpha^{-1}} \frac{\beta(\lambda)}{\lambda - \theta}\, d\lambda \tag{A.2}$$

Since $\beta(\lambda)$ is an antisymmetric function of λ, Eq. (A.2) can be written more simply as follows:

$$\log F_{\alpha b}(\theta) = \pi^{-1}\int_{\alpha^{-2}}^{b^{-2}} \frac{\beta(\lambda^2)}{\lambda^2 - \theta^2}\, d\lambda^2 \tag{A.3}$$

Hence,

$$F_{\alpha b}(\theta) = \exp\left(\pi^{-1}\int_{\alpha^{-2}}^{b^{-2}} \frac{\beta(\lambda^2)}{\lambda^2 - \theta^2}\, d\lambda^2\right) \tag{A.4}$$

To prove the uniqueness of the above result, we assume that there exists a second function $F_2(\theta)$ which also satisfies the conditions listed in above. It follows that $F_2(\theta)/F_{\alpha b}(\theta)$ must be analytic at every point in the

entire θ plane since $F_{\alpha b}(\theta)$ has no zeros and the non-analyticities of $F_2(\theta)$ and $F_{\alpha b}(\theta)$ cancel for $\alpha^{-1} \leq |\theta| \leq b^{-1}$. Moreover, the value of $F_2(\theta)/F_{\alpha b}(\theta)$ is 1 at infinity. It follows from Liouville's Theorem that $F_2(\theta)/F_{\alpha b}(\theta)$ is everywhere equal to unity, or that $F_2(\theta) = F_{\alpha b}(\theta)$, and $F_{\alpha b}(\theta)$ is unique.

Since the integral of Eq. (A.4) is hyperelliptic, it is generally not possible to express $F_{\alpha b}(\theta)$ in terms of elementary functions. However, this is not the case if $\alpha^{-2} = b^{-2}$ or if $\alpha^{-2} = a^{-2}$. In the former case, i.e. when $\alpha^{-2} = b^{-2}$, the integration is carried out over a contour of zero length. Hence $F_{\alpha b}(\theta) = 1$ if $\alpha^{-2} = b^{-2}$. When $\alpha^{-2} = a^{-2}$, the contour of integration extends along the full length of the cut on the real θ^2 axis between a^{-2} and b^{-2} associated with $R(\theta^2)$.

It can easily be verified that the conditions listed above are satisfied for $\alpha^{-2} = a^{-2}$ if

$$F_{\alpha b}(\theta) = \frac{R(\theta^2)}{2(a^{-2}-b^{-2})(\theta^2-c^{-2})} \quad , \tag{A.5}$$

where c^{-2} is the zero point of $R(\theta^2)$ and $2(a^{-2}-b^{-2})$ is the value of $R(\theta^2)/(\theta^2-c^{-2})$ at infinity.

A.2. Numerical Evaluation of $F_{\alpha b}(\theta)$

In this study, $F_{\alpha b}(\theta)$ is evaluated numerically for problems in which $b < \alpha < a$. Integration by parts of the integral of Eq. (A.4), followed by the substitution of $\log (\lambda^2-\theta_0^2) - \int_{\theta_0^2}^{\theta_2} (\lambda^2-\theta^2)^{-1} d\theta^2$ for $\log (\lambda^2-\theta^2)$ makes it possible to compute $F_{\alpha b}(\theta)$ is a step-by-step procedure for the following equation:

$$F_{\alpha b}(\theta) = \exp\left[\pi^{-1}(-\beta(\alpha^{-2})\log(\alpha^{-2}-\theta^2) - \int_{\alpha^{-2}}^{b^{-2}} \beta'(\lambda^2)\log(\lambda^2-\theta_0^2)d\lambda^2 + \int_{\theta_0^2}^{\theta^2} M(\theta^2)d\theta^2)\right] \tag{A.6}$$

where $\beta'(\lambda^2) = d\beta(\lambda^2)/d\lambda^2$, θ_0^2 is any arbitrarily chosen fixed point in the θ^2 plane, and $M(\theta^2)$ is the function defined by the integral

$$M(\theta^2) = \int_{\alpha^{-2}}^{b^{-2}} \frac{\beta'(\lambda^2)}{\lambda^2 - \theta^2}\, d\lambda^2 \quad . \tag{A.7}$$

Since $M(\theta^2)$ and $\beta'(\lambda^2)$ are expressible in terms of elementary functions, the integrals of Eq. (A.6) can be evaluated numerically by the methods described in Chapter 5. It follows that the value of $F_{\alpha b}(\theta)$ can be obtained without difficulty at any point in the complex θ plane.

It can easily be verified that $\beta'(\lambda^2)$ and $M(\theta^2)$ are defined as follows:

$$\beta'(\lambda^2) = -\frac{D_1(\lambda^2)}{(D_2(\lambda^2)(\lambda^2-a^{-2})^{1/2}(b^{-2}-\lambda^2)^{1/2})}$$

where

$$\begin{aligned} D_1(\lambda^2) = {} & 8(b^{-2}-a^{-2})\lambda^6 + 8(a^{-2}-2b^{-2})b^{-2}\lambda^4 \\ & + 6.0(a^{-2}+b^{-2})b^{-4}\lambda^2 - 4.0\, a^{-2}b^{-6} \quad , \\ D_2(\lambda^2) = {} & -16(b^{-2}-a^{-2})\lambda^6 + b^{-2}(24b^{-2}-16a^{-2})\lambda^4 \\ & -8b^{-6}\lambda^6 + b^{-8} \quad , \end{aligned} \tag{A.8}$$

$$M(\theta^2) = \beta'(\theta^2) \times R(\theta^2) + \frac{1}{16(b^{-2}-a^{-2})} \sum_{i=1}^{3} \frac{R(\lambda_i^2)}{\lambda_i^2 - \theta^2} \; Q(\lambda_i^2) \tag{A.9}$$

where the λ_i^2 (i=1,2,3) denote the three roots of $D_2(\lambda^2) = 0$

and where

$$P(\theta^2) = - \log \left(\frac{b^{-2} - a^{-2}}{2\sqrt{\theta^2-a^{-2}}\sqrt{b^{-2}-\theta^2}}\right)$$

$$+ \log \left(\frac{\sqrt{\alpha^{-2}-a^{-2}}\sqrt{b^{-2}-\alpha^{-2}} + \sqrt{\theta^2-a^{-2}}\sqrt{b^{-2}-\theta^2}}{\alpha^{-2} - \theta^2}\right.$$

$$\left. + \frac{a^{-2} + b^{-2} - 2\theta^2}{2\sqrt{\theta^2-a^{-2}}\sqrt{b^{-2}-\theta^2}}\right)$$

and

$$Q(\lambda_i^2) = \frac{D_1(\lambda_i^2) + 1/2\; D_2(\lambda_i^2)}{(\lambda_i^2-\lambda_j^2)(\lambda_i^2-\lambda_k^2)\sqrt{\lambda_i^2-a^{-2}}\sqrt{b^{-2}-\lambda_i^2}} \qquad i \neq j \neq k \neq i$$

A.3. The Asymptotic Expansion of $F_{\alpha b}(\theta)$ about the Edge of the Region of Contact

It is convenient in computing the asymptotic expansion of $F_{\alpha b}(\theta)$ about $\theta^2 = \alpha^{-2}$ to rewrite Eq. (A.4) in the form

$$F_{\alpha b}(\theta) = \exp\left(\pi^{-1} \int_{\alpha^{-2}}^{b^{-2}} \frac{\beta(\lambda^2) - \beta(\theta^2)}{\lambda^2 - \theta^2}\, d\lambda^2 + \pi^{-1} \int_{\alpha^{-2}}^{b^{-2}} \frac{\beta(\theta^2)}{\lambda^2 - \theta^2}\, d\lambda^2\right) \tag{A.10}$$

The first integral of Eq. (A.10) defines a function which varies smoothly for values of θ^2 in the vicinity of α^{-2}. If this function is denoted by

$L(\theta^2)$, it can easily be verified that Eq. (A.10) can be rewritten in the form

$$F_{\alpha b}(\theta) = \exp(\pi^{-1}L(\theta^2)) \cdot \left(\frac{b^{-2} - \theta^2}{\alpha^{-2} - \theta^2}\right)^{B(\theta^2)/\pi} \tag{A.11}$$

As asymptotic expansion of $F_{\alpha b}(\theta)$ about the points $\theta^2 = \alpha^{-2}$ results in the following series:

$$F_{\alpha b}(\theta) \simeq (\alpha^{-2}-\theta^2)^{-\beta(\alpha^{-2})/\pi}\left\{1+\frac{\beta'(\alpha^{-2})}{\pi}(\alpha^{-2}-\theta^2)\log(\alpha^{-2}-\theta^2) + ...\right\}$$

$$\left\{C_0 + C_1(\theta^2-\alpha^{-2}) + ...\right\} \tag{A.12}$$

where the infinite series in the second set of braces is a Taylor series expansion of

$$\exp(\pi^{-1}L(\theta^2))(b^{-2}-\theta^2)^{\beta(\alpha^{-2})/\pi+\beta'(\alpha^{-2})(\theta^2-\alpha^{-2})/\pi + \ldots}$$

about $\theta^2 = \alpha^{-2}$. That is to say,

$$C_0 = \exp(\pi^{-1} L(\alpha^{-2}))(b^{-2}-\alpha^{-2})^{\beta(\alpha^{-2})/\pi} \tag{A.13}$$

and so on.

APPENDIX B. STEP DISCONTINUITIES IN THE STRESSES ACROSS THE MACH FRONTS FOR THE CONE

The vertical stress for the problem in which a cone indents superseismically can be computed at any point in the half space from the equation:†

$$\sigma_y(r,y,t) = \int_{\theta_{11}^2}^{\bar{\theta}_{11}^2} I_1(\theta_1^2) \cdot \frac{\partial \omega}{\partial \theta_1^2} \, d\theta_1^2 + \int_{\theta_{22}^2}^{\bar{\theta}_{22}^2} I_2(\theta_2^2) \frac{\partial \omega}{\partial \theta_2^2} \, d\theta_2^2 \qquad \text{(B.1)}$$

where
$$I_i(\theta_i^2) = \int_0^{\theta_i^2} I_i'(\theta^2) d\theta^2 \qquad i = 1,2 \qquad \text{(B.2)}$$

$$I_1'(\theta_1^2) = \frac{A_1}{2(b^{-2}-a^{-2})} \frac{(b^{-2}-2\theta_1^2)^2}{(a^{-2}-\theta_1^2)^{1/2}(\alpha^{-2}-\theta_1^2)^{3/2}} ,$$

$$I_2'(\theta_2^2) = \frac{A_1}{2(b^{-2}-a^{-2})} \frac{4\theta_2^2(b^{-2}-\theta_2^2)^{1/2}}{(\alpha^{-2}-\theta_2^2)^{3/2}} , \qquad \text{(B.3)}$$

$$t - r\cos\omega\theta_i - y(c_i^{-2}-\theta_i^2)^{1/2} = 0 , \qquad \text{(B.4)}$$

$$t - r\theta_{ii} - y(c_i^{-2}-\theta_{ii}^2)^{1/2} = 0 , \qquad \text{(B.5)}$$

and A_1 is defined by Eq. (4.48). Equation (B.4) is used to compute $\partial\omega/\partial\theta_i^2$. The result is

$$\frac{\partial \omega}{\partial \theta_i^2} = \frac{t - yc_i^{-2}/(c_i^{-2}-\theta_i^2)^{1/2}}{2\theta_i^2(r^2\theta_i^2 - (t - y(c_i^{-2}-\theta_i^2)^{1/2})^2)^{1/2}} \qquad i = 1,2 \qquad \text{(B.6)}$$

† Equation (B.1) is obtained from Eqs. (2.57), (2.88), (3.14) and (4.50).

As in Chapter 5, we denote the P- and S-wave components of σ_y by σ_y^P and σ_y^S, respectively. To compute the value of σ_y^P at a point behind the Mach front shown in Fig. 19,† we evaluate the first integral of Eq. (B.1) along contour of the type shown in Fig. 12b. This contour begins a θ_{11}^2, crosses the real θ_1^2 axis to the left of α^{-2}, and ends at $\bar{\theta}_{11}^2$. If the point at which σ_y^P is being computed lies just behind the Mach front, the value of θ_{11}^2 will be real and slightly greater than α^{-2}. As a result, a contour of integration can be chosen which is situated in the immediate vicinity of α^{-2}, i.e. a contour such as C_3 of Fig. 12b. The value of $I_1(\theta_1^2)$ along this contour can be found by integrating termwise the asymptotic expansion of $I_1'(\theta_1^2)$ about α^{-2}. The final result is the following infinite series:

$$I_1(\theta_1^2) \simeq C_0 + C_1/(\alpha^{-2}-\theta_1^2)^{1/2} + C_2(\alpha^{-2}-\theta_1^2)^{1/2} + O(\alpha^{-2}-\theta_1^2)^{3/2} ,$$

where
$$C_1 = \frac{A_1}{(b^{-2}-a^{-2})} \frac{(b^{-2}-2\alpha^{-2})^2}{(a^{-2}-\alpha^{-2})^{1/2}} ,$$
$$C_2 = -\frac{A_1}{2(b^{-2}-a^{-2})} \frac{b^{-2}(8a^{-2}-b^{-2}) - 4\alpha^{-2}(4a^{-2}+b^{-2}) + 12\alpha^{-4}}{(a^{-2}-\alpha^{-2})^{3/2}} \qquad (B.7)$$

and where C_0 is a constant of integration yet to be determined.

The function $\partial\omega/\partial\theta_i^2$ has a branch cut outward along the real θ_i^2 axis from the point $\theta_i^2 = \bar{\theta}_{ii}^2$. At this point there is a square root singularity. An asymptotic expansion of this function about θ_{ii}^2 results in the following series:

$$\frac{\partial\omega}{\partial\theta_i^2} \simeq \frac{1}{i(\theta_{ii}^2-\theta_i^2)^{1/2}} (D_0 + D_1(\theta_{ii}^2-\theta_i^2) + D_2(\theta_{ii}^2-\theta_i^2)^2 + \ldots)$$

† That is, the Mach front which is tangent to the front of the P wave.

where $$D_0 = \frac{(t - yc_i^{-2}/(c_i^{-2}-\theta_{ii}^{-2})^{1/2})}{(r^2 + y^2 - ty/(c_i^{-2}-\theta_{ii}^2)^{1/2})^{1/2} \cdot 2\theta_{ii}^2} \tag{B.8}$$

with t, y and r satisfying Eq. (B.5) with i = 1. A straightforward but lengthy computation gives the coefficients of the remaining terms in the series.

Using Eqs. (B.7) and (B.8), we express the integrand of the first of the integrals of Eq. (B.1) in series form, and, as a result, obtain the following series approximation of σ_y^P:

$$\begin{aligned}\sigma_y^P = &\int_C \frac{C_0 D_0 \, d\theta_1^2}{i(\theta_{11}^2-\theta_1^2)^{1/2}} + \int_C \frac{C_1 D_0 \, d\theta_1^2}{i(\alpha^{-2}-\theta_{11}^2)^{1/2}(\theta_{11}^2-\theta_1^2)^{1/2}} \\ &+ \int_C \left(\frac{D_1 C_1 (\theta_{11}^2-\theta_1^2)^{1/2}}{i(\alpha^{-2}-\theta_1^2)^{1/2}} + \frac{C_2 D_0 (\alpha^{-2}-\theta_1^2)^{1/2}}{i(\theta_{11}^2-\theta_1^2)}\right) d\theta_1^2 \\ &+ \ldots\end{aligned} \tag{B.9}$$

where C is the contour of integration described previously.

The integrand of the first integral in (B.9) is analytic on and within the contour of integration, except at the point $\theta_1^2 = \theta_{11}^2$ where there is a square root singularity. Despite the presence of this singularity, it can easily be shown that the value of this integral is zero. Evaluating the remaining terms in the series gives the following result:

$$\sigma_y^P \simeq -2\pi C_1 D_0 + (\pi D_1 C_1 - \pi C_2 D_0)(\theta_1^2-\alpha^{-2}) + O(\theta_1^2-\alpha^{-2})^2 \tag{B.10}$$

The variation with time at a point in the vicinity of the Mach front can be computed from Eqs. (B.5) and (B.10). The result is

$$\sigma_y^P(r,y,t) = 0 \qquad \text{for } t < t_{PM}$$

$$= 2\pi C_1 D_0 + \pi \frac{(D_1 C_1 - C_2 D_0)}{r - y\alpha^{-1}/(a^{-2}-\alpha^{-2})^{1/2}} (t-t_{PM})$$

$$+ O(t-t_{PM})^2 \qquad \text{for } t \geq t_{PM}$$

where t_{PM} is the time at which the Mach front reaches the point in question. It can be verified from Eqs. (B.8) and (B.11) that the magnitude of the stress behind the Mach front depends on the distance of the point in question below the y = 0 surface and the interval of time following the arrival of the front. This is in contrast to the results obtained for the superseismic wedge problem. It was found (see Sec. 5.2.1) that the value of σ_y^P was constant at every point between the Mach front and the cylindrical front of the P wave.

The value of σ_y^S at points in the vicinity of the Mach front which is tangent to the S wave is computed by methods analogous to those described above. The final result of these computations are the equations

$$\sigma_y^S = 0 \qquad \text{for } t < t_{SM}$$

$$\simeq 2\pi B_1 D_0 + \frac{\pi(D_1 B_1 - B_2 D_0)(t-t_{SM})}{r - y\alpha^{-2}\sim(b^{-2}-\alpha^{-2})^{1/2}} + O(t-t_{SM})^2 \qquad \text{for } t \geq t_{SM} \tag{B.12}$$

where

$$B_1 = -\frac{4A_1\alpha^{-2}(b^{-2}-\alpha^{-2})^{1/2}}{(b^{-2}-a^{-2})}\ , \tag{B.13}$$

D_0 is defined by Eq. (B.8), and r, y and t satisfy Eq. (B.5) with i = 2. The remaining B_i's and D_i's can be computed without difficulty from Eqs. (B.3) and (B.6).

The asymptotic character of the P- and S-wave components of the remaining stresses and velocities in the vicinity of the two Mach fronts is determined by computation similar to those described above.

APPENDIX C. THE COMPUTATION OF $\dot{\sigma}_y^S$ FOR THE CONE WHEN THE CONTACT SPEED IS IN THE SECOND INTERMEDIATE RANGE

The following equation defines the equivoluminal component of $\dot{\sigma}_y$ for the problem in which a rigid cone indents a half space in such a way that $b < \alpha < a$, i.e. in such a way that α is in the second intermediate range of contact speeds:†

$$\dot{\sigma}_y^S = \mathrm{Re}\int_{\theta_2^2}^{\alpha^{-2}} \frac{I(\theta^2)\cdot F_{\alpha b}(\theta)}{G(\theta^2)(\alpha^{-2}-\theta^2)^2}\, d\theta^2 \tag{C.1}$$

where
$$I(\theta^2) = 8\theta^2(a^{-2}-\theta^2)^{1/2}(b^{-2}-\theta^2)^{1/2}(c^{-2}-\theta^2)/R(\theta^2), \tag{C.2}$$

$$G(\theta^2) = (r^2\theta^2 - (t - y(b^{-2}-\theta^2)^{1/2})^2)^{1/2}\ , \tag{C.3}$$

$F_{\alpha b}(\theta)$ is defined by Eq. (A.4), and θ_2 is defined implicitly by the equation

$$t - \theta_2 r - y(b^{-2}-\theta_2^2)^{1/2} = 0 \tag{C.4}$$

It was pointed out in Sec. 5.4.2 that $\dot{\sigma}_y^S$ is singular on the surface in the r, y, t space defined by Eq. (C.4) when $\theta_2 = \alpha^{-1}$. This surface is shown schematically in Fig. 18. To compute the value of $\dot{\sigma}_y^S$ at points near this surface, it is convenient to rewrite Eq. (C.1) in the form

$$\dot{\sigma}_y^S = \mathrm{Re}\int_{\theta_0^2}^{a^{-2}} \frac{I(\theta^2)\, F_{\alpha b}(\theta^2)}{(\alpha^{-2}-\theta^2)^2 G(\theta^2)}\, d\theta^2 + \mathrm{Re}\int_{\theta_2^2}^{\theta_0^2} \frac{I^*(\theta^2)\, F^*_{\alpha b}(\theta^2)}{(\alpha^{-2}-\theta^2)^2 G^*(\theta^2)} \tag{C.5}$$

† Equation (C.1) is obtained from Eqs. (4.50), (2.57) and (3.40).

where $I^*(\theta^2)F^*_{\alpha b}(\theta)$ denotes the asymptotic expansion of $I(\theta^2)F_{\alpha b}(\theta)$ about α^{-2}, $G^*(\theta^2)$ denotes the asymptotic expansion of $G(\theta)$ about θ_2^2, and θ_0^2 is a fixed point on the real θ^2 axis slightly to the left of α^{-2}. (See Fig. 29.)

The first integral of Eq. (C.5) defines a function of θ_2^2 which varies smoothly for all $\theta_2^2 > \theta_0^2$. The value of this function can be computed without difficulty by the numerical integration procedures described in Chapter 5.

The second integral of Eq. (C.5) defines the component of $\dot{\sigma}_y^S$ which is singular on the Mach front shown in Fig. 18, i.e. on the surface along which $\theta_2 = \alpha^{-1}$. It can easily be verified from Eqs. (C.2), (C.3) and (A.12) that the integrand is defined by an infinite series of the form

$$\frac{I^*(\theta^2)\, F^*_{\alpha b}(\theta)}{G^*(\theta^2)(\alpha^{-2}-\theta^2)^2} \simeq \frac{A_0 + A_1(\alpha^{-2}-\theta^2) + A_2(\alpha^{-2}-\theta^2)\log(\alpha^{-2}-\theta^2)+\ldots}{(\theta_2^2-\theta^2)^{1/2}(\alpha^{-2}-\theta^2)^{2+\beta(\alpha^{-2})/\pi}} \tag{C.6}$$

where $\beta(\alpha^{-2})$ is the value of the argument of $F_{\alpha b}(\theta)$ at α^{-2} and A_i's are complex-valued constants which can be determined in a straightforward manner from the equations above.

Term-by-term integration of the series defined by (C.6) results in the following approximation for the singular component of $\dot{\sigma}_y^S$:

$$\int_{\theta_2^2}^{\theta_0^2} \frac{I^*(\theta^2)F^*_{\alpha b}(\theta)}{G(\theta^2)(\alpha^{-2}-\theta^2)^2} \simeq \frac{B_0}{(\alpha^{-2}-\theta_2^2)^{3/2+\beta(\alpha^{-2})/\pi}} + \frac{B_1}{(\alpha^{-2}-\theta_2^2)^{1/2+\beta(\alpha^{-2})/\pi}} + \frac{B_2\log(\alpha^{-2}-\theta_2^2)}{(\alpha^{-2}-\theta_2^2)^{1/2+\beta(\alpha^{-2})/\pi}} + \ldots \tag{C.7}$$

where

$$B_0 = -A_0 \int_1^{\lambda_0} \frac{d\lambda}{\lambda^{2+\beta(\alpha^{-2})/\pi_{(\lambda-1)}^{1/2}}}$$

$$B_1 = -A_1 \int_1^{\lambda_0} \frac{d\lambda}{\lambda^{1+\beta(\alpha^{-2})/\pi_{(\lambda-1)}^{1/2}}} - A_2 \int_1^{\lambda_0} \frac{\log \lambda d\lambda}{\lambda^{1+\beta(\alpha^{-2})/\pi_{(\lambda-1)}^{1/2}}}$$

$$B_2 = -A_2 \int_1^{\lambda_0} \frac{1 \quad d\lambda}{\lambda^{1+\beta(\alpha^{-2})/\pi_{(\lambda-1)}^{1/2}}} \qquad \text{(C.8)}$$

and $$\lambda_0 = \frac{\alpha^{-2} - \theta_0^2}{\alpha^{-2} - \theta_2^2} \quad .$$

The integrals defining the B_i's can be evaluated numerically by the methods described in Chapter 5. When $\theta_2^2 < \alpha^{-2}$, i.e. for a point behind the surface on which $\dot{\sigma}_y^S$ is singular, the contour of integration is deformed around the singular point in the manner shown in Fig. 29.

The method used to compute $\dot{\sigma}_y^S$ can also be applied to the determination of the S-wave component of the remaining stresses and velocities.

ERRATA

Page	Line* or Eq.	
2	7	developed <u>by</u> Smirnov and Sobolev
13	5^-	$\Delta =$
20	(2.17)	$\frac{df(\theta)}{d\theta}\left[\frac{\partial^2\theta}{\partial x^2} + \ldots\right.$
26	2	... but <u>is</u> less ...
26	3^-	... can be satisfied ...
30	(2.45)	in the first equation read $\frac{\sqrt{c_2^{-2} - \theta_2^2}}{\delta_2'}$
30	4	$\Psi'(\theta_2) = \frac{d\Psi(\theta_2)}{d\theta_2}$
30	(2.47)	in the second equation, first integrand read $(b^{-2}+2\theta^2-2\underline{a}^{-2})$
32	(2.49)	in the first equation, $-2\theta\sqrt{b^{-2}-\theta^2}\ \Psi'(\theta)$ in the second equation, $2\theta\sqrt{a^{-2}-\theta^2}\ \Phi'(\theta)$
32	(2.51)	$\sum_y^*$, in the first equation $-2\theta\sqrt{b^{-2}-\theta^2}\ \Psi'(\theta)$ in the second equation, $2\theta\sqrt{a^{-2}-\theta^2}\ \Phi'(\theta)$ $+ (b^{-2}-2\theta^2)\ \Psi'(\theta)$
32	3^-	... where $\sum_y^*$ ...
33	(2.53)	$\sum_y = \mathrm{Re}\sum_y^*$
33	3^-	<u>then</u>
34	10^-	... θ_1 and θ_2 half planes ....
35	10	$\Phi'(\theta_1)$

*A superior minus sign indicates a number counted from the bottom of the page.

Page	Line* or Eq.	
39	(2.64)	$\Phi'(\theta_1)$
39	(2.65)	I_v
44	(2.71)	$u_x = \underline{Re}\ \{....\}$ $u_y = \underline{Re}\ \{....\}$
47	5	... approximation of σ_x:
47	3^-	$\theta_i - c^{-1}$
50	2^-	... <u>are</u> found ....
54	(2.88)	in the third equation read $d\tau_1$, ... $d\tau_{n-1}$ $d\tau_n$
63	(3.8)	in the fourth equation read τ_{ry}
66	2^-	... without difficulty†. (Footnote reference)
67	(3.18)	in the second equation read σ_{y2}
68	(3.20)	in the second equation read $\dot{\tau}_{ry}(r,t) =$
69	(3.21)	in the second equation read $\dot{\tau}_{ry}(\theta_o) =$
70	2	... between 0 and + ∞ .
72	(3.25)	in the second equation read $\dot{\tau}_{ry}(\theta_o) =$
72	4^-	the radial in the denominator reads $\sqrt{\theta^2-\theta_o^2}$
74	1	... loaded area.
76	(3.32)	in the second equation read $\tau^{*'}_{xy} = 0$
79	(3.39)	in the first equation close the parenthesis at the end of the line in the second equation open parenthesis before $\partial^2/\partial\tau^2$ and close at the end
81	(3.42)	in the first equation read F i in the last equation on Page 81 close the parenthesis at the end.
84	(3.44)	line two ends ... $d\theta^2) + \sigma^R_\omega$
86	4^-	left <u>of</u> a^{-2}

Page	Line* or Eq.	
87	(3.48)	read $\sqrt{c^{-1}-\theta_2}$ in the denominator of the second term
88	(3.48)	in the third equation, first line read $(b^{-2}-2c^{-2})^2$ the second line begins with a minus sign
89	1	in the first term read $\sqrt{1-c^2/a^2}$
90	2⁻	... more direct than that ....
91	9⁻	... $(a^{-2}-\theta_1^2)^{1/2}$ ...
94	(3.59)	in the first equation read = $\tau^p_{ry} = 0$ for $t < t_p$
94	4⁻	... which define ...
96	(3.61)	in the first equation read $\sqrt{(r^2+y^2)/b^2-t^2}$
97	(3.62)	in sixth equation read (r^2+y^2) in the denominator
100	(3.66)	read F μ
101	(3.69)	the equation number is (3.69)
111	11⁻	.... along the segments of ...
113	12⁻	This is the condition ....
125	2⁻	read $\frac{d\sigma_y^*(\theta^2)}{d\theta^2} = \ldots$
132	9	... it can easily be verified ...
136	8	... can then be rewritten ...
136	(4.66)	read U (ξ, t-τ)
139	(4.73)	read $\sigma_y(x,t) =$
		in the second line read $(-\alpha^{-1} + \theta)$ in the denominator
139	(4.74)	read $\frac{\partial\sigma_y(x,t)}{\partial\theta_o}$

Page	Line* or Eq.	
139	(4.75)	read $\sigma_y^{\,o}\ (r-r_o,\ \omega-\omega_o,\ \tau)$
142	(4.84)	read $R(\theta^2)$
142	(4.87)	read $0 \leq r \leq \infty$ in the first equation
148	(5.10)	... for $\alpha^{-1} < \theta_1\ (t) \leq$ ...
149	(5.13)	read $4I_2\ \dfrac{\theta_2{}^j + \theta_2{}^{j+1}}{2}$
150	(5.18)	read $-4\mu b^2\ V\alpha^{-2}$
152	(5.23)	in the numerator read $\sqrt{a^{-1}+\theta}$
153	(5.28)	read ... $-y_o\ (b^{-2} - (a^{-1}+m\Delta\theta)^2)^{1/2} = 0$
156	11⁻	... Secs. 5.2.1 and 5.2.2.
156	5⁻	... step-by-step ...
158	(5.38)	read $\sigma_y^{*'}\ (\theta_1)$
161	7 and 8	... associated with the P wave passes ....
162	8	... function.
162	(5.48)	read ... $4\sigma_y^{\,S}(t_2^{\,*} + (2j+1)\Delta t)$ ...
163	5⁻	read $\theta_2(t_2) > \alpha^{-1}$
164	(5.53)	$\dot{\sigma}_y^{\,S} \simeq$ Re { } + ...
169	12⁻	... than the square root ...
170	(6.6)	in the third equation read .. $\left[\dfrac{iB_1}{\ldots} + \dfrac{iB_2}{\ldots}\right]$
171	3	$\sigma_y\ (\xi, y, t)$
171	5⁻	.. up to <u>and</u> immediately following ...
173	(6.10)	... $\simeq$ - Re ( ) ....
174	9	<u>d</u>ominant

Page	Line* or Eq.	
174	(6.11)	read $\int_0^1 \frac{id\lambda}{\lambda^{1+\beta/\pi}\sqrt{1-\lambda}}$
178	1	read $A_1 \alpha^2 + A_1 \alpha^4 \theta^2 + \ldots$
185	Ref. 22	read ... ser. geofiz ...
185	Refs. 22 & 26	read Pod"yapol'skii
228	2^-&1^-	read ... listed above ...
232	(A.11)	exponent reads $\beta(\theta^2)/\pi$

PART 1 - GOVERNMENT

Administrative & Liaison Activities

Chief of Naval Research
Department of the Navy
Washington, D. C. 20360
Attn: Code 423
439 (2)
468

Director
ONR Branch Office
495 Summer Street
Boston, Massachusetts 02210

Director
ONR Branch Office
219 S. Dearborn Street
Chicago, Illinois 60604

Commanding Officer
ONR Branch Office
Box 39, Navy 100
c/o Fleet Post Office
New York, New York 09510 (5)

Commanding Officer
ONR Branch Office
207 West 24th Street
New York, New York 10011

Director
ONR Branch Office
1030 E. Green Street
Pasadena, California 91101

U. S. Naval Research Laboratory
Attn: Technical Information Div.
Washington, D. C. 20390 (6)

Defense Documentation Center
Cameron Station
Alexandria, Virginia 22314 (20)

Army

Commanding Officer
U. S. Army Research Off. Durham
Attn: Mr. J. J. Murray
CRD-AA-IP
Box CM, Duke Station
Durham, North Carolina 27706

Commanding Officer
AMXMR-ATL
Attn: Mr. J. Bluhm
U. S. Army Materials Res. Agcy.
Watertown, Massachusetts 02172

Watervliet Arsenal
MAGGS Research Center
Watervliet, New York
Attn: Director of Research

Redstone Scientific Info. Center
Chief, Document Section
U. S. Army Missile Command
Redstone Arsenal, Alabama 35809

Army R & D Center
Fort Belvoir, Virginia 22060

Technical Library
Aberdeen Proving Ground
Aberdeen, Maryland 21005

Navy

Commanding Officer and Director
Naval Ship Research & Development Center
Washington, D. C. 20007
Attn: Code 042 (Tech. Lib. Br.)
700 (Struc. Mech. Lab.)
720
725
800 (Appl. Math. Lab.)
012.2 (Mr. W. J. Sette)
901 (Dr. M. Strassberg)
941 (Dr. R. Liebowitz)
945 (Dr. W. S. Cramer)
960 (Mr. E. F. Noonan)
962 (Dr. E. Buchmann)

Aeronautical Structures Lab
Naval Air Engineering Center
Naval Base, Philadelphia, Pa. 19112

Naval Weapons Laboratory
Dahlgren, Virginia 22448

Naval Research Laboratory
Washington, D. C. 20390
Attn: Code 8400
8430
8440

Navy (cont'd)

Undersea Explosion Research Div.
Naval Ship R & D Center
Norfolk Naval Shipyard
Portsmouth, Virginia 23709
Attn: Mr. D. S. Cohen
Code 780

Nav. Ship R & D Center
Annapolis Division
Code 257, Library
Annapolis, Maryland 21402

Technical Library
Naval Underwater Weapons Center
Pasadena Annex
3202 E. Foothill Blvd.
Pasadena, California 91107

U. S. Naval Weapons Center
China Lake, California 93557
Attn: Code 4062 Mr. W. Werback
4520 Mr. Ken Bischel

Naval Research Laboratory
Washington, D. C. 20390
Attn: Code 8400 Ocean Tech. Div.
8440 Ocean Structures
6300 Metallurgy Div.
6305 Dr. J. Krafft

Commanding Officer
U. S. Naval Civil Engr. Lab.
Code L31
Port Hueneme, California 93041

Shipyard Technical Library
Code 242 L
Portsmouth Naval Shipyard
Portsmouth, New Hampshire 03804

U. S. Naval Electronics Laboratory
Attn: Dr. R. J. Christensen
San Diego, California 92152

U. S. Naval Ordnance Laboratory
Mechanics Division
RFD 1, White Oak
Silver Spring, Maryland 20910

U. S. Naval Ordnance Laboratory
Attn: Mr. H. A. Perry, Jr.
Non-Metallic Materials Division
Silver Spring, Maryland 20910

Supervisor of Shipbuilding
U. S. Navy
Newport News, Virginia 23607

Shipyard Technical Library
Building 746, Code 303TL
Mare Island Naval Shipyard
Vallejo, California 94592

U. S. Navy Underwater Sound Ref. Lab.
Office of Naval Research
P. O. Box 8337
Orlando, Florida 32806

Technical Library
U. S. Naval Ordnance Station
Indian Head, Maryland 20640

U. S. Naval Ordnance Station
Attn: Mr. Garet Bornstein
Research & Development Division
Indian Head, Maryland 20640

Chief of Naval Operation
Department of the Navy
Washington, D. C. 20350
Attn: Code Op-03EG
Op-07T

Special Projects Office
(CNM-PM-1) (MUN)
Department of the Navy
Washington, D. C. 20360
Attn: NSP-001 Dr. J. P. Craven

Deep Submergence Sys. Project
(CNM-PM-11)
6900 Wisconsin Ave.
Chevy Chase, Md. 20015
Attn: PM-1120 S. Hersh

U. S. Naval Applied Science Lab.
Code 9832
Technical Library
Building 291, Naval Base
Brooklyn, New York 11251

Director Aeronautical Materials Lab.
Naval Air Engineering Center
Naval Base
Philadelphia, Pennsylvania 19112

Navy (cont'd)

Naval Air Systems Command
Dept. of the Navy
Washington, D. C. 20360
Attn: NAIR 03 Res. & Technology
320 Aero. & Structures
5320 Structures
604 Tech. Library

Naval Facilities Engineering
Command
Dept. of the Navy
Washington, D. C. 20360
Attn: NFAC 03 Res. & Development
04 Engineering & Design
04128 Tech. Library

Naval Ship Systems Command
Dept. of the Navy
Washington, D. C. 20360
Attn: NSHIP 031 Ch. Scientists for R & D
0342 Ship Mats. & Structs.
037 Ship Silencing Div.
052 Shock & Blast Coord.
2052 Tech. Library

Naval Ship Engineering Center
Main Navy Building
Washington D. C. 20360
Attn: NSEC 6100 Ship Sys. Engr. & Des. Dept.
6102C Computerated Ship Des.
6105 Ship Protection
6110 Ship Concept Design
6120 Hull Div. - J. Nachtsheim
6120D Hull Div. - J. Vasta
6132 Hull Structs. - (4)

Naval Ordnance Systems Command
Dept. of the Navy
Washington, D. C. 20360
Attn: NORD 03 Res. & Technology
035 Weapons Dynamics
9132 Tech. Library

Air Force

Commander WADD
Wright-Patterson Air Force Base
Dayton, Ohio 45433
Attn: Code WWRMDD
AFFDL (FDDS)

Wright-Patterson AFB (cont'd)
Attn: Structures Division
AFLC (MCEEA)
Code WWRC
AFML (MAAM)
Code WCLSY
SEG (SEFSD, Mr. Lakin)

Commander
Chief, Applied Mechanics Group
U. S. Air Force Inst. of Tech.
Wright-Patterson Air Force Base
Dayton, Ohio 45433

Chief, Civil Engineering Branch
WLRC, Research Division
Air Force Weapons Laboratory
Kirtland AFB, New Mexico 87117

Air Force Office of Scientific Res.
1400 Wilson Blvd.
Arlington, Virginia 22209
Attn: Mechs. Div.

NASA

Structures Research Division
National Aeronautics & Space Admin.
Langley Research Center
Langley Station
Hampton, Virginia 23365
Attn: Mr. R. R. Heldenfels, Chief

National Aeronautic & Space Admin.
Associate Administrator for Advanced
Research & Technology
Washington, D. C. 20546

Scientific & Tech. Info. Facility
NASA Representative (S-AK/DL)
P. O. Box 5700
Bethesda, Maryland 20014

National Aeronautic & Space Admin.
Code RV-2
Washington, D. C. 20546

Other Government Activities

Commandant
Chief, Testing & Development Div.
U. S. Coast Guard
1300 E Street, N. W.
Washington, D. C. 20226

Director
Marine Corps Landing Force Devel. Cen.
Marine Corps Schools
Quantico, Virginia 22134

Director
National Bureau of Standards
Washington, D. C. 20234
Attn: Mr. B. L. Wilson, EM 219

National Science Foundation
Engineering Division
Washington, D. C. 20550

Science & Tech. Division
Library of Congress
Washington, D. C. 20540

Director
STBS
Defense Atomic Support Agency
Washington, D. C. 20350

Commander Field Command
Defense Atomic Support Agency
Sandia Base
Albuquerque, New Mexico 87115

Chief, Defense Atomic Support Agcy.
Blast & Shock Division
The Pentagon
Washington, D. C. 20301

Director Defense Research & Engr.
Technical Library
Room 3C-128
The Pentagon
Washington, D C. 20301

Chief, Airframe & Equipment Branch
FS-120
Office of Flight Standards
Federal Aviation Agency
Washington, D. C. 20553

Chief, Division of Ship Design
Maritime Administration
Washington, D. C. 20235

Deputy Chief, Office of Ship Constr.
Maritime Administration
Washington, D. C. 20235
Attn: Mr. U. L. Russo

Mr Milton Shaw, Director
Div. of Reactor Devel. & Technology
Atomic Energy Commission
Germantown, Md. 20767

Ship Hull Research Committee
National Research Council
National Academy of Sciences
2101 Constitution Avenue
Washington, D. C. 20418
Attn: Mr. A. R. Lytle

PART 2 - CONTRACTORS AND OTHER TECHNICAL COLLABORATORS

Universities

Professor J. R. Rice
Division of Engineering
Brown University
Providence, Rhode Island 02912

Dr. J. Tinsley Oden
Dept. of Engr. Mechs.
University of Alabama
Huntsville, Alabama

Professor M. E. Gurtin
Dept. of Mathematics
Carnegie Institute of Technology
Pittsburgh, Pennsylvania 15213

Professor R. S. Rivlin
Center for the Application of Mathematics
Lehigh University
Bethlehem, Pennsylvania 18015

Professor Julius Miklowitz
Division of Engr. & Applied Sciences
California Institute of Technology
Pasadena, California 91109

Professor George Sih
Department of Mechanics
Lehigh University
Bethlehem, Pennsylvania 18015

Dr. Harold Liebowitz, Dean
School of Engr. & Applied Science
George Washington University
725 23rd Street
Washington, D. C. 20006

Universities (cont'd)

Professor Eli Sternberg
Div. of Engr. & Applied Sciences
California Institute of Technology
Pasadena, California 91109

Professor Paul M. Naghdi
Div. of Applied Mechanics
Etcheverry Hall
University of California
Berkeley, California 94720

Professor Wm. Prager
Revelle College
University of California
P.O. Box 109
La Jolla, California 92037

Professor J. Baltrukonis
Mechanics Division
The Catholic Univ. of America
Washington, D. C. 20017

Professor A. J. Durelli
Mechanics Division
The Catholic Univ. of America
Washington, D. C. 20017

Professor H. H. Bleich
Department of Civil Engr.
Columbia University
Amsterdam & 120th Street
New York, New York 10027

Professor R. D. Mindlin
Department of Civil Engr.
Columbia University
S. W. Mudd Building
New York, New York 10027

Professor F. L. DiMaggio
Department of Civil Engr.
Columbia University
616 Mudd Building
New York, New York 10027

Professor A. M. Freudenthal
Department of Civil Engr. &
Engr. Mech.
Columbia University
New York, New York 10027

Professor B. A. Boley
Department of Theor. & Appl. Mech.
Cornell University
Ithaca, New York 14850

Professor P. G. Hodge
Department of Mechanics
Illinois Institute of Technology
Chicago, Illinois 60616

Dr. D. C. Drucker
Dean of Engineering
University of Illinois
Urbana, Illinois 61803

Professor N. M. Newmark
Dept. of Civil Engineering
University of Illinois
Urbana, Illinois 61803

Professor A. R. Robinson
Department of Civil Engr.
University of Illinois
Urbana, Illinois 61803

Professor S. Taira
Department of Engineering
Kyoto University
Kyoto, Japan

Professor James Mar
Massachusetts Inst. of Tech.
Rm. 33-318
Dept. of Aerospace & Astro.
77 Massachusetts Ave.
Cambridge, Mass. 02139

Professor E. Reissner
Dept. of Mathematics
Massachusetts Inst. of Tech.
Cambridge, Mass. 02139

Professor William A. Nash
Dept. of Mechs. & Aerospace Engr.
University of Mass.
Amherst, Mass. 01002

Library (Code 0384)
U. S. Naval Postgraduate School
Monterey, California 93940

Professor Arnold Allentuch
Dept. of Mechanical Engineering
Newark College of Engineering
323 High Street
Newark, New Jersey 07102

Universities (cont'd)

Professor E. L. Reiss
Courant Inst. of Math. Sciences
New York University
4 Washington Place
New York, New York 10003

Professor Bernard W. Shaffer
School of Engrg. & Science
New York University
University Heights
New York, New York 10453

Dr. Francis Cozzarelli
Div. of Interdisciplinary
Studies and Research
School of Engineering
State Univ. of N. Y.
Buffalo, New York 14214

Professor R. A. Douglas
Dept. of Engr. Mechs.
North Carolina State
University
Raleigh, North Carolina 27607

Dr. George Herrmann
The Technological Institute
Northwestern University
Evanston, Illinois 60201

Professor J. D. Achenbach
Technological Institute
Northwestern University
Evanston, Illinois 60201

Director, Ordnance Research Lab.
Pennsylvania State University
P. O. Box 30
State College, Pennsylvania 16801

Professor Eugene J. Skudrzyk
Department of Physics
Ordnance Research Lab.
Pennsylvania State University
P. O. Box 30
State College, Pennsylvania 16801

Dean Oscar Baguio
Assoc. of Struc. Engr. of
the Philippines
University of Philippines
Manila, Philippines

Professor J. Kempner
Dept. of Aero. Engr. & Applied Mech.
Polytechnic Institute of Brooklyn
333 Jay Street
Brooklyn, New York 11201

Professor J. Klosner
Polytechnic Institute of Brooklyn
333 Jay Street
Brooklyn, New York 11201

Professor A. C. Eringen
Dept. of Aerospace & Mech. Sciences
Princeton University
Princeton, New Jersey 08540

Dr. S. L. Koh
School of Aero., Astro. & Engr. Sc.
Purdue University
Lafayette, Indiana 47907

Professor R. A. Schapery
Purdue University
Lafayette, Indiana 47907

Professor E. H. Lee
Div. of Engr. Mechanics
Stanford University
Stanford, California 94305

Dr. Nicholas J. Hoff
Dept. of Aero. & Astro.
Stanford University
Stanford, California 94305

Professor Max Anliker
Dept. of Aero. & Astro.
Stanford University
Stanford, California 94305

Professor J. N. Goodier
Div. of Engr. Mechanics
Stanford University
Stanford, California 94305

Professor H. W. Liu
Dept. of Chemical Engr. & Metal.
Syracuse University
Syracuse, New York 13210

Professor Markus Reiner
Technion R & D Foundation
Haifa, Israel

Universities (cont'd)

Professor Tsuyoshi Hayashi
Department of Aeronautics
Faculty of Engineering
University of Tokyo
BUNKYO-KU
Tokyo, Japan

Professor J. E. Fitzgerald, Ch.
Dept. of Civil Engineering
University of Utah
Salt Lake City, Utah 84112

Professor R. J. H. Bollard
Chairman, Aeronautical Engr. Dept.
207 Guggenheim Hall
University of Washington
Seattle, Washington 98105

Professor Albert S. Kobayashi
Dept. of Mechanical Engr.
University of Washington
Seattle, Washington 98105

Officer-in-Charge
Post Graduate School for Naval Off.
Webb Institute of Naval Arch.
Crescent Beach Road, Glen Cove
Long Island, New York 11542

Librarian
Webb Institute of Naval Arch.
Crescent Beach Road, Glen Cove
Long Island, New York 11542

Solid Rocket Struc. Integrity Cen.
Dept. of Mechanical Engr.
Professor F. Wagner
University of Utah
Salt Lake City, Utah 84112

Dr. Daniel Frederick
Dept. of Engr. Mechs.
Virginia Polytechnic Inst.
Blacksburgh, Virginia

Industry and Research Institutes

Dr. James H. Wiegand
Senior Dept. 4720, Bldg. 0525
Ballistics & Mech. Properties Lab.
Aerojet-General Corporation
P. O. Box 1947
Sacramento, California 95809

Mr. Carl E. Hartbower
Dept. 4620, Bldg. 2019 A2
Aerojet-General Corporation
P. O. Box 1947
Sacramento, California 95809

Mr. J. S. Wise
Aerospace Corporation
P. O. Box 1300
San Bernardino, California 92402

Dr. Vito Salerno
Applied Technology Assoc., Inc.
29 Church Street
Ramsey, New Jersey 07446

Library Services Department
Report Section, Bldg. 14-14
Argonne National Laboratory
9700 S. Cass Avenue
Argonne, Illinois 60440

Dr. M. C. Junger
Cambridge Acoustical Associates
129 Mount Auburn Street
Cambridge, Massachusetts 02138

Dr. F. R. Schwarzl
Central Laboratory T.N.O.
Schoenmakerstraat 97
Delft, The Netherlands

Research and Development
Electric Boat Division
General Dynamics Corporation
Groton, Connecticut 06340

Supervisor of Shipbuilding, USN,
and Naval Insp. of Ordnance
Electric Boat Division
General Dynamics Corporation
Groton, Connecticut 06340

Dr. L. H. Chen
Basic Engineering
Electric Boat Division
General Dynamics Corporation
Groton, Connecticut 06340

Dr. Wendt
Valley Forge Space Technology Cen.
General Electric Co.
Valley Forge, Pennsylvania 10481

Dr. Joshua E. Greenspon
J. G. Engr. Research Associates
3831 Menlo Drive
Baltimore, Maryland 21215

Industry & Research Inst. (cont'd)

Dr. Walt. D. Pilkey
IIT Research Institute
10 West 35 Street
Chicago, Illinois 60616

Library Newport News Shipbuilding
& Dry Dock Company
Newport News, Virginia 23607

Mr. J. I. Gonzalez
Engr. Mechs. Lab.
Martin Marietta
MP - 233
P. O. Box 5837
Orlando, Florida 32805

Dr. E. A. Alexander
Research Dept.
Rocketdyne D. W., NAA
6633 Canoga Avenue
Canoga Park, California 91304

Mr. Cezar P. Nuguid
Deputy Commissioner
Philippine Atomic Energy
Commission
Manila, Philippines

Dr. M. L. Merritt
Division 5412
Sandia Corporation
Sandia Base
Albuquerque, New Mexico 87115

Director
Ship Research Institute
Ministry of Transportation
700, SHINKAWA
Mitaka
Tokyo, Japan

Dr. H. N. Abramson
Southwest Research Institute
8500 Culebra Road
San Antonio, Texas 78206

Dr. R. C. DeHart
Southwest Research Institute
8500 Culebra Road
San Antonio, Texas 78206

Dr. M. L. Baron
Paul Weidlinger, Consulting Engr.
777 Third Ave. - 22nd Floor
New York, New York 10017

Mr. Roger Weiss
High Temp. Structs. & Materials
Applied Physics Lab.
8621 Georgia Ave.
Silver Spring, Md.

Mr. William Caywood
Code BBE
Applied Physics Lab.
8621 Georgia Ave.
Silver Spring, Md.

Mr. M. J. Berg
Engineering Mechs. Lab.
Bldg. R-1, Rm. 1104A
TRW Systems
1 Space Park
Redondo Beach, California 90278

Security Classification

DOCUMENT CONTROL DATA - R & D

(Security classification of title, body of abstract and indexing annotation must be entered when the overall report is classified)

1. ORIGINATING ACTIVITY (Corporate author)	2a. REPORT SECURITY CLASSIFICATION
University of Illinois, Urbana, Illinois Department of Civil Engineering	Unclassified
	2b. GROUP

3. REPORT TITLE

EXACT SOLUTIONS OF SOME DYNAMIC PROBLEMS OF INDENTATION AND TRANSIENT LOADINGS OF AN ELASTIC HALF SPACE

4. DESCRIPTIVE NOTES (Type of report and inclusive dates)

Report

5. AUTHOR(S) (First name, middle initial, last name)

Robinson, Arthur R.
Thompson, J. Carl

6. REPORT DATE	7a. TOTAL NO. OF PAGES	7b. NO. OF REFS
September 1969	240	39

8a. CONTRACT OR GRANT NO.	9a. ORIGINATOR'S REPORT NUMBER(S)
N0014-67-A-0305-0010	Structural Research Series No. SRS-350
b. PROJECT NO.	
c.	9b. OTHER REPORT NO(S) (Any other numbers that may be assigned this report)
d.	None

10. DISTRIBUTION STATEMENT

Qualified requesters may obtain copies of this report from DDC.

11. SUPPLEMENTARY NOTES	12. SPONSORING MILITARY ACTIVITY
	Office of Naval Research, Structural Mechanics Branch, Navy Department, Washington, D. C.

13. ABSTRACT

In this report the method of self-similar potentials is used to solve certain problems which involve the frictionless indentation of a linearly elastic half space by a rigid die. Solutions which are exact within the limits of the classical theory of elasticity are obtained for the early stages of contact for any problem in which the surface of the die is smooth. For problems in which the die is wedge- or cone-shaped and indents the half space at a constant rate, the solution for the entire process is given. The stress and velocity fields for the wedge and cone problems are considered in detail.

This report includes an exposition of the method of self-similar potentials and of the procedure based on this method for solving two-and three-dimensional problems involving transient loads acting at interior or surface points of a homogeneous linearly elastic half space. The asymptotic character of the disturbance near the wave fronts and near the surface wave is determined in detail for both the two-and three-dimensional problems in which the source of the disturbance is an impulse applied normal to the surface of the half space.

14. KEY WORDS	LINK A		LINK B		LINK C	
	ROLE	WT	ROLE	WT	ROLE	WT
Waves in Solids						
Dynamic Contact Stresses						